AUTOMOTIVE CAE COMPANION

Knowledge for Tomorrow's Automotive Engineering

2025
2026

carhs
Empowering Engineers

automotive
CAE**Companion**
2025/2026

Engineering

CAE Tools

Modeling of
Materials &
Connections

CAE Theory

Safety

carhs.training gmbh

Siemensstrasse 12
63755 Alzenau
Germany

Tel. +49 6023 9640 60
Web www.carhs.de
E-Mail trainingcenter@carhs.de

Table of Contents

Virtual Testing-Based Assessment:
Why is CAE becoming even more important?

Virtual testing-based assessment refers to the systematic evaluation and certification of a product using data generated from virtual simulations instead of physical tests. It’s about using simulation results to determine whether a product fulfills legal or consumer requirements.

Today, virtual testing-based assessment is not yet an accepted standard; legal and consumer assessments are still almost entirely based on physical testing. However, there are compelling reasons to rapidly transition to virtual testing for future assessments.

Time-to-Market and Cost Efficiency:
Global market dynamics demand accelerated product development cycles that significantly reduce both time and cost for legal and consumer assessments – despite growing regulatory and safety requirements.

Life-Cycle Management and Over-the-Air (OTA) Updates:
Modern automobiles are defined by their software, which controls all vehicle functions – including safety-critical systems. As new functions are introduced during a vehicle’s life cycle, the need for updates and subsequent re-validation arises. Physical testing for each update would be cost-prohibitive; only virtual testing allows new functions and software patches to be validated efficiently before deployment via OTA updates.

CAE at the Core:
CAE is at the heart of virtual testing, and its role is rapidly expanding as the software-defined vehicle becomes a reality. Without CAE and virtual testing, the future of the automobile is unthinkable.

Your Guide: The New automotive CAECompanion
Whether you want to deepen your understanding of CAE and virtual testing, improve your simulation skills, or stay informed about the latest developments in the field, the 2025 automotive CAECompanion is your ultimate guide. Join us on this journey of exploration and discovery – and unlock the full potential of CAE and virtual testing in the future of the automotive industry.

Alzenau, April 2025

For the whole team at carhs.training

Constantin Hoffmann
Managing Director

In-house Seminars
Seminars at your site - efficient, flexible and customized

Are you looking for an individual and customized training for your employees?

Most of the seminars from our training program can also be booked as in-house seminars in English or German language. Whether on your company site or at another venue of your choice, the scale of our in-house seminars is tailored to your needs.

Your advantages

- You retain full cost control. We offer attractive fixed prices for our in-house seminars, depending on the number of participants and the related service.
- Even for a small number of participants you can save a lot of money compared to the individual booking of seminars. Additionally, there are no costs for travel and time of your employees.
- We respect your target dates as far as possible – also upon short notice in „urgent cases“.
- You benefit from our professional organization and the top-quality seminar manuals.
- Our lecturers answer your individual questions.
- Even if you are interested in very specific questions – we are looking for a qualified lecturer and develop the seminar.

Many of our customers have integrated our in-house seminars into their company's training program.

„At BMW we faced the challenge to train a large number of employees with different professional backgrounds as simulation engineers for crash and occupant safety. Based on their successful CAE Intensive Training program carhs.training developed an individual multi week training program for us. This training program combined theory, software and project training in an ideal manor. We were very pleased about the success and the professional handling of the project. We can recommend carhs.training to companies that have individual and complex training needs as a partner for the design and execution of the training.“

Dr. Wolf Bartelheimer
Manager Frontal Protection Small Cars
BMW AG

Take advantage of this offer, too! We will be pleased to prepare you an individual offer.

Contact person

Dr. Dirk Ulrich
Tel. +49 6023 9640 66
dirk.ulrich@carhs.de

References:

ACTS, AIT, ARRK, AUDI, Autoform, ARAI, AZOS, Bentley Motors, Bertrandt, BMW, Bosch, Brose, CATARC, Continental, CSI, Daimler, Dalphimetal, Delphi, Dura Automotive, EDAG, Faurecia, Ford, F.S. Fehrer Automotive, FEV, Global NCAP, Grammer, HAITEC, Honda, Hopium, Hyundai, IAV, IABG, IDIADA, IEE, JCI, IVECO, IVM, Key Safety Systems, Kistler, Kube, LEAR, Lotus, Magna, Mahindra & Mahindra, MAHLE, MESSRING, MGA, NEVS, Next.e.GO Mobile, Opel, Open Air Systems, PATAC, Porsche, PSW, SAIC, SMP, SMSC, SEAT, Siemens, StreetScooter, TAKATA, TASS, Tata, TECCON, TECOSIM, TTTech, TÜV Süd, Valeo, VIRTUAL VEHICLE, Vinfast, Visteon, Volkswagen, Webasto, ZF

Attractive prices

With reference to our regular seminar fees we offer attractive discounts on our in-house seminars:

1 Day Seminar	
Discount	for the
30%	5th - 8th participant
60%	9th - 12th participant
70%	13th - 16th participant
75%	17th - 20th participant
80%	from the 21st participant

2 Day Seminar	
Discount	for the
50%	5th - 8th participant
70%	9th - 12th participant
75%	13th - 16th participant
80%	17th - 20th participant
85%	from the 21st participant

Seminar Guide

Here you find the courses you need to get your job done!

Legend

- ▶ Seminar/Event that focusses on this topic
- ▶ Seminar/Event that deals with this topic (among others)

Durability & Fatigue

Crash & Safety

Materials

Car Bodies

NVH - Noise Vibration Harshness

CAE Methods & Tools

Additive Manufacturing

Haven't found what you need?
Get in touch with us!

☎ **+49 6023 9640 60**

Online Training - Safe, Convenient & Efficient

Driven by recent travel restrictions, online seminars have quickly become a highly attractive alternative to face-to-face seminars. This allows us to continue to offer our customers access to almost all of our events. As an attendee, you save time and travel expenses and have the opportunity to better integrate course attendance into your regular work. In case of individual online seminars we can adapt them to your specific needs in terms of time and content. In addition, we have expanded our seminar program with numerous open online seminars.

This is what customers of our online seminars say:

„In August 2020 we conducted an online training course on HV battery safety with a particular focus on crash safety[1]. With the COVID travel restrictions it was the only option available to us. And to be honest we expected that it would be a somewhat compromised course without the benefit of face to face contact, but the best that we could do in the circumstances.

The course well and truly exceeded expectations. *The content was excellent and Rainer is clearly a global expert in this field. Clear and compressive material, well organized and well presented. We were able to dive deeper on topics of particular interest whenever needed. An extra session was added also for this purpose. Technically the delivery of content in the online format was seamless. Several times this course has been mentioned as* ***the example of how useful training can be "when done right".***

In terms of logistics – ***an online course spread over a period of several days was absolutely ideal.*** *Engineers from several sites could attend easily. Engineers could maintain productivity in their normal work schedules without the downtime (or cost) associated with travel. In terms of cost, convenience and effectiveness – this is really the ideal way to run a training course for a large group.* ***In summary, the course was excellent and is likely now the model we will use for group training courses into the future.*** *With or without travel restrictions."*

Stewart Sheffield, Lead Technical Specialist - Vehicle Safety, VINFAST TRADING AND PRODUCTION LLC

[1] VINFAST conducted the seminar "Crash Safety of Hybrid- and Electric Vehicles" led by Rainer Justen in August 2020.
See details of this couse on page 162.

And here is what a trainer says about online seminars:

„Online seminars have the advantage that, as an alternative to a compact 2-day seminar, they can also be conducted in more individual sessions. These can also extend over a longer period, e.g. 1-2 weeks. The individual modules can be scheduled on the sidelines or completely outside of regular working hours. The scheduling can also be adapted more individually to the participants' wishes, as binding hotel and room bookings are no longer necessary. Travel expenses and travel times are also eliminated. Last but not least, ***concentration and thus learning success increase significantly with short learning intervals.****"*

Rainer Justen, Manager Vehicle Safety E-Mobility, Mercedes-Benz AG

Rainer Justen is our trainer for the seminar "Crash Safety of Hybrid- and Electric Vehicles".
See details of this couse on page 162.

To get an offer for an individual online seminar get in touch with

Dr. Dirk Ulrich
Tel. +49 6023 9640 66
dirk.ulrich@carhs.de

Seminars at carhs.training - Your Benefits

Free parking

The carhs TrainingCenter in Alzenau offers plenty of free and secure parking spaces for our course participants. You don't have to plan any time for searching for a parking space and can start your course in a relaxed way.

Free EV charging

You can use our charging station for electric and hybrid vehicles free of charge during your course attendance at the carhs TrainingCenter in Alzenau. Two 11 kW type-2 charging stations are available at your disposal.

Electronic seminar materials

You will receive the seminar documents from us as a PDF file for storage on your computer. You can also bring your computer with you to the course and work directly in the PDF file.

Fair cancellation policy

We know that sometimes something interferes. Therefore you can cancel your seminar registration free of charge until 4 weeks before the course and until 2 weeks before the course only a lump sum of 100 Euro will be charged. You can send a substitute participant at any time. So you can register early for your seminar of choice without any risk and benefit from the → early bird rates.

Early bird rates reduce your costs

Early registrations give us and the course participants planning security. We return the favour with a significantly lower early booking price for both seminars and conferences.

All-round catering during the seminar

You don't have to bring anything: During the seminar you will be provided with snacks, fresh fruit and drinks in the breaks and we invite you to lunch with all course participants and trainers - this is the opportunity to network.

Small group sizes for maximum learning success

Our courses take place in small group sizes to ensure optimal interaction with the trainers and between students.

And WiFi?

Of course, WiFi is also available free of charge at the carhs TrainingCenter in Alzenau. However, we recommend that you not be distracted while attending the seminar. But that is of course your choice.

On Site & Online

Most of our events and seminars are available both for on-site and online attendance. You can choose if you want to talk face to face with other attendees and trainers or if you want to take part from your office or even from your home.

automotive **CAE** GRAND CHALLENGE

May 19 – 20, 2026
Frankfurt / Hanau
Germany

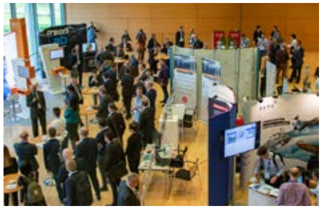

Computer simulation has become an indispensable tool in automotive development. Tremendous progress in software and computer technology makes it possible today to assess product and process performance before physical prototypes have been built. Despite of significant progress in simulation technology and impressive results in industrial application there remains a number of challenges which prevent a "100 % digital prototyping". We at carhs.training call these Grand Challenges.

Automotive CAE Grand Challenge offers a Platform for Dialogue

The automotive CAE Grand Challenge stimulates the exchange between users, scientists and software developers in order to solve these challenges.
Annually the current, critical challenges in automotive CAE are being identified through a survey among the simulation experts of the international automotive industry. In the conference one session is dedicated to each of the most critical challenges, the so-called Grand Challenges. In each session CAE experts from industry, research and software development will explain the importance of the individual Challenge for the virtual development process and talk about their efforts to solve the challenge.

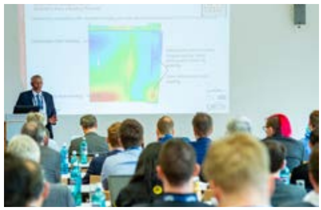

Automotive CAE Grand Challenges

Annually we determine the important current challenges of automotive CAE – the so-called "Grand Challenges" - through a survey among the CAE experts of the international automotive industry. These "Grand Challenges" will form the topics of the sessions of the following automotive CAE Grand Challenge conference:

Who should attend?

The conference intends bringing together industrial users, researchers and software developers to discuss these current, critical challenges of automotive CAE and to initiate collaboration between these groups to help overcoming the Grand Challenges of automotive CAE. The presentation program of the conference provides both experts and beginners valuable information for their daily work. The possibility to meet and exchange with all stakeholders of automotive CAE is a great opportunity. In the accompanying exhibition participants can receive additional information from leading companies of CAE.

Facts

May 19 – 20, 2026

Hanau, GERMANY & ONLINE

www.carhs.de/grandchallenge

ON SITE & ONLINE

Virtual Testing for Vehicle Safety Assessment in Consumer Protection Tests and Regulations

Course Description

Vehicle type approval based on virtual test procedures has been possible for some time for a limited number of specific regulations in the area of automotive safety. However, there have been very few actual applications so far. Currently the continually increasing demands of organizations in the area of consumer protection are leading to a noticeable acceleration in the development and acceptance of procedures for virtual testing as an alternative or supplement to physical testing. There are also corresponding efforts by legislators to directly implement virtual test procedures in new regulations for assessment of vehicle safety.
This course offers an introduction to virtual testing-based vehicle safety assessment for both consumer testing and regulatory requirements. The fundamental processes are discussed that ensure traceable data flow while safeguarding confidential data protection requirements that lead to acceptance of simulation results for certification, homologation or NCAP assessment. The current status of various virtual testing initiatives, their timelines and remaining obstacles will be explained. The validation of models and simulation tools for virtual assessments will be shown. For test procedures that can already be applied physically, approved corresponding virtual test methods are already available. However, for virtual assessments methods based on HBMs (human body models) other approaches must be developed. These will also be discussed in detail.

Course Objectives

Course participants will understand the current status of virtual testing for safety assessments in the automotive industry. They will be able to understand the relevant processes and learn the wording and terms to discuss with legislators and NCAP organizations. Additionally, they will understand what new requirements to expect in the future in the area of Virtual Testing based assessment for both NCAP and regulatory requirements.

Who should attend?

The course is intended for CAE managers and engineers, project and product managers at OEMs, suppliers and engineering service providers, as well as for individuals responsible for achieving vehicle safety requirements and relationships with authorities and testing organizations.

Course Contents

- Introduction to vehicle safety assessment based on virtual testing
  - Background, motivation, definitions of VT based testing procedures
  - Global overview, VT adoption timelines
  - Overview of EU research projects (e.g. IMVITER, OSCCAR, VIRTUAL)
  - Methods of model traceability
- Virtual Testing in consumer protection tests
  - Euro NCAP Virtual Testing: Developments and schedules (pedestrian protection CoHerent, occupant protection: Far-Side, Frontal impact, VT for evaluating active safety (crash avoidance)
  - C-NCAP and C-IASI Virtual Testing: current plans and status
  - IIHS plans to improve whiplash assessment through virtual testing
- Virtual Testing in legal requirements
  - Overview of virtual testing in legal regulations of vehicle safety
  - Example: UNECE Informal Working Group Deployable Pedestrian Protection Systems (DPPS)
  - Future plans and challenges of virtual testing in UNECE Informal Working Group Equitable Occupant Protection (EqOP)
- Human Models in Virtual Testing
  - Challenges and requirements to use Human Body Models (HBMs) for VT based assessment

Instructor

Dr.-Ing. Andre Eggers (German Federal Highway and Transport Research Institute (BASt))
is a researcher at BASt (German Federal Highway and Transport Research Institute) since 2006 working in the area of biomechanics, evaluation of dummies, human models and virtual testing. He studied mechanical engineering at the Technical University of Hamburg and Biomedical Engineering at Wayne State University. 2013 he completed his doctorate at the Technical University of Berlin. He contributed to several European research projects like IMVITER, THORAX, ASSESS, SENIORS and OSCCAR. He is representing BASt in Euro NCAP working groups related to injury criteria and virtual testing.

Facts

04.-05.06.2025	204/4490	Alzenau	2 Days	1.450,- EUR till 07.05.2025, thereafter 1.750,- EUR	
25.-26.11.2025	204/4489	Alzenau	2 Days	1.450,- EUR till 28.10.2025, thereafter 1.750,- EUR	
05.-10.03.2026	204/4628	Online	4 x 4 Hrs.	1.450,- EUR till 05.02.2026, thereafter 1.750,- EUR	

Latest info about this course

Engineering Seminar

Early Increase of Design Maturity of Restraint System Components in the Reduced Prototype Vehicle Development Process

Course Description

The number of hardware prototypes available for the development of restraint systems and restraint system components is declining steadily due to an increasing cost pressure in automotive development. In the project schedule the availability of hardware (restraint system components and / or vehicle environments) shifts to the late vehicle development phases. As a result, ensuring the required degree of maturity of restraint system components, in addition to the sole functional development of seat belts and airbag, necessitates new strategies and development paths.

In this seminar, current risks in the development of seat belts and airbags are addressed and ideas for the early increase of maturity are elucidated. This is done by explaining the link between milestones in the development schedule, the functional requirements of restraint system components, the development duration of restraint system components and the description of approaches for the creation of substitutes of vehicle environments in the early development process. In addition the project schedules of conventional vehicle development processes and prototype-reduced development processes of base line models and derivatives are shown. Interactions of the development of seat belts and airbags with surrounding components (e.g. trim parts) are also discussed.

Course Objectives

The course provides thoughts and ideas for a successful approach in the development of restraint systems within vehicle development processes in which only a small number of prototypes are available for verification and optimization of the systems.

Who should attend?

The seminar is aimed at engineers and project managers of restraint systems and restraint system components development, as well as heads of teams or departments in the field of passive safety, which want to gain, in addition to the pure functional development of restraint systems, an overview of the requirements of the prototype-reduced restraint system development with regard to achieving and ensuring the necessary degree of maturity of belts and airbags.

Course Contents

- Overview and differences of vehicle development schedules
  - Standard project schedule
  - Prototype-reduced development of lead series
  - Prototype-reduced development of derivatives
- Safety belts
  - Examples of requirements for safety belts
  - Prerequisites and timing for functional development
  - Timing for homologation and certification
  - Ideas / possibilities for creating vehicle environments
  - Interactions with surrounding components
- Airbags
  - Examples of requirements for airbags
  - Prerequisites and timing for functional development
  - Ideas / possibilities for creating vehicle environments
  - Interactions with surrounding components

Instructor

Sandro Hübner (EDAG Engineering GmbH) studied mechanical engineering at the University of Applied Sciences Schmalkalden. After completing his studies he worked as an engineer in the FEM laboratory of Schmalkalden University of Applied Sciences. From 2003 he worked as a CAE engineer for occupant safety at EASi Engineering GmbH. In 2006, he moved to EDAG Engineering GmbH as a CAE engineer for vehicle safety and has been project manager for vehicle safety and CAE since 2013.

Facts

20.-21.05.2025	166/4542	Online	2 x 4 Hrs.	890,- EUR till 22.04.2025, thereafter 1.090,- EUR
05.11.2025	166/4543	Alzenau	1 Day	890,- EUR till 08.10.2025, thereafter 1.090,- EUR

Latest info about this course

Engineering Seminar

Crashworthy and Lightweight Car Body Design

Course Description

In the development of a car body different - sometimes conflicting - design requirements have to be met. Depending on the intended drive unit, the fulfilling of the crash regulations considering the lightweight principles is a key task. Therefore, it is mandatory that designers have a good understanding of the crash behavior of mechanical structures. The combination of knowledge about mechanics and the ability to use modern design tools allows for an efficient development process without unnecessary design iterations.

Course Objectives

The objective of the seminar is to present new methods for crashworthy car body design. At the beginning of the course the mechanical phenomena of crash events will be discussed. Subsequently modern development methods (CAD design and crash simulation) will be treated. Thereafter modern implementations of safety design measures will be presented. Mathematical optimization of structural design - which is increasingly used in industry - will be covered at the end of the course.

Who should attend?

This 2 day course addresses designers, test and simulation engineers as well as project leaders and managers working in car body development and analysis.

Course Contents

- Mechanics of crash events
  - Accelerations during collisions
  - Structural loading during collisions
  - Examination of real crash events
  - Stability problems
  - Plasticity
- Lightweight principles for the car body design
  - Lightweight design rules
  - Car body design
  - CAE conform design
- Crash simulation
  - Finite Element modeling of a car body
  - Finite Element analysis with explicit methods
  - Possibilities and limitations
- Technical implementation of safety measures
  - Energy absorbing members
  - Car bodies
  - Electric car bodies
  - Safety systems
  - Pedestrian protection
  - Post crash
- Use of mathematical optimization procedures in real world applications
  - Approximation techniques
  - Optimization software & strategies
  - Shape and topology optimization

Instructor

Prof. Dr.-Ing. Axel Schumacher (University of Wuppertal) studied mechanical engineering at the universities of Duisburg and Aachen. He received his doctorate on structural optimization from the University of Siegen. Following research projects for Airbus were focused on the optimization of aircraft structures. Thereafter he worked in the CAE methods development department of Adam Opel AG as project leader for structural optimization. From 2003 - 2012 he was a professor at the University of Applied Sciences in Hamburg and taught structural design, passive safety and structural optimization. Since 2012 he has been professor at the University of Wuppertal, where he holds the chair for optimization of mechanical structures..

Facts

06.-07.05.2025	188/4527	Alzenau	2 Days	1.450,- EUR till 08.04.2025, thereafter 1.750,- EUR	
10.-13.11.2025	188/4528	Online	4 x 4 Hrs.	1.450,- EUR till 13.10.2025, thereafter 1.750,- EUR	

Design of Composite Structures

Course Description

Since the mass is one of the main factors influencing the fuel consumption of vehicles, increasing demands to reduce energy usage and CO2 emissions, force the automotive industry to consider the use of alternative designs and new materials. Composite materials have proven their potential to reduce the weight of structures in many applications (e.g. aerospace and motorsports). As composites have a special set-up and behave completely different than traditional materials, engineers must learn how to employ these materials to take advantage of their special characteristics in the design of vehicle structures. In the seminar real world examples are used to create a basic understanding of designing composite structures. Then the theoretical and practical foundations of composite design are explained.

Course Objectives

After participating in the seminar participants are able to design and develop composite structures. They understand the specific requirements of composite structures and the related design concepts. In the seminar special attention is directed to the concurrent consideration of loading, design and manufacturing related requirements. Accordingly, the different designs - integral, differential, fully laminated and sandwich - are addressed. The seminar also provides knowledge about preliminary design and FE analysis based on classical laminate theory.

Who should attend?

This seminar is especially designed for engineers and technicians who work in the development departments of automotive manufacturers, suppliers and engineering service providers and deal with the design and development of composite components.

Course Contents

- Introduction
- Elastic behavior of composite materials
- Failure of composite materials
- Mechanics of composite materials and structures
- Joining technologies for composites
- Design of composite structures
- Fatigue and strength of composites

Instructor

Dr.-techn. Roland Hinterhölzl (University of Applied Sciences Upper Austria) has been heading the Professorship Composite Materials and the study degree program "Lightweight Design and Composite Materials" at the University of Applied Sciences Upper Austria since 2016. From 2010 to 2016 he was head of the numerical simulation department of the Institute for Carbon Composites at the Technical University of Munich. The focus of his work is on process simulation and structural analysis for the automotive and aviation industries. Dr. Hinterhölzl received his doctorate in 2000 at the University of Innsbruck on the simulation of the time-dependent behavior of composite materials, after he had spent several months at the Department of Aerospace Engineering and Engineering Mechanics at the University of Texas at Austin and CRREL (USA). Subsequently, he developed innovative composite components at the aerospace supplier FACC AG and headed the structural analysis department.

Facts

17.-18.11.2025	135/4566	Alzenau	2 Days	1.450,- EUR till 20.10.2025, thereafter 1.750,- EUR

Latest info about this course

Engineering Seminar

Crash-Course Additive Manufacturing

Course Description

Additive manufacturing processes (3D printing) are becoming increasingly important. While this technology was initially used to produce prototypes and models, additive manufacturing processes are now also finding their way into series production. If you have not yet had the time to deal with this exciting technology, this seminar is the right place for you. In one day, you will gain a practical insight into the world of layer-by-layer manufacturing, learn about different processes and get some initial pointers as to what the next steps might be for your company.

Who should attend?

The seminar is aimed at specialists and managers from manufacturing companies who are considering the use of additive manufacturing processes and would like to gain an initial overview about the processes, possible applications and implementation models. However, it also addresses specialists from companies, such as production or design engineers, who already have initial experience in dealing with additive manufacturing processes and are considering their industrial use.

Course Contents

- Fundamentals of additive manufacturing processes
- Potentials and challenges
- Process chain of additive manufacturing
- Professional applications in industry and perspectives for future applications
- Business models and possibilities for implementation in the industrial environment

Instructor

Prof. Dr. Fabian Riß - Technical University of Applied Sciences Rosenheim has been responsible for the teaching and research area of lightweight construction and additive manufacturing processes at Rosenheim Technical University since 2019. Before joining the university, he held various positions in research and industry in the field of additive manufacturing along the entire process chain. Most recently he worked for the European space company Ariane Group as an expert in additive manufacturing technology.

Facts

01.09.2025	202/4450	Alzenau	1 Day	890,- EUR till 04.08.2025, thereafter 1.090,- EUR	

Implementation of Additive Manufacturing Processes in Corporate Environments

Course Description

You have already received a crash course in additive manufacturing and have already gained initial experience? Now where do you go from here? What are the next steps? But you don't really know what is suitable for you and your company? Then you should mark this seminar. During the event, you will receive information and practical knowledge on how you can introduce additive manufacturing processes in your company, what needs to be taken into account in the context of approvals and qualifications, and what business models may be possible in addition to component production.

Who should attend?

The seminar is aimed at company specialists, such as production or design engineers, who already have initial experience in dealing with additive manufacturing processes and are thinking about taking the step to industrial use.

Course Contents

- Process selection
- Component selection
- Strategy for implementation in the company

Instructor

Prof. Dr. Fabian Riß - Technical University of Applied Sciences Rosenheim has been responsible for the teaching and research area of lightweight construction and additive manufacturing processes at Rosenheim Technical University since 2019. Before joining the university, he held various positions in research and industry in the field of additive manufacturing along the entire process chain. Most recently he worked for the European space company Ariane Group as an expert in additive manufacturing technology.

Facts

02.-03.09.2025	203/4451	Alzenau	2 Days	1.450,- EUR till 05.08.2025, thereafter 1.750,- EUR	

Design for Additive Manufacturing

Course Description

Additive manufacturing technologies offer new opportunities for product design. However, contrary to popular belief, appropriate design guidelines also apply here, such as known for cutting processes. If these are used only to a limited extent or not at all, this can have a significant impact on process stability and manufacturing costs. In order to counteract this, this seminar imparts the necessary knowledge as well as the methods and aids to make the best possible use of the existing potential of additive manufacturing processes for the product.

Who should attend?

The seminar is aimed at designers and developers of companies who want to find out what a production-oriented design for additive manufacturing should look like. But production technicians are also welcome to attend the seminar, because it certainly helps to better understand the customer requirements.

Course Contents

- Product development for additive manufacturing
- Design recommendations
- Lightweight design and functional integration
- Bionics
- Functional design

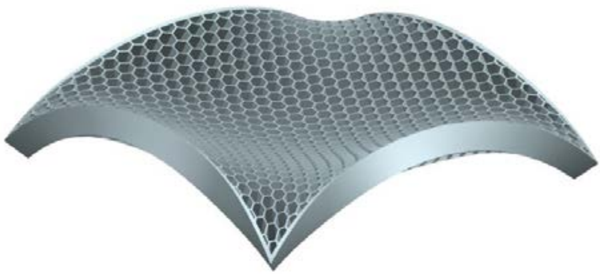

Instructor

Prof. Dr. Fabian Riß - Technical University of Applied Sciences Rosenheim has been responsible for the teaching and research area of lightweight construction and additive manufacturing processes at Rosenheim Technical University since 2019. Before joining the university, he held various positions in research and industry in the field of additive manufacturing along the entire process chain. Most recently he worked for the European space company Ariane Group as an expert in additive manufacturing technology.

Facts

04.-05.09.2025	191/4452	Alzenau	2 Days	1.450,- EUR till 07.08.2025, thereafter 1.750,- EUR

The Minimum Area Discrepancy Method (MADM): A New Tool to Correlate Force Displacement Responses and Improve CORA Accuracy

The development of computing capability has led to an ever-increasing use of numerical modelling in science and engineering. It is essential to validate any numerical model in order to ensure credibility of the results. Usually, the response of a model is compared to that of the represented system for a set of (physical) experimental test configurations. Physical testing rely on instrumentation most often in the form of accelerometers or force transducers which measure accelerations and forces respectively. These outputs can in turn be post-processed and compared against a set of engineering criteria. Readings from transducers as a function of time can be correlated using a "CORrelation and Analysis" (CORA) rating. Others, like force vs deflection responses, usually cannot be used in CORA due to the fact that functional values (Y-axis) are not unique with respect to X-axis values. As an example, a force reading of 1.5kN (Y-value) occurs for multiple displacement (X-axis) values, as illustrated in Figure 1.

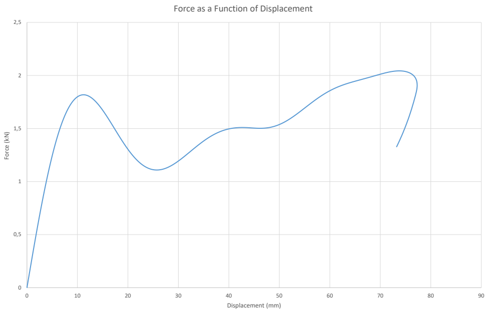

Figure 1: Typical Force vs Deflection curve

The MADM introduces a method to calculate a correlation coefficient for "typical" force-displacement signals in order to rate how close they are to test response. The MADM correlation criteria utilises an area method and aims to maximise area overlap; a complete (maximum) overlap indicates perfect correlation.

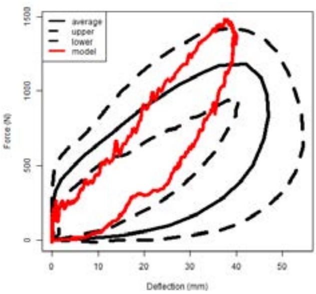

Figure 2: Typical CAE response against test corridors

Figure 2 contains an example of numerical analysis results (labelled "model") which can be overlaid on the test data represented by the "upper" "lower" and "average" test-corridors.

Based on Figure 2 three areas can be defined:

- A_{model}: area between the model and the average corridor.

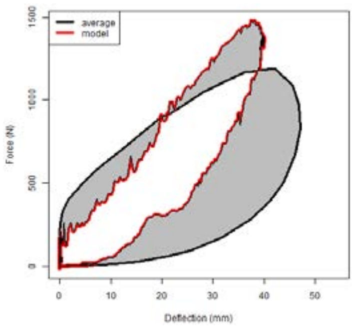

- A_{lower}: area between the lower corridor and the average corridor

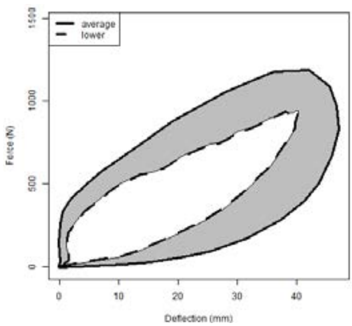

- A_{upper}: area between the upper corridor and the average corridor

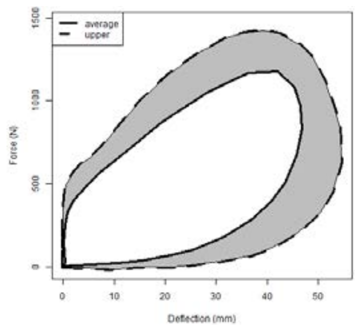

Using these definitions MADM can now be introduced using the following steps. Firstly, the ratio 'R' can be calculated as Equation 1:

$$R = \frac{A_{model}}{\frac{(A_{upper} + A_{lower})}{2}}$$

Equation 1: Calculation of R: area ratio overlap between the CAE model and the test corridors

'R' represents the ratio of (A_{model}) the area between the simulation and the average test response to the average area between the upper and lower test corridors. The ratio 'R' is normalised and referred to as the MADM correlation number which is subsequently adjusted to suit the desired degree of correlation, by changing the values of n and m in Equation 2.

$$MADM_{n,m} = \frac{1}{1 + nR^m}$$

Equation 2: MADM Generic Form

MADM has been tested in the development of a thorax spring model assembly [1] for which the springs characteristics were optimised for low impact and high impact energy (n=1 and m=2).

Low impact Energy:

$MADM_{1,2}$ (initial) = 0.79; $MADM_{1,2}$ (final) = 0.93

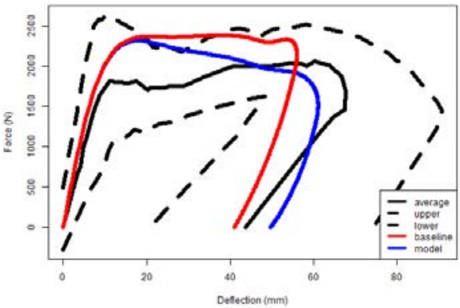

Figure 3: Low Impact Energy Scenario (Initial CAE response - RED; Optimised Response MADM - BLUE))

High Energy:

$MADM_{1,2}$ (initial) = 0.89; $MADM_{1,2}$ (final) = 0.92

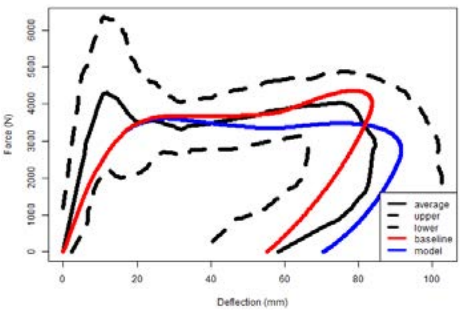

Figure 4: High Impact Energy Scenario (Initial CAE response - RED; Optimised Response MADM - BLUE))

MADM can also be employed following a CORA assessment rating to refine the correlation level, as illustrated in Figure 5. MADM can therefore be implemented as an add-on to current engineering processes. In this case, the authors suggest the combinations n=1 and m=2 or n=3 and m=2 to make MADM and the CORA ratings congruent.

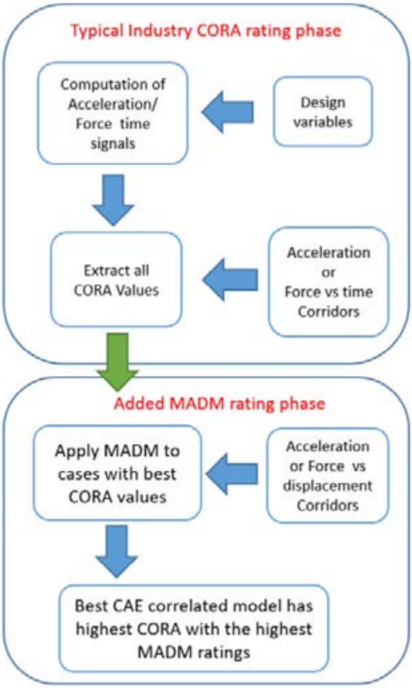

Figure 5: New framework linking CORA and MADM

The MADM Correlation tool is available:

- As a free Win64 download (GUI and Batch): figshare.com/authors/Christophe_Bastien/12013418
- In Oasys T/HIS: www.oasys-software.com/dyna/software/t-his/

References:

[1] Peres, J., Bastien, C., Christensen, J., & Asgharpour, Z. (2019). A Minimum Area Discrepancy Method (MADM) for Force Displacement Response Correlation. Computer Methods in Biomechanics and Biomedical Engineering, 22(11), 981-996.

[2] Bastien, C., Diederich, A., Christensen, J., & Ghaleb, S. (2021). Improving Correlation Accuracy of Crashworthiness Applications by Combining the CORA and MADM Methods. Proceedings of the Institution of Mechanical Engineers, Part D: Journal of Aut. Engineering.

Dr. Christophe Bastien & Dr. Jesper Christensen (Centre for Future Transport and Cities (CFTC), Coventry University, UK).

Comparison of Reduced Order Model Approaches for Electrical Machines

The Finite Element Method (FEM) is a versatile, accurate and widely accepted method to simulate and analyze different aspects of the electromagnetic performance of electrical machines. However, there are also many aspects for which it is more efficient or rather the only possible approach to solve them in a system simulator, where electric circuits and mechanical subsystems can be simulated as one coupled system. This requires a representation of the electrical machine, which behaves in all regards as the FEM model but with a considerable reduction in computational complexity.

The generic term for such a model is reduced order model or short ROM. In the following, several approaches to construct ROMs by means of FEA will be investigated and compared with each other in terms of accuracy, performance, convergence and energy conservation properties. The machine used for this comparison is a 3-phase interior permanent magnet synchronous machine (IPMSM) with a rated peak current $I_{rated} = 195$ A, a rated torque $T_{rated} = 340$ Nm and 4 pole pairs. All FEM results have been obtained in 2D using CST Studio Suite® [1] under the assumption of lossless operation. The system simulator used for the comparison was Dymola [2], a system simulator based on the Modelica language.

Approaches to obtain ROMs

All ROMs have in common that they map the input quantities, namely the currents and the rotor angle, onto the output quantities, magnetic flux linkages and torque. However, the mapping can be based either on phase quantities or alternatively on their respective quantities in the DQ-coordinate frame. The transformation between the two coordinate frames is given by the so called dq0-transformation [3]. No matter what coordinate frame is chosen, first a discretization of the input space (currents and rotor angle) is required to then capture the outputs (flux linkage and torque) as result of FEM analysis. After having simulated the discrete mapping between inputs and outputs, as next step a continuous mapping must be created for use in the system simulator.

In particular both a creation of lookup tables in phase- as well as in DQ-coordinate frame has been performed. To make the mapping continuous, a requirement for system simulation, the lookup tables, being phase- or DQ-ones, have been interpolated both linearly as well as with an Akima spline.

The grid for creating the lookup in terms of phase quantities was generated in the following way: The phase currents I_u and I_v have both been swept in 21 steps from $-1.2 \cdot I_{rated}$ to $1.2 \cdot I_{rated}$. Assuming a star connection of the 3 phases (see Fig. 1a) the 3rd phase current is given by $I_W = -(I_u + I_V)$. For each of the resulting $21 \cdot 21 = 421$ current vectors $(I_u, I_V, -(I_u + I_V))$ the rotor has been rotated in 0.75° steps from 0° to 90° such that 120 positon steps per electrical period have been performed. The FEM outputs for each grid point are $(\psi_u, \psi_V, \psi_W, T)$ where ψ_i stands for the flux linkage in the $_i$-phase and T for the torque. When creating an interpolated lookup table from this data it is advantageous to reduce the degree of freedom by the transition of the circuit representation shown in Fig. 1a to the one in Fig. 1b. This transition does not change both line voltages V_{ij} and phase currents I_i. Therefore the outer behavior of the machine is not altered at all but one should keep in mind that there is no longer any way to obtain the phase voltages.

The grid in DQ-coordinate frame is generated with the same 120 position steps as above but with 21 current steps both in I_d and I_q from $-1.2 \cdot I_{rated}$ to $1.2 \cdot I_{rated}$. The FEA analysis is driven with the phase currents obtained by transforming (I_d, I_q) into phase currents by the dq0 transformation. The output of the FEA is as above $(\psi_u, \psi_V, \psi_W, T)$ but instead of using this data as is, the same dq0-transformation which transforms the currents is used to transform the flux linkages as well. However, the 0-component of the flux linkage does not vanish since it is not perfect balanced anymore. But using the transition from Fig. 1, one can remove the impact of the 0-component and therefore the output data for the lookup is made of (ψ_d, ψ_q, T).

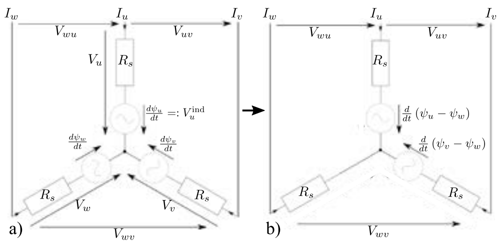

Figure 1: By the transition from a) to b) the number of degree of freedom is reduced by one. Therefore the number of operations inside the ROM is reduced.

To interpolate the lookup tables we have used NDTable from the SDF library shipped with Dymola. Linear and Akima spline interpolation used here are directly available in NDTable.

One additional approach for creating a machine's ROM is the one shipped with CST Studio Suite®. The grid calculated by FEM analysis is exactly the same as in the DQ-case described above. However, the idea is not to interpolate fluxes and torque independently but instead interpolating a vector-valued function $f(I_d, I_q, \theta) = (\psi_d, \psi_q, T)$ in such a way that energy-conservation is satisfied by construction. CST Studio Suite® encapsulates this type of ROM into a functional mockup unit (FMU) [4], which can be directly imported into Dymola.

Results

The schematic of the common test case for the different implementations of ROMs is shown in Fig. 2a. A speed profile (Fig. 2b) is applied on the shaft of the machine and a load resistance of 1Ω per phase is attached. Now the underlying ROM of the machine itself is replaced with ROMs of the different flavours described above.

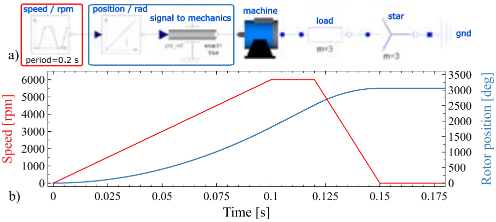

Figure 2: a) Schematic of the generator setup in the system simulator. The speed (red curve) is given and a load of 1Ω (load) is attached to each phase of the ROM based machine representation (machine).

The resulting torques and interlinked flux linkages $\psi_u - \psi_w \coloneqq \psi_{uw}$ are shown in Fig. 3. The reason to look at ψ_{uw} as a relevant quantity is justified by Fig. 1b which shows the electric part of the machines schematic implemented in all of the different ROM approaches as well as the FEM reference (solid red).

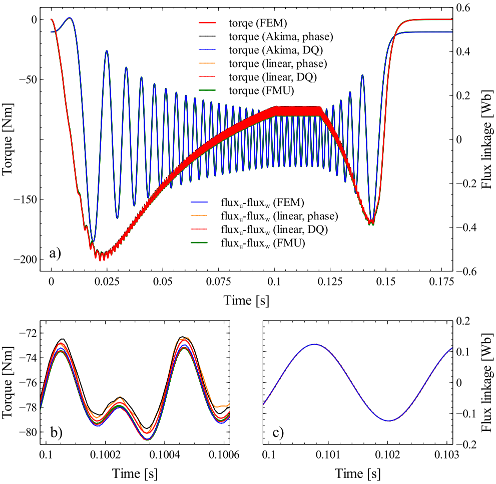

Figure 3: Torque and interlinked flux linkage calculated using the schematic shown in Fig. 2 with different ROM approaches. The plots b) and c) magnify a small cutout of the torque and flux linkage respectively.

One sees in Fig 3a, which shows the complete timeline, that all approaches yield results quite similar to each other. So all of them seem to work reasonable well. However, if one looks at the magnified cutout Fig. 3b and 3c for torque and ψ_{uw} respectively, one can observe small differences in magnitude (in the order of 0.7% with respect to the FEM result) and, especially in the case of the interpolations based on phase quantities (black and orange dashed-dotted curves), somewhat distorted curve shapes for the torque. The distortion is more pronounced in the case of linear interpolation as expected. However, when the interpolation is performed in the DQ-coordinate frame both linear and spline interpolation give rather similar torques. A difference in the compared flux linkage quantity ψ_{uw} can hardly been seen even when magnified.

Interesting is also a comparison of the execution times for the different ROM approaches.

Approach	abs. runtime [s]	rel. runtime [%]
Phase, linear	1.44	50
Phase, Akima	7.32	254
DQ, linear	0.814	28
DQ, Akima	5.61	195
FMU	2.88	100
FEM	14000	486111

All system analyses have been performed with the variable step size DASSL integration method (default method in Dymola) with an accuracy set to 10^{-8} and an output step size of 10 µs. The FEM analysis was performed with constant step size forward Euler method with the step size of 10 µs. Last but not least the various methods can be distinguished by their energy conserving behavior. To compare this the total energy given by

$$\int_0^t \left(P_{gap}(t') - P_m(t')\right) dt'$$

where

$$P_{gap} = I_u \cdot \frac{d\psi_{uw}}{dt} + I_v \cdot \frac{d\psi_{vw}}{dt}$$

is the instantaneous power in the magnetic field and $P_m = T \cdot \omega$ the mechanical power, is shown in Fig. 4. Energy conservation holds if (i) in the region of constant speed (green ellipse in Fig. 4) the average of total energy over a period stays constant and (ii) the total energy comes back to its initial value when the speed approaches 0. Looking at the results reveal that only the FMU approach and the FEM results are strictly energy conserving. All the flux, torque interpolation approaches in contrast violate this fundamental physical property in the order of 5 to 10%.

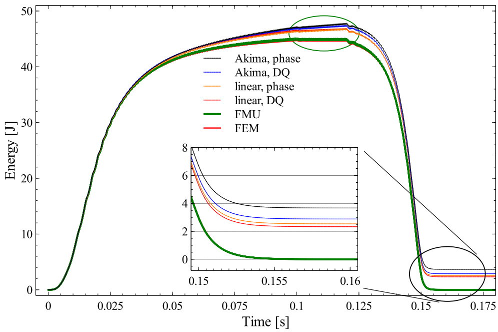

Figure 4: Total energy vs time in the machine simulated with the different ROM approaches. Energy is conserved if it returns to its initial value and remains constant in the region of constant energy (green ellipse).

Conclusion

Various approaches for ROM creation for PMSM's were described and compared with each other with regard to accuracy, execution speed and energy conservation. It was demonstrated that the violation of energy conservation resulting from look-up table based methods is not negligible even if the results show only small deviation compared with FEM. To fulfil energy conservation one has to incorporate this property in the interpolation of the vector-valued function $f(I_d I_q, \theta) = (\psi_d \psi_q, T)$.

References

[1] https://www.3ds.com/products-services/simulia/products/cst-studio-suite

[2] https://www.3ds.com/products-services/catia/products/dymola

[3] Gieras, J. F.: "Permanent Magnet Motor Technology", CRC Press, 2009

[4] https://fmi-standard.org/

CAE Wissen by courtesy of Christian Kremers, Adrian Scott, Nikolas Weber, SIMULIA, Dassault Systèmes.

Basics: Consistent Units

Background

Finite-Elemente-Programs require the usage of consistent unit systems. In structural mechanics the SI-Systems and the mm-t-s (Millimeter-Ton-Second) system have proved their worth.

What does consistent mean?

Derived units can be expressed in terms of fundamental units without conversion factors:

1 Force Unit = 1 Mass-Unit * 1 Acceleration-Unit

1 Acceleration-Unit = 1 Length-Unit / (1 Time-Unit)^2

1 Density-Unit = 1 Mass-Unit / (1 Length-Unit)^3

Mass	Length	Time	Force	Pressure/Stress	Energy
kg	**m**	**s**	**N**	**Pa**	**J**
kg	cm	s	1.0e-02 N	1.0e+02 Pa	1.0e-04 J
kg	cm	ms	1.0e+04 N	1.0e+08 Pa	1.0e+02 J
kg	cm	µs	1.0e+10 N	1.0e+14 Pa	1.0e+08 J
kg	mm	ms	kN	GPa	J
g	cm	s	dyne	dy/cm²	erg
g	cm	µs	1.0e+07 N	Mbar	1.0e+07 Ncm
g	mm	s	µN	Pa	nJ
g	mm	ms	N	MPa	mJ
ton	**mm**	**s**	**N**	**MPa**	**mJ**
lbf-s²/in	in	s	lbf	psi	lbf-in
kgf-s²/mm	mm	s	kgf	kgf/mm²	kgf-mm
kg	mm	s	mN	kPa	µJ
g	cm	ms	dN	1.0e+05 Pa	1.0e-01 J

Enabling Exploration and Analysis of Design Changes and Results over many Crash Simulations

Numerical simulations play an important role in the automotive product development process. Particularly in the CAE-based crashworthiness analysis process, the large number of design possibilities combined with increasing requirements and regulations for crash safety lead to large so-called development trees. These reflect the many undertaken design measures and corresponding simulation runs performed until given design criteria are met. A key challenge is to learn useful designs from a set of model changes and corresponding simulation results, for example to mitigate undesired deformations. The complex and diverse data to be studied suggests the use of AI approaches to handle the complexity of the evaluation. However, most existing machine learning methods are not directly applicable to the analysis of CAE data. On the one hand they require large amounts of training data, which are not available because simulations are computationally intensive, and on the other hand the data are high-dimensional, where the dimensionality is given by the size of the finite element meshes. We have developed approaches specifically adapted to CAE simulations that overcome these limitations. Specifically, we employ our own approaches to provide an overview of many simulations, in particular to analyse design changes that lead to similarities or exceptions in deformations and mesh functions, as well as their propagation over time. In addition to the simulation outputs, the design measures as input to the simulations are very heterogeneous, including changes in geometry, in material parameters, or in welds. We also address the challenge of representing measure information as features for machine learning algorithms. Together, our approaches can significantly improve the CAE-based product design process.

Laplace Beltrami shape feature approach

We investigate suitable similarity concepts to arrange the simulation results in an overview diagram, e.g., to reflect the different deformation modes. A dimensionality reduction approach based on the Laplace-Beltrami (LB) operator is used, which can be thought of as a „Fourier-decomposition for geometries”. This novel approach allows a clustering of many simulations based on their crash behavior using these "geometric Fourier-modes”.

In detail, the proposed approach [1] uses one reference surface shape. A discrete version of the LB operator on the reference mesh surface is computed. This operator is invariant under isometric transformations, which means that deformations of the surface over time or corresponding surfaces from other simulations that have essentially the same distance along the surface will result in the same surface operator. Now, the eigenvectors of the matrix representation of the discrete LB operator reflect invariant surface features that can be used to represent simulation results. Formally, for any mesh function f of a simulation result spectral coefficients α_j are computed, allowing to write f as a linear combination of eigenvectors ϕ_j:

$$f = \sum_{j=1}^{N} \alpha_j \phi_j \, , \alpha_j = \langle f, \phi_j \rangle$$

where N is the number of nodes. Note that usually only a few coefficients are needed to represent relevant variations, resulting in a dimensionality reduction. These coefficients have proved useful as low-dimensional coordinates to cluster, for example, deformation changes. The geometric features can be calculated for all components of interest, where a component consists of one or more parts defined in the FE-model.

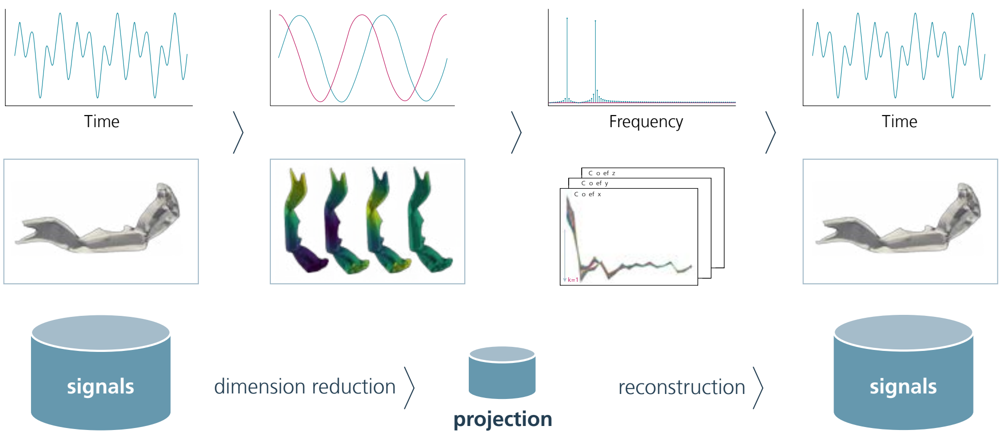

Figure 1: Schematic illustration of the “Fourier”-decomposition for geometries.

Representation of Model Changes

Design measures include changes in geometry, in material parameters, or in welds. For example a modification of the B-Pillar might include a geometrical change of a structural member, e.g., a cut or extension, which could require changes in the weld connections or of material thickness. These combined measures are called a semantic design measure. To appropriately deal with all these changes we have developed and implemented a corresponding structured digital representation. Ongoing work is to further extend the semantics of this representation, including components, and on making it available for filtering and searching (semantic) design measures.

Clustering in latent space

For visualization purposes the number of coefficients is limited to three. Using the geometric features, an optimization algorithm will select three coefficients per component and time step that show the best overall separation into clusters. A density based clustering algorithm is then applied to identify clusters, i.e., simulations that behave similarly, and outliers, i.e., simulations that behave significantly different. Furthermore, cluster representatives provide a quick overview of different general deformation modes or functional behavior.

Identify the simulations or components with the largest deviations

To further automate the process, an outlier score is computed per simulation. The outlier score is mainly based on the distance of the simulation from the cluster means, with respect to the deformations or other selected mesh functions. After an aggregation over all time steps and a normalization the outlier score allows a ranking of the simulations with respect to their deviations from the other analyzed simulations.

In addition to a score per simulation, we developed a component score that helps to find patterns in the deviations per component across all simulations and all time steps. The component score is based on the difference between the component of the considered outlier simulation and the reference simulation. Several suitable metrics and methods are available for distance calculation and aggregation. The aim of the analysis is to see if there are components in the group of outlier simulations that always show large deviations compared to the simulations within clusters.

Interactive Exploration

A 3D visualization of the coefficients of the shape features allows a seamless interactive and easy-to-use exploration and analysis of different components, together with selected mesh functions. It provides an intuitive overview of the similarities and exceptions in the simulation results with respect

Figure 2: Various simulations are arranged based on the proposed geometry-driven features. Simulations forming clusters and outliers can be easily examined using SimExplore's web-based application for interactive visualization.

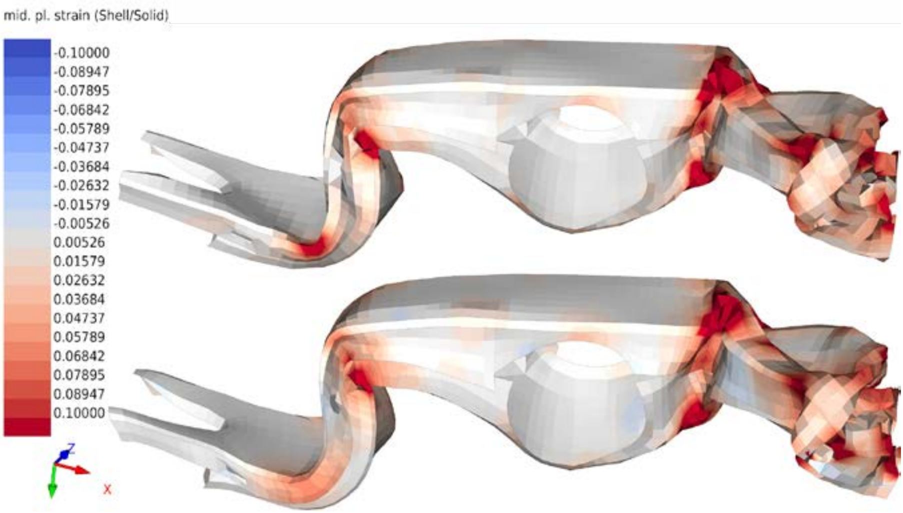

Figure 3: Fast reconstruction of a component using geometry-driven features. Above shows the component with original displacement and function (mid. Pl. strain (Shell/Solid)) at time t=13ms, below the same component with reconstructed displacement and function using first 100 eigenvectors is shown. Data from open FE-model of 1994 Chevrolet C2500 Pickup (US NCAP).

to the selected functions. Clusters and outliers can be easily investigated in this representation by accessing additional information. For example, by selecting in the visualization a point representing a simulation, one can quickly see the corresponding mesh function in a 3D viewer, or other relevant data from the selected simulation run. For outliers it will be possible to easily investigate connections to design measures, based on the introduced structured data representation.

Conclusion

The described LB-shape feature approach, as well as the clustering and scoring, are included in SCAI's SimExplore software tool. It supports CAE engineers in their simulation data analysis workflow by providing a browsable overview of many crash simulation results, e.g., in terms of clusters and outliers based on deformations and mesh functions. In particular, SimExplore provides a web-based application for interactive visualization.

The capabilities of the LB-shape feature approach have been investigated using industrial data, for example in [2], [3]. Therein, we examine simulation data from a robustness analysis of a vehicle front-end crash load case where the wall thicknesses of several selected components have been varied. The simulation results are analysed to identify similarities as well as outliers in the deformation behaviour.

Overall, this novel and patented LB-shape feature approach enables not only automatic classification of simulation behavior, but also rapid visualization and interactive analysis. SimExplore thus represents a breakthrough towards an automatic event detection for car crash simulations within the overall crashworthiness data analysis process.

References

[1] R. Iza-Teran and J. Garcke. A geometrical method for low-dimensional representations of simulations. SIAM/ASA Journal on Uncertainty Quantification, 7(2):472–496, 2019

[2] D. Steffes-lai, M. Pathare, and J. Garcke. Towards a Framework for Automatic Event Detection for Car Crash Simulations. In NAFEMS World Congress 2021, 2021

[3] J. Garcke, R. Iza-Teran, M. Pathare, P. Schwanitz, D. Steffes-lai. Identifying similarities and exceptions in deformations and mesh functions comparing many simulation results automatically. SIMVEC Kongress, Baden-Baden 2022, VDI Berichte 2407:277-288, ISBN: 978-3-18-092407-6, 2022

CAE Wissen by courtesy of Dr. Daniela Steffes-lai, Dr. Rodrigo Iza-Teran, Mandar Pathare, Prof. Dr. Jochen Garcke - Fraunhofer SCAI, Sankt Augustin, Germany.

Battery Testing and Multi-Physics Simulation Approaches

Introduction & Motivation

With respect to several standards and regulations, battery packs must pass certain tests related to their abuse behavior. Consequently, specific requirements have to be addressed and considered within the design process. Especially, the thermal propagation, induced by one cell and resulting in a catastrophic failure of the whole battery pack, must absolutely be mitigated or avoided. Hence, a deep understanding of the abuse behavior of the applied battery cells and their interaction in the battery pack are required for an efficient design and optimization of the battery system's overall safety behavior.

Methodology

In order to improve the battery pack's safety behavior in a time and cost-efficient way, a multi-physical simulation model of a battery cell capable to resemble the cell's behavior during thermal runaway is required. Considering the course of events in an abuse scenario, a battery cell may first be mechanically loaded. Once a specific amount of deformation happened, an internal short circuit may arise. Due to the high currents associated with the short circuit, the cell starts to heat up. Finally, exothermic reactions of the cell components start to take place once the corresponding temperature levels have been exceeded and the thermal runaway is in full progress. Hence, a predictive simulation model needs to be capable to describe the interaction between mechanical, electromagnetical and thermal events. In order to describe a thermal runaway and its initiation, the interaction between mechanical, electromagnetical and thermal events needs to be modelled. A sketch of the multi-physical nature of battery cells is exemplified in Figure 1.

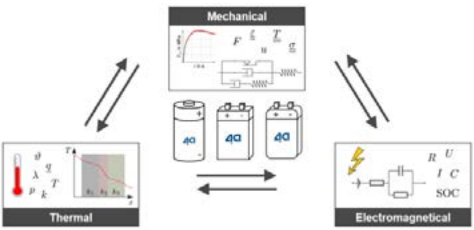

Figure 1: Sketch of the multi-physical nature of battery cells

First, specific characterization tests have to be conducted at single cell level, which serve as a basis for the generation of a corresponding multi-physical simulation model of the battery cell.

For this purpose, some terminologies and tests are described in the following, which are essential for modeling and parameter identification of the material models describing the cell behavior in terms of their thermal abuse characteristics.

C-rate:

The C-rate is a measure to describe the charge and discharge rate of a lithium-ion battery. In particular, it represents the rate at which a battery is charged or discharged in relation to its capacity.

It is defined as the ratio between the battery's charge or discharge current and its capacity. For example, a battery with a capacity of 1 ampere-hour (Ah) that is charged or discharged at a rate of 1 C requires a current of 1 ampere (A) to do so. A battery charged or discharged at a rate of 2 C, a current of 2 A, and so on.

It should be noted that the C-rate is a relative measure that depends on the capacity of the battery being charged or discharged. For example, a C-rate of 1 for a small battery corresponds to a much lower current than a C-rate of 1 for a larger battery.

The C-rate is an important factor for lithium-ion battery applications because exceeding the recommended C-rate can result in shortened battery life, reduced performance, and even safety hazards such as overheating and fires. Manufacturers typically specify a maximum charge and discharge C-rate for their batteries to avoid these problems.

For numerical modeling of the electrical behavior of a battery cell, C-rate tests are performed at a low charge/discharge rate (e.g. C/10 test) to enable the basic equation parameters of the material model to be determined. In the aforementioned C/10 test, a current is applied for charging and discharging that corresponds to a charge increase respectively decrease of 10% of the cell capacity per hour.

An example result of a C/10 with an appropriately applied current can be seen in Figure 2.

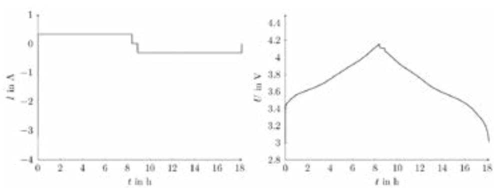

Figure 2: Result of a C/10 test in loading and unloading direction

4a HPPC-Test:

HPPC stands for Hybrid Pulse Power Characterization. It is a test commonly used to characterize the performance of lithium-ion batteries under realistic driving conditions in electric vehicles (EVs).

In HPPC testing, a series of current pulses of varying strength and duration are applied to the battery or cell while the voltage response is measured. This helps determine how the battery, or cell, responds to different power demands and how its internal resistance and other characteristics change over time.

The HPPC test is a valuable tool for evaluating the performance and durability of lithium-ion batteries under realistic operating conditions. It can help identify weak points and failure modes in battery cells and optimize battery management systems and control algorithms for electric vehicles.

For realistic modeling of electrical behavior using surrogate models, this test serves as a basis for meaningful model fitting. Figure 3 shows a schematic HPPC test profile.

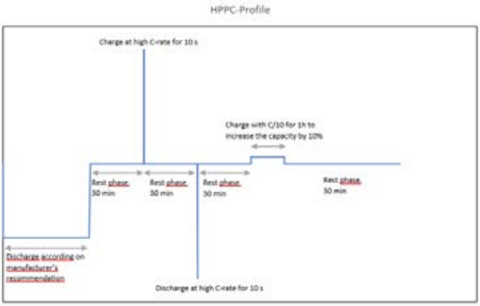

Figure 3: 4a HPPC-Test

By combining the two tests, i.e. C/10 and HPPC test, a more efficient electrical characterization capability is created. A corresponding load profile of such a 4a HPPC test is shown in Figure 4.

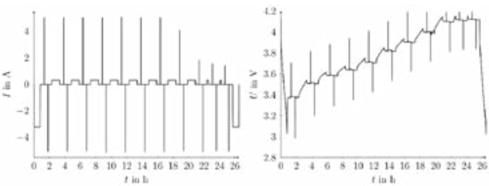

Figure 4: 4a HPPC test profile; Applied current and resulting voltage

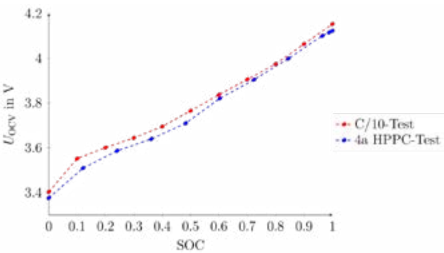

Figure 5: Comparison of the mean OCV(SoC) curves generated via a C/10 and a 4a HPPC test

As can be seen in Figure 5, the OCV(SoC) curves generated by the two tests (C/10 and 4a HPPC) show almost identical behavior.

Abuse testing:

As already noted, there are various misuse scenarios (electrically, thermally or mechanically triggered) that can lead to critical states in battery cells. These can occur individually or in combination. Ultimately, all scenarios lead to an internal short circuit and, depending on the respective state of charge of the battery or cell, to a thermal runaway.

This article takes a closer look at the thermal and mechanical abuse cases as examples.

In order to characterize the thermal abuse behavior (i.e. thermal runaway behavior), overheating experiments of battery cells can be performed. For example, a fully charged cylindrical cell (100% SoC) can be heated with constant power at a certain position, e.g. at the bottom surface. To track the thermal behavior, the battery cell must be sensorized with several thermocouples at different positions. This is accomplished by placing multiple thermocouples at different positions, e.g., on the heating element, on the surface of the cell, in the vent path above the cell, and further away in the enclosed air volume, to record the temperature evolution during the experiment.

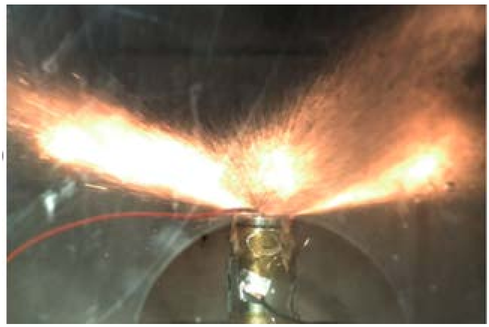

Figure 6: Single cell thermal runaway experiment

Figure 6 shows a snapshot of a fully sensorized battery cell during a single cell thermal runaway experiment.

This allows on the one hand to define boundary conditions for the simulation, and on the other hand to compare the temperature profile of the simulation with the measured data and to validate the model. Furthermore, the cell voltage is measured to detect the failure of the separator and the occurrence of an internal short circuit (ISC).

In the mechanical abuse scenario, a mechanical load is applied to a cell (e.g. a plane-crush load) and the behavior, i.e. the applied force, the time evolution, the displacement, the temperature and the battery voltage are detected. A representative illustration of the test setup is shown in Figure 7.

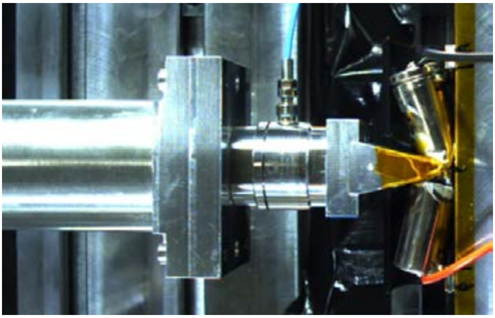

Figure 7: Plane crush test set-up

As in the thermal abuse case, the temperature measurement can be realized using thermocouples, whereby the data generated in this way are solely used as validation of the simulation results of the mechanical load case. The displacement detected in the experiment is applied as a boundary condition in the simulation of the mechanical abuse event and the resulting force, as well as temperature and stress response, are determined using the multi-physics simulation approach defined in Figure 1.

<u>Modeling of the electrothermal behavior of battery cells in terms of their thermal abuse behavior</u>

When discharging a lithium-ion battery, lithium ions migrate from the negative electrode to the positive electrode and back when charging. The corresponding electrical behavior as well as the heat generated by the current flow can be well described with equivalent circuit models, e.g. a Randels circuit model. These models are generally simple, but capable of capturing the battery dynamics for various operating conditions.

These equivalent models are electrical circuits consisting of an ideal voltage source, an internal resistor and n RC elements in parallel connection, where n is the order of the considered model. A schematic representation of the equivalent circuit is illustrated in Figure 8.

In this model, the RC circuits provide damping effects, which usually appear in the measured voltages. Here, the circuit elements are not constant, but a function of the state of charge, temperature, and current direction, i.e., OCV = OCV(SoC, T, I).

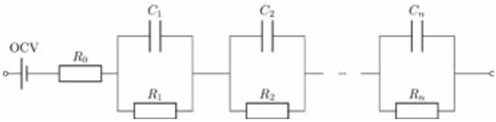

Figure 8: Randels circuit model of order n

By this definition, Randels equivalent circuit has a wide range of validity; however, the effort required to calibrate the model, depending on the number of parallel circuits, can quickly become very high. A good compromise between accuracy and parameter identification effort is offered by the first order equivalent circuit shown in Figure 9. This reduces the number of parameters to be identified to only 4, namely the open circuit voltage (OCV), 2 ohmic resistors (R_0,R_1) and a capacitance (C_1), assuming that the OCV source depends only on the SoC.

The numerical implementation of this Randels equivalent circuit is implemented e.g. in LS-Dyna. Here the realization of an electric field is achieved by coupling single Randels circuits ($R_{0,k}$, $R_{1,k}$, $C_{1,k}$) with the k-nodes of the collectors under the following assumptions:

- Equal potential difference and flow of the same current between the accounts of the collectors
- The circuit is interpreted as a series circuit
- Possibility of conversion of parameters by comparison with equivalent purely single Randels circuit

$$R_0 = k \cdot R_{0,k}, \quad R_1 = k \cdot R_{1,k}, \quad C_1 = \frac{C_{1,k}}{k}.$$

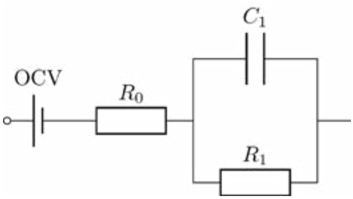

Figure 9: First order equivalent circuit model

Additionally, the reversible heat generation, i.e. the entropic heat coefficient, which is the change of the cell's OCV with respect to temperature, needs to be considered in the model and hence identified in an additional experiment. Together with the Joule heating term, the total heat generation of the cell can be described.

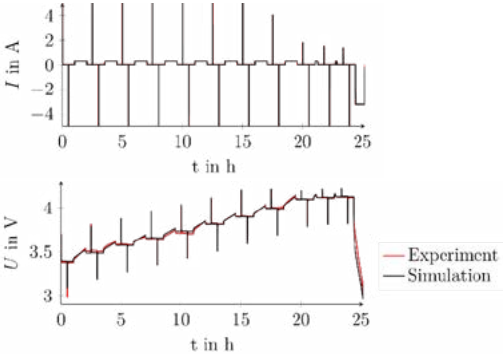

Figure 10: Comparison of test and simulation data of an 4a HPPC test

In order to finally model the electrothermal behavior of a battery cell, a standardized and automatable model generation methodology is introduced and applied. LS-Dyna offers a practicable method for solving the governing equations, using the so-called Batmac approach to model the multi-physical behavior of the cell. The model features a first order Randles circuit to describe the electrical behavior. For this purpose, the four unknown model parameters must be optimized using the aforementioned HPPC test data. As can be seen in Figure 10, the optimization results in a very good agreement between simulation and test, which creates the basis for multi-physical modeling.

Additionally, Joule heating and reversible heat generation are considered, and the electromagnetic solver is coupled with the thermal solver. The ISC is modelled using the keyword *EM_RANDLES_SHORT, wherein a user-defined function can be implemented to define the ISC initiation criterion and the associated short-circuit resistance. For the present study, ISC initiation is modelled to take place once a corresponding initiation temperature is reached. Finally, the exothermal reaction is modelled using the keyword *EM_RANDLES_EXOTHERMIC_REACTION. Again, a user-defined function can be programmed to define the initiation criterion and the additional heat source. In this study, initiation is defined to take place once a specific temperature is exceeded. The heat generation is described by a generalized Arrhenius function and takes place until a specified maximum amount of heat has been generated.

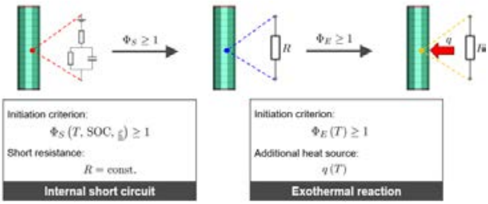

Figure 11: Modelling approach of the ISC and the exothermal reaction within the Batmac model in LS-Dyna

<u>Mechanical modelling of battery cells</u>

For modeling the mechanical behavior of battery cells, LS-Dyna with its available material and damage models provides a sound basis for a realistic numerical representation of the actual behavior. In this article, mechanical modeling focuses on the behavior of a cylindrical 18650 cell.

In the recent past, different strategies for mechanical modeling have been established. On the one hand, there are detailed approaches, which are specifically based on the layer structure of a battery cell, on the other hand, partially homogenized approaches are used, which do not resolve the layer structure of the anode-separator-cathode layers in detail, but consider it as a homogenized material. Both approaches have advantages and disadvantages, detailed models have the disadvantage of a considerably longer simulation time, whereas the layer structure provides a detailed resolution of the mechanical behavior. With the homogenized modeling approaches, this detailed representation is not obtained, but has considerably shorter simulation times and in the overall system of the battery cell, a similarly representative overall behavior of the cell is obtained as is the case with the detailed models. The model considered in this article therefore refers to the homogenized approach, which is more common in practice.

For a homogenized approach, the jelly roll can be considered as the homogenized part and the shell casing as the shell placed around the jelly roll. It is recommended to model the jelly roll using solid elements and the shell casing using shell elements.

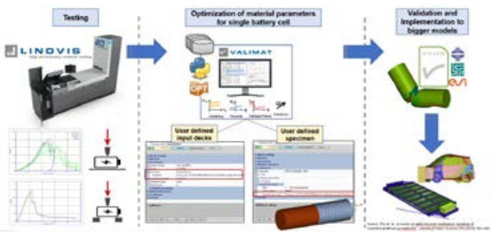

Figure 12: Automated modelling approach for mechanical load cases of battery cells

Since the shell casing consists of either aluminum or steel, modeling with the LS-Dyna material model *MAT_PIECEWISE_LINEAR_PLASTICITY is the most practical approach. There are several models that can be applied to model the jelly roll, but the most practical solutions are the LS-Dyna models *MAT_CRUSHABLE_FOAM, *MAT_MODIFIED_CRUSHABLE_FOAM as well as *MAT_MODIFIED_HONEYCOMB, whereas the model *MAT_CRUSHABLE_FOAM was used in the illustrated example. The behavior of battery cells in compression test, especially for pouch cells, exhibits a concave shaped stress-strain curve, which is characteristic for compressible foams with low plateau stress. Moreover, this model offers the possibility to define different properties for tension and compression. In tension, it provides an elastic response with a cut-off limit for the tensile strength.

Considering an additional failure model, e.g. LS-Dyna model *MAT_ADD_EROSION, it is also possible to account for the damage during the mechanical load.

Based on the experimental data and a reverse engineering approach (more details can be found in the section "Material Parameter Identification - Reverse Engineering"), simulation models for single cells can be generated using the procedure schematically shown in Figure 11.

Validation results and Discussion

To prove the practicality of the resulting models, some experiments are shown as examples.

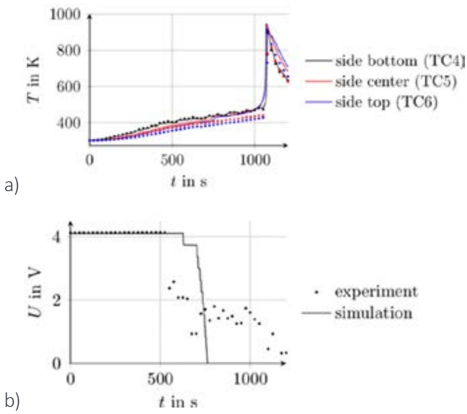

Figure 13: Electrothermal simulation results compared to experimental data; a) Temperature development over time; b) Voltage drop due to internal short

For both the electrothermal, Figure 13, and mechanical simulations, Figure 14, it is clearly evident that the simulation approaches show good agreement between the experiment and the simulation and reflect the battery behavior realistically.

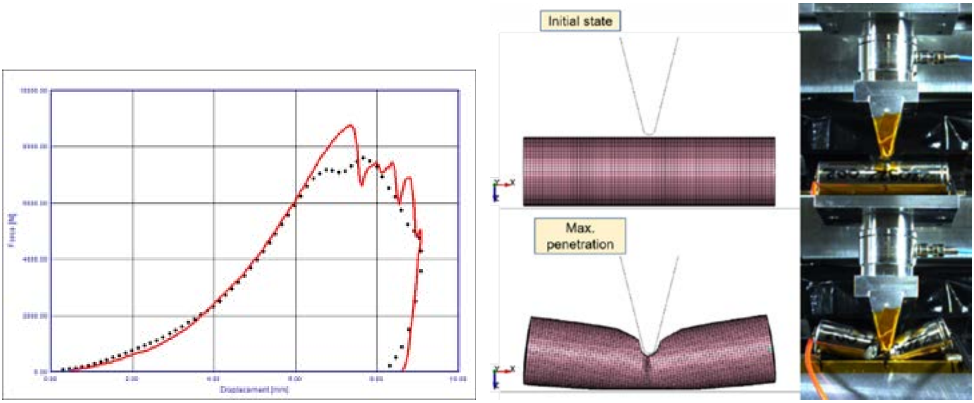

Figure 14: Mechanical simulation results (solid line) compared to the experimental data (dotted line)

CAE Wissen by courtesy of Christoph Schober - 4a engineering GmbH

Filling Simulation of Hydrogen Tanks

Gaseous storage

Hydrogen is often stored in gaseous form at pressures between 200 and 900 bar. One speaks of CGH2 (compressed gaseous hydrogen) in this context.

The following tank systems are used:

- Type 1: Steel tank
- Type 2: Liner (inner container) made of metal, partially surrounded by carbon fibre winding
- Type 3: Metal liner, completely surrounded by carbon fibre winding
- Type 4: Plastic liner, completely surrounded by carbon fibre winding

Type 1 is cheap, but too heavy for mobile use. This is why mainly type 3 and type 4 tanks are used in the automotive sector.

Inside, the tanks are often coated with plastic, which limits the locally tolerable temperatures of the tank to approx. 80 °C.

The tank should be filled in as short a time as possible (high pressure drop between the high-pressure intermediate storage tank and the tank system), and neither the maximum permissible gas temperature nor the maximum permissible tank pressure must be exceeded.

Figure 1: Hydrogen tank truck

Liquid storage

The storage of liquid hydrogen in cryogenic tanks is not the subject of this article.

Refuelling

The simulation of the filling process of a hydrogen tank as a zero-dimensional model is roughly possible via the solution of corresponding differential equations and is suitable for estimating the maximum occurring average temperatures in the tank as well as the filling times. According to [1], a comparison between experiment and calculation shows that the modelling of the heat transfer into the tank wall is absolutely necessary in order to achieve meaningful results. In contrast, the pressure and temperature decrease in the high-pressure bundle during refuelling has only a minor influence and can be neglected. The modelling of the real gas behaviour has a significant influence because of the pressure dependence. The differences between perfect and ideal gas behaviour are not significant due to the small temperature variations. Essential for the quality of the analytical calculation is the formulation of the heat transfer, which is dependent on the velocity during the inflow process.

Local effects cannot be resolved by a zero-dimensional model, of course. During refuelling, the gas flows in via a pipe with high flow velocities. If the jet hits the tank wall, an increased dynamic pressure temperature is created. This local temperature in the wall is limited.

Optimisation potential

The local peak temperature can be optimised and limited to a permissible value by a correspondingly clever choice of the inflow angle. This can increase the inflowing mass flow and reduce the refuelling time. However, transient CFD models are required for optimisation under the above aspects.

3D simulation

The 3D calculation of refuelling processes by Merkle CAE Solutions is carried out with the STAR-CCM+ software as a transient simulation assuming a turbulent flow (k-ε-model) with hydrogen as a compressible fluid with real gas properties (Redlich-Kwong).

The following assumptions are made:

The filling of a tank with hydrogen is carried out using an exemplary example with a constant supply pressure of 350 bar at 20 °C for the entire duration of the simulation.

To avoid instabilities at the beginning of the simulation, the supply pressure is numerically brought to the target value of 350 bar within about half a second. For the 3D simulation, an adaptive time step method is used, which determines the respective current time step width in the interval [10e-7 s; 10e-2 s] depending on the convective CFL number occurring in the flow. The target value for the CFL number should be about 100 on average and may reach a maximum value of

1000. This Courant-Friedrichs-Lewy number (CFL number or Courant number) is used in numerical flow simulation for the discretisation of time-dependent partial differential equations. It indicates the maximum number of cells by which a quantity under consideration moves per time step:

$$c = u\,\Delta t / \Delta x$$

Were c is the Courant number, u the velocity, Δt the discrete time step and Δx the discrete place step. This is motivated by the CFL condition, which states that explicit Euler methods can only be stable for $c < 1$. However, this would mean very small time steps, which result in very high computing times.

Since the flow velocities are very high and the model must not be too coarse, this limit can therefore generally not be observed for economic reasons (computing time).

However, Star CCM+ has smoothing procedures that enable a stable solution with comparatively high CFL numbers. The decisive factor is always the convergence behaviour of the simulation.

At the beginning of the simulation, when the supply pressure is still low, the time step size is approx. 1.5e-3 s and then decreases rapidly. As the supply pressure approaches 350 bar, the time increment decreases due to the high velocities in the system and finally approaches an almost constant value of about 8e-6 s.

With this small time step size, a complete simulation of the filling process on a smaller cluster would take about 6 months!

Due to the high time required for calculation, the complete filling process cannot be simulated in a practicable response time.

However, the simulation results suggest that pressure rise, mass flow, etc. are constant during most of the filling process. From this, corresponding filling times can be analytically derived by extrapolation.

Let's now take a closer look at the individual effects during filling:

The expanding gas cools down strongly immediately after leaving the filling tube. The local temperature here reaches temperatures of -240 °C at the beginning of the simulation.

Due to the compression of the gas, the gas temperature in the bottle increases over time. After 1.5 seconds, the gas temperature averaged over the bottle volume is about 150 °C and remains constant thereafter.

The effects relevant for optimisation occur in the first few seconds. The inlet angle in particular is crucial for minimising temperature peaks on the inner wall of the tank.

The optimisation goal is to keep the heat transfer coefficient between the gas jet and the inner tank wall as uniform as possible. Here, it is already apparent in comparison to the analytical solution, which assumes a value for the inner wall, that the local fluctuations are considerable.

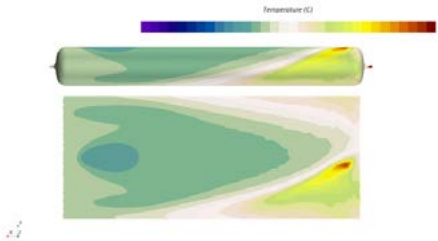

Figure 2: Temperature distribution of gas Inlet angle 1

Figure 2 shows the temperature distribution at the beginning of the filling process in the gas near the wall with a poorly selected inflow angle of the filling pipe.

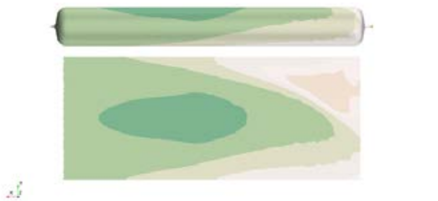

Figrue 3: Temperature distribution of gas Inlet angle 2

Figure 3 shows the temperature distribution at the beginning of the filling process in the gas with optimised inflow conditions at the same time and with the same mass flow. The locally occurring temperature peaks can obviously be avoided.

Summary

The results show that 3D CFD simulations are capable of optimising the filling of hydrogen tanks with reasonable effort. For this, however, one must limit oneself to the relevant time periods, as the calculation times explode very quickly. Comparisons with calculations over the entire period confirm the correctness of the assumptions made.

Thus, a delicate touch is required when networking the tanks and setting the solvers in order to keep optimisations within economic limits.

The optimum inflow angle of the feed pipe is strongly dependent on the tank geometry and can be determined with the help of simulation by evaluating the conditions at the beginning of the fuelling condition.

CAE Wissen by courtesy of Stefan Merkle, Merkle CAE Solutions GmbH

Distortion Management in Multi-stage Welded Assemblies

The prevention of shape deviations and material changes due to welding is a challenging issue, which often leads to difficulties to solve in practice. With welding simulation it is possible to calculate welding distortion, residual stresses and the microstructure changes in advance. Welding assembly often takes place in several stages. For multi-stage weld assemblies, the deformations from previous sub-assemblies must also be taken into account in the simulation. This extends the welding simulation to a manufacturing simulation. The FabWeld software was developed by Dr. Loose GmbH to efficiently create simulation models for multi-stage assembly.

In welded constructions, several questions arise that can be answered by simulation. Distortion management is about adjusting the welding distortion so that the geometry of the finished structure is within required tolerances. Simulation allows the analysis and design of manufacturing at an early stage of the design planning of components and assemblies. This makes it possible to identify manufacturing challenges at an early stage and to plan and implement necessary improvement measures in good time.

The goal is to save resources, especially raw materials, personnel, time and thus costs. This is achieved by the simulation, because the production can start error-free without time loss and run-in loops.

Validation of weld structure simulation

Welding structure simulation as a special application of the finite element method considers the effects from welding on the entire component. The input variable is the heat input from the welding heat source. This is applied in the form of a so-called equivalent heat source. This means that any fusion welding process can be modeled, regardless of how the fusion heat is generated. Of course, all boundary conditions must be taken into account in the model. This includes the clamping device, heat dissipation through clamping or cooling jaws and tacking.

Results from the weld structure simulation include geometry change due to welding, weld distortion, residual stresses and plastic strains, and if the microstructure transformation calculation is included, hardness, microstructure state after welding and the resulting changing yield strength.

Goldak Technologies Inc, Dr. Loose GmbH and TIME - Technology Institute for Metal & Engineering have demonstrated the predictive accuracy of weld structure simulation in a joint research project using a welded orthotropic plate, 1200 mm x 600 mm, two longitudinal stiffeners, 3 transverse stiffeners.

Deformation normal to the plate were measured with cable wire sensors. At the same locations, the vertical distortion from the simulation was evaluated. Figure 1 shows an example of the result of the validation test on displacement cable wire sensor 4. The graph compares the vertical deformations measured with cable wire sensor with the calculated vertical deformations. The vertical distortion is calculated correctly during the entire welding process. This proves that the applied calculation method of transient weld structure simulation is able to accurately reproduce the deformation behavior during the entire welding process. This finding is new, as previously only final results, i.e. the state after welding and cooling, were used for validation. In order to fully use weld structure simulation to analyze welding, the simulation results must also be accurate throughout the process. For example, this comes into play when the gap formations during welding are to be investigated in order to check the clamping or tacking concept.

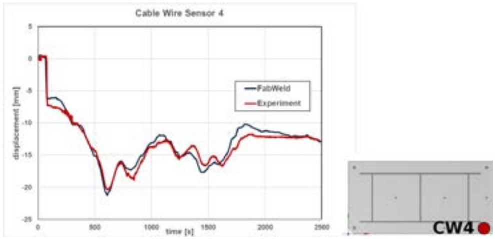

Figure 1: Validation result. Calculated deformation vs. measured deformation.

Simulation-based distortion optimization using the example of a battery tray

A battery tray for electromobility is manufactured from extruded aluminum profiles. A GMA cold wire process is used. Assembly takes place at three stations with a substation:

Station 1: Assembly of the base plate
Substation 1.1: Subassembly of bushings to outer cross members
Station 2: Assembly of base plate with outer cross members
Station 3: Assembly of inner cross members

In order to obtain accurate results when simulating the welded assembly, the clamping process with the resulting distortions must be mapped correctly. If individual components or subassemblies already deviate from the nominal geometry, clamping distortion will occur when they are clamped in the fixture. Welding generates the thermal distortion. When the clamping forces are released during unclamping, unclamping distortion occurs, which represents springback. All distortion components together result in the distortion. The clamping process must be mapped realistically in the simulation in order to achieve exact calculation results.

The simulation of the assembly requires a multi-stage simulation. In the simulation, as in reality, components or subassemblies are added, clamped and welded from manufacturing station to manufacturing station.

Assembly simulation can be used to analyze whether critical gaps occur during production. When the bottom profiles of the battery tray example are welded, a gap is formed towards the end between the center profile and the profile adjacent to it. The gap forms in both the vertical and lateral directions (Fig. 2). The vertical gap can be significantly reduced by optimizing the clamp position.

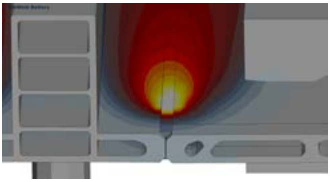
Figure 2: Gap formation during welding of the assembly

From the multi-stage assembly simulation, the station where the greatest distortion occurs can first be determined. In our example, this is station 1 with the welding of the floor profiles. The station where the largest warpage occurs is also the station where the compensation measures are most effective. The distortion caused by the warping of the slab is explained by the eccentricity between the center profile gravity line and the longitudinal welds. The improvement in variant 2 is due to the fact that the longitudinal welds are now arranged symmetrically to the center line of gravity. The improvement in station 1 has a direct effect on the total distortion. Fig. 3 shows the vertical distortion after complete cooling for variant 1 with unsplit center profile and Fig. 4 for variant 2 with split center profile.

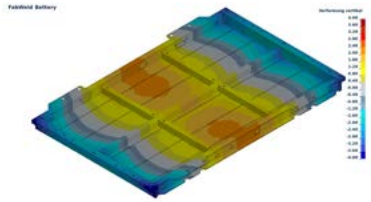
Figure 3: Variant 1, final vertical distortion

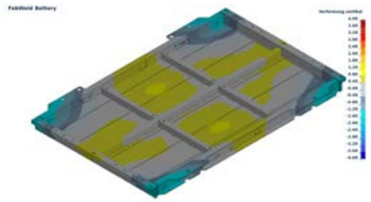
Figure 4: Optimization of variant 2, final vertical distortion

This example clearly shows how profitably assembly simulation can be used in the design phase. If the welding distortion is determined precisely at this early stage, it is possible to minimize welding distortion efficiently with geometry changes that do not require a great deal of effort.

CAE Wissen by courtesy of Dr.-Ing. Tobias Loose, Dr. Loose GmbH, Walzbachtal, Germany, loose@dr-loose-gmbh.de, www.dr-loose-gmbh.de / www.fabweld.de

Latest info about this course

Engineering Seminar

Pedestrian Protection - Development Strategies

Course Description

Euro NCAP annually adjusts details in its pedestrian rating protocols and even U.S. NCAP plans to introduce a pedestrian protection assessment.

Stricter injury criteria, modified testing areas and a new legform impactor require the thorough knowledge of the requirements and a strict implementation of the requirements in the development process.

In the introduction the seminar informs about the different impactors that are used for pedestrian safety testing. Thereafter the various requirements (regulations and consumer tests) are explained and compared.

The focus of the seminar is on the development strategy: Which decisions have to be taken in which development phase? What are the tasks and priorities of the person in charge of pedestrian protection? As a background, ideas and approaches towards the design of a vehicle front end in order to meet the pedestrian protection requirements are discussed. In addition to that, the seminar explains how the function of active bonnets can be proven by means of numerical simulation. This includes both, the pedestrian detection that need to be proven with various impactors or human models, as well as the proof that the bonnet is fully deployed at the time of impact.

Who should attend?

The seminar is intended for development, project or simulation engineers working in the field of vehicle safety, dealing with the design of motor vehicles with regard to pedestrian protection.

Course Contents

- Introduction with an overview of current requirements regarding pedestrian protection
  - Legal requirements (EU, UN Regulations, Japan, GTR)
  - Consumer tests (e.g. Euro NCAP, U.S. NCAP, JNCAP, KNCAP)
- Presentation and discussion of the design and application of the impactors
  - Leg impactors (Flex PLI, Upper Legform, aPLI)
  - Head impactors (Child head, Adult head)
- Methods in numerical simulation, testing and system development
- Requirements on the design of vehicle front ends for pedestrian protection
- Development strategy
  - Interaction between simulation and testing
  - Integration in the vehicle development process
- Solutions to fulfill the requirements
  - Passive solutions
  - Active solutions (active bonnets, airbags)

Instructor

Maren Finck (carhs.training gmbh) is a Project Manager at carhs.training gmbh. From 2008 - 2015 she worked at EDAG as a project manager responsible for vehicle safety. Previously, she worked several years at carhs GmbH and TECOSIM as an analysis engineer with a focus on pedestrian safety and biomechanics.

Facts

05.-07.08.2025	152/4546	Online	3 x 4 Hrs.	1.450,- EUR till 08.07.2025, thereafter 1.750,- EUR	English
03.-04.11.2025	152/4547	Alzenau	2 Days	1.450,- EUR till 06.10.2025, thereafter 1.750,- EUR	German

Functional Development: Pedestrian Protection - Lower Leg Impact

Requirements/Critical Target Values:

- UN R127:

  Impactor: Flex PLI Legform Impactor
  Test Conditions: 40 km/h (11.1 m/s), 0°, 75 mm over ground
  Criteria:

Tibia Bending Moment	< 340 Nm (up to 264 mm: 380 Nm)
MCL Elongation	< 22 mm
ACL/PCL Elongation	< 13 mm

- Euro NCAP

  Impactor: aPLI
  Test Conditions: 40 km/h (11.1 m/s), 0°, 25 mm over ground
  Criteria:

Score	maximum Score	0 Points
Femur Bending Moment	< 390 Nm	≥ 440 Nm
Tibia Bending Moment	< 275 Nm	≥ 320 Nm
MCL Elongation	< 27 mm	≥ 32 mm

Procedures:

- Use of full vehicle models (impact area: detailed models of all components; motor package can be rigid)
- High detailing for bumper, radiator, grill, optional accessories (head light cleaning system, parking sensors etc.)
- Proper material characterization for plastic parts is required incl. failure definition
- Connection modeling is highly significant (clips, sliding components)
- Use of validated impactor model
- Typical simulation duration: 40 ms (up tp complete rebound → legform impactor completely separated from vehicle)

Critical Modeling Parameters:

- Strain rate dependency of materials in the impact area
- Details of spatial discretization

Evaluation Criteria:

- Femur Bending Moment
- Tibia Bending Moment
- MCL Elongation
- For the optimization: Plot the above criteria vs. displacement to identify jamming

Main Influencing Factors:

- Geometry of vehicle front (impact points, impact behavior)
- Material stiffness at impact point (potential for optimization)
- Stiffness of geometrical package
- Clearance between outer bumper shell and bumper beam (minimum 80 mm, filled with energy-absorbing foam or deformation elements)
- No jamming elements (e.g. parking sensors) should be placed directly in front of the bumper beam
- Homogeneous support of the impactor along the full vehicle width is required.
- Sharp stiffness gradient should be avoided.

Functional Development: Pedestrian Protection - Head Impact

Requirements/Critical Target Values:

- UN R127.02 (127.03; 7 July 2024 new types, 7 July 2026 new registrations):

  Impactors: 3.5 kg & 4.5 kg Headform Impactor
  Test Conditions & Criteria:

Child/Small Adult Adult	3.5 kg / 35 km/h (9.7 m/s) / 50° BLE/WAD 1000 - WAD 1700 / Bonnet rear edge **2024:** BLE/WAD 1000 - WAD 1700 4.5 kg / 35 km/h / 65° WAD 1700 - Bonnet rear edge/WAD 2100 **2024:** WAD 1700 - WAD 2500 / Windscreen rear edge - 130 mm, Monitoring for the cowl area.
HIC_{15}	< 1000 (1/2 of the child head impact area AND 2/3 of the total impact area) <1700 (remaining area) **2024:** < 1000 for 2/3, HIC < 1700 for 1/3 of the entire test area (but at least 2/3 < 1000 on bonnet) Until 2028, repetition of windscreen tests is allowed, if HIC value is untypically high due to unexpected breaking behavior of the glass.

- Euro NCAP:

  Impactors: 3.5 kg & 4.5 kg Headform Impactor
  Test Conditions & Criteria:

Child/Small Adult Adult	3.5 kg / 40 km/h (11.1 m/s) / 50° BLE/WAD 1000 - WAD 1500 Adult 4.5 kg / 40 km/h (11.1 m/s) / 65° / 45° for roof testing WAD 1500 - WAD 2500 (if points between WAD 1500 and 1700 are on bonnet, use child head) Performance prediction for all grid points required from manufacturer. In 2023 & 2024 re-testing in case of atypical windscreen fracture is allowed.	
Score	maximum Score	0 Points
HIC_{15}	< 650	≥ 1700

Procedures:

- Use of full vehicle models (impact area: detailed models of all components; engine package can be rigid)
- High detailing for bonnet attachments, hinges, locks, sealing structures, bonnet shock damper, head light attachments, windshield wiper assemblies
- Connection modeling is highly significant (spot welds, adhesives etc.)
- Use of validated material model for windshield failure
- Use of validated impactor model
- Typical simulation duration: 20 ms

Critical Modeling Parameters:

- Strain rate dependency of materials in the impact area
- Details of spatial discretization

Evaluation Criteria:

- Head Injury Criterion (HIC_{15})
- For the optimization: use of acceleration - displacement diagrams to identify jamming

Main Influencing Factors:

- Geometry of vehicle front (impact points, impact behavior)
- Material stiffness at impact point (potential for optimization)
- Stiffness of geometrical package (sheet metal thickness, structural reinforcements in direction of impact, inlays, application of adhesives)
- Clearance between bonnet outer shell and package (min. 60 - 80 mm free displacement required, otherwise an active bonnet should be considered)
- No jamming elements (e.g. bonnet shock dampers, wiper axles) should be packaged directly in the impact area
- Homogenous support of the impactor along the full bonnet/vehicle width is required (e.g. muffin-like structure for the bonnet inner shell).
- Sharp stiffness gradient should be avoided.

Co-hosted with

BGS Böhme & Gehring GmbH

Engineering Event

20th PraxisConference Pedestrian Protection

The first Conference in the Test Lab

The unique concept of the PraxisConference, which was jointly designed and developed by BGS Böhme & Gehring GmbH and carhs.training gmbh, ideally combines the expertise of a top-class conference with the conciseness of live tests, highly instructive practical demonstrations and detailed explanations on the vehicle. The PraxisConference has been held annually since 2006 at the Federal Highway Research Institute (BASt) and has established itself as the world's largest meeting of experts on pedestrian protection.

Top-class Experts

In the lecture session of the conference, representatives from the automotive industry, authorities and institutions will speak about current developments and research projects. International experts will report on the progress of the committees working on legislation and consumer protection test procedures (NCAP). Other presentations will show practical experience in the execution of tests and present new solutions for pedestrian protection.

What is special about the PraxisConference: Hands-on Pedestrian Protection

As the name suggests, the PraxisConference is not a normal conference, but brings together theory and practice. On both conference days there is a detailed practical session. On the first day, the current test methods for pedestrian protection will be presented in the laboratory and on the BASt outdoor area, both for passive safety and for active safety. On the second day of the conference, automobile manufacturers will present the pedestrian protection measures of their current models directly on the exhibited vehicle and will provide deep insights into the respective solutions.

More than Pedestrian Protection

When the conference started in 2006, it was still all about pedestrian protection. In the meantime the topic has been broadened: All vulnerable road users (VRU) are addressed, including cyclists and motorcyclists.

Who should attend?

The PraxisConference is aimed at both experts and newcomers in the field of VRU protection. Experts receive an update on current legal and technical developments and use the conference to exchange experiences with colleagues. Beginners will get a very practice-oriented overview of the topic and can use the event to establish contacts with pedestrian protection experts.

Facts

25.-26.06.2025

Bergisch Gladbach, GERMANY & ONLINE

www.carhs.de/pkf

1.660,- EUR till 28.05.2025, thereafter 1.920,- EUR, ONLINE 990,- EUR

ON SITE & ONLINE

Latest info about this course

Engineering Seminar

Workshop Pedestrian Protection and Low Speed Crash

Course Description

While pedestrian protection works best when sufficient deformation space is available, for example by means of component failure, damage to the vehicle must be kept to a minimum for the UN R42, FMVSS 581 and RCAR tests. In this workshop, the aim is to extend the scope of the simulation engineers' work to include function development. This also includes the implementation of component changes and the solution of conflicting objectives. Thus, both disciplines (pedestrian protection and low speed crash) first present their requirements and design criteria, and then search for features that enable the resolution of the target conflicts. Subsequently, the tasks of the function developers are worked out in detail, from the definition of a design strategy to the preparation of tests, including hardware acquisition, up to the final release. The focus is on method transfer instead of training design criteria, which the participants usually master very well due to their daily work.

Course Objectives

First, the involved groups (Pedestrian Protection and Low Speed Crash) present their respective development goals and constraints to each other to provide a basis for solving the target conflicts. Then the physics of the relevant load cases are worked out in order to technically solve target conflicts. In the final part, the participants are prepared to take on the role of a function developer.

Who should attend?

The one-day workshop is aimed particularly at CAE engineers from the fields of pedestrian protection and low speed crash. Both regularly face conflicting targets when designing the vehicle front end.

Course Contents

- Mutual presentation of legal and consumer protection requirements
  - Test areas on the vehicle
  - Load cases
  - Criteria and limit values
  - Consequences of non-compliance
  - Design criteria
- Target conflicts
  - Recognize
  - Avoid
  - Disassemble
  - Solve
- Function development
  - Dealing with time schedules
  - Determination of the design space and derivation of a development strategy
  - Pushing through of component changes
  - Test hardware: planning and logistics
  - Test execution: ensuring reproducible results
  - Homologation

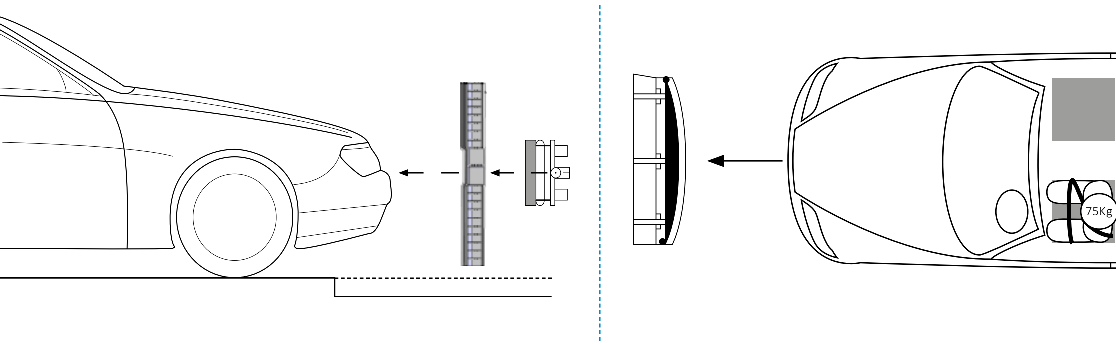

Instructor

Maren Finck (carhs.training gmbh) is a Project Manager at carhs.training gmbh. From 2008 - 2015 she worked at EDAG as a project manager responsible for vehicle safety. Previously, she worked several years at carhs GmbH and TECOSIM as an analysis engineer with a focus on pedestrian safety and biomechanics.

Facts

06.10.2025	192/4548	Alzenau	1 Day	890,- EUR till 08.09.2025, thereafter 1.090,- EUR	

Addressing the Fatigue Challenge of Additive Manufacturing

Additive Manufacturing (AM) allows the production of complex components layer by layer, using only the necessary material. The AM processes can however lead to local artifacts in the printed structure like variable surface roughness, porosities and microstructure which are not well understood nor well controlled. Additionally, there is a lack of CAE tools with predictive quality of complex dynamic performance that can account for the effect of such local artifacts. In this article a novel method and software implementation is presented that enables to account in an efficient manner for the effect of the above-mentioned AM induced local artifacts in the fatigue performance simulation of 3D printed metal components.

What is the Fatigue Challenge of Additive Manufacturing?

Several AM process factors have an influence on the induced fatigue performance. The AM process is less controlled than the conventional manufacturing process and leads to process-induced fatigue-influencing artifacts. These fatigue-influencing artifacts are highly dependent on the geometry, and therefore exhibit a local nature.

All of this makes it challenging to predict the fatigue performance of AM materials. The AM fatigue challenge is illustrated in Figure 1. Key influencing factors of fatigue performance are the microstructure, porosities, surface roughness and residual stress. Fatigue life of any printed product is always a result of the combined influence of multiple local factors. It is not possible to separate these factors in a printed component, and it is not possible to have one mathematic model describing the interaction and separated impact of these factors [1].

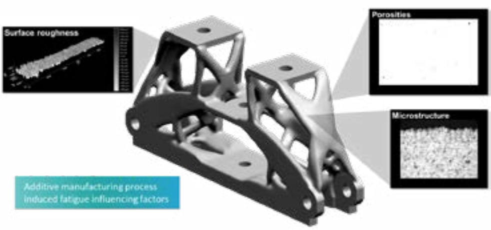

Figure 1: A major challenge of AM: the fatigue life of a 3D-printed structure is influenced by several factors (© Siemens Digital Industries Software)

AM enables the production of complex geometries, often resulting from topology optimized shapes like the component depicted in Figure 1. The quality of the 3D-printed component will depend on several AM processes and design related aspects. For example, the build direction will implicitly impact the orientation of the different surfaces of the printed geometry. Since the surface roughness of a 3D-printed component also depends on the overhang angle (the angle between the build plate plane (x-y) and the overhanging surface tangent in the x-z (or y-z) plane), a different orientation of the component in the build tray will lead to a different distribution of the surface roughness. One may want to optimize the use of build space and stack several instances of the same component with different orientations in the build to produce as many as possible components in one shot. Having oriented several components in a different manner will lead to components with different distribution of surface roughness, porosity distribution and local microstructure. Figure 2 illustrates the same for surface roughness.

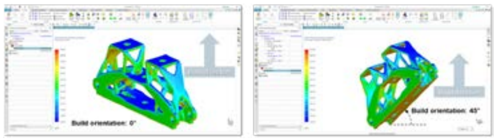

Figure 2: Automatic feature extraction: surface roughness as a function of overhang angle in Simcenter 3D (© Siemens Digital Industries Software)

Since surface roughness is a major influencing factor for fatigue, the different components will exhibit different fatigue behavior, even though they have the same geometry and they have been produced with the same machine and from the same material.

Furthermore, the residual stress in the part during the additive manufacturing process and the different heat treatments applied after the manufacturing process also influence the fatigue performance of the component.

To enable the 3D printing of safety-critical, load-bearing components, it is vital to be able to predict the effect of AM-induced local artifacts on the fatigue life of the produced part. To achieve this, predicting the local artifacts is only one piece of the puzzle. One must also have the means to directly assess the impact of AM-induced local artifacts on the fatigue behavior of the 3D-printed material. Furthermore, a durability solver is needed that can handle local fatigue-influencing artifacts in an efficient manner. The following section will detail these aspects.

Using Machine Learning to accurately predict the local fatigue performance of AM structures

The fatigue performance of the 3D-printed material depends on several aspects such as the manufacturing process and material used, geometry and loading conditions, microstructure, residual stress, surface roughness, porosities and post treatments (surface and volume treatments). When characterizing the fatigue performance of a material, typically the sample geometry, manufacturing process and loading related aspects are all fixed. The effects of the remaining parameters are then assessed. However, in the case of AM, many of the conditions are tightly linked to each other. For example, the build orientation will implicitly impact the surface roughness of the sample and the microstructure (since the layer-by-layer deposition will favor certain growth paths of the metal grains). As mentioned in the previous paragraph, in a complex 3D-printed component, many combinations of these factors are present, and one should have data on all encountered combinations of fatigue-influencing factors, in order to be able to assess the fatigue performance accurately. This means that characterizing the fatigue performance of a 3D-printed material inevitably leads to a huge test campaign to cover as many combinations of factors as possible. It also leads to a significant challenge to derive models which can fit and enable the assessment of un-tested combinations.

Siemens Digital Industries Software (DI SW) has developed a new approach to assess the fatigue performance of 3D-printed components by leveraging on the power of machine learning [2][3].

Going back to the example of the component from Figure 2, to be able to accurately predict the fatigue performance of this 3D-printed part, a material model is needed that can predict the effect the AM-induced local artifacts have on the fatigue property of the material. A machine learning (ML) based material model has been developed that relies on a limited set of training data. This ML model can fit the multi-attribute space of SN curves (Wöhler curves) experimentally determined for a set of different conditions (orientation in the build, different surface treatments, heat treatments, etc.) and can predict the SN curve for untested combinations of conditions. The ML material model has been integrated as an AM enhancement module in our open durability solver environment to account for the effect of the AM-induced local fatigue-influencing factors [4].

Experimental data needed for training the ML algorithm has been produced using the experimental setup and test procedure as described in sources [2] and [5]. This includes specimens printed by 3D Systems according to a fixed set of processing parameters, for which the fatigue testing was performed by the Manufacturing Processes and Systems (MAPS) department of KU Leuven, using an Instron ElectroPuls E10000 while considering a variety of surface and heat treatments [5]. Bearing in mind the cost of fatigue testing on additively manufactured components, it is unrealistic to test all possible parameter combinations. Also, coupon level testing may not allow the replication of all possible conditions, that, for example, could be encountered in thin-walled sections or near internal cavities. Therefore, a methodology is required that is capable of extrapolating fatigue properties for a multitude of artifacts based on a minimal set of test results. Machine Learning (ML) is employed for that purpose, using a so-called Gaussian Process Regression. The benefit of this approach over more classical interpolation/extrapolation approaches is that it makes minimal assumptions on allowable mathematical models to approximate the test data. This is important, given the complex interactions between different parameters and the limited data available for calibration.

The ML approach was implemented, extending the existing durability solver in Simcenter 3D Specialist Durability. The inputs that influence the fatigue properties can be defined per region or per element. In addition, they can be entered by the user, via a file or with an automatic tool that assigns fatigue-relevant parameters to each element as presented in Figure 2.

A schematic representation of the workflow is given in Figure 3. It efficiently links together the AM-induced fatigue-influencing factors with the effect they have on the local fatigue property of the 3D-printed material to enable an AM-enhanced durability solution. On the bottom, the ML approach is depicted, which takes the predicted local artifacts as inputs and returns the estimated corresponding local SN curves to the durability solver. On the top, the CAD model (1) is illustrated, which is required for the FE analysis (for which the results are not shown) and the automated feature extraction tool (2) that will predict the local AM-induced fatigue-influencing factors needed as input for the ML model (3). Subsequently, the AM-enhanced durability simulation can be performed. The user-defined loads are not included in the illustration.

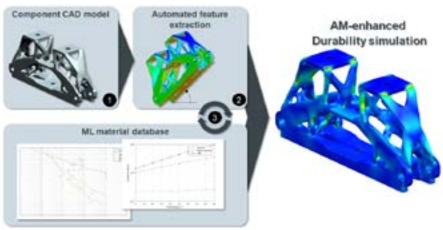

Figure 3: Machine Learning-enhanced Fatigue Analysis of AM components in Simcenter 3D. Schematic depiction of the workflow for durability computations of additively manufactured parts using a machine learning extension to predict material properties (© Siemens Digital Industries Software)

The workflow presented above enables the user to, for example, assess the impact that orientation of the component in the build tray has on the fatigue performance. In the above described case with several instances of the same component with different orientations in the build tray, using the approach shown in Figure 3, the user can predict the local surface roughness for a selected build orientation of the component. The surface roughness is available per element in the model, which is passed to the ML material model along with other relevant parameters such as the heat treatment of the selected material. The machine learning material model will be used to derive the local SN curves at each surface element of the structural mesh that corresponds with the CAD geometry model according to the local fatigue-influencing factors. To calculate the durability performance of the whole printed component, a durability calculation is then conducted using the AM-enhanced Simcenter 3D Specialist Durability solution.

This performs the damage accumulation for the entire structure according to the local conditions, including two new and highly important features: the efficient handling of local material properties, and the mapping of local SN curves on the model. This virtual approach avoids potentially hundreds, if not thousands of tests, by using machine learning together with a limited test set, resulting in a model that can interpolate/extrapolate for untested conditions.

Results & Outlook

Applying machine learning to more accurately model fatigue life performance of additive manufactured components has several benefits. First, no inferences are needed on how the combination of different artifacts affect fatigue life. Furthermore, the approach is flexible, accounts for local phenomena, requires limited testing, enables accurate extrapolation and enables the study of the impact of different factors in an uncoupled manner (which is often impossible to achieve based on experimental data).

Figure 4 shows the results for a blind test to validate the model. The ML algorithm has been trained with a subset of experimentally obtained SN curves corresponding to different combinations of factors. Some combinations have been withheld from the training set, more specifically the cases of 90 degree oriented samples that have been machined and submitted to hot isostatic pressing treatment (HIP) and the cases of machined, 50 degree oriented fully annealed (FA) and HIP-ed samples. In Figure 4 the red solid lines represent the predicted SN curves for the aforementioned unseen cases, also giving a corresponding confidence interval for them (dashed lines). The actual test results have been then plotted on top of the predictions, shown with blue circles in the picture. This shows the good correlation of the predictions with the actual measurements.

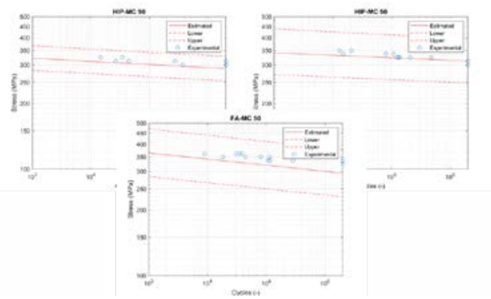

Figure 4: Results: Machine Learning for Fatigue Life Prediction of AM Components Accounting for Localized Material Properties (© Siemens Digital Industries Software)

The AM-enhanced durability simulation in Simcenter 3D Specialist Durability, combines the best of both worlds of experimental data and physics-based modelling. It is also possible to purely rely on experimental and/or simulation data. A customized durability analysis can be performed, leveraging Open Solver technology (of the Simcenter 3D Specialist Durability Solver) to calculate the durability performance of a structure, accounting for the key fatigue-influencing factors: the surface roughness, as shown in this article, and other localized phenomena (void-rich areas, residual stress, etc.). One ongoing work is the prediction of the fatigue performance/SN curves relying on multi-scale modelling, based on a method developed by Ghent University [6].

Acknowledgements

The authors gratefully acknowledge the IBO project FATAM ("Fatigue of Additive Manufactured components - Relating AM process conditions to long-term dynamic performance of metallic AM parts", 2017-2020), which fits in the MacroModelMat (M3) research program, coordinated by Siemens (Siemens Digital Industries Software, Belgium) [7] and funded by SIM (Strategic Initiative Materials in Flanders) [8] and VLAIO (Flemish government agency Flanders Innovation & Entrepreneurship) [9].

References

[1] H. Erdelyi, "ML-enhanced Fatigue Analysis of AM Components", Formnext 2019, Frankfurt, Germany, November 19-22, 2019.

[2] N. Lammens, H. Erdelyi, T. Craeghs, B. Van Hooreweder, W. Van Paepegem, "Effect of process induced artifacts on the fatigue life estimation of additive manufactured metal components", ESIAM19, Trondheim, Norway, September 9-11, 2019.

[3] M. Schultz, N. Lammens, M. Hack, H. Erdelyi, "Machine Learning Enhanced Durability Analysis of Additively Manufactured Lightweight Components", NAFEMS Nordic Seminar, CAE in support of Sustainability and Durability, Billund, Denmark, Nov. 25-26, 2019.

[4] N. Lammens, M. Schulz, M. Hack, H. Erdelyi, "Local Fatigue Parameter Prediction of Additively Manufactured Components using Machine Learning", Fatigue 2020, Downing College, Cambridge, UK, June 29 – July 1, 2020.

[5] C. Elangeswaran, A. Cutolo, G.K. Muralidharan, C. de Formanoir, F. Berto, K. Vanmeensel, B. Van Hooreweder, "Effect of post-treatments on the fatigue behaviour of 316L stainless steel manufactured by laser powder bed fusion", International Journal of Fatigue, Vol. 123, pp. 31-39, 2019.

[6] T.D. Dinh, J. Vanwalleghem, H. Xiang, H. Erdelyi, T. Craeghs, W. Van Paepegem, "A unified approach to model the effect of porosity and high surface roughness on the fatigue properties of additively manufactured Ti6-Al4-V alloys", Additive Manufacturing, Vol. 33, 101139, May 2020.

[7] MacroModelMat (M3) research program, coordinated by Siemens (Siemens Digital Industries Software, Belgium): https://www.sim-flanders.be/research-program/m3

[8] SIM, Strategic Initiative Materials in Flanders: https://www.sim-flanders.be/

[9] VLAIO, Flemish government agency Flanders Innovation & Entrepreneurship: https://vlaio.be/nl/andere-doelgroepen/flanders-innovation-entrepreneurship

CAE Wissen by courtesy of Nicolas Lammens, Matthias Schulz, Hunor Erdelyi, Stijn Donders and Michael Hack, Siemens Digital Industries Software

Latest info about this course

Engineering Seminar

Introduction to Fatigue Analysis

Course Description

Fatigue damage is a significant threat for developers, manufacturers and vendors of many products. A high number of recalls within the automotive industry and spectacular accidents of trains and airplanes dramatically emphasize that. Fatigue damage might bear high risk to human life and financial stability of manufacturers like OEMs in transportation industry. Failure due to cyclic loading of products during service also has a great impact on the image of a car manufacturer and therefore should be avoided.

Fatigue is a complex issue with many different factors influencing durability and involving large scatter of individual parameters like loads or material data. Experimental as well as virtual methods are available to investigate the risk of a product failure due to cyclic loading. Modern simulation methods, like the finite element method, require specific emphasis on modeling for the assessment of stresses suitable for further fatigue postprocessing.

This seminar provides insight into modern durability analysis covering everything from issues of required experimental tests to stress analysis using the FEM and an introduction of different concepts for computational durability assessment. Statistical aspects of fatigue data and probability issues on product reliability will be covered as well. Several examples will be presented and discussed.

Who should attend?

The seminar is aimed at product developers, analysis engineers and managers who are responsible for product reliability involving cyclic loading and durability.

Course Contents

- Fatigue damage, examples and mechanisms
- What stresses do I need? Modeling and stress analysis using FEA for durability
- Obtaining SN-curves and statistical issues involved
- Cycle counting
- Factors affecting fatigue life and synthetic SN-curves
- Stress based and strain based fatigue evaluation
- Introduction to multiaxial fatigue theories

Instructor

Prof. Dr.-Ing. Klemens Rother (Munich University of Applied Sciences) studied mechanical engineering at Munich University of Applied Sciences and the Department of Mechanics, Metallurgy and Materials Science at Michigan State University, East Lansing, USA. He earned his doctorate in the field of computational durability at University of Dortmund. Since 1986 he has been working in various positions in industry, e.g. more than 15 years in senior management for structural integrity and CAE consulting services.

Since 2008 he is professor at the University of Applied Sciences in Munich, faculty of mechanical, automotive and aircraft engineering. He teaches strength, lightweight design, durability and conceptual design. He is also head of a master's program in computational engineering. His main research focuses on CAx-supported product development and structural integrity.

Facts

SEMINAR ON DEMAND

You can book this seminar as an in-house seminar directly at your site or as an online seminar. Alternatively, if you are interested in the course, you can make a reservation. As soon as a sufficient number of participants has been reached, we will arrange a specific course date with the interested parties.

DURATION	LANGUAGE
2 Days	 

Computational Approaches and Simulation of Progressive Damage in Composite Structural Components

Simulation of Fatigue Damage in Composite Materials

Composite materials impose new demands on testing, production and simulation. The combination of various materials, various fiber topologies and manufacturing methods results in numerous influences that simulations must be taken into account to manufacture components with optimum properties.

Different damage mechanisms must be distinguished. On a material (micro-scale) level: the damage mechanism can be, for example, a matrix crack, fiber-matrix debonding, fiber breakage, or delamination, Figure 1

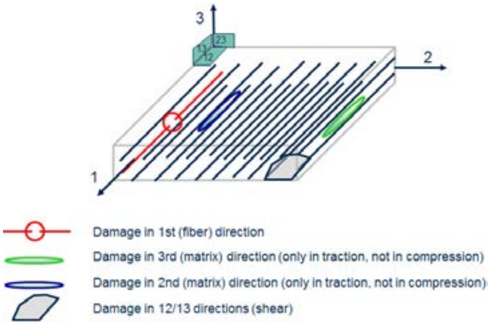

Figure 1: Damage in the layer (© Siemens PLM)

Different types of load, for example, static load, shock (impact) and fatigue loading lead to different damages, which may also interact.

Although such damage may emerge early on in the useful life of the component, complete failure only happens much later. Nevertheless, changes in local stiffness and stress redistribution can develop, which, in turn, may affect the behavior during the lifetime. Accordingly, different approaches to simulation are required.

Continuous Damage Model

In the continuous damage model (CDM), damage influences are homogenized at the layer level in the directions dictated by fiber alignment, In other words damage is considered parallel and transverse to the fiber direction as well as shear damage.

The advantage of these approaches is the ability to describe damage based on different load types (static, shock, fatigue) using the same or compatible models and therefore can be combined. This also means that many material parameters for the different types of load only need to be determined once.

A further crucial advantage of this modeling approach is the fact that material parameters are used at the layer level and thus need only be determined once. No further tests are necessary when the layup design is changed.

Fatigue Behaviour in three stages

Various damage mechanisms are at work in composite materials. Early damage with substantial loss of stiffness is typically followed by an extended phase of stability prior to the failure phase, Figure 2. Comparative testing is more feasible for a stiffness fall-off curve graph than a SN-curve, which is usually used for fatigue, as the point of failure is scattering much more than the stiffness behavior of the test specimen.

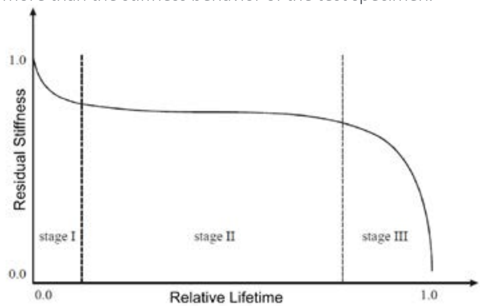

Figure 2: Typical phases of stiffness fall-off (© Siemens PLM)

A simplified (i.e. one-dimensional without interaction to other damage modes) model with fatigue damage behavior in three stages as derived from [2] can be written as

$$\frac{dD}{dN} = c_1 \sigma_a exp\left(-c_2 \frac{D}{\sqrt{\sigma_a}}\right) + c_3 D \sigma_a^2 exp(c_5(\sigma_a - c_4))$$

Where *dD/dN* denotes the damage of one cycle (here in stresses σ_a) at the pre-damage *D*.

These curves could also be replaced by virtual tests instead of using graphed stiffness reduction measurements. These would calculate the stiffness reduction curves based on pure material characteristics and a precise production simulation. Research projects investigating this issue are underway [4].

Hybrid approaches – measuring master data that are then adjusted based on local properties such as voids, moisture etc. – are also key options within this process. For short-fiber reinforced components, see [5] as an example.

Computational Process for Recurring Loads

In principle, the effect of any change in stiffness on local stresses must be calculated throughout the model. While this is, in principle, numerically possible, the pure number of stress cycles make it practically infeasible.

It is more logical to take the global effect of stiffness changes into consideration when significant changes occur, while always taking local effects into consideration. A closer look at the special case of block loads (i.e. the repetition of the same load stress cycle) allows the local effect of the stress cycle to be first calculated, then extrapolated using the stiffness fall-off curve. This extrapolation also allows an estimate of when a recalculation (a so-called N-Jump) is required at the global level.

Good results have been achieved over the last 15 years for composite materials with woven fibers using this method.

Complex Loads

As already mentioned in the introduction, the load collectives to be investigated in the vehicle industry are complex, with varying amplitude and multiple, non-proportional loads. A simple approach with extrapolation no longer possible here, which is why a typical estimate is often made using SN-curve-based methods and all the aforementioned disadvantages (layup-dependent, high test scattering).

In this case there is now an extension to the n-jump method for complex loads that uses cumulative damage based on hysteresis operator theory [6,7] for local damage accumulation (local stiffness fall-off calculation). These methods can accurately map typical non-linear accumulation when calculating stiffness reduction, while considering correctly the effects on other damage modes.

One special aspect is the ability to implement any linear and non-linear damage accumulation methods using this method. An open interface allows research institutes and research departments to add their own extensions.

This methodology was developed alongside extensions to stiffness reduction rules and new methods for determining material curves. Details of the methodology and corresponding test method insights are presented in [7].

Damage between the Layers

CDM can also be used for accurate predictions when calculating delamination between layers and taking damage within the layers into account [9,10].

The complex calculations involved in delamination simulation induce that the focus for fatigue calculation is not on the delamination process itself but on the statement questioning whether delamination occurs. The first tools measuring whether an existing short crack between the layers continues to grow during an operating load collective are undergoing tests. They take into account the damage, or stiffness in the layers, that prompts a change to the intermediate layer load. Further investigations into delamination from the border and the behavior of larger cracks are what follow, to round off the computational tool.

Conclusion and Outlook

Switching from metal to composite materials is far more complex than switching from one metal to another metal. Retaining a testing and simulation level equivalent to that for metals and treating a composite material as a “black metal” would result in restricting the effect of many of the positive composite material characteristics. The goal of lightweight design would remain elusive. This is why the damage simulation methods and process chains need to be adapted. Openness allowing extensions to the various simulation scales is key, given the considerable potential for development here.

Firstly, the right simulation tools can be used such that many tests can be performed more efficiently. Secondly, production processes and designs can be simulated from an early stage. This allows design and production studies to achieve better and also lighter vehicles in the simulation phase.

References

[1] Küssner, M. E. N.: Simcenter for the predictive validation of composite materials. Simulation von Composites – Bereit für Industrie 4.0? Hamburg, NAFEMS DACH, 2016

[2] v. Paepegem, W.: Fatigue Damage Modelling with the phenomenological residual stiffness approach. In: A. Vassilopoulos, Fatigue Life Prediction of Composites and Composite Structures, 2010, pp. 102-138

[3] Ladevèze, E.; Le Dantec, P.: Damage modelling of the elementary ply for laminated composites. Composite Science and Technology, 43,1992, pp. 252-267

[4] M3, S., 2014, M3 - SIM-Flanders. Retrieved from SIM-Fladers: www.sim-flanders.be/research-program/m3

[5] Jain, A.; v. Paepegem, W.; Verpoest, I.; Lomov, S.: A feasibility study of the Master SN curve approach for short fiber reinforced composites. I Journal of Fatigue, 2016, pp. 264-274

[6] Brokate, M.; Sprekels, J.: Hysteresis operators. 1996, New York, Springer

[7] Carrella-Payan, D.; Magneville, B.; Hack, M.; Naito, T.; Urushiyama, Y.; Yamazaki, T.; v. Paepegem, W.: Implementation of fatigue model for unidirectional laminate based on finite element analysis: theory and practice. Frattura ed Integritá Strutturale 38, 2016, pp. 184-190

[8] v. Paepegem, W.: Development and finite element implementation of a damage. PhD Thesis, 2002, U Gent

[9] Bruyneel, M.; Delsemme, P.; Groupil, A.; Jetteur, J.; Lequesne, C.; Naito, T.; Urushiyama, Y.: Damage modeling of laminated composites: validation of the inter-laminar damage law in SAMCEF at the coupon level for UD plies. World Congress of Comp Mechanics, 2014, Barcelona

[10] Bruyneel, M.; Delsemme, P.; Groupil, A.; Jetteur, J.; Lequesne, C.; Naito, T.; Urushiyama, Y.: Damage modeling of laminated composites: validation of the intra-laminar damage law in SAMCEF at the coupon level for UD plies. European Conference on Composite Material ECCM16, 2014, Sevilla

CAE Wissen by courtesy of Dr. Michael Hack, Siemens PLM Software in Kaiserslautern.

Operational Strength under Consideration of Random Loads in the Frequency Domain

Dynamic loads characterized by randomness frequently lead to system failure through material fatigue in vibratory mechanical structures. In order to correctly account for this random character, it is necessary to observe the stochastic load over a longer period of time. This requires long measurement series for measurement-based determination. In order to ensure that the random process is stationary, it is also necessary to observe the stochastic properties over the course of several measurement series.

Description of stochastic processes

The aforementioned considerations make only limited allowance for the conclusion that determination of the stochastic process can be made using individual realizations (individual measurement series). Consequently, the function *p(x)* is used to characterize the stochastic process, which indicates the probability that the signal *x(t)* lies in the interval [*x,x+Δx*]. The temporal correlation of the random process is described using the spectral power density $S_X(f)$, whereby *f* designates the frequency. Especially in the case that *p(x)* corresponds to a normal distribution, the distribution parameters (arithmetic mean and variance) can be determined from the spectral power density $S_X(f)$.

Linear mechanical systems under stochastic excitation

If a linear, time-invariant mechanical system is excited by transfer function *h(t)* over a normally distributed load signal *x(t)*, it can be demonstrated that the equivalent stress history

$$y(t) = \int_{-\infty}^{+\infty} x(\tau)h(t-\tau)d\tau$$

is also distributed normally. The equivalent stress history can be transformed into the frequency domain by means of the Fourier transformation. In particular, *Y(f) = H(f) · X(f)* results, whereby *Y(f), H(f) and X(f)* designate the Fourier transforms of the equivalent stress history, the transfer function and the load signal. The power density spectrum of the input signal delivers the power density spectrum of the equivalent stress by means of the relationship $S_Y(f) = H(f) \cdot S_X(f) \cdot H^*(f)$. Here, H^* is the conjugate complex and transposed transfer function. The frequency-dependent transmission behavior *H(f)* of a linear mechanical structure can be determined effectively by a frequency-based response analysis with a unit load using finite element methods (Fig. 1).

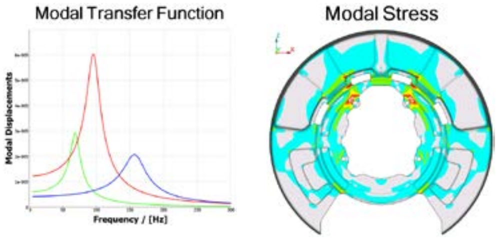

Figure 1: Modal transfer functions (left) and modal stress result for mode 2 (right).

Operational strength of stochastic processes

For normally distributed equivalent stress histories, it is possible to specify probability densities in particular, which allow counting of the stress cycles which occur (rainflow classification) to be carried out on a probabilistic basis. Following from this, operational strength forecasts can be derived. Especially for narrow-band signals, it can be shown by means of analysis that a Rayleigh distribution results for the oscillation amplitudes of the equivalent stress. An estimation of the distribution parameters can be carried out using the spectral equivalent stress power density $S_Y(f)$ with the help of moments of the *k* order

$$m_k = \int_{-\infty}^{+\infty} f^k \, S_Y(f)df$$

Dirlik [1] developed an empirical distribution density function for counting stress cycle amplitudes (probability density function) based on Monte-Carlo simulations which is also applicable for broad-band signals. Further approaches for the distribution densities of oscillation amplitudes can be found in the works of Zhao-Baker [2], Tovo – Benasciutti [3], as well as Petrucci – Zuccarello [4], among others. A representation of the overall process is shown in Fig. 2.

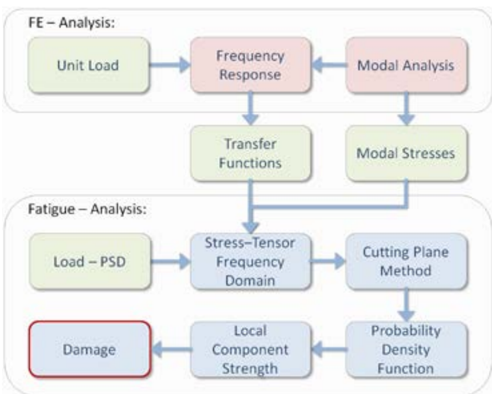

Figure 2: Spectral fatigue process

Example – Operational strength of a brake protection plate

Using the example of a brake protection plate, operational strength analyses [5] were carried out in the time domain and in the frequency domain and were compared. The center of the wheel (Fig. 3 at left) was taken as the excitation point for the measured acceleration load. The corresponding excitation PSD of the acceleration is shown in Fig. 3 at the right.

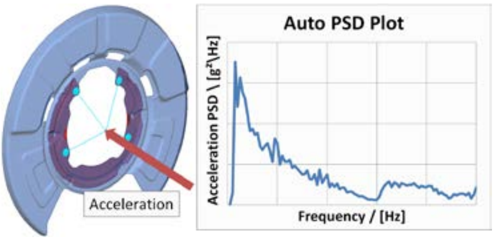

Figure 3: FE model with acceleration at center node (left). Power spectral density of acceleration load (right).

The results of the operational strength analyses in the time domain and in the frequency domain are shown in Fig. 4. One can see that the locality of the highly damaged areas demonstrates very good correlation. The absolute damage values of the analysis in the frequency domain are about 80% higher on average than the damage values of the analysis in the time domain. This difference primarily results from the fact that the load time series only shows a single realization of the stochastic process. The damage result of the spectral analysis, however, delivers the expected value over all realizations of the process (described by the PSD). In addition to the good correlation of the damage results, the main advantage of the analysis in the spectral domain is the fact that the computation times are often shorter.

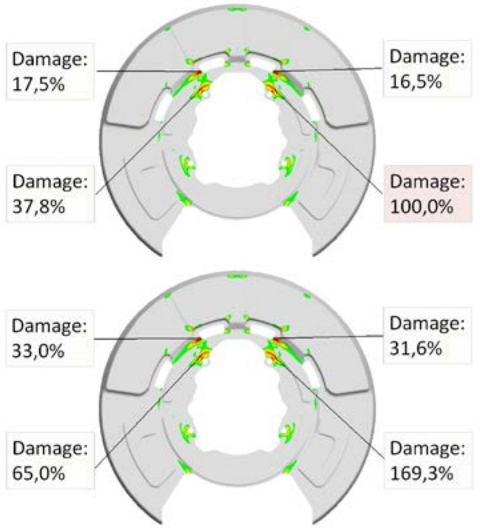

Figure 4: Fatigue result of time domain approach (top). Fatigue result of spectral approach (bottom).

Literature

[1] T. Dirlik. Application of Computers in Fatigue Analysis. PhD thesis, The University of Warwick, 1985.

[2] W. Zhao and M. J. Baker. On the probability density function of rainflow stress range for stationary gaussian processes. Int. J. Fatigue, 14(2):121{ 135, March 1992.

[3] D. Benasciutti and R. Tovo. Spectral methods for lifetime prediction under wide-band stationary random processes. Int. J. Fatigue, 27(8):867{877, 2005.

[4] G. Petrucci and B. Zuccarello. On the estimation of the fatigue cycle distribution from spectral density data. Proceedings of the institution of mechanical engineers part C - J. Eng. Sci., 213(8):819{831, 1999.

[5] http://www.femfat.com/Papers.4940.0.html
W. Hinterberger, O. Ertl, C. Gaier and H. Fleischer. Spektrale Schädigungsanalyse für multiaxial stochastisch belastete Komponenten.

CAE Wissen by courtesy of Engineering Center Steyr, Austria, Author: Dr. Walter Hinterberger.
For more information see www.femfat.com

Fatigue Calculation of Short Fiber Reinforced Plastics using Injection Molding Simulation Results

Introduction

As part of a research project, the fatigue behavior of short fiber reinforced plastics was investigated [3-9]. The goal was to develop practical methods for predicting the lifetime of dynamically loaded plastic components. A variety of tests were conducted on samples and components (static and cyclic), leading to the development of lifetime evaluation methods based on injection molding simulation results. Additionally, relationships between various material parameters were identified. This now allows for the estimation of complex anisotropic material parameters using simple input data such as matrix material, fiber content and tensile strength.

Workflow - From process simulation to fatigue calculation

Unlike a standard simulation of an isotropic material, an injection molding simulation is additionally required for predicting the local fiber orientation in fiber-reinforced plastics. In general, the following data is needed for a complete simulation including lifetime calculation:

- A finite element (FE) structure consisting of nodes and elements. The FE mesh for the injection molding simulation is significantly finer than for strength analysis. Mapping of the injection molding simulation results is required.
- Stresses due to external dynamic loads. The stress analysis must be performed using local orthotropic material parameters.
- Load-time histories that characterize the time-varying loads.
- The distribution of fiber orientation and concentration as a result of the injection molding simulation.
- The distribution of residual stresses as a result of the injection molding simulation.
- Static material parameters and specimen SN curves for loads along and transverse to the fiber orientation.

An established simulation chain is shown in Figure 1. It consists of an injection molding simulation tool such as MOLDFLOW, an FE solver such as ABAQUS for stress analysis, and a durability analysis software such as FEMFAT for fatigue calculation.

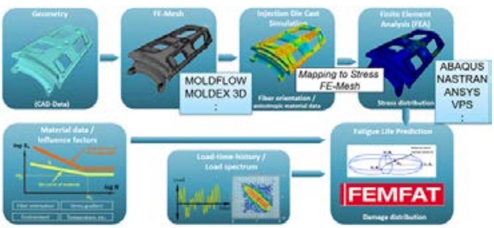

Figure 1: Representation of the simulation process for short fiber reinforced plastics

Fatigue assessment for short fiber reinforced plastics

For short fiber reinforced plastics, the failure mechanisms differ significantly from metallic materials. Figure 2 shows the fracture surface of a tested sample, revealing the separation of the matrix from the fibers.

Figure 2: SEM image of the fracture surface of a sample made of PA 6T/6I-GF40MX2

Additional influences on the lifetime of short fiber reinforced plastics include:

- Fiber orientation, material orthotropy
- Participating materials in the fiber-matrix system
- Frequency dependence
- Moisture absorption
- Environmental media (oil, brake fluid, water/glycol)
- Bonding seams
- Aging
- ...

By far, the most significant influence is the material orthotropy caused by fiber distribution and fiber orientation. These can be fully described by a symmetric 3x3 second-order tensor. The orientation tensor includes the following information:

- The three eigenvectors determine the principal directions of orthotropy.
- The three eigenvalues λ_i represent the proportions of fibers in the three principal directions of orthotropy, see Figure 3.

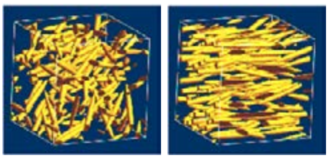

Figure 3: Left: randomly oriented fibers (λ_1=33%, λ_2=33%, λ_3=33%), Right: almost completely aligned fibers parallel to each other (λ_1=98%, λ_2=1%, λ_3=1%)

The distribution of orientation tensors in a component made of short fiber reinforced plastic can be determined through an injection molding simulation.

Static and cyclic specimen tests were conducted at Montanuniversität Leoben to investigate orthotropy [3]. Figure 4 shows SN curves for a polyamide with 40% glass fiber content under tensile-compressive loading along and transverse to the fiber orientation. The standard specimen (long) was produced by injection molding into a corresponding mold, while the short specimen was taken from injected plates.

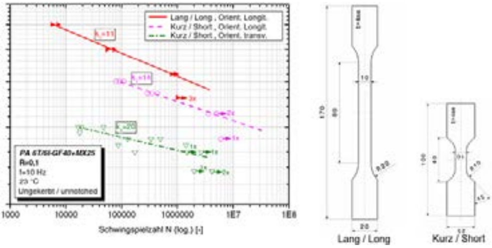

Figure 4: Left: Influence of fiber orientation on the lifetime Right: Sample geometries

Static material properties (modulus of elasticity, tensile strength, yield strength) and measured SN curves for tensile-compressive loading along and transverse to the fiber orientation are input data for the lifetime calculation of orthotropic materials in FEMFAT. For this purpose, the existing critical plane method has been extended by using different SN curves in each plane depending on the orientation of the plane with respect to the fiber orientation. First, the SN curve parameters (endurance limit, slope, cyclic stress ratio) are determined in the three principal directions of orthotropy. For given fiber fractions λ_1, λ_2, and λ_3, these parameters can be determined through linear interpolation, as shown in Figure 5 on the left. The symbol w represents any parameter such as modulus of elasticity, tensile strength, endurance limit, etc. w_1, w_2, and w_3 are the interpolated parameters in the principal directions of orthotropy. In the next step, the material parameters in the plane defined by the normal vector v are again calculated through interpolation. A simple sinusoidal variation of the material parameters is assumed when rotating the plane by 90 degrees from one principal direction of orthotropy (e.g., e_1) to another (e.g., e_2).

$$\frac{w_1 x^2 + w_2 y^2 + w_3 z^2}{\left(x^2 + y^2 + z^2\right)^{\frac{3}{2}}} = 1$$

The closed surface described by this equation is shown in Figure 5 on the right.

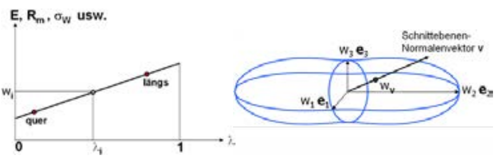

Figure 5: Interpolation of material parameters, left: first in the principal directions of orthotropy based on two measured values and given λ_i, i = 1, 2, 3; right: then in the cutting plane.

Another peculiarity of short fiber reinforced plastics is that the linear damage accumulation 0according to Palmgren/ Miner should be extended by the exponent b [1-2]:

$$D = \left(\frac{n_1}{N_1}\right)^b + \left(\frac{n_2}{N_2}\right)^b + \left(\frac{n_3}{N_3}\right)^b + \cdots + \left(\frac{n_{i-1}}{N_{i-1}}\right)^b + \left(\frac{n_i}{N_i}\right)^b$$

These methods have been implemented in the durability analysis software FEMFAT.

Generation of material data for short fiber reinforced plastics

In contrast to long-established and conventional materials such as steel or aluminum, the available data for short fiber reinforced materials is very limited. Moreover, the testing effort is significantly higher due to the anisotropy, requiring different direction-dependent tests.

Over a period of 15 years, within the scope of three research projects, the necessary tests were conducted for various matrix-fiber combinations, leading to the development of a material generator for short fiber reinforced plastics. This material generator has also been integrated into the durability analysis software FEMFAT. As a result, material data can be estimated for the following matrix-fiber combinations:

Matrix	PPA dry	PPA conditioned	PEEK	PEEK
Fiber type	Glass	Glass	Glass	Carbon
Matrix	PA66 dry	PA66 conditioned	PP	PA12
Fiber type	Glass	Glass	Glass	Glass

For the mentioned fiber/matrix combinations, both static and dynamic material data are estimated in the longitudinal and transverse directions to the fiber orientation. Additionally, parameters for isothermal temperature influence are calculated. In total, over 60 different parameters are determined, and a ready-to-use dataset is generated. To estimate these data, only a few inputs are required:

- Matrix material
- Fiber material (primarily glass fiber supported)
- Fiber content in mass or volume %.

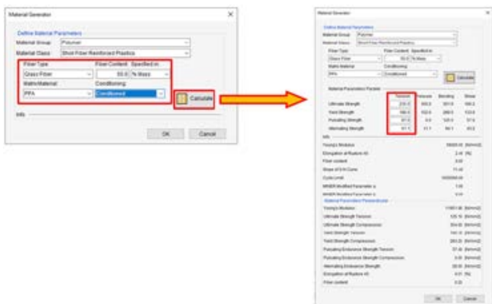

Figure 6: Implementation of the material generator for short fiber reinforced plastics in FEMFAT

In addition to the aforementioned data, inputting the tensile strength and/or yield strength of the matrix is recommended. These data are usually provided by the manufacturer. Additional material data can also be incorporated at any stage of the material generation process.

Application examples

Belt pulley

As an existing serial component in the automotive industry, a belt pulley was tested and analyzed. For the orthotropic stress analysis and lifetime calculation, the finite element (FE) mesh from the injection molding simulation was used. The elements in the FE mesh are small, and it consists of 1.5 million linear tetrahedral elements, as shown in Figure 7 on the left. On the right, the injection molding simulation model with the melt inlet channels can be seen. In Figure 8, the stress distribution calculated with ABAQUS and the damage distribution calculated with FEMFAT are shown. The failure location was correctly predicted, and the absolute lifetime was within the scatter range.

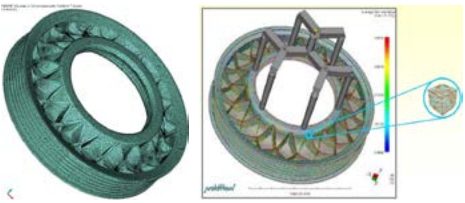

Figure 7: Left: Finite element (FE) model of the pulley   Right: Injection molding simulation with MOLDFLOW

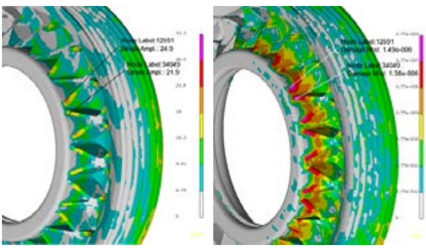

Figure 8: The distribution of stress amplitude calculated with ABAQUS and the distribution of damage calculated with FEMFAT

Ring spanner

Another example that was analyzed is a ring spanner (Figure 9). The mesh consists of approximately 200,000 elements. Initially, isotropic analyses were performed using material properties in the longitudinal and transverse directions to the fibers. This resulted in a difference in lifetime of a factor of 7. Then, calculations were carried out using an orthotropic material. As expected, the result fell between the two results obtained with the isotropic material.

It is worth noting that, when considering the orthotropy of the material, the predicted critical location did not occur at the highest stress point but rather at the injection point, where the fibers are randomly distributed. This was also verified on the test bench, highlighting the suitability of lifetime simulation considering fiber orientation from the injection molding simulation.

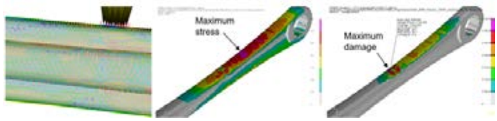

Figure 9: Ring spanner, left: Fiber orientation at the injection point, middle: Distribution of stress amplitude calculated with ABAQUS, right: Distribution of damage calculated with FEMFAT.

References

[1] Zago A., Springer G.S., “Life Prediction of Short Fiber Composites”, Final Report to BMW AG, Department of Aeronautics and Astronautics, Stanford University, July 2000.

[2] Brune M., Zago A., „Lebensdauerberechnung für kurzglasfaserverstärkte Thermoplaste“, VDI-Gesellschaft Kunststofftechnik, Kunststoffe im Automobilbau, Tagung Mannheim 13./14. März 2002, pp. 129-145.

[3] Brune M., Fleischer H., Guster Ch., Balika W., "Rechnerische Lebensdauerabschätzung für Bauteile aus kurzglasfaserverstärkten Kunststoffen“, VDI-K Mannheim, 2006, pp. 321-342.

[4] Gaier C., Dannbauer H., Werkhausen A., „Fatigue Life Prediction of Short Fiber Reinforced Plastic Components“,NAFEMS Seminar Simulating Composite Materials and Structures, 6.-7. November 2007, Bad Kissingen.

[5] Gaier C., Dannbauer H., Werkhausen A., „Festigkeitsbewertung von Komponenten aus kurzfaserverstärkten Kunststoffen“, NAFEMS Magazin, 8. Ausgabe, Dezember 2007 Nr. 3, pp. 23-33.

[6] Gaier C., Fleischer H., Guster C., Pinter G., "Einfluss von Faserorientierung, Temperatur und Feuchtigkeit auf das Schwingfestigkeits-verhalten von spritzgegossenen kurzfaserverstärkten Thermoplasten", DVM-Bericht 136 „Einflussgrößen auf die Betriebsfestigkeit bei der Bauteil- und Systementwicklung“, 36. Tagung des DVM-Arbeitskreises Betriebsfestigkeit, 8.-9. Oktober 2009, Darmstadt, pp. 121-132.

[7] Gaier C., Unger B., Dannbauer H., “Multiaxial Fatigue Analysis of Orthotropic Materials”, 29èmes Journées de Printemps organisées par la Commission de Fatigue de la SF2M (Société Française de Métallurgie et de Matériaux), Influence des procédés sur la tenue en fatigue, Paris - 19-20 mai 2010, pp. 155-162.

[8] Gaier C., Fleischer H., Guster C., Pinter G., “Einfluss von Faserorientierung, Temperatur und Feuchtigkeit auf das Ermüdungsverhalten von kurzfaserverstärkten Thermoplasten”, Materialprüfung, Materials Testing, Volume 52, 7-8/2010, Carl Hanser Verlag, München, pp. 534-542.

[9] Gaier C., Unger B., Dannbauer H., “Multiaxial fatigue analysis of orthotropic materials”, Revue de Métallurgie, Volume 107, number 9, 2010, EDP Sciences 2011, pp. 369-375.

CAE Wissen by courtesy of Engineering Center Steyr, Austria.

Vibration Fatigue Analysis of Solder Joints

Introduction

The trend towards electrification of vehicles requires an increased number of electronic components which need to withstand different environmental influences, like thermal, vibration and static loading. In the following, vibrational loads, as specified in different standards (e.g. LV124) [1] will be treated. Those standards define stochastic, deterministic vibration profiles as well as shock loads that an electric drive must endure during a test scenario to guarantee the vehicles function. An essential part of the e-drive is the inverter, which includes printed circuit board assemblies (PCBA). These consist of the printed circuit board (PCB) and different surface mounted devices (SMD), which are connected by solder joints. The mechanical integrity of these joints is essential for the function of the inverter. Therefore, it must be ensured that these solder joints can endure the specified mechanical loads. Predicting possible damages in an early design phase by virtual testing can save additional design loops as well as physical testing and therefore development costs.

Simulation process

The vibration fatigue analysis of solder joints requires an accurate finite element model of each individual solder joint. Due to the large number of SMDs on an Inverter PCB (up to thousands) it would be impractical to model all solder joints manually, thus the model generation needs to be automated. In the simulation process this is achieved by automatically placing simplified finite element SMD models (using shell and beam elements) on a shell model of the PCB. The solder joint which represents the connection between PCB and SMD, are included via sub-models.

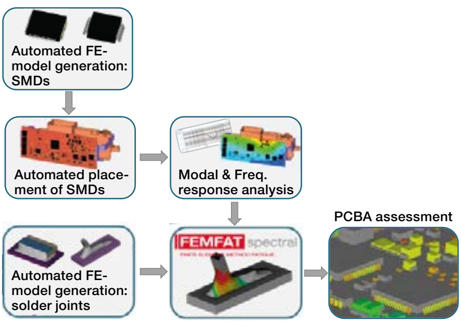

Figure 1: Simulation process

The resulting overall PCBA model is then used to conduct a modal reduced steady state dynamic analysis. In a subsequent FEMFAT analysis, the damage can be automatically assessed. This is achieved by mapping the frequency-dependent movement of each solder joint onto the detailed sub-model. For more details see [2].

Finite-element model

To make this process efficient, a database for SMDs is used every time an overall PCBA model is built (see Figure 1). For each SMD package type this database contains a simplified model (consisting of beams and shells) and a detailed solder joint model (solid-meshed).

Overall model: When modelling a new PCBA the PCB itself usually is modelled with shell elements. Nevertheless, the inhomogeneous material distribution due to the complex composition of layers, traces and drills has to be considered. An automated process takes the coordinate information of every finite element of the meshed PCB and maps it over the layer composition retrieved from ODB++ export (from e-CAD). For every element the enclosed materials are homogenized into one material which gets assigned to the corresponding finite element of the PCB.

Subsequently all SMDs are automatically placed onto the PCB from the database using the Pick&Place export (from e-CAD). The beams of the simplified SMD models, representing the pins, are connected with ABAQUS substructure elements with two interface nodes carrying the reduced stiffness matrix of the corresponding detailed solder joint model (see Figure 2) [3].

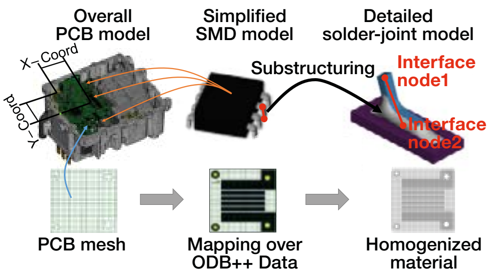

Figure 2: Structure of FE model generation

Simplified SMD model: If a new SMD package needs to be added to the database its geometry data has to be specified from the datasheet. An algorithm takes this data as an input and automatically generates a simplified SMD model using beam and shell elements and adds it to the database.

Detailed solder joint model: The shape of the solder joint depends on the solder-type (see Figure 3) as well as the size of the solder pad. After specifying this data, the automated process utilizes a parametric CAD model as well as a parametric solder joint FE-model of the corresponding solder-type.

The solder meniscus shape is automatically calculated and takes physical parameters like surface tension during the soldering process and gravity into consideration [4]. The resulting geometry of the solder meniscus is imported into the FE-preprocessor where it is automatically meshed and stored in a database similar to the simplified SMD model.

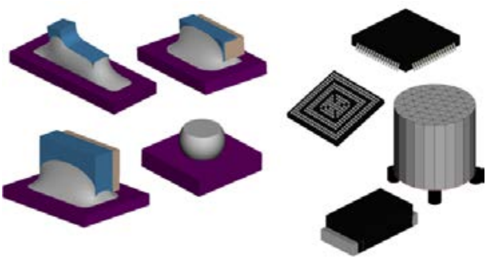

Figure 3: Left: solder joint sub models, right: simplified SMD models

Fatigue life prediction

A modal analysis followed by a frequency response analysis needs to be carried out for the overall model. The nodal displacements of both interface nodes from each substructure element are exported for every frequency and all degrees of freedom. Additionally for each new detailed solder joint model in the database a static stress analysis with unit-displacements is conducted in all 6 degrees of freedom separately for both interface nodes of the sub-model. Both results together form the input for a solder joint fatigue calculation.

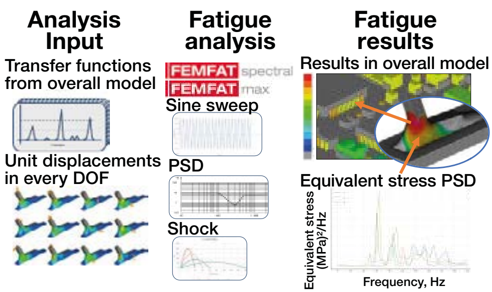

Figure 4: Durability assessment process

Fatigue assessment: Stochastic load profiles like PSDs can be used as a direct input in FEMFAT Spectral. If a deterministic signal needs to be calculated (e.g. sine sweep or mechanical shock), the software tool Harmonic is used to generate the load-time history from the frequency response behavior which is the input for a subsequent FEMFAT Channel-Max analysis. The material data (ultimate strength, yield strength, S-N curve, etc...) for the FEMFAT analysis is based on literature like [5]. For each solder joint an analysis job is automatically created and calculated. The maximum damage value of each solder joint is exported into one overall result file for further post processing.

FE - post processing

In the postprocessor the overall result file can be loaded to the overall model of the PCBA. The maximum damage value of each solder joint is assigned to the corresponding sub-structure element. This allows a quick identification of problematic areas on the PCBA. For the critical solder joints the result files from FEMFAT can be reviewed to receive detailed information about the location of the highest damage on the solder joint as well as critical frequencies and load directions.

Usually, movement of the critical SMD is sufficient improvement to mitigate the occurring damage. Furthermore, application of additional mounting points or adhesives on the PCB can reduce the overall mobility of the PCBA and therefore lower the solder joint damage values.

Conclusion

Using automatization and different sub-structuring and sub-modelling techniques a process was developed which time and cost efficiently calculates the vibration fatigue of each solder joint on a PCBA for deterministic and stochastic load cases. Application of this simulation process allows the identification of critical solder joints in an early design phase where improvements can prevent costly defects during later tests or even during operation.

Even though this paper concentrates on the vibration fatigue calculation of solder joints, other loading types also have to be considered. Especially for thermal loads as well as pre-tension loads during assembly automated analysis processes exist. All those methods are available in a software tool that assist an efficient assessment of PCBAs [6].

References

[1] Volkswagen Aktiengesellschaft, LV 124, Wolfsburg, 2013.

[2] H. Ziegelwanger and W. Hinterberger, Fatigue analysis of solder-joints for vibration and shock, St. Valentin: MAGNA Powertrain, 2021.

[3] Dassault Systemes, SIMULIA User Assistance 2020, Dassault Systemes, 2020.

[4] K. A. Brakke, "The Surface Evolver," Experimental Mathematics, vol. 1, no. 2, pp. 141-165, 1992.

[5] N. Barry, Lead-free Solders for High-Reliability Applications: High-Cycle Fatigue Studies, University of Birmingham, 2008.

[6] Engineering Center Steyr, "CAE/Simulation: NVH", Available: https://engineering.mpt.magna.com/engineering/nvh.

CAE Wissen by courtesy of Engineering Center Steyr, Austria. Authors: C. Neubacher, Dr. W. Hinterberger

Reshaping Automotive Components with Advanced RBF Mesh Morphing

Automotive industry is relying more and more on Computer Aided Engineering and high-fidelity simulations are today trusted enough to reduce drastically the number of physical prototypes that are often limited to the final validation stage of the new product. FEA (CSM) is well established for structural analysis so that the strength, the durability, the comfort and the crashworthiness of automotive components can be anticipated. CFD (usually VOF) is widely adopted for external aero, internal flow, cooling. Just to name a few of the daily applications performed by design engineers in the automotive industry.

There is a growing demand for optimization tools. All the automotive companies are striving for improved products for many different reasons: competition, regulations, greener and safer products. But optimization is not enough because we need robustness and we want to be sure that component will preserve the initial specifications within a certain range for the whole life. Digital twins (powered by AI and reduced models) and digital shadows (replica of as built parts) are emerging technologies, strictly connected to CAE, and intended to target not a generic part, but a specific actual one. There is furthermore another important driver: additive manufacturing is today a main stream technology which opens new solution for the design and new challenges for the maintenance.

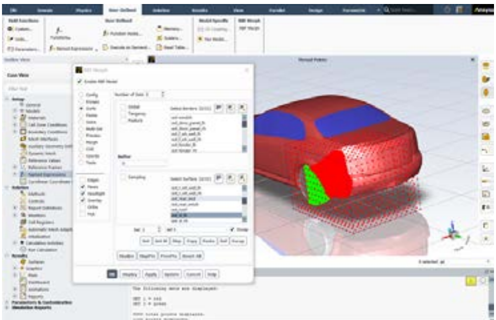

Figure 1: The RBF Morph Fluids software is integrated in the CFD solver Ansys Fluent. The RBF set-up for changing the boat tail angle of the car is represented. The morphing action is localized in the Domain box, the red points on the tail are controlled to change its angle, the green points allows preserving the shape of the wheel. The right side of the car receives the same morphing action with a symmetry constraint.

In this landscape shape control is a paramount and advanced mesh morphing provides a good help. Mesh morphing is a technology that allows to reshape an existing CAE model ready to run (a CFD model complete of initial data and boundary conditions, an FEA model with loads and constraints ready to run) by updating the position of the mesh nodes (all the nodes or for local subset). The use of radial basis functions [1] makes mesh morphing precise and effective allowing to have the full control of surfaces (up to be node-wise) and volumes (gently propagating the deformation of surfaces into the full solid mesh).

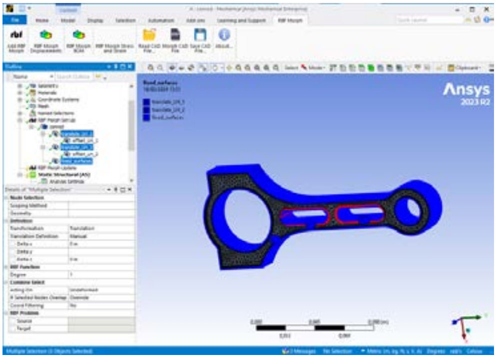

Figure 2: The RBF Morph Structures software is integrated in the FEA solver Ansys Mechanical. The RBF set-up for changing the size of the lightening holes of the connecting rod is represented. The holes are controlled making their position and size parametric (A,B) the external surface (C) is constrained.

The software RBF Morph, the first industrial solution on the market based on RBF mesh morphing, offers advanced RBF mesh morphing for fluids and structures [2,3]. The UI, available as a Stand Alone software, as a Fluent Add-On and as an ACT Extension for Mechanical, is represented in figures 1 and 2.

Mesh morphing can be used mainly in two ways: parameter-based, parameter-free. Adding parameters to an existing CAE model (changing of a thickness, a length, and angle) allows to enable parameter-based optimizations making the original CAE model parametric.

Figure 3: The automated workflow enabled by mesh morphing. New CAE variations are automatically generated making the baseline CAE model parametric. Design exploration and generation of synthetic big data to train reduced order model are substantially simplified with respect to the conventional approach based on parametric CAD and remeshing.

The ability of generating shape variations with parameters (figure 3) allows to enable optimization according to zero-order methods (the shape parameters are used as input) and/or to local methods (steepest descent gradient when derivatives of KPI versus input parameters are available). The same orchestration tools can be used for robust design (in this case instead of input parameters we have their uncertainty focused). Last, but not least, the ability to create variations allows to generate synthetic big data ready to train AI so that reduced order models can be defined and deployed.

Mesh morphing is adopted for parameter-free situations as well. This is occurring for shape optimization cases in which the results computed by the CAE solver (local stress, flow results, adjoint sensitivities) are used to locally reshape surfaces adding in this case packaging and manufacturing constraints. There are other scenarios that can be targeted: non conformal parts can be studied by morphing the baseline CAE onto the actual shape, evolution of the shape due to the working scenario (erosion, repair, snow deposition, fauling).

The first example described is about crashworthiness [4]. In this study both the aforementioned approaches are adopted demonstrating advanced mesh morphing for the quick evaluation of crash performances of a car bonnet (figure 4). The existing LS-DYNA model of the Honda Accord is firstly morphed to represent a new car (in the example the Chevrolet Silverado), then parameters are added so that the desired level of deceleration are achieved. In the first morphing action the new style is used as a target, then parameters are added so that the shape is changed and variations of the explicit transient job are submitted getting the desired KPI.

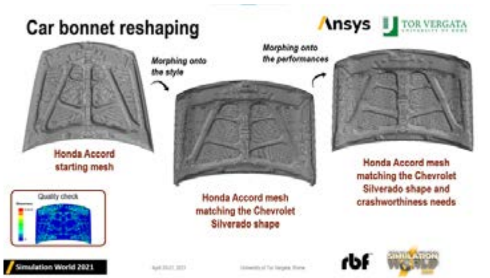

Figure 4: In the picture a solution presented at Ansys Simulation World 2021 by the University of Rome Tor Vergata is shown. The study demonstrates how an existing FEA model for LS-DYNA (the bonnet of a car complete of external style surface, internal structures, welds and interfaces with the chassis) can be transformed to represent a different car and then controlled to match its crashworthiness' requirements.

The second example is about flow optimization, in the specific the shape of a Formula 3 F3-19 Dallara [5] is controlled with the aim of reducing drag force (figure 5). 14 design parameters are introduced to control the front wing end plate, the mirror and the bargeboard. The adjoint solver is in this case exploited to compute the derivatives of the KPI (drag) with respect to the high number of parameters. It's worth to notice that a single run (CFD + adjoint) allows to compute all the 14 derivatives. A local optimization method allows in this case to go for the optimum.

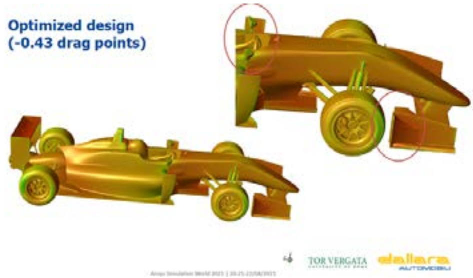

Figure 5: In the picture a solution presented at Ansys Simulation World 2021 by Dallara is shown. The study demonstrates how shape sensitivity map computed by the adjoint CFD solver of Ansys Fluent can be used to compute and combine the effect of 14 different local shape modifications getting a good reduction of the overall drag.

The third (figure 6) and fourth (figure 7) applications here presented are about powertrain optimization showing how the same BGM method [6] can be used to improve the durability of an internal combustion engine [7] and of an electric motor [8].

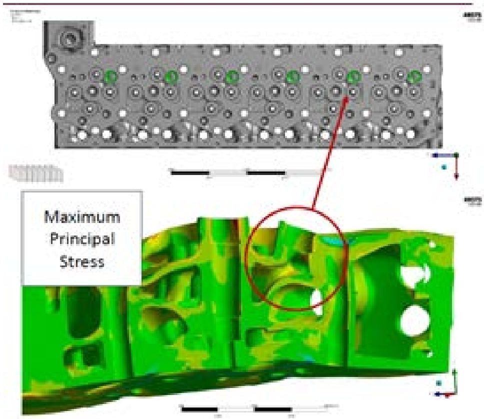

Figure 6: This picture shows how Cummins Inc. reduced the stress on the head of an internal combustion engine.

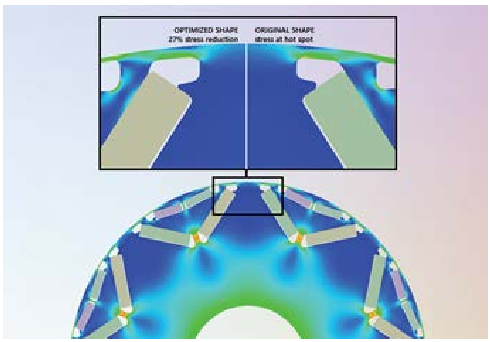

Figure 7: The picture shows how the pockets of the rotor of a Tesla-like electric motor are reshaped to reduce the stress.

For the thermal engine the mitigation of a hotspot in the engine head in a district close to the exhaust valve housing is conducted under a complex multi-physics analysis where the intake and exhaust flows, the liquid coolant flow and the thermos-structural analysis of the block are conducted at the same time. The shape evolves by adding/removing material according to the local level of stress on surfaces getting a 15% reduction of the hot-spot stress. The same BGM approach is used for the rotor of an electric motor. In this case the structural analysis is coupled with an EM one. The shape of the pocket is changed getting a 27% stress reduction.

The last two automotive examples reported (figure 8 and figure 9) are related to motorbikes. Shape parameters can be added to the CFD model so that drag and lift can be finely controlled. In the example the mock up model of a MotoGP is parametrized and an improvement of 23% in downforce, together with a 3.5% drag reduction is achieved [9]. Structural optimization of the wheel rim of a Ducati Panigale [10] is conducted considering the stress at critical braking getting a lighter and less stressed (-21%) version of the component.

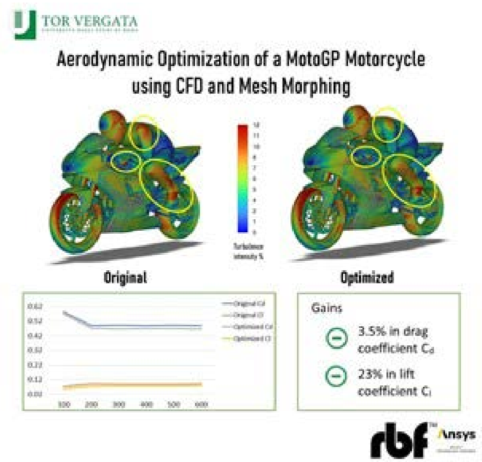

Figure 8: The picture shows how mesh morphing allows to reduce the drag and increase downforce of motoGP motorbike.

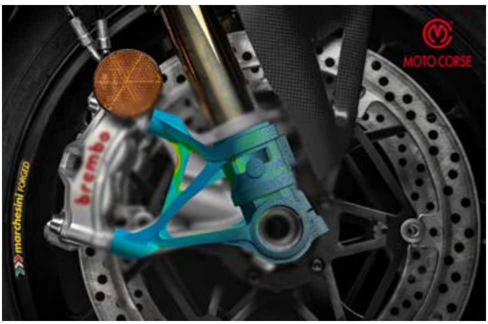

Figure 9: This picture shows how Moto Corse company managed to reduce the weight of the front wheel hub for a Ducati Panigale motorbike.

References

[1] Biancolini, M.E. Fast Radial Basis Functions for Engineering Applications (2017), Springer pp. 1-357.

[2] RBF Morph Fluids web page https://www.rbf-morph.com/add-on-ansys-fluent/

[3] RBF Morph Structures web page https://www.rbf-morph.com/act-module/

[4] Marco Evangelos Biancolini, Leonardo Geronzi. Integrating RBF Morph and LS-DYNA into Ansys Workbench and Mechanical for car bonnet crash optimization. Ansys Simulation World 2021. https://www.rbf-morph.com/wp-content/uploads/2021/04/RBF-Morphand-LSDYNAintoAnsysWorkbenchandMechanical.pdf

[5] Elisa Serioli, Corrado Groth, Simona Invernizzi, Marco Evangelos Biancolini. Fast and cost efficient CFD optimization by means of adjoint and RBF mesh morphing: a perspective from Dallara. Ansys Simulation World 2021. https://www.rbf-morph.com/wp-content/uploads/2021/04/FastandcostefficientCFDDallara.pdf

[6] Porziani, S., Groth, C., Waldman, W., Biancolini, M.E. Automatic shape optimisation of structural parts driven by BGM and RBF mesh morphing (2021) International Journal of Mechanical Sciences, 189, art. no. 105976.

[7] Porziani S., Groth C., Zhang H., Biancolini M.E. Stress mitigation of a thermal engine head block using the bioinspired BGM-FEM method. AIAS2023 6-9 September, Genova, Italy. https://www.rbf-morph.com/wp-content/uploads/2023/10/Aias2023RBFMorph_Porziani.pdf

[8] C.Groth, M.Marra, S.Porziani, M. Schubert, M.E. Biancolini. Advancing Structural Optimization of an Electric Motor Rotor through Mesh Morphing Techniques. AIAS2023 6-9 September, Genova, Italy. https://www.rbf-morph.com/wp-content/uploads/2023/10/Aias-2023RBFMorph_Porziani.pdf

[9] F. Ricci. Aerodynamic Optimization of a MotoGP Motorcycle using CFD and Mesh Morphing. BsC thesis, University of Rome Tor Vergata 2023. https://www.rbf-morph.com/wp-content/uploads/2024/01/FRicciRBFMorph_presentationeng.pdf

[10] Andrea Ridolfi, Luca Mancini, Chirianni Francesco, Felici Alessandro, Mirasoli Gabriele, Stefano Porziani, Marco Evangelos Biancolini. Ottimizzazione di un componente motociclistico attraverso il biological growth method. A&C. Analisi e Calcolo. 2020. https://www.rbf-morph.com/wp-content/uploads/2021/05/Analisiecalcolo2021.pdf

CAE Wissen by courtesy of Prof. Marco Evangelos Biancolini
Dipartimento di Ingegneria dell'Impresa "Mario Lucertini"
Università di Roma Tor Vergata

Latest info about this course

Engineering Seminar

Design for Durability - Lightweight Car Bodies and Fatigue

Course Course Description

Today lightweight design is of paramount importance in car body development. The objective is to save both material and energy during manufacturing as well as during use. All of this without sacrificing technical function, economy and safety of people and environment. Due to the inherent approach of lightweight construction to reach for the limits the load-bearing capacity of designs are often reached and the demand for durability - that is, adequate fatigue strength over the entire service life - suddenly comes to the fore.

Course Objectives

In the seminar first the basic principles of durability are presented with particular regard to the design of car bodies. Then the design principles of modern lightweight body construction are taught. In addition, the use of numerical simulation and mathematical optimization within the modern car body development process is explained.

After participating in the seminar, the participants will understand the influence of cyclical loading on the design of car bodies, will be able to identify problems in the design and will be able to resolve them using appropriate design methods. They understand how the fatigue analysis and geometric optimization enable the modern virtual development process.

Who should attend?

The seminar is aimed at engineers and technicians in the development departments of automotive manufacturers, suppliers and engineering service providers who deal with the design, construction, simulation and development of vehicle bodies, with special regard to durability.

Course Contents

- Remarkable cases of damage
- Loads and stresses during driving
  - Cyclic loading
  - Special loads
  - Misuse load cases
- Crack initiation and fracture behavior
  - Material fatigue
  - Failure criteria
  - Learning from real cases of damage
- Material and component strength
  - Finite life fatigue strength and endurance limit, Wohler curves
  - Fatigue strength under variable stress amplitude, Gassner curves
  - Scatter of fatigue strength
- Influence factors
  - Design, shape
  - Mean stress
- Lifetime (fatigue) simulation
  - Fatigue damage definition
  - Fatigue damage accumulation
  - FEA based fatigue analysis
- Design principles for lightweight car bodies
  - Direct load paths
  - Typical load paths in car body
  - Large moment of inertia
  - Filigree design of structures
  - Support through curvature
  - Intentional stiffening
  - Function integration
  - Framework design vs. shell structures
  - Application to practice-relevant cases

Instructor

Prof. Dr.-Ing. Udo Jung (THM University of Applied Sciences) studied mechanical engineering at the Technical University Darmstadt and promoted in the field of fatigue and finite element analysis at the Institute of Materials Science at the TU Darmstadt. At Adam Opel AG, he initially worked as a development engineer in the analysis department and introduced the fatigue life analysis in virtual vehicle development. Subsequently, he took over the management of the simulation and test methodology in the central durability laboratory. Since 2005 he has been a university professor for lightweight design and durability as well as construction and FE methods at the Technische Hochschule Mittelhessen (THM) at Friedberg Campus. In the field of research, he is at the forefront of the Competence Center for Automotive, Mobility and Materials Research (AutoM). He also heads the TransMIT Center for Lightweight Design and Durability of TransMIT Gesellschaft für Technologietransfer mbH, Giessen.

Facts

29.10.2025	170/4544	Alzenau	1 Day	890,- EUR till 01.10.2025, thereafter 1.090,- EUR	

Modern Fatigue Life Prediction of Welded Joints - Modeling, Definition and Evaluation

Introduction

Welded joints have a significant influence on the fatigue life of vehicle components due to considerably lower dynamic strength values. An efficient definition of the welds as well as the reliable evaluation of multiaxial loads represent additional challenges, especially for large welded structures. In order to meet these requirements, the Engineering Center Steyr has developed methods and tools which are demonstrated on the basis of the lifetime evaluation of a bus structure.

Problem description

A substructure of a bus (MockUP) was used for the investigations using a FE model consisting of shell elements with 3.6 million degrees of freedom.

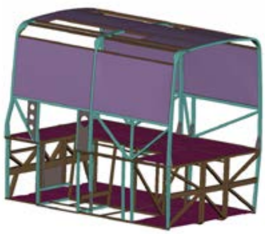

Figure 1: FE-Model of a bus substructure (MockUP)

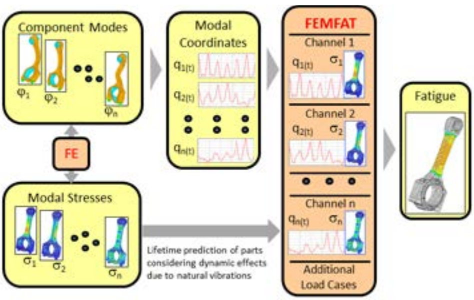

Figure 2: Workflow of a modal fatigue analysis

A modal approach was chosen for the simulation of the loads. The mode basis was determined using FEM and the participation factors of the individual modes in the total deformation were determined for each point in time in the multi-body simulation. In the fatigue life assessment tool FEMFAT the modal stresses are superimposed with the time histories of the mode participation factors and the local multiaxial stress-time history is obtained.

This method is applied for each driving maneuver and the resulting damages are summed up

Weld seam definition

The definition of the welding seams in the bus structure was fully automated. Based on geometrical information, the seam lines are detected fully automatically and the joint type is automatically assigned based on the topology (butt joint, T-joint, ...). The preprocessor FEMFAT visualizer enables the check and correction of the 846 fully automatically generated weld seam definitions within a few hours.

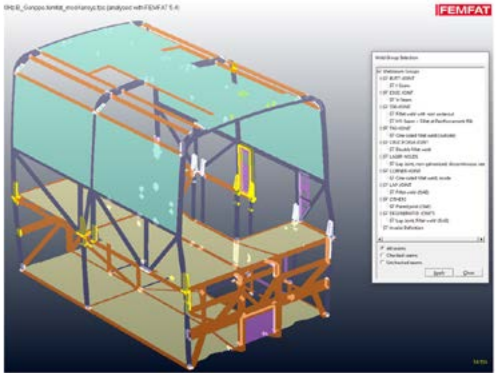

Figure 3: Visualization of the weld seams in the FE model - checked (yellow) and unchecked (white) seams

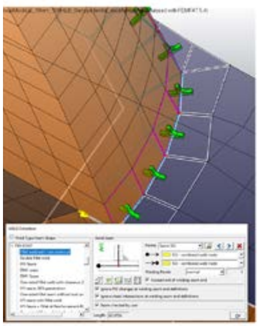

Figure 4: Visualization of the joint type/seam shape and the weld seam elements

A further significant reduction in effort is achieved by using generic default joints and considering a worst-case situation (e.g. T-joint web plate with root and toe notches on both sheet sides).

Fatigue life evaluation of the welds

In order to be able to perform a weld seam evaluation for such large structures efficiently and with high accuracy, a notch-based approach is applied. The notch factors determined from Radaj models for root and toe as well as seam start and end for each joint type and seam shape are stored in a database. In the damage calculation, the FE stresses of the shell elements are then scaled up with the corresponding notch factors and evaluated with the SN curves, which are also stored in the database for each evaluation point (root/toe, start/end).

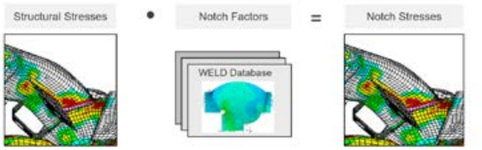

Figure 5: Workflow of notch stress based weld seam evaluation with shell models

Thus, despite simple shell modeling, you get detailed lifetime results. Not only the various assessment points are evaluated, but also the three stress components (normal stress perpendicular $\sigma_{\perp}$ and parallel $\sigma_{||}$ to the seam as well as shear stress τ) are considered.

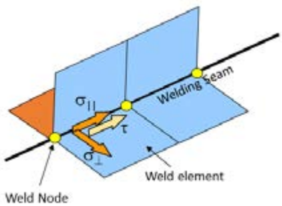

Figure 6: Stress transformation in local seam direction

$\sigma_{\perp,notch} = \sigma_{\perp,nominal} \bullet \beta_{\perp}$

$\sigma_{||,notch} = \sigma_{||,nominal} \bullet \beta_{||} \cong \sigma_{||,nominal} + \nu \bullet (\sigma_{\perp,notch} - \sigma_{\perp,nominal})$

$\tau_{notch} = \tau_{nominal} \bullet \beta_{\tau} \cong \tau_{nominal} \bullet (\beta_{\perp} + 1)/2$

$\beta_{\perp}$, $\beta_{||}$, and β_{τ}, are the notch factors for the individual stress components. These are stored in a weld seam database for all assessment points of each joint.

In order to account for the influence of the multi-axiality of the stress state, an equivalent utilization degree a_V is formed from the damages *D* of the individual stress components using the corresponding SN curve inclination *k*:

$$a_V = \sqrt{a_{\perp}^2 + a_{||}^2 + f \cdot a_{\perp} \cdot a_{||} + a_{\tau}^2}$$

with $a_{\perp} = D_{\perp}^{1/k}$, $a_{||} = D_{||}^{1/k}$, $a_{\tau} = D_{\tau}^{1/k\tau}$

The equivalent damage D_V is then calculated from the equivalent utilization degree a_V using a weighted averaged slope keff : $D_V = a_V^{keff}$

The mixed term $(a_{\perp} \cdot a_{||})$ is weighted with a factor *f*, where *f* can have values between -1 and +1:

$$f = -\cos\left\{2 \cdot \arctan\left[abs\left(\frac{X_{min}}{X_{max}}\right)\right]\right\}$$

X_{min} and X_{max} characterize the multiaxiality of the stress-time history according to DVS 1608

This avoids an erratic distribution of the damage along the seam, and on the other hand, slightly negative stress components do not immediately lead to very conservative results.

Analysis results

With the described analysis process, it is possible to carry out a detailed fatigue lifetime assessment of the welded joints, even for very large and complex structures.

In the following, the damage results at a welding node of the bus structure are shown as an example.

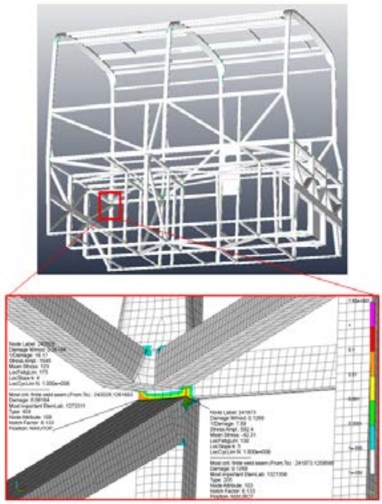

Figure 7: Fatigue analysis results of the welds

In summary, the following advantages can be noted:

- Very short processing time with high accuracy of results
- Damage analysis for base material and welded joints in one calculation run
- Detailed information about the critical point (root/toe, seam beginning/end, sheet side)
  → easier derivation of improvement measures

CAE Wissen by courtesy of Engineering Center Steyr GmbH, DI Klaus Hofwimmer

NVH - Background, Practice and Simulation Methodology

Course Description

In order to ensure the long-term success of a brand in the automotive sector, it is mandatory today to have a targeted design of the vibration and acoustic behavior of its products and thus achieve a high "perceived quality" of the company's vehicles. This functional design objective is generally called "NVH Noise, Vibration & Harshness".

After vibration comfort has been one of the core objectives of vehicle development for a long time, the acoustics in the passenger compartment more recently also became a competitive criterion, which today receives a lot of attention in the automotive industry.

The tasks of the NVH design can be divided into 3 areas:

- 1. Elimination of annoying vibrations.
- 2. Elimination of noise.
- 3. Design of the vehicle character.

To meet these design objectives, extensive developments in the fields of measurement technology and simulation methodology have been undertaken in recent years.

Course Objectives

In the two-day seminar, first the basics of NVH are presented. In this emphasis is placed on the physical background to understand the complex relationships in this field. Furthermore, the possibilities and limitations of simulation in the NVH area are explained using practical examples.

Who should attend?

Newcomers and development engineers who wish to gain an overview of the topic. Designers and engineers who want to broaden their knowledge about NVH criteria in the vehicle development process. Simulation engineers from engineering service suppliers that are looking to enter the NVH simulation or want to optimize their services. Project managers and senior executives from vehicle and component development who want to gain a better understanding of the background of the NVH methods.

Course Contents

- Introduction
  - Tasks & objectives
  - Historical development of NVH
  - NVH in the design process
- Basics of structural dynamics
  - Fundamentals
  - Frequency analysis
  - Modeling
  - Modal analysis
- Basics of acoustics
  - Sound propagation
  - Acoustic parameters
  - Room acoustics
  - Psychoacoustics
- Problem analysis in NVH
  - Noise sources
  - Analytical methods
- NVH measures
  - Basic concepts
  - Relevant components
  - Example: Isolation package
- Simulation methods
- Load cases in the NVH vehicle development process
- CAE Practice: Applications and examples from the areas:
  - Engine mounting
  - Body development
  - Chassis development
  - Optimization methods

Instructors

Prof. Dr.-Ing. Dietmar Jennewein (Darmstadt University of Applied Sciences) studied mechanical engineering at the University of Kaiserslautern. He received his PhD in 1998 in the field of vibration technology. He then joined the Adam Opel AG in the "Vehicle Simulation" department and worked in the NVH group on the analysis of vehicle vibration and vehicle acoustics using the FEM. Since 2001, Mr. Jennewein has been responsible as a group leader for all NVH simulation activity at Opel. He also led a multidisciplinary team for the metrological validation of the calculation procedure. Since 2011 he has been a professor at the University of Applied Sciences Darmstadt and lectures in the subjects of engineering mechanics, control and automotive engineering.

Prof. Dr.-Ing. Alexander Zopp (RheinMain University of Applied Sciences) studied mechanical engineering at the Technical University of Darmstadt. He received his PhD in 2000 in the field of finite elements in acoustics. He then joined Adam Opel AG to work in the Vehicle Simulation Department. In the NVH group he analyzed vehicle vibration and vehicle acoustics with the FEM. Later, Mr. Zopp introduced the Statistical Energy Analysis (SEA) in the development process of Opel to expand the detectable frequency range in the simulation. He was responsible for the global simulation methodology in the high frequency range in the GM group. Since 2011, Mr. Zopp served as Group Head of NVH simulation at Opel. Since 2013 he has been a professor at the RheinMain University of Applied Sciences and lectures in the subjects finite elements, engineering mechanics, machine dynamics and NVH.

Facts

	#				
29.09.-02.10.2025	153/4550	Online	4 x 4 Hrs.	1.450,- EUR till 01.09.2025, thereafter 1.750,- EUR	English
23.-24.02.2026	153/4632	Alzenau	2 Days	1.450,- EUR till 26.01.2026, thereafter 1.750,- EUR	German

Theory and Application of Multibody Systems in Automotive Development

Multibody system modeling plays a key role in the development of an efficient automobile. The design of quieter multibody systems is one important aspect of automotive development. Under the typical operating conditions of an automobile, the transmission system or gearbox is a major sources of noise and vibration. Multibody system modeling, such as analyzing the vibroacoustics of a gearbox, can help improve system designs and reduce noise radiation.

Understanding Vibration and Noise Path in a Transmission System

Transmission systems or gearbox assemblies are typically made up of a number of components, including the housing, gears, shafts, and bearings. Under the operating conditions of a typical gearbox, noise radiates through the surroundings. This is due to unwanted forces on the housing and bearings. Also, power is transmitted from shaft to shaft. Another factor that contributes to vibration and noise is the flexibility of certain parts, including the bearings, housings, and gear mesh. In fact, the gear mesh is the main source of the vibration and noise. Structural vibration, experienced in this scenario as noise radiation within the gearbox surroundings, typically follows the path shown below:

Figure 1: Typical noise path in a transmission system

Transmission Error within a Transmission System

Transmission errors (TE) are usually associated with gear whine. What actually is a transmission error? Consider two rigid gears with a perfect involute profile. The output gear's rotation is a function of both the input rotation as well as the gear ratio. Because the input shaft constantly rotates, the output shaft does as well. There are many reasons to modify a gear tooth profile, like gear runout, tooth tip, misalignment, and root relief. Geometrical errors and modifications such as these can cause errors in the output gear rotation. This phenomena is called the transmission error. Gear tooth deflection under dynamic loading can also add to the TE, which is then called the dynamic transmission error (DTE).

Noise in a Transmission System

Let's have a brief look on different types of noise that can be generated by gear meshing; namely the whine and rattle. Gear whine is a common type of gearbox noise that is present when the gearbox runs under loaded conditions. The noise is due to the vibration of the meshing gear teeth, because of transmission errors in the meshing and the varying contact ratio. Gear whine occurs at the multiples of the meshing frequency. Gear rattle, on the other hand, happens when a gearbox runs under unloaded or lightly loaded conditions. When diesel buses and trucks idle, they exhibit gear rattle. Gear rattle is induced by impact, and often caused by the presence of unloaded gear pairs in a gearbox. One of the main controlling parameters of gear rattle is backlash which cannot be completely eliminated, as it is required for lubrication purposes. However, gear rattle can sometimes be minimized by adjusting the amount of the gearbox backlash.

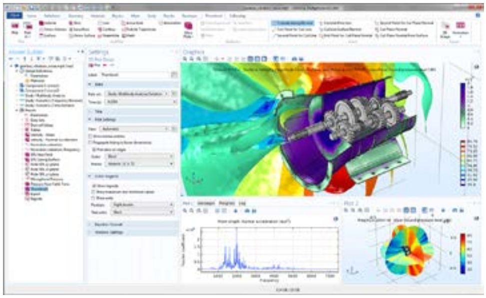

Figure 2: A gearbox modeled using COMSOL Multiphysics®.

Model of a Synchromesh Gearbox

Modern gearboxes are quite complex, often including many gears meshing at once. Minimizing gear whine and rattle in such a gearbox to acceptable levels can be challenging. By simulating such complex systems accurately, engineers can design less noisy gearboxes. The COMSOL Multiphysics® software enables simulation engineers to identify noise and vibration problems with accuracy, enabling them to propose viable real-world solutions that are within the accepted design constraints. Using the COMSOL® software, engineers can optimize designs that already exist by reducing noise, and analyze new designs early on in the development process.

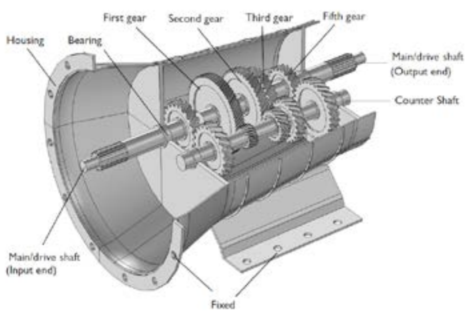

Figure 3: Geometry of a five-speed synchromesh gearbox for a manual transmission vehicle.

Let us use a five-speed synchromesh gearbox for our numerical modeling and simulation example. The goal of our simulation is to perform a noise and vibration analysis using two steps: multibody and acoustics analyses. The multibody study computes the gear and housing vibration dynamics in the time domain at a specific engine speed as well as output torque. The acoustics analysis involves computing the sound pressure levels that are outside of the gearbox over a wide frequency range, with the noise source as the gear housing's normal acceleration.

The details of the arrangement of gears in the gearbox are shown below. The helical gears help transfer power from the drive shaft's input end to the counter shaft, then to the drive shaft's output end.

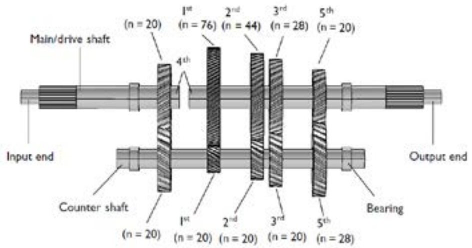

Figure 4: The gear arrangement without synchronizing rings.

The properties of the modeled helical gears include:

- Pressure angle: 25 [deg]
- Helix angle: 30 [deg]
- Gear mesh stiffness: 1e8 [N/m]
- Contact ratio: 1.25

The counter shaft's gears are fixed to the shaft, but the drive shaft's gears are able to rotate freely. A single gear is fixed on the shaft at a time, which is achieved in the real world via synchronizing rings. The model includes hinge joints, and an activation condition makes it so they can be conditionally engaged or disengaged with the drive shaft.

Both the shafts are assumed rigid. They are connected to the housing via hinge joints. We assume that the housing is flexible; mounted on a chassis; and, at one end, connected to the engine. The simulated driving conditions include:

- Engine speed: 5000 [rpm]
- Load torque: 1000 [Nm]
- Engaged gear: 5

To simulate the noise radiation in the surroundings, an air domain is set up outside of the gearbox. A one-way coupling is used to connect the acoustics and multibody dynamics studies, as the exterior fluid is air. With this setup, we can infer that the gearbox housing vibrations are affecting the fluid, and we can neglect the feedback coming from the acoustic waves to the structure. We perform the acoustics analysis for a wide frequency range and solve the multibody analysis in the time domain. The FFT solver is used to convert housing accelerations to the frequency domain from the time domain.

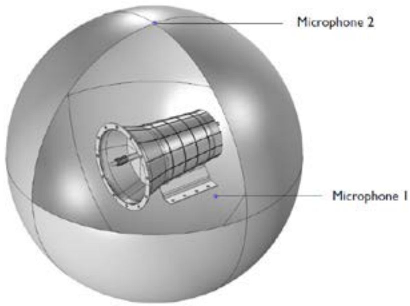

Figure 5: The air domain that encloses the gearbox, with two microphones for noise level.

Analyzing the Results of a Gearbox Model

To see that the normal acceleration is a function of time, you can pick a point on the gearbox housing and refer to the time history of the normal acceleration at that point. The FFT solver can be used to transform these results to the frequency domain and compute the vibration frequency. Looking at the frequency response plot, there is more than one dominant frequency in the normal acceleration of the housing. The housing vibration is dominant in the 1000–3000-Hz frequency band.

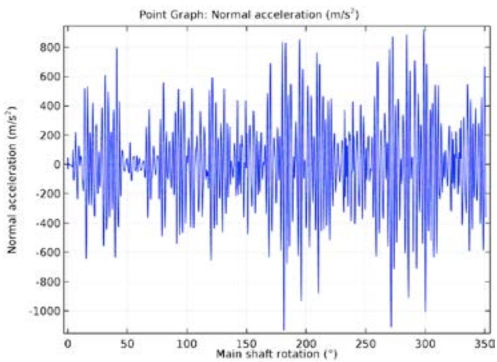

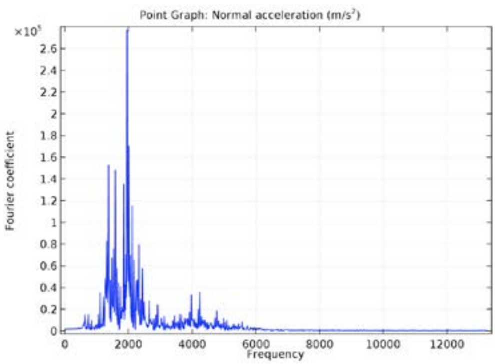

Figure 6: Normal acceleration of the gearbox housing, showing the time history (top) and frequency spectrum (bottom).

The gearbox housing's normal acceleration is applied on the acoustics domain's interior boundaries as a source of noise. To avoid exterior boundary reflections to the surrounding domain, a spherical wave radiation condition is applied. The settings enable you to perform an acoustics analysis, including computing the near-field sound pressure level, as well as on the gearbox housing surface at a range of frequencies. To better understand the noise radiation directivity, you can generate plots of the far field at different planes and frequencies.

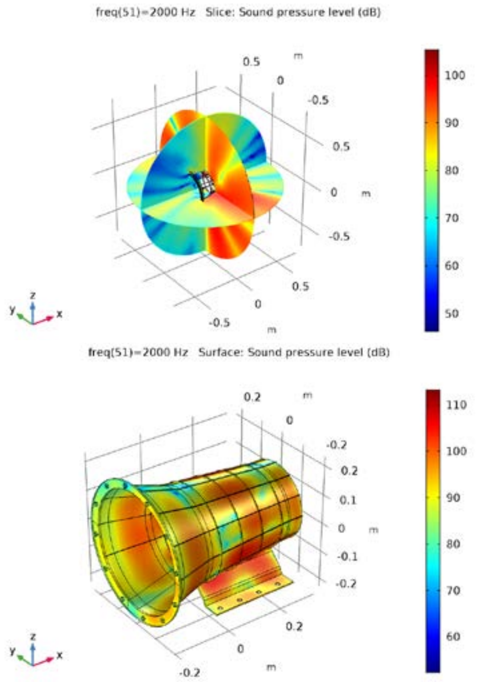

Figure 7: Near-field sound pressure level (top) and gearbox surface sound pressure level (bottom).

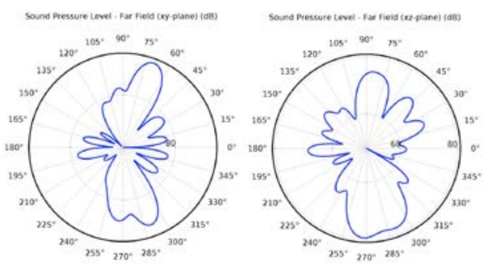

Figure 8: Sound pressure level in the far field at 1 m in xy-plane (left) and the xz-plane (right).

You might want to determine how the sound pressure varies by location, which can be done by putting two microphones in specified placements.

Microphone	Placement	Position
1	Side of the gearbox	(0, - 0.5 m, 0)
2	Top of the gearbox	(0, 0, 0.75 m)

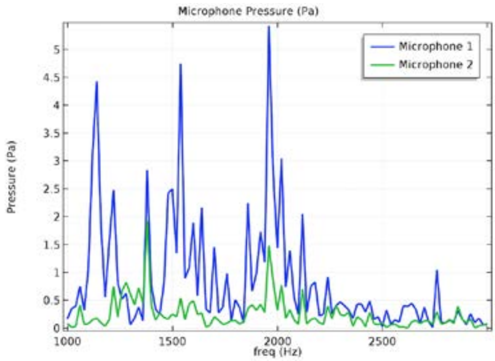

Figure 9: The pressure magnitude's frequency spectrum at two microphone locations.

The pressure response at the two microphone locations shows the frequency content that exists in the noise. What if you could actually hear the noise captured with each microphone as if performing a lab experiment? By putting Java® code into a method in COMSOL Multiphysics® and using the magnitude and phase information of the pressure as functions of frequency, this is possible. To get the time-domain acoustics results, on the other hand, you can transform the frequency domain results via the FFT solver, which helps to see the transient wave propagation in the gearbox's surrounding area.

Conclusion

To accurately compute noise radiation in a gearbox, you can couple multibody analyses and acoustics simulations. This technique is useful early on in your design process, because it enables you to optimize the gearbox design by minimizing noise radiation for a specific range of the gearbox's operating speeds. In order to move the simulation closer to a physical experiment, there is even the capability of including methods to hear the noise that the gearbox generates.

CAE Wissen by courtesy of Pawan Soami and Brianne Christopher – COMSOL Group

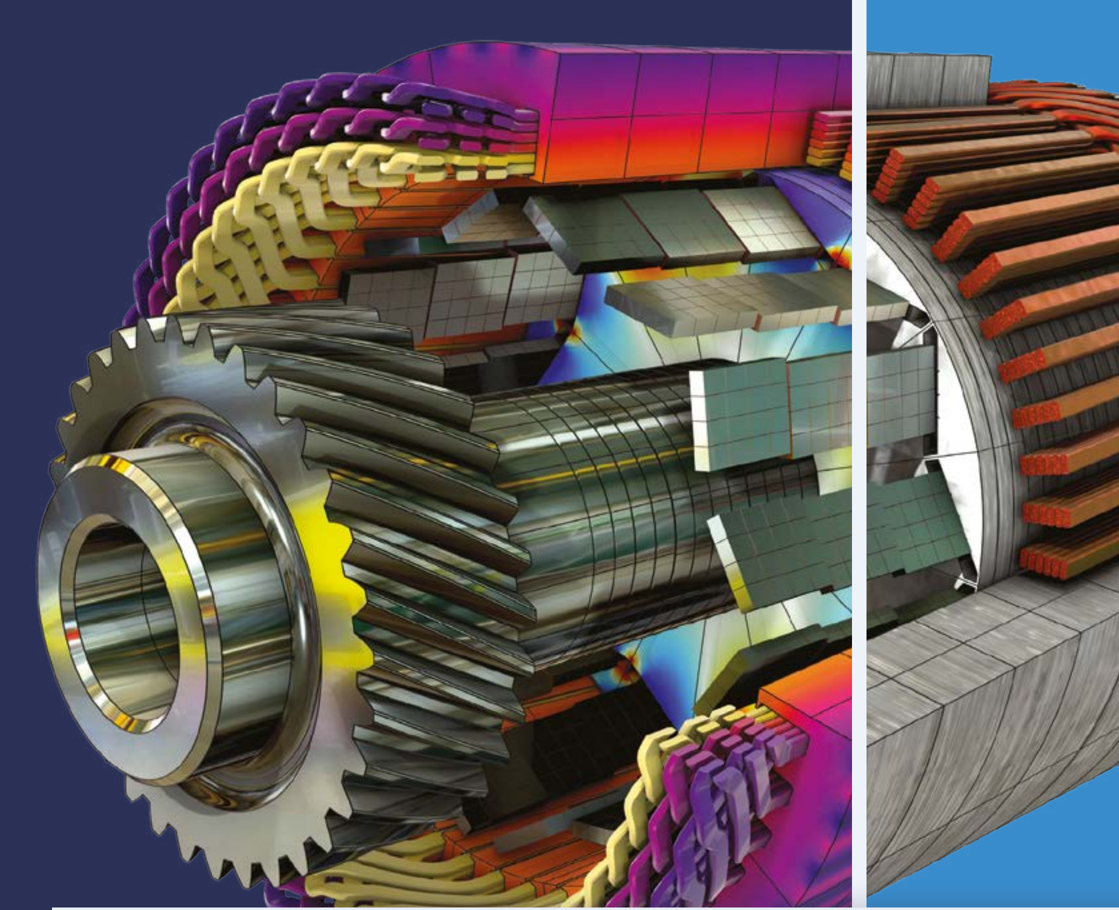

Design and Simulation of Vehicle Vibration

Course Description

The vibration characteristics of vehicles have a significant influence on driving performance and ride comfort. Therefore the design of the vehicle structure with regard to vibration targets is an integral part of the car body design process. Numerical simulation has become an indispensable tool within this process. The evaluation and optimization based on simulation results is only effective if the user has a profound knowledge about the underlying theories, the idealizations of reality associated with the simulation and the integration of simulation results in the product development process. In this one-day seminar the design and validation process of the vehicle structure's vibrational properties within the product development process will be presented. In particular, information on the theory of mechanical vibrations, the practical modeling and on the commonly used FE solvers Abaqus and Nastran will be provided. This information will be illustrated using practical examples from car body development.

Course Objectives

To understand the relationships of functional requirements and their design and simulation within the product development process. To Increase the knowledge about mechanical vibration theory as a basis for correct modeling and application of finite element software in vibration analysis. To expand the knowledge regarding vibration phenomena in vehicles and targeted design using computational methods.

Who should attend?

Engineers who are new in functional design and simulation. Designers, test engineers and technicians who want to expand their knowledge regarding the full vehicle design process. Simulation services providers who want to increase their understanding of vehicle vibrations to optimize their contribution to the car body design process. Project managers and managers from the vehicle and component development, who want to gain a better understanding of simulation methods.

Course Contents

- Functional requirements
  - Passive safety
  - Vibrations and acoustics
  - Durability
  - Fatigue life
- Product Development Process
  - Phases
  - Integrated design
  - Integrated validation
- Vibration requirements
  - Excitation sources
  - Targets
  - Conflicting goals
- Theory of Mechanical Vibrations
  - Categorization of oscillations
  - Free vibrations
  - Modal quantities
  - Forced oscillations
  - Resonances
  - Modal decoupling
- Modeling
  - System definition
  - Frequency range
  - System boundaries, boundary conditions
  - Structural model
  - Characteristic values and functions
  - Beam and shell theory
- FE simulations
  - Beam and shell elements
  - Numerical solution procedures
  - Eigen-value solvers
  - FEA software programs
  - Vibration analysis with Nastran and Abaqus
  - Assessment of simulation results
- Examples

Instructor

Prof. Dr.-Ing. Dietmar Jennewein (Hochschule Darmstadt) studied mechanical engineering at the University of Kaiserslautern. He received his PhD in 1998 in the field of vibration technology. He then joined the Adam Opel AG in the "Vehicle Simulation" department and worked in the NVH group on the analysis of vehicle vibration and vehicle acoustics using the FEM. Since 2001, Mr. Jennewein has been responsible as a group leader for all NVH simulation activity at Opel. He also led a multidisciplinary team for the metrological validation of the calculation procedure. Since 2011 he has been a professor at the University of Applied Sciences Darmstadt and lectures in the subjects of engineering mechanics, control and automotive engineering.

Facts

10.10.2025	125/4631	Alzenau	1 Day	890,- EUR till 12.09.2025, thereafter 1.090,- EUR	

Topology Optimization for Crash-loaded Structures

By using mathematical topology optimization methods, new structural layouts are generated. These methods are efficient in the field of structural design, taking into account linear structural properties and linear static loading conditions. E.g. the homogenization method introduced by M. Bendsøe and N. Kikuchi in 1988 (Comput. Methods Appl. Mech. Eng. 71:197–224) minimizes the mean compliance considering a mass constraint. Therefore, they divide the design space into a large number of small voxel and decide - based on an analytical sensitivity - for every voxel, is there material or not. After this optimization, the engineer has a good proposal and the possibility for the interpretation and the generation of a CAD model of the component.

The consideration of the mean compliance is much too simple for the optimization of crash-loaded structures. When crash load cases have to be considered, the special characteristics of the highly non-linear dynamic crash problems have to be taken into account. Large deformations and displacements occur during a crash incident. The used material laws are mostly nonlinear because the kinetic energy is absorbed by plastic deformation. For the correct prediction of the material behavior, strain rate dependencies and complex failure criterions have to be considered. The majority of the forces is transmitted via contacts. In additional to that, the crash simulation is much more complicate as the linear simulation of structures:

- non-smooth structural behavior
- not enough material data
- important scatterings of the material data
- mesh-dependent results
- physical bifurcations
- simulation bifurcations

In the topology optimization we deal with all these problems. We have requirements like:

- consideration of special acceleration values like the HIC values
- energy absorption,
- special force levels,
- smooth force-displacement curves,
- smooth acceleration-time curves,
- special force paths for special loadcases,
- high stiffness of special parts, e.g. parts in a main force paths in the passenger domain,
- low stiffness of special parts, e.g. at positions of the head contact of a pedestrian,
- special safety criteria, e.g. for the deformation of battery cells.

One of the first approaches in the area of topology optimization for crashworthiness was the work of R.R. Mayer et. al. in 1996 (Int. J. Numer. Methods Eng. 39:1383–1403). Their optimization method is based on the voxel method and an optimality criterion is used to maximize the energy absorption at specific weighted times. A resizing algorithm is utilized for the alteration of the design variables and a threshold algorithm is used to delete finite elements from the structure.

In the "**Hybrid Cellular Automaton (HCA)**" method of N.M. Patel et al. published in 2009 (J. Mech. Des. 131:061013.1–061013.12) an optimality criterion is used which is based on a homogenous distribution of the inner energy density. The design space is divided into cells in which the finite elements have an artificial density. These artificial densities have influence on the mechanical properties of the finite elements and are used as design variables for the optimization. The inner energy density distribution is homogenized with a material distribution rule, which changes the design variables. Neighborly relations can be taken into account by the "Cellular Automaton Lattice". Displacement, mass and force constraints can be considered in the optimization.

In order to be able to use the homogenization method mentioned above, which is based on the analytical sensitivities of the individual voxels, you can work with **substitute load cases** in a nested loop approach. These substitute load cases are derived from the complete crash simulation in the outer loop and can be mapped on a linear static voxel model in the inner loop.

The "**Equivalent Static Loads Method (ESLM)**" of G.J. Park published in 2011 (Struct. Multidisc. Optim. 43:319–337, 2011) uses artificial loads, which are generated in that way, that the deformation fields of the model in the outer loop and of the model in the inner loop are the same. Equivalent static loads are calculated for some discrete times of the nonlinear dynamic simulation. The linear static optimization in the inner loop is performed with a multiple loading condition using these equivalent static loads. Good topology optimization results can be found in an extension of the ESLM, published from J. Triller et. al. (Struct. Multidisc. Optim. 65:65-89, 2022). Another way to generate substitute load cases is to use the contact forces determined during the crash simulation. P. Clemens et. al. (Structures 55 (2023) p. 2013–2022) published an approach for crash-loaded deep-drawn components. An optimization result of this approach can be seen in figure 1. Goal is the maximization of the stiffness considering a mass constraint, a sheet-metal thickness side constraint, a constant wall thickness constraint in the whole structure, a no undercuts constraint in deep-drawing direction and no ribs constraint.

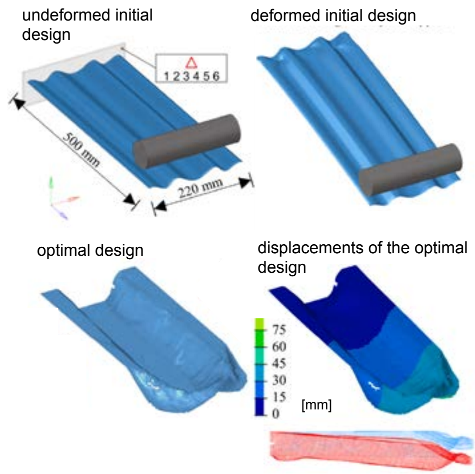

Figure 1: Nested optimization of the topology and shape optimization of a crash-loaded deep-drawn component

The "**Graph and Heuristic based Topology optimization (GHT)**" of C. Ortmann et. al. (Struct. Multidisc. Optim. 47:839–854, 2013 & 64:1063–1077, 2021) was developed because of the limitations of the previous voxel-based methods. The approach combines topology, shape and sizing optimization and use established finite element shell models for the crash simulation. The optimization task is divided into an outer optimization loop which performs the topology optimization and an inner optimization loop which performs the shape and sizing optimization (figure 2).

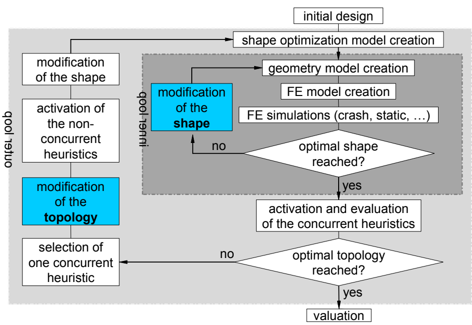

Figure 2: Basic optimization scheme of the Graph and Heuristic based Topology optimization (GHT)

The inner loop is carried out with mathematical optimization algorithms while the outer loop uses heuristics (rules), which are derived from expert knowledge. E.g.:

- delete unnecessary components,
- support fast deforming components in order to avoid buckling,
- balance energy density,
- use deformation space,
- smooth structure to simplify structures.

The basis for the modification of the geometry by the optimization software and for the automatic creation of input decks for the crash simulation is a flexible description of the geometry using mathematical graphs.

The first application is the optimization of profile cross-section of the structure abstracted by a planar graph, which reduces the geometric optimization problem to the second dimension, although the structure itself and all performed simulations are three dimensional. The first example is an academic application (figure 3): A simple frame structure clamped on the left side. A sphere with a mass of 1.757 kg hit the structure with an initial vertical velocity of 6.25 m/s. Two optimization tasks are considered:

1. minimize the maximum intrusion with a constraint of the mass ≤ 0.027 kg

2. minimize the maximum acceleration with a constraint of the intrusion ≤ 49 mm

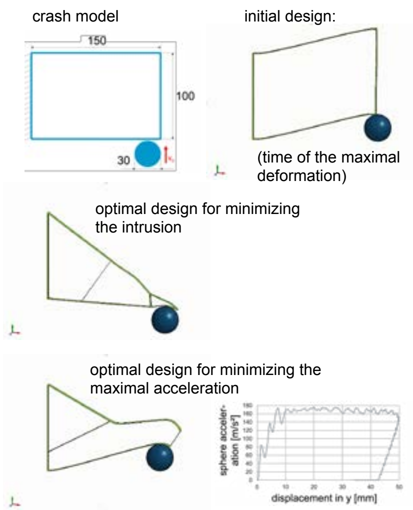

Figure 3: Topology optimization of a 2D-frame

The second example is a submodel of an automotive rocker again a pole (figure 4). The optimization task is to find the optimal topology and shape of the cross section of the rocker profile. The goal is the minimization of the maximal force at a moved rigid wall, so that some stiffness constraints and the manufacturing constraints are fulfilled.

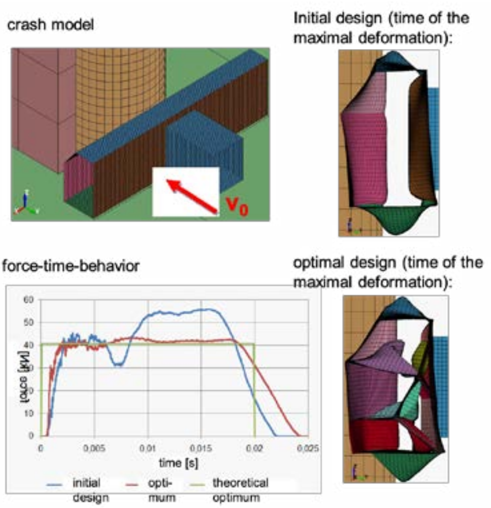

Figure 4: Topology optimization of a rocker

Especially the force-intrusion curve of the optimal result is impressively, because it is nearby the theoretical optimum (constant level during the entire crash time).

The third example is the optimization of a three-dimensional frame structure (F. Beyer et. al., Struct. Multidisc. Optim. 63:59-73, 2021). Profiles can be arranged by GHT. In this example (figure 5), all profiles in a structure should have the same cross-section and the same wall thickness.

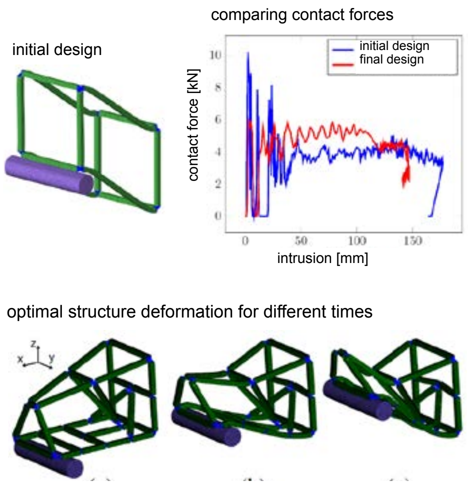

Figure 5: Topology optimization of a 3D-space structure

The optimizer has to minimize the maximum occurring contact force considering an intrusion constraint and a mass constraint.

The outer frame shape has been tapered in the shape optimization in the front upper area. The framework can be divided into two areas. The front area near the impact is more flexible, while additional profiles have been developed in the rear area near the clamping. As a result, the rear of the frame provides the rigidity needed to stop the cylinder before intrusion constraint.

An overview of the current possibilities of the GHT can be found in H. Altenbach et. al. (2024): Progress in Structural Mechanics, Chapter 10 “How Mechanically Inspired Design Rules Help in the Topology Optimization of Structures with Highly Nonlinear Behavior”.

CAE Wissen by courtesy of Prof. Axel Schumacher, Bergische Universität Wuppertal

Latest info about this course

Engineering Seminar

Structural Optimization in Automotive Design
Theory and Application

Course Description

In recent years numerical simulation has gained importance in all engineering disciplines. In the automotive industry the development process evolved from an experiment based to a virtual development process. Through this move towards simulation, mathematical optimization also gained importance and new opportunities for its application have been opened within the development process. Only a few years ago it would have been unthinkable to find the optimal cross section and the number and location of ribs for a cast part through mathematical optimization, which is now common practice.

As there exists no single optimization method that is suited for all problems it is important to gain an overview over various optimization methods and their characteristics. In the seminar the most popular and reliable optimization methods will be presented. The focus will be on the explanation of the basic concepts and ideas rather than on the detailed mathematical derivations and formulations.

Emphasis will be on practical applications. Possibilities for using optimization methods will be demonstrated through many industrial examples.

The following questions will be answered in the seminar:

- Which optimization methods are suited for which problems and which are not?
- How big is the optimization effort?
- How can the optimization effort be minimized?
- Which possibilities exist for the formulation of different optimization problems?
- What can lead to failure of an optimization?

Course Objectives

At the end of the seminar participants will have gained an overview over different optimization disciplines and procedures, the areas of application and their individual limitations.

Who should attend?

The seminar is suited for engineers and technicians from research and development departments, users that intend to enlarge or fresh up their background knowledge and newcomers that want to get an overview of the subject.

Course Contents

- Local and global optimization methods and coupled strategies
- Approximation methods
- Lagrange function, dual method
- Optimality criteria methods
- Bionic optimization procedures (CAO, SKO, evolutionary algorithms, optimization with particle swarms)
- Coupling with FEM
- Formulation of optimization problems
- Sensitivity analysis
- Determination of important variables and variable reduction
- Sizing
- Shape optimization, use of morphing techniques, topology optimization
- Robustness optimization
- Multi disciplinary and multi objective optimization
- Numerous application examples

Instructor

Prof. Dr. Lothar Harzheim (Opel Automobile GmbH) worked in the Group of Professor Mattheck on the development of the optimization programs CAO and SKO, before joining the simulation department of Opel. At Opel he is responsible for optimization, bio engineering and robustness. In this position he not only introduced and applied optimization methods but has also developed software for topology optimization. Prof. Dr. Harzheim regularly holds seminars for applied structural optimization and teaches at the Technical University of Darmstadt. He is the author of the book "Strukturoptimierung: Grundlagen und Anwendungen".

Facts

27.-30.10.2025	112/4563	Online	4 x 4 Hrs.	1.450,- EUR till 29.09.2025, thereafter 1.750,- EUR	English
03.-04.03.2026	112/4630	Alzenau	2 Days	1.450,- EUR till 03.02.2026, thereafter 1.750,- EUR	German

Robust Design Strategies for CAE-based Virtual Prototyping in the Automotive Industry

Due to a highly competitive market, the development cycles in the automotive industry have to be constantly reduced while the demand regarding performance, cost and safety is rising. CAE-based virtual prototyping and robustness evaluation helps to meet these market requirements. A CAE-based robustness evaluation creates a set of possible design variations regarding the naturally given input scatter. A stochastic analysis methodology is used to generate the sample set. Depending on the criteria, variance-based or probability based robustness evaluation have to be utilized. In variance-based procedures, a medium sized number (100 to 150) of input variables are generated by Latin Hypercube Sampling (LHS). The primary goal of robustness evaluations is the determination of a variation range of significant response variables and their assessment by using definitions of system robustness like limit value violations. By running a sample set of around 100 Latin Hypercube samples, reliable estimation of event probabilities up to 1 out of 1000 (2 to 3 Sigma range) is possible. For rare event probability estimations like 1 out of 1000000 (4 to 6 Sigma range), probability-based robustness evaluation is necessary. The secondary goal is the identification of correlations between input and response scatter as well as a quantification of "physical" and "numerical" scatter of result variables.

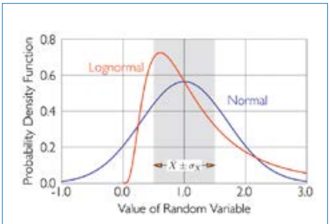

Figure 1: Normal versus Lognormal distribution, the figure visualizes that both distributions may have the same mean and standard variation but very different probability in the tails

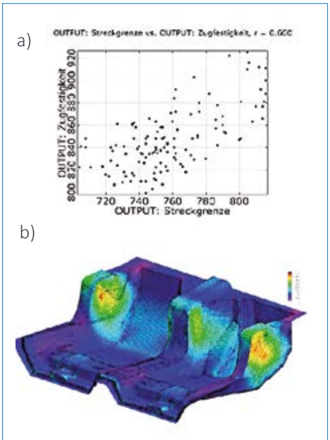

Figure 2:
a) correlation of scattering material parameter/

b) random field of initial stresses after forming process

The definition of the uncertainties forms the base for the stochastic generation of the sampling set. Because robustness evaluation requires knowledge of input scatter influence, the best available know-how needs to be transformed in the definition of input scatter including type of distribution function, correlation of single parameter or spatial correlations (random fields).

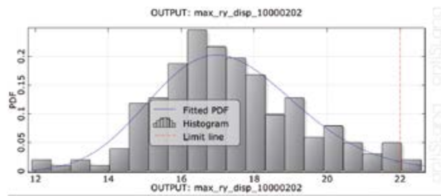

Statistic data			
Min:	11.9	Max:	22.58
Mean:	17.31	Sigma:	2.006
CV:	0.1159		
Skewness:	0.264	Kurtosis:	3.115
Fitted PDF: Log-Normal			
Mean:	17.31	Sigma:	2.006
Limit x = 22			
P_rel:	0.989474	1 - P_rel:	0.0105263
P_fit:	0.98349	1 - P_fit:	0.0165101
Sigma-Level:	2.33581		

Figure 3: Histogram for Robustness evaluation; the violation probability of the limit 22 is estimated at 1 to 2%

Within the framework of optiSLang the Metamodel of Optimal Prognosis (MOP) algorithms and the measurement of forecast quality (Coefficient of Prognosis-CoP) of the correlation model were developed to provide automatic reduction of dimensionality to the most important parameter. This is combined with automatic identification of the meta-model which shows the best forecast quality of variation for every important response value. At the same time, the amount of CAE solver calls necessary to reach a certain forecast quality can be minimized. This technology allows successful application of CAE-based robustness evaluation as a standard process to CPU intensive applications in the automotive industry.

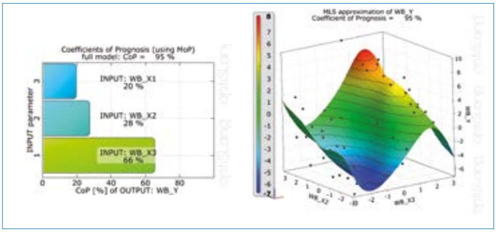

Figure 4: Coefficient of Prognosis (CoP) using the Metamodel of Optimal Prognosis (MoP) to quantify the input variable contribution to the response variable variation

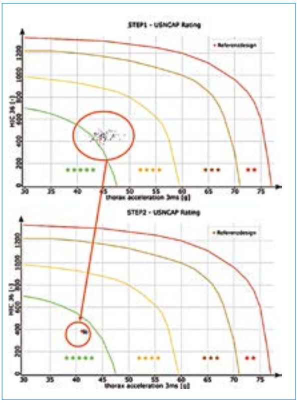

Figure 5: Visualization of robustness improvement of passive safety performance: upper diagram shows the scatter at milestone 1; lower diagram shows the scatter at final milestone of the virtual product development process

The goal of robustness evaluations for passive car safety applications is to investigate and improve the robustness of the restraint systems to fulfill consumer ratings and legal regulations of crash tests. Figure 5 shows an example how a restraint system was improved by FE-modeling and physical modifications to move the mean value and to reduce the response scatter.

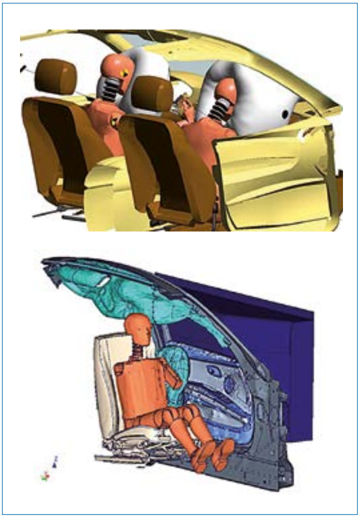

Figure 6: For passive safety applications multi body as well as finite element models are used in robustness evaluation

In passive safety applications, using MBS or FE-models, the quantification of numerical noise has become an important part of robustness evaluation. In other words, by investigating the quantity of numerical noise, an assessment of model quality is possible. Nowadays, by developing a reliable quantitative estimation of numerical noise robustness, the evaluation of passive safety applications is applied to regular procedures in virtual prototyping. It is necessary to provide state-of-the-art technology for the consideration of test setup (dummy positioning, crash pulse), airbag (mass flow, venting, permeability), sensors, belt system, door/interior stiffness and scatter of friction (Fig. 6). Besides the influencing dummy scatter, also the consideration of geometric body scatter in white car is a topic of interest. Automation of post processing is a key feature for productive serial use. Starting from response variation overview, the engineer can identify the critical response values regarding to variation (Fig. 7).

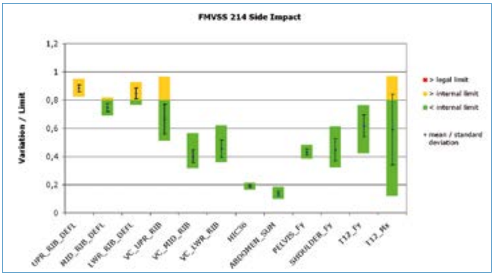

Figure 7: Summary of variation of all important responses for load case FMVSS 214

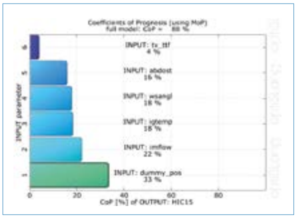

Figure 8: Coefficient of Prognosis for Variation of HIC15 values

In the serial use, the following added value can be expected concerning the dimensioning and increase of the restraint systems robustness:

1. Those scattering input parameters are identified that have significant contribution to important response scatter.
2. Model weaknesses are detected and numerical noise of significant vehicle performance variables is reduced.
3. The model robustness/stability and the quality of prognosis of crash-test computations are increased.
4. Robustness problems of the restraint systems are recognized and in cases of high violation of limits solved or improved by re-design of components.

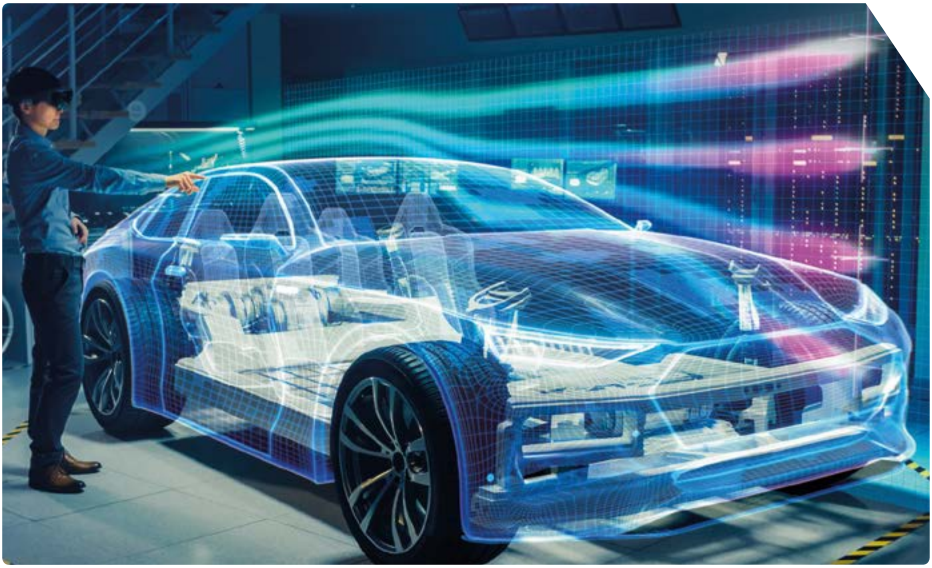

Stochastic Fracture of Polymer Materials

Polymer is a chemical notion comprising many different materials that strongly differ from the physical behavior of metals. All polymers consist of stochastically entangled long chain molecules. The differences relate to the number of crosslinks between them (Figure 1).

Figure 1: Molecular structure of polymers.

Due to their disordered structure, material properties as the tensile strength have a high statistical spread, compared to metals. In what follows, two acrylic glasses, one brittle and one impact resistant modified PMMA, are exemplified due to their stochastic fracture behavior.

Test Procedure

The fracture behavior under uniaxial stress state is examined in tensile tests on specimens which are milled out from injection moulded plates. The dimensions of the tensile specimen are given in Fig. 2.

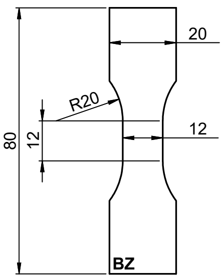

Figure 2: Geometry of BZ tensile specimen.

As the force-displacement curves in Fig. 3 indicate, load is applied reproducibly. Only the point of failure varies in a wide range, following a so far unknown distribution.

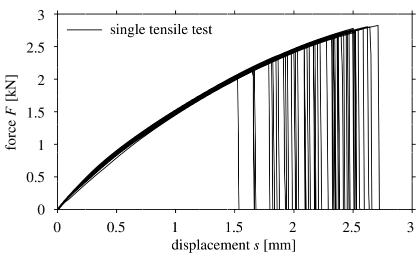

Figure 3: Force-displacement curves of 50 tensile tests on PMMA.

As an observable we choose the fracture strain that can be computed directly via the measured local displacements by digital image correlation (DIC). Using highspeed cameras, the local strain is determined at the position of the initial crack. A finite element analysis of the test allows for the examination of the stress triaxiality

$$m = -\frac{p}{\sigma_{\mathrm{vM}}} = \frac{\frac{1}{3}(\sigma_1 + \sigma_2 + \sigma_3)}{\sqrt{\frac{1}{2}[(\sigma_1 - \sigma_2)^2 + (\sigma_2 - \sigma_3)^2 + (\sigma_3 - \sigma_1)^2]}}$$

of the specimen which is shown in Fig. 4. The area of the initial crack is checked for a stress triaxiality of 1/3, i.e. a uniaxial stress state.

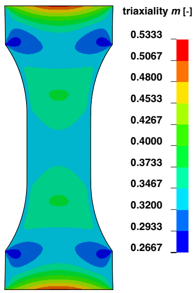

Figure 4: Stress triaxiality within specimen.

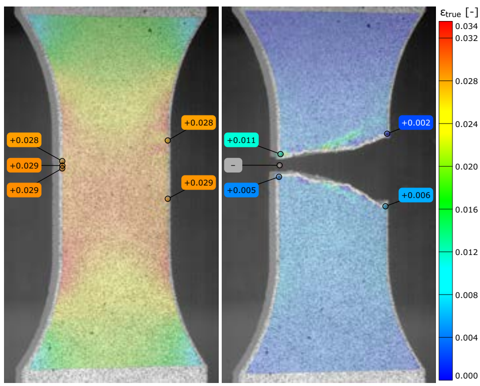

Figure 5: True strains received from DIC and initial crack in the area of uniaxial tension one picture before (left) and after failure (right).

If this condition is fulfilled, the corresponding strain is taken from the DIC analysis one picture before failure, see Fig. 5. In this manner, samples of at least 30 fracture strains are determined for different haul-off speeds.

Distribution Fitting

So far, the information on the probability for each fracture strain to occur is missing. Here, a so-called probability estimator is utilized. The n fracture strains ε_i of a sample are ordered ascendingly that $\varepsilon_1 \leq \varepsilon_2 \leq \ldots \leq \varepsilon_n$. Then, by WEIBULL's estimator

$$p_i = \frac{i}{n+1}$$

an occurrence probability p_i is assigned to each fracture strain, dependent on its position i in the order. Having the empirical data prepared, a probability distribution function P(ε) is to choose their reproduction. For the modified PMMA we consider exemplarily the 3-parameter Weibull distribution, whose cumulative distribution function (CDF) is given to

$$P(\varepsilon) = 1 - \exp\left[-\left(\frac{\varepsilon-\varepsilon_0}{\eta}\right)^{\beta}\right]$$

Its parameters β and η are fitted on the calculated pairs of values ($\varepsilon_i \mid p_i$) by minimization of the weighted residual sum of squares

$$WRSS = \sum_{i=1}^{n} [p_i - P(\varepsilon_i)]^2 \psi[P(\varepsilon_i)].$$

In this study we give higher weight to the lower function tail by

$$\psi(u) = \frac{1}{u}$$

which will show later to result in the best fit for the modified PMMA. The goodness of the gained fit is evaluated by the lower-tail generalized ANDERSON-DARLING test, whose test statistic is calculated by

$$A^2_{G,LT} = n\left\{\frac{1}{2} - 2p_n(1-u_n) - p_n^2 \ln(u_n) + \sum_{i=1}^{n-1}\left[p_i^2 \ln\left(\frac{u_{i+1}}{u_i}\right) + 2p_i(u_i - u_{i+1})\right]\right\}$$

The inspection of the goodness-of-fit of several probability functions identified the 3-parameter Weibull distribution as best reproduction of the empirical data. The fit results for five different tensile velocities on the modified PMMA are displayed in Fig. 6.

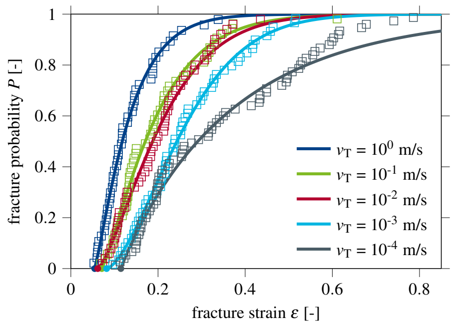

Figure 6: Fracture behaviour of modified PMMA at different haul-off speeds. Fit of 3-parameter Weibull distribution.

Detecting Outliers

For the brittle PMMA, the detection of the most suitable distribution is not that clear. Fig. 7 shows the fit of a bimodal Weibull distribution (BMW) on the quasi-static fracture strains.

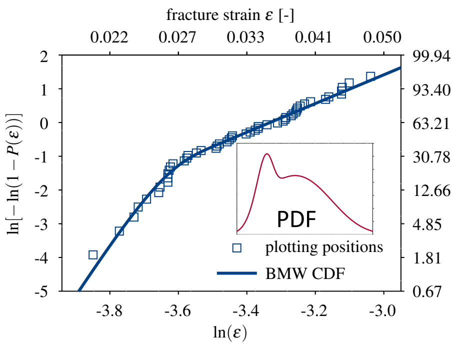

Figure 7: Quasi-static fracture strains fitted with bimodal Weibull distribution, visualized in Weibull Plot. In small: corresponding probability density function.

For visualization matters, the CDF is plotted on transformed axes. In this so-called Weibull plot, a Weibull distribution becomes a straight line. Thus, the bilinear progression of the empirical data points indicates the existence of two different populations in the sample. Indeed, a second inspection of the specimens shows two different fracture criteria. The group of lower fracture strains result from significant machining-flaws on the milled surface as demonstrated in the right picture of Fig. 8, where the view is vertical to the fracture surface (A).

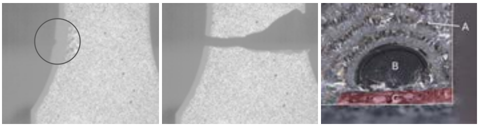

Figure 8: Initial crack arising from significant machining-flaw (left/ middle), confirmed by fracture mirror (B) within notch root (C) (right).

By search for the fracture mirror, the position of the initial crack can reliably be detected. Specimens with a starting point in a surface defect are then defined as outliers. In doing so, for the current sample a unimodal progression of the empirical data is reached. The best fit is gained by the Gaussian distribution. The five distribution functions are plotted in Fig. 9.

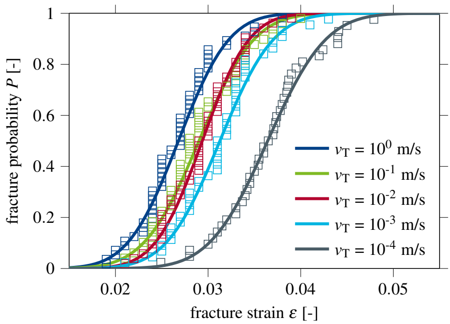

Figure 9: Fracture behaviour of brittle PMMA at different haul-off speeds. Fit of Gaussian distribution for stochastic simulations.

For a quick check on a sample the Gaussian distribution is a good reference. Its parameters can easily be estimated by μ = mean(ε_i) and σ = std(ε_i).

Application in Numerical Simulation

Both diagrams in Figures 6 and 9 demonstrate a characteristic behavior of polymeric materials. The statistical spread of the fracture strain declines with increasing strain rate. At the same time, the fracture strain level is reduced. This motivates a consideration of a strain-rate-dependent, stochastic fracture criterion in numerical simulation.

By knowledge of the probability distribution function P(ε) that reproduces the population of empirical data best, random fracture strains for a FE simulation are generated by the method of inverse transform sampling. A generator provides uniformly distributed random numbers R from 0 to 1. These inserted in the inverse CDF produce fracture strains of respective distribution. For the 3-parameter Weibull distribution this can be computed by

$$\varepsilon_{\text{rand}} = P^{-1}(R) = \varepsilon_0 + \eta[-\ln(1-R)]^{\frac{1}{\beta}}.$$

In order to obtain Gaussian distributed random fracture strains, two uniformly distributed random numbers are generated respectively, producing two sample points

$$\varepsilon_{\text{rand},1} = \mu + \sigma\sqrt{-2\ln(R_1)}\sin(2\pi R_2),$$

$$\varepsilon_{\text{rand},2} = \mu + \sigma\sqrt{-2\ln(R_1)}\cos(2\pi R_2).$$

For consideration of the strain rate, corresponding CDFs are chosen between which the fracture strain is then interpolated.

In summary, the stochastic fracture behavior of polymer materials must be taken into account for the safe design of components under both quasi-static and dynamic loading. Strain-rate dependent distribution functions are necessary to describe the fracture behavior adequately. Gaussian distributions for brittle plastics and Weibull distributions for ductile plastics seem to be first choice. Stochastic simulation is a useful tool in this context in which limiting quantiles have to be defined individually for each material.

CAE Wissen by courtesy of the Institute for Mechanics and Materials at the THM, University of Applied Sciences, Giessen.

Applus+ DatapointLabs

Testing more than 1800 materials per year

Expert Material Characterization and Model Calibration for Automotive Applications

Meet automotive industry challenges for CAE process and quality assurance:

- Characterize the properties of your materials to industry specifications
- Create robust and reliable material cards
- Accurately simulate the behavior of your materials
- Gain deeper insights into the performance of materials critical to automotive R&D

Automotive OEM Properties Testing

Composites, Plastics, Foams, Rubbers, Metals

- Tensile
- Compressive
- Shear
- Flexural
- Thermal

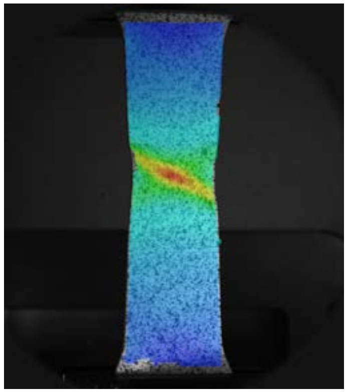

TestPaks® for CAE

CAE-ready material files for simulation

- Ansys LS-DYNA
- Altair Radioss
- Abaqus
- Autodesk Moldflow
- Ansys
- Altair Multiscale Designer
- ESI

See our online Test Catalog for all TestPaks supporting 30+ simulation codes.

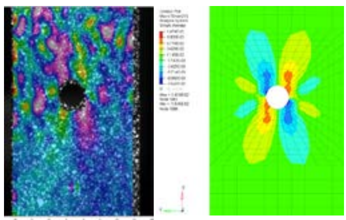

CAETestBench™

Validation of simulation

- Measure solver accuracy prior to use in product applications to gain confidence that the simulation replicates real-life physical behavior

Test Catalog

www.datapointlabs.com

Founded in 1995

Tel: +1-607-266-0405

EU: +353 86 898 0355

A2LA ACCREDITED ISO/IEC 17025:2017

Nadcap Administered by PRI ACCREDITED Non Metallic Materials Testing Materials Testing Laboratories

Introduction to the Python Programming Language

Course Description

Python is a modern programming language that is increasingly used in the field of Scientific Computing. Together with the environment scipy Python is an open source alternative to the commercial software MATLAB. A series of CAE software products, including the Pre-Processor ANSA, the solvers ABAQUS and PAM-CRASH and the Post-Processor META, are already using Python as an integrated scripting language. Python puts the emphasis on well-readable code, so beginners can learn the language very quickly. Nevertheless, Python is a powerful programming language and can also be used for larger projects. Further advantages of Python are the platform independence and the very extensive standard library supplied.

Course Objectives

The seminar provides a comprehensive introduction to the basics of the Python programming language. It also includes an introduction to object-oriented programming. Practical exercises, such as processing text-based files from the CAE world, will be treated. After the seminar, participants will be able to acquaint themselves with the Python interfaces of CAE software products.

Who should attend?

The seminar is aimed at newcomers to the Python language. Experience in other scripting or programming languages would be an advantage but is not a requirement.

Course Contents

- Basic concepts of the Python programming language
  - Introduction to the language
  - Data and control structures, functions
- Advanced topics
  - Processing of data
  - Important modules of the Python standard library
  - Examples from scientific computing
  - Modularization in bigger Python projects
- Practical exercises

Instructor

Dr. André Backes (TECOSIM Technische Simulation GmbH) studied Mathematics at the University of Duisburg. From 2000 to 2006 he was a researcher at the Institute for Mathematics at the Humboldt University in Berlin. His PhD studies at the chair for Numerical Mathematics introduced him to the field of CAE. Since 2006 he works at TECOSIM GmbH and among other topics specialized in NVH. In the area of Virtual Benchmarking he helped developing the TECOSIM-owned process TEC|BENCH where also the Python language was used. In current research projects he investigates the use of Python-based methods for data analysis and machine learning in the CAE process. Since 2020 he has been working at TECOSIM Stuttgart.

Facts

20.-21.05.2025	161/4558	Alzenau	2 Days	1.450,- EUR till 22.04.2025, thereafter 1.750,- EUR	German
02.-05.12.2025	161/4559	Online	4 x 2 Hrs.	1.450,- EUR till 04.11.2025, thereafter 1.750,- EUR	English

Application of Machine Learning to solve Engineering Problems

The concept of Machine Learning

The idea of artificial intelligence is to replace human made evaluations and decisions by a software based automatic process. One possible way is to build a rule-based software system where expert knowledge is implemented in a very explicit way. Disadvantage of this concept is sophisticated maintenance of such a system and also the fact that for many human made decisions explicit defined rules even are not specified. Looking to complex engineering systems we find a similar situation. Despite the fact that a lot of engineering systems can be described by physical laws for example in terms of differential equations there are also many huge systems derived for example from coupling several smaller systems where the input output behavior is not obviously well known. In real world systems we are additionally faced to stochastic inputs like noise which is unpredictable from a certain analytical point of view. Thus, as well in simulations as in testing activities we are faced to complex unpredictable correlations between input and output. This situation leads to the idea to learn these correlations from existing data.

Data Preparation and Feature Engineering

Data preparation and feature engineering are fundamental steps in the machine learning process. The quality of data and the skilful choice of extracted data features decide about the success when applying machine learning methods. A main step where necessary effort is underestimated in most cases is the process of collecting and providing the complete set of data to be investigated. In many cases there are several sources of data that have to be made comparable in order to be processed in a common way.

Figure 1 shows data points divided in three different classes. The left diagram visualizes the original data using the features "x" and "y" and the right diagram visualizes the features "magnitude" and "angle" arising from polar coordinate transformation of the original data

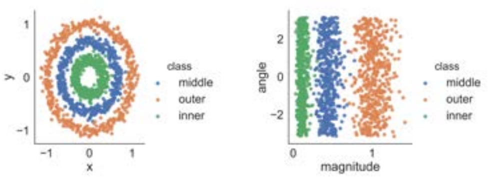

Figure 1: Left: Data described by features "x" and "y"; Right: Data described by features "angle" and "magnitude"

The programming language Python offers a lot of tools and packages for data preparation, visualization and machine learning. Figure 2 shows the table of data visualized in figure 1 stored in a DataFrame data structure from Python package pandas.

	x	y	magnitude	angle	class
0	0.736031	-0.011317	0.541869	-0.015375	middle
1	-0.444005	-0.588433	0.543394	-2.217205	middle
2	0.884205	-0.655863	1.211974	-0.638203	outer
3	-0.096443	-0.934155	0.881946	-1.673673	outer
4	-1.008296	0.188571	1.052220	2.956709	outer
	...	...	...	...	...
1495	-0.207368	0.389135	0.194428	2.060413	inner
1496	-0.383191	0.142339	0.167096	2.785933	inner
1497	0.149809	-0.345030	0.141489	-1.161166	inner
1498	-0.252743	-0.152214	0.087048	-2.599523	inner
1499	0.123888	-0.241328	0.073587	-1.096518	inner

Figure 2: DataFrame data structure from Python package pandas

Classification

Machine learning can treat different types of problems, mainly the two different tasks classification and regression. In classification tasks a decision has to be made between at least two or more classification types. A very famous popular example using artificial neural networks is to distinguish between pictures of cats and dogs. Engineers are now asked to find suitable engineering applications. Imaginable examples for engineering classification types might be: Does a given structure resist under defined loads (yes/no)? Will there be an acoustic resonance problem (yes/no)? Will the driver survive (yes/no)?

The following figures show some examples of machine learning classification methods. The intention of each method is to learn the decision regions for the different classes from the given training data. The red lines visualize the boundaries of these automatically determined regions. It must be stressed that it is not primarily the machine learning intention to separate the training data classes exactly. Main focus is to generate smart decision boundaries in order to predict future data almost correctly. Thus the quality check of a machine learning model must be performed using separate test data which were not included in the training data set. The effect that the machine learning model has too much explicit focus onto the training data is called overfitting. The overfitting effect can have different reasons for example the choice of a model with too high complexity or even to less data at all.

Figure 3 shows the very simple Nearest Neighbor Classifier where the class of a data point is defined by the nearest data point of the training data set in terms of a suitable metric. The visualization shows overfitting for the original data in the left diagram but very useful linear decision boundaries in the right diagram for the transformed data set.

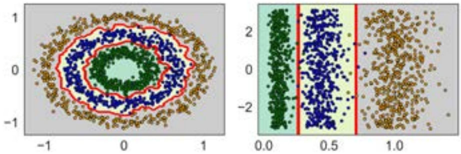

Figure 3: Nearest Neighbor Classification. Left diagram shows overfitting

Figure 4 shows a very naive application of the Decision Tree Classifier. Here both diagrams show overfitting. Decision Trees are very powerful but we have to use them correctly in order to get acceptable decision boundaries. A generalization of Decision Trees is for example the concept of Random Forests which overcome the problem of overfitting.

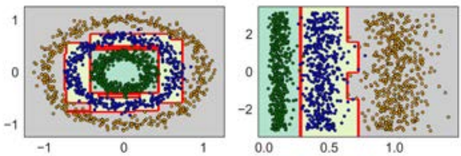

Figure 4: Naïve application of the Decision Tree Classifier leads to unusable overfitting decision regions

Figure 5 shows the application of Linear Regression to the polar coordinate transformed data set. Linear Regression is only applicable for linear separable data, thus it cannot be applied to the original circular shaped data. Comparing figures 3 and 5 we can see that Nearest Neighbor Classification and Linear Regression on the transformed data lead to similar decision boundaries.

All classification methods discussed here can be found in the Python package scikit-learn. Additional methods not mentioned yet are the famous Support Vector Machines and Neural Networks. Using Neural Networks is appropriate especially in case of huge amount of data and a high number of features. To study neural networks in deep the Python package keras is a good choice which is a user friendly interface for the Google software TensorFlow.

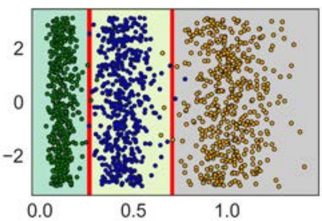

Figure 5: Classification by Linear Regression

Regression

In regression tasks the intention is to predict a continuous value depending on several input parameters. This situation actually is given in almost every engineering system.

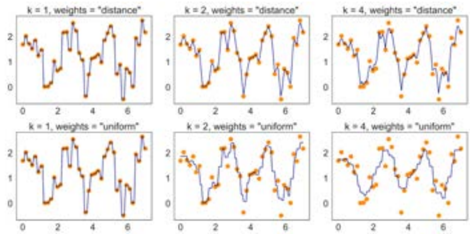

Figure 6: Regression using k nearest neighbor method with different values for k and two different options how to weight neighbor values

Figure 6 shows several examples of using the Nearest Neighbor method for regression in one dimension. The parameter k describes the number of neighbors included in the evaluation. In addition the parameter "weights" defines the way different neighbors are taken into account. The varying parameters lead to different treatment of noise and outliers in the data. Remarkable is that this method can be used in exactly the same way for data in arbitrary higher dimensions.

Clustering

The classification and regression tasks discussed before belong to the concept of supervised learning. This concept assumes already classified labeled training data. In case of data sets without given classification clustering methods might help to identify such data clusters, of course without any semantic interpretation in the first step. This type of machine learning methods is called unsupervised learning. One intention of applying such methods might be to find and extract significant features automatically. The Python package scikit-learn provides several different clustering methods.

Model Selection and Model Parameter Optimization

Beside suitable data preparation and feature engineering an appropriate choice of the machine learning model leads to successful machine learning applications. In addition to several implemented machine learning methods the Python package scikit-learn also offers efficient tools to identify optimal model parameters. The optimal choice of such parameters always depends on the individual data.

Dimensionality Reduction

Machine learning methods are in general remarkably scalable with respect to the number of features and number of data. Nevertheless it is always recommendable to consider feature reduction in order to increase the performance by dimensionality reduction of the machine learning task. There a two relevant ways of feature reduction methods, feature selection and feature extraction, both implemented in the Python package scikit-learn. Feature selection figures out which subset of the given features are really significant for the machine learning task. A well known method of feature extraction is principal component analysis. The underlying coordinate transformation might be critical for engineering applications due to the undefinded physical meaning of extracted features. Figure 7 shows that a pairplot visualization can help to identify redundant features.

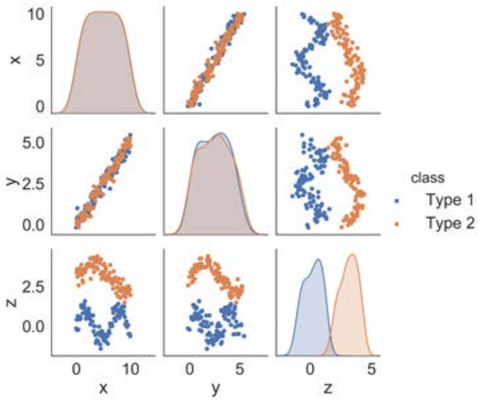

Figure 7: Pairplot of features x, y and z, shows linear dependency of x and y

Conclusion

Machine Learning can help to automate classification and regression tasks based on existing data. The machine learning ecosystem of the programming language Python offers several tools for using these machine learning methods to process and understand own existing data sets. For machine learning applications in engineering context engineers are requested to interpret their challenges in a suitable way such that learning from existing data becomes possible and fruitful.

Internet links for Python packages

- Programming language Python https://www.Python.org
- Anaconda https://www.anaconda.com
  Python distribution including management of packages for machine learning
- Pandas https://pandas.pydata.org
  Data preparation using the DataFrame data structure
- Scikit-Learn https://scikit-learn.org
  Methods for data transformation and machine learning
- Keras https://keras.io
  Interface to Google's software TensorFlow for using artificial neural networks
- Matplotlib https://matplotlib.org,
  Seaborn https://seaborn.pydata.org
  Tools for data vizualization

Literature

Albon, C. (2018). Python Machine Learning Cookbook: Practical solutions from preprocessing to deep learning. O'Reilly UK Ltd.

Müller, A. C., & Guido, S. (2016). Introduction to Machine Learning with Python: A Guide for Data Scientists. O'Reilly UK Ltd.

Zheng, A., & Casari, A. (2018). Feature Engineering for Machine Learning Models: Principles and Techniques for Data Scientists. O'Reilly UK Ltd.

CAE Wissen by courtesy of Dr. André Backes, Technical Manager, TECOSIM Technische Simulation GmbH

Python based Machine Learning with Automotive Applications

Course Description

The topic of Artificial Intelligence (AI) is currently becoming more and more important, in particular in areas where processes are automated and many data are processed. Especially in automotive area as well in the virtual development process as in the field of testing, numerous applications are conceivable in this context. A part of artificial intelligence is machine learning, which is becoming increasingly important in addition to classical rule-based expert systems. This current development is due to the generation of ever-larger datasets (big data) as well as more powerful computers for their processing.

Especially in the automotive environment, extensive data are generated in the context of simulation or testing, for which an automated analysis is often sought. In addition to the classical interpretation of individual simulation or testing results, the methods of machine learning allow a new view at models and results. Based on the analysis of numerous results (big data), e.g. from parameter studies, it is possible to derive Artificial Intelligence using methods of machine learning, which is then used to evaluate further simulations or tests.

Python is currently the most popular programming language for data analysis and machine learning. The freely available Python library Scikit-Learn provides a user-friendly entry to the relevant procedures. Especially the application of artificial neural networks (Deep Learning) has become very popular lately. The software TensorFlow developed by Google and the Python library Keras based on it provide a beginner-friendly access.

Course Objectives

The seminar gives an introduction to machine learning based on the programming language Python. This includes, as a start, topics of data analysis, preparation and visualization.

In the second step, methods of machine learning are studied using the Python packages Scikit-Learn and Keras or TensorFlow. Practical exercises will deepen the topics discussed and discuss possible applications in CAE or testing. An important aspect of data analysis is the extraction of features from CAE or testing data for the use in machine learning. After the seminar participants will be able to tackle the implementation of their own tasks. This also includes evaluating various methods of machine learning regarding their applicability to one's own tasks and to deepen the methods based on the discussed Python packages.

Who should attend?

The seminar addresses participants coming from CAE or testing field who want to take the first steps in machine learning based on their Python knowledge. It is assumed that basic Python knowledge - e.g. as it is conveyed in the carhs.training seminar Introduction to the Python Programming Language of the same trainer - exists.

Course Contents

- Basics of data analysis with Python
  - Data structures
  - Concepts of data preparation
  - Extraction of features for machine learning methods
  - Data visualization
  - The Python packages Numpy, Scipy, Pandas, Matplotlib
- Machine Learning with Python
  - Methods for classification and regression analysis
  - The Python Package Scikit-Learn
  - Deep Learning and Neural Networks with Keras, TensorFlow
- Applications motivated by CAE or testing background
  - Introductory examples
  - Discussion of possible deeper applications
  - Procedure for implementing your own ideas

Instructor

Dr. André Backes (TECOSIM Technische Simulation GmbH) studied Mathematics at the University of Duisburg. From 2000 to 2006 he was a researcher at the Institute for Mathematics at the Humboldt University in Berlin. His PhD studies at the chair for Numerical Mathematics introduced him to the field of CAE. Since 2006 he works at TECOSIM GmbH and among other topics specialized in NVH. In the area of Virtual Benchmarking he helped developing the TECOSIM-owned process TEC|BENCH where also the Python language was used. In current research projects he investigates the use of Python-based methods for data analysis and machine learning in the CAE process. Since 2020 he has been working at TECOSIM Stuttgart.

Facts

02.-05.06.2025	185/4560	Online	4 x 2 Hrs.	1.450,- EUR till 05.05.2025, thereafter 1.750,- EUR
27.-28.10.2025	185/4561	Alzenau	2 Days	1.450,- EUR till 29.09.2025, thereafter 1.750,- EUR

Artificial Intelligence and Machine Learning for ADAS and ADS - Introduction and Basics

Course Description

The functions of automated driving - no matter what degree of automation - usually require the application of modern artificial intelligence techniques in order to be able to realize the desired functionalities at all. The aim of this seminar is to present the basic methods of Artificial Intelligence and Machine Learning. The methods should be demonstrated with concrete examples from the fields of assisted and automated driving. Care is also taken about validation, verification and safeguarding of the related models and AI-based software components.

Course Objectives

This seminar provides an overview and a brief introduction to the relevant methods of Artificial Intelligence and Machine Learning, so that both developers and managers can clearly decide which methods and procedures are relevant for their applications and which possible pitfalls they should consider in the application.

Who should attend?

Developers and (project) managers who have not yet had deep experience with the methodology and want to get a quick overview and introduction to the use of artificial intelligence.

Course Contents

- Introduction of data-based development versus analytical and rule-based approaches
- Overview of the different procedures and areas of application
- Artificial Neural Networks, Deep Learning, various variants and architectures
- Decision and regression trees
- Support Vector Machines
- Validation and safeguarding of models, sampling procedures, robustness assessment
- Data preparation and problem parameterization
- Meta modeling and model committees

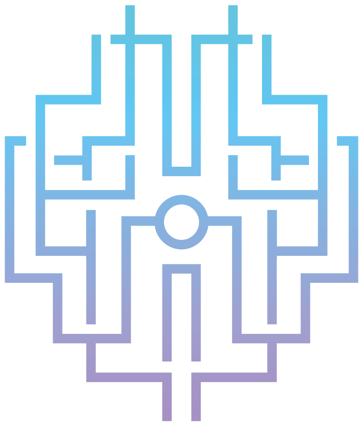

Instructor

Dr. Andreas Kuhn (Andata Entwicklungstechnologie GmbH) studied Technical Mathematics and Mechanical Engineering at the Technical University of Vienna. After his dissertation on the simulation of special satellite formations for the European Space Agency, he began his professional career in crash simulation at BMW. After further years as a consultant for stochastic simulation at EASI Engineering GmbH (today carhs), he founded ANDATA in 2004, where he is responsible for development and research as managing partner. Since 2009 he has also been co-owner of Automotive Safety Technologies GmbH in Gaimersheim. His professional interests are founded in effective and efficient development, validation and assessment methods for complex, safety-critical systems. In particular, he has been working for more than 20 years on the development and combined application of methods from the fields of artificial intelligence, machine learning, advanced simulation methods, scenario-based approaches and according process models in the virtual development of vehicles and autonomous robots. His current activities are the development and implementation of cooperative, networked, automated driving strategies for effective traffic automation.

Facts

21.-22.10.2025	186/4485	Alzenau	2 Days	1.450,- EUR till 23.09.2025, thereafter 1.750,- EUR	German

Latest info about this course

CAE Tools Seminar

Simulation for Automated Vehicles - Introduction to Scenarios, ODDs and Validation

Course Description

The complexity of modern driver assistance systems and automated driving functions sometimes requires completely new methods and approaches for their development, validation and testing. In particular, the wide coverage and analysis of functions with numerical simulation over the entire operating range (the so-called Operational Design Domain) is an indispensable tool for the effective and efficient development of appropriate vehicle functions. The course is about presenting the basics of scenario-based and data-based development and putting them in a holistic context.

Course Objectives

The course provides an overview and a brief introduction to the relevant scenario management methods for simulation and data-centric development and validation of automated driving functions. Some key basic principles in the development of complex systems are to be taught.

Who should attend?

The seminar addresses employees of automotive manufacturers, suppliers, engineering service providers, government agencies and research institutions, who are engaged in the development and validation of automated driving functions. In particular, method and process developers, simulation and test engineers are also addressed, who are responsible to implement corresponding processes and methods in their companies to ensure safe development and assessment of automated driving functions.

Course Contents

- Overview of the basic functions of automated driving
- Basics of Scenario and Data-based development
- Basics in Machine Learning, Data Mining and Artificial Intelligence
- Stochastic Simulation, Monte-Carlo-Simulation, Design-of-Experiments
- Optimization and automated calibration
- Robustness and complexity management
- Anomaly and fault detection
- Development processes for complex systems and software, top-down versus bottom-up
- Functional requirements management
- Validation and verification
- Definitions Operational Design Domain
- Effectiveness assessment of system functions and components
- Quality management for simulation data

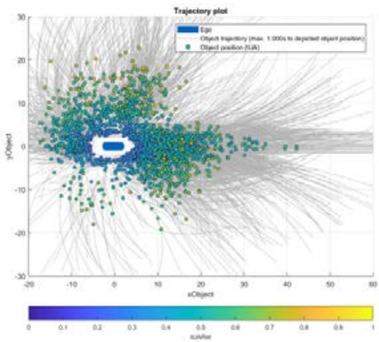

Instructor

Dr. Andreas Kuhn (Andata Entwicklungstechnologie GmbH) studied Technical Mathematics and Mechanical Engineering at the Technical University of Vienna. After his dissertation on the simulation of special satellite formations for the European Space Agency, he began his professional career in crash simulation at BMW. After further years as a consultant for stochastic simulation at EASI Engineering GmbH (today carhs), he founded ANDATA in 2004, where he is responsible for development and research as managing partner. Since 2009 he has also been co-owner of Automotive Safety Technologies GmbH in Gaimersheim. His professional interests are founded in effective and efficient development, validation and assessment methods for complex, safety-critical systems. In particular, he has been working for more than 20 years on the development and combined application of methods from the fields of artificial intelligence, machine learning, advanced simulation methods, scenario-based approaches and according process models in the virtual development of vehicles and autonomous robots. His current activities are the development and implementation of cooperative, networked, automated driving strategies for effective traffic automation.

Facts

25.-26.09.2025	187/4487	Alzenau	2 Days	1.450,- EUR till 28.08.2025, thereafter 1.750,- EUR	

A Computer Method to Calculate Occupants' Pre-Crash Kinematics under extreme Braking in Rotated Seat Arrangements

The introduction of automated Level 5 driving technologies will revolutionise the design of vehicle interiors and seating configurations, improving occupant comfort and experience. It is foreseen that pre-crash emergency braking and swerving manoeuvres will affect occupant's posture, which could lead to potential interactions with a vehicle interior trim and occupants to occupant's head collisions. A method is proposed to calculate the occupant's head envelope inside vehicle cabins in rotated seat arrangements [1].

STEP 1: Validation of the Madymo Active Human Model (AHM) kinematics

The research used two different sets of volunteer tests experiencing vehicle manoeuvres, based in the first instance on 22 50th percentile fit males wearing a lap-belt (OM4IS), while the other dataset is based on 87 volunteers with a BMI range of 19 to 67 kg/m² wearing a 3-point belt (UMTRI), as per Figure 1. Unique kinematics corridors were defined [2], as a function of belt configuration and vehicle manoeuvre, to calibrate an AHM using a multi-objective optimisation coupled with a Correlation and Analysis (CORA) rating.

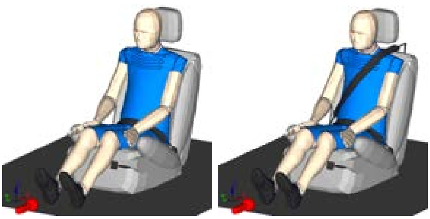

Figure 1: AHM kinematics setups (R: OM4IS; L: UMTRI)

The Optimum AHM parameters for a lap-belt configuration are provided in Table 1 [2].

Activation	Neck	0.5
	Spine	3.0
	Shoulder	3.0
	Elbow	3.0
	Hip	0.5
	Knee	0.5
Head Orientation	Head	0
Awareness	Neck_CCR	0.6
	Reaction Time	0.0 ms
Strength	Global	2.86
	Neck	↑
	Arms	↑
	Legs	↑

Table 1: Optimum Madymo AHM parameters for lap-belt

Research has proven that the standard AHM activation settings were adequate in 3-point seatbelt scenarios [2].

STEP 2: Creating a Design of Experiment (DOE) to compute the kinematics of an occupant wearing a 3-point seatbelt in rotated seating arrangement.

The occupant is placed in a sled model where a braking pulse is applied. To represent the effect of different driving directions, the Acceleration Angle direction (AA) is rotated, as per Figure 2. For example, 90° implies a swerving acceleration.

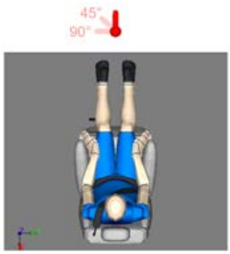

Figure 2: Rotated Seat Arrangement. The red arrow indicates the driving direction

The following design domain is computed:

- AA: varied from 0° to 360° in steps of 22.5°
- The Seat Back Angle (SBA): varied from 20° to 60° in steps of 8°.

Figure 3: SBA change. Left 20°, middle 45° and right 60°

STEP 3: Reduced Order Model (ROM) creation of occupant kinematics, varying only AA.

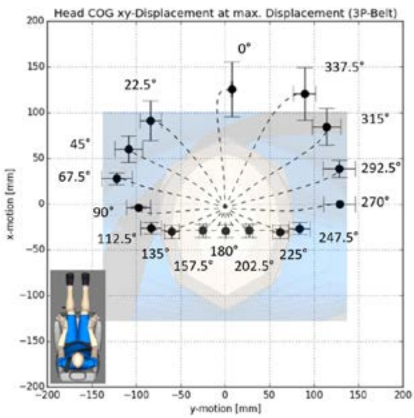

Figure 4: Head kinematics for a 20° SBA

The DOE kinematic responses are plotted in Figure 4.

In order to capture all the kinematic responses for a varying AA and constant SBA, a ROM model is created using Hexagon ODYSSEE Lunar. This ROM is then tested against scenarios containing AA values outside the DOE. The CORA value of this ROM prediction was compared to the Madymo X and Y displacement responses, considering the dispersion corridors evaluated in previous research [2]. Table 2 and Figure 5 suggest that the ROM model's predictions are excellent.

Case	SBA	SA	CORA	ISO/TR 9790
1	20	10	0.99	excellent
2	28	280	0.98	excellent
3	36	50	0.97	excellent
4	45	280	0.91	excellent
5	52	100	1.00	excellent
6	60	190	0.93	excellent

Table 2: ML Validation Test

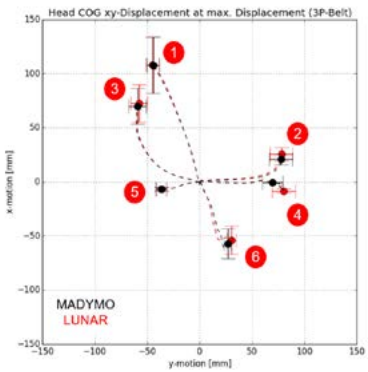

Figure 5: ML prediction of head motion for a varying SA

STEP 4: Reduced Order Model (ROM) creation of occupant kinematics varying both AA and SBA.

The same process is undertaken as STEP 3, but ensuring that the ROM model was tested with unknown values both for AA and SBA. Overall, the CORA results are excellent, except for point 7, which may require more data points in its area to improve predictions (Table 3).

Case	(SBA)	(SA)	CORA	ISO/TR 9790
7	25	10	0.68	good
8	30	280	0.98	excellent
9	40	50	1.00	excellent
10	50	280	0.95	excellent
11	50	100	0.97	excellent
12	55	190	0.95	excellent

Table 3: ML Validation Test, varying SA and SBA values outside the DOE

The differences in kinematics predictions are presented in Figure 6. The ROM model has successfully captured the maximum head excursions.

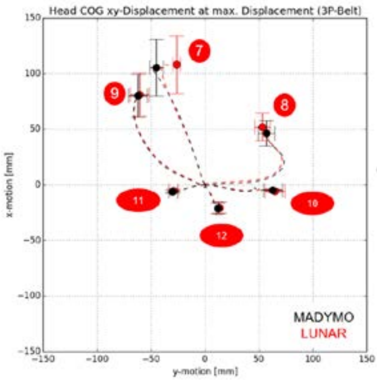

Figure 6: ML prediction of an AHBM's head motion, for a varying SA and SBA (maximum excursion)

STEP 5: Compute the head kinematics envelope.

Using the ROM models in STEP 3 or STEP 4, the head envelope can be calculated in seconds and used for future cabin designs to improve occupants' protection.

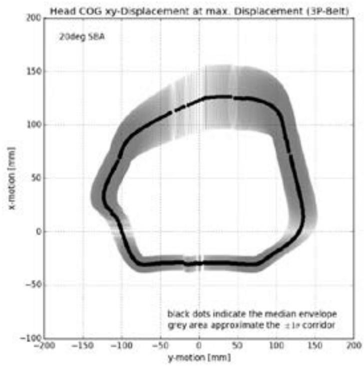

Figure 7: Kinematics Envelope for 20° SBA (max displ.)

References:

[1] Diederich A, Bastien C, Blundell M. The prediction of autonomous vehicle occupants' pre-crash motion during emergency braking scenarios. Proceedings of the Institution of Mechanical Engineers, Part D: Journal of Automobile Engineering. 2023;0(0). doi:10.1177/09544070231153262

[2] Diederich A, Bastien C, Ekambaram K, Wilson A. Occupant pre-crash kinematics in rotated seat arrangements. Proceedings of the Institution of Mechanical Engineers, Part D: Journal of Automobile Engineering. 2021;235(10-11):2818-2842. doi:10.1177/09544070211004504

CAE Wissen by courtesy of Dr. Christophe Bastien: aa3425@coventry.ac.uk Prof. Mike Blundell: cex403@coventry.ac.uk Alexander Diederich: diederia@uni.coventry.ac.uk

Consideration of Seating Comfort in Virtual Seat Development

Seating comfort is the essential customer requirement in virtual seat development. In this very early seat development phase, seating comfort tools like CASIMIR/Automotive offer the possibility to consider various comfort aspects with a set of manikins representing different human percentiles and anthropometries. Based on these simulations of the occupied seat, it is possible to determine the comfort-relevant parameters such as seat pressure distributions, transfer functions, etc. A typical workflow for virtual comfort assessment is shown below (Fig. 1).

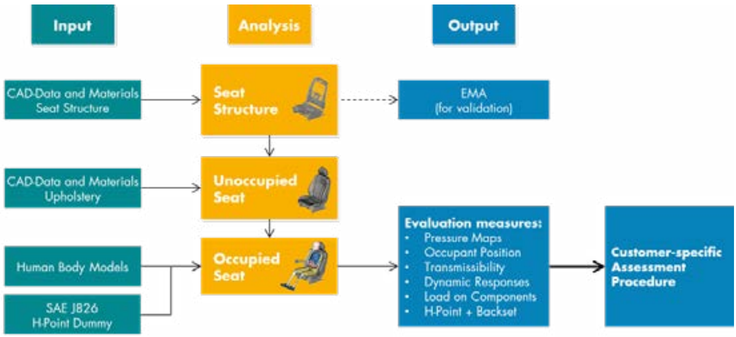

Figure 1: Virtual seating comfort workflow

This workflow is analogous to CAE workflows for other applications. You may start with either CAD data or with a mesh from other tasks like crash and adapt it to the needs for comfort simulation. The material properties of the foam and trim material are used to set up the unoccupied seat. Then, the seat is occupied with either a human body model for comfort or the SAE J826 dummy for H-Point simulation. As an output from static comfort simulation, the user gets e.g. the pressure distribution at the interface between human body model and the seat (Fig. 2). For dynamic seating comfort, it is possible to determine the seat transmissibility etc. Based on this, seating comfort may be assessed.

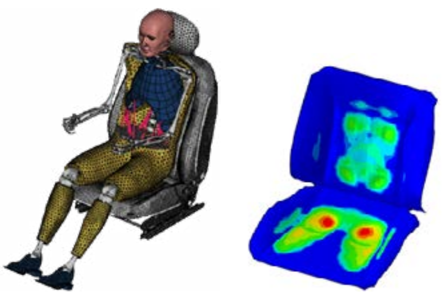

Figure 2: Occupied seat with CASIMIR m50 manikin and seat pressure distribution

In contrast to the established test-based seat development, this virtual development workflow allows for a detailed view into the seat and also into the human body model, and the investigation of a large number of variants in a short time. This allows for example to evaluate the potential of new manufacturing procedures like additive manufacturing for individualized seats. This „customizing“ will be an important alternative to standardized products in the future. New, 3D-printed materials – so-called lattice structures – enable new degrees of design freedom in material properties since it is possible to vary the stiffness locally within in one part without an additional effort. Compared to classic PU foams, they can be used to create completely individualized seats or seating experiences. In order to thoroughly test this novel concept and material before reaching the prototype stage and to make the process more efficient, the CASIMIR/Automotive software was used.

The additively manufactured structures and their material parameters were mapped, simulations of seating comfort were carried out, and reliable and reproducible results have been obtained without need for subjective and lengthy tests with human subjects.

In specific, the project was to compare the different materials for seat cushions and to show the potential of local 3D stiffness variations, (Fig. 3).

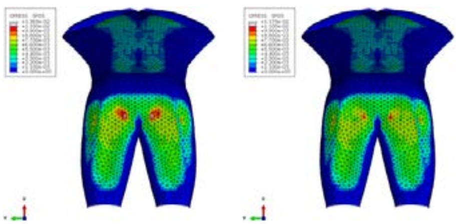

Figure 3: Example comparison of the seat pressure distribution of a seat cushion made of a homogeneous PU foam (left) and inhomogeneous, locally adapted lattice structure (right) for a m50 human model on a seat

The study showed that even for different percentiles, the seat with inhomogeneous lattice material resulted in a more even pressure distribution, resulting in lower load peaks at the ischial tuberosities and a more comfortable seating experience. In addition, the engineers found in the test that by locally adjusting the material parameters, the overall height of the seat cushion could be significantly reduced and thus the amount of material used is much smaller compared to classic foams.

This was found by not only looking at the pressure distribution on the seat surface as is usually done by pressure map sensors in prototype testing, but by looking into the seat, especially into the local foam deformation, (Fig. 4). The approach is to visualize and quantify the volumetric strain distribution (VSD) to identify the regions with low foam utilization.

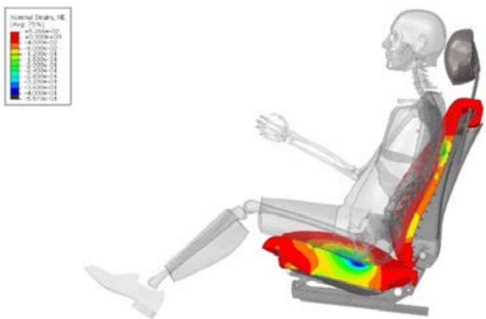

Figure 4: Example of an occupied seat and the strain distribution within the foam

A simulation of different foam designs (thickness) can prove that there is no or only minimal impact on comfort. In some cases, this may even increase comfort due to a larger portion of foam in the comfortable compression range. A novel method to easily visualize this effect, is to calculate the amount of foam in each compression state and to plot it over the material curve, providing a quite good idea of how much foam is in the different stiffness ranges, (Fig. 5).

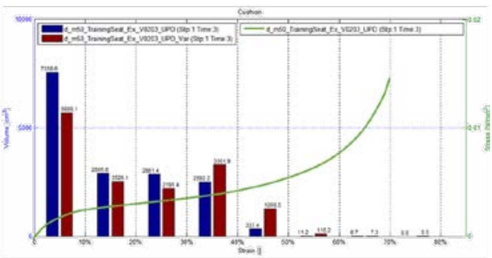

Figure 5: Distribution of the compression state of an original cushion geometry and a variant with better foam utilization

Besides looking into the seat, it is possible to have a view inside the human body which may also lead to a better understanding of discomfort. With a more detailed muscle representation in the buttock and thigh regions of a special manikin, it is possible to look inside the human body and in the main contact areas with the seat, (Fig. 6).

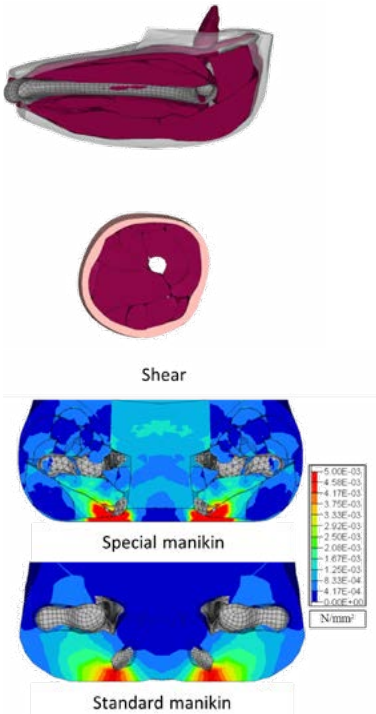

Figure 6: Representation of individual muscle instead of homogeneous tissue, comparison of shear distribution for special and standard manikin

This allows for a more realistic look at the shear as well as the compression distribution inside the seated human body, compared to the standard manikin with homogeneous tissue. These insights may be used to detect discomfort when sitting for a longer period of time in the same posture and to identify uncomfortable postures more easily.

Summarizing, the application of this virtual workflow allows for a comprehensive analysis of seating comfort in early design stages and the acceleration of development times and reduction of the use of physical prototypes. This workflow does not only reflect the physical test-based method but gives a tool at hand to get a deeper insight and to perform more targeted seat development considering comfort.

CAE Wissen by courtesy of Dipl.-Ing. Jörg Hofmann, Dr.-Ing. Georg Enß (Wölfel Engineering GmbH + Co. KG, www.woelfel.de/casi)

HUMAN MODELING AND SIMULATION
IN AUTOMOTIVE ENGINEERING

Human Modeling and Simulation in Automotive Engineering

The application of numerical simulation with digital human models offers exciting new opportunities in automotive engineering. The use of human models in the areas of safety, comfort, and ergonomics can overcome the limitations imposed by the use of real humans or their mechanical surrogates, thus enabling further optimization of automotive designs. In addition, human modeling and simulation is opening the new era of virtual testing for safety assessment and homologation.

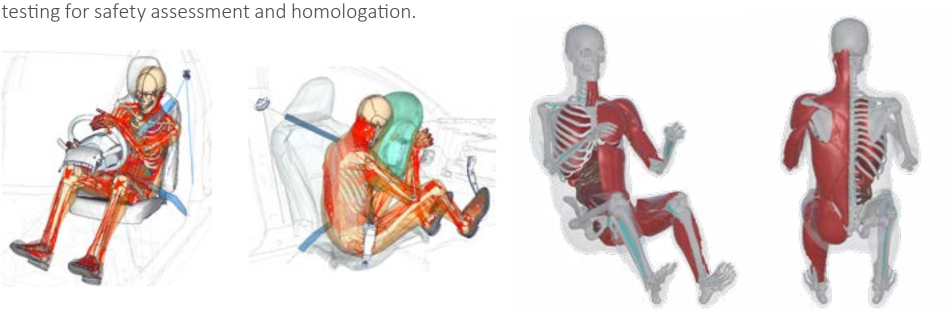

Focus Topic 2025

Autonomous vehicles will bring significant comfort benefits to passengers. However, safety cannot be compromised for alternative seating positions. Human Modeling and Simulation is currently the only technology that will allow assessment of occupant protection for new car interior architectures with flexible seat arrangements.

In 2025 the **11th International Symposium Human Modeling and Simulation in Automotive Engineering** will be held in China for the first time. The symposium aims to continue and advance the dialog between researchers, software developers and industrial users of human models. Presentations by renowned researchers, software developers and industrial users from around the world on biomechanical research, digital human models and their application in automotive engineering will guarantee a unique and highly relevant conference.

ON SITE & ONLINE

Facts

30.-31.10.2025

Shanghai, CHINA & ONLINE — NEW VENUE

www.carhs.de/humo

English / Chinese with simultaneous translation

THUMS Version 6 AM50, AF05, AM95 Occupant Models

Background and Objective:

Total Human Model for Safety (THUMS) has been developed for simulating crash-induced injuries. The previous model, Version 5, enabled to simulate muscular reactions of relaxed and braced occupants during braking and occupant kinematics in vehicle collisions. The new model, Version 6 was developed based on Version 4 while Version 5 was based on Version 3. The detailed internal organs and brain models in Version 6, originated from Version 4, enables to analyze injury mechanisms of relaxed and braced occupants in vehicle collisions. Version 6 is available in three body sizes: AF05 (small female), AM50 (midsize male) and AM95 (large male).

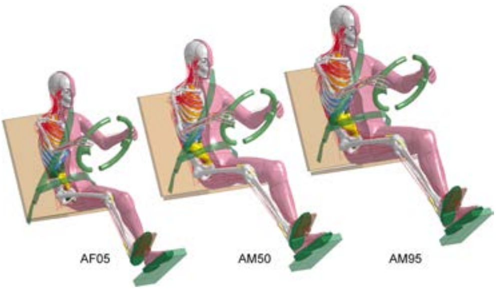

Figure 1: THUMS V6 Model Family

Features of Version 6:

High resolution CT scan image data was used to represent the human body structure. The geometry of the internal organs and the connection with the surrounding parts were carefully duplicated in the model as well as those of the brain. A total of 262 muscle elements was implemented into Version 6 to represent the muscle-tendon complexes in the whole body. A controller model was developed to activate muscle elements to simulate relaxed and braced states. Validations were conducted against 38 series of PMHS and volunteer test data. The validation cases included both component tests and whole body tests. THUMS Version 6 can be used for vehicle crash simulations by simply replacing the dummy model. Positioning tools may be necessary to adjust the posture to the target. The time step of Version 6 is 0.15 microsecond. The total model size is 1.9 million elements.

Muscle Activation Controller:

The muscle states such as relaxed and braced are represented by the muscle activation controller. The muscle activation levels are updated at each time step based on displacement and force of the monitoring points. The controller consists of two closed-loop feedback controls for posture and force. The posture control works to maintain the initial posture while the force control generates forces exerted in the braced state. The proportional-integral-derivative (PID) method is used for the control system. The relaxed state can be simulated using the posture control while both posture and force controls are necessary to represent the braced state.

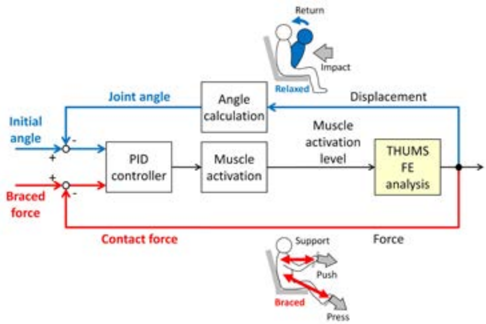

Figure 2: Muscle Activation Controller

Example Application:

Version 6 enables to simulate occupant posture change due to evasive maneuvers, such as braking and steering, taking into account the muscle states.

Version 6 can be used for research of integrated safety systems including precrash safety technology.

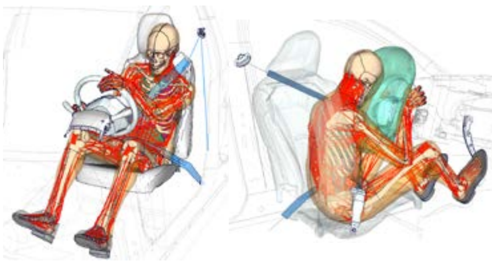

Figure 3: THUMS applications steering and crash

CAE Wissen by courtesy of TOYOTA MOTOR CORPORATION and Toyota Central R&D Labs., Inc.

Global Human Body Model Consortium (GHBMC) Detailed and Simplified Occupant Modeling

The GHBMC

In 2006, a consortium of automakers was formed to fund the development of human body finite element models for use in crash injury biomechanics research as part of the Global Human Body Model Consortium (GHBMC) project. Centers of Expertise were identified across the globe and regional models were developed and validated based on the expertise of each institution. The unique objective of the GHBMC is to consolidate world-wide research and development activities in human body modeling into a single global effort to advance crash safety technologies. Today, the GHBMC family of human models consists of 13 models representing both detailed and simplified versions of the small female, average male, and large male in occupant and pedestrian postures. Models were developed to replicate the biomechanics and kinematics of the human body in various scenarios, allowing for truly human-centered design of safety systems. Since 2014, the GHBMC models are exclusively licensed to both academic and commercial users through Elemance, LLC.

Detailed and Simplified Model Development

Detailed GHBMC models are designed for prediction of crash-induced injury metrics and criteria, including highly complex bones and internal organs, optimal for use in a wide variety of applications. The Simplified models are developed with fewer elements and less complex constitutive models for a faster run time (up to 50x faster). Simplified models include kinematic joints for ease of positioning and are designed for modularity. Recent advances in model development include the latest version of the detailed average male (M50 O version 6.0), updated simplified pedestrian models certified for use with Euro NCAPs Pedestrian Protocol (TB024) and new simplified occupant models incorporating active musculature.

Figure 1: M50-O Version 6.0 Front and Rear View

M50-O Version 6.0

Since the first release of the GHBMC M50-O, the model has undergone more than 100 unique validation simulations ranging from the tissue level to the full body level. As of April 2022, the latest version of the M50-O available for use is v6.0. Since the start of the GHBMC program, over 200 scientific articles have been published in the peer-reviewed literature detailing their use. A detailed listing of these publications can be found at www.elemance.com/resources.

Version 6.0 of the M50-O features:

- Three "age targeted" versions of the M50-O model are now available at 24, 42, and 70 years old (YO). Body shape, mass, and cortical bone properties were adjusted to account for the aging process (Figure 2).
- In the development of the M50-O+aged models, 120 individual material properties were adjusted to match literature data on age related biomechanical property changes.
- Over 100 pre-coded outputs that can be used for subsequent postprocessing (e.g. local nodes at head CG for calculating HIC, section planes in cervical spine for calculating NIJ)
- A fully deformable axial skeleton including all vertebral bodies and joint articulations. No rigid constraints used from skull to sacrum.
- Redesigned abdominal contact scheme reduces the number of contacts in the model from 214 in v5.1 to 131 in v6.0, providing reduced run time and greater stability.
- All model licenses include access to Metriks, a custom software for post-processing injury metrics from GHBMC simulation outputs (Figure 3).

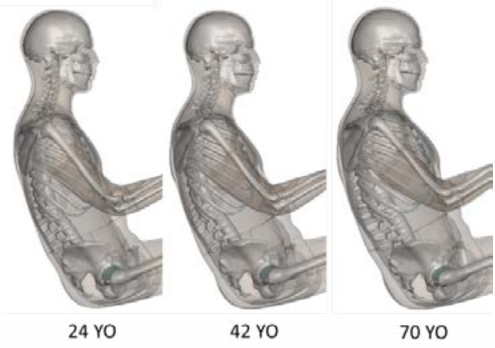

Figure 2: Depiction of aged models developed from the baseline M50-O. Aged models were developed by adjust body shape, mass, and cortical bone properties

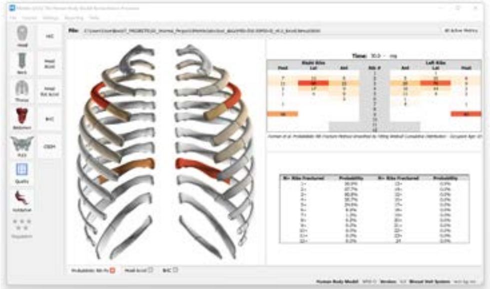

Figure 3: Metriks tool for post-processing GHBMC simulation outputs

Simplified Models with Active Muscle

The GHBMC model family now offers models with active muscle. Based on the simplified models of the average male (M50-OS) and small female (F05-OS), active musculature has been implemented through the use of a closed-loop PID controller as depicted in Figure 5. For the PID controller, muscle activation levels were determined through the use of Equation (1) - Equation (3). Gain factors for the PID controller in Equation (4) were optimized with LS-Opt using data from volunteer sled tests. Gain factors were determined for the musculature in the lower extremities, the upper extremities, the trunk and neck. As a result, a validated muscle activation PID controller is now available in both the M50-OS and F05-OS models. An example of the effect of active muscles can be seen in the braced responses of the M50-OS and F05-OS models when compared to a relaxed response (see Figures 4-5). In these images, the transparent model represents the relaxed response and the opaque model represents the braced condition.

Figure 4: M50-OS in braced test

Figure 5: F05-OS in braced test

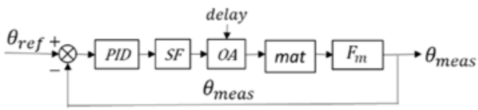

Figure 6: PID Controller feedback system for muscle activation in the M50-OS model, *SF*: Sigmoid function, *OA*: Overall activation, *mat*: Hill-Type muscle material model, *Fm*: Muscle force, *θmeas*: Measured angle, *θref*: Reference angle

$$AL_i(t) = A_i^0 + C_i \cdot s_i \tag{1}$$

$$s_i = \frac{1}{1 + e^{(-9.19 * w_j + 4.60)}} \tag{2}$$

$$w_i = \sum_j R_{ij} \cdot u_i(t) \tag{3}$$

$$u_j(t) = k_{Pj} \cdot e_j(t) + k_{Ij} \cdot \int_0^t e_j(\tau) d\tau + k_{Dj} \cdot \frac{de_j(t)}{dt} \tag{4}$$

with

AL Activation level

u_i PID controller output

e_i error

A_i^0 Initial Activation

C_i Co-contraction

s_i Sigmoid Function based on firing rate of motor neurons

R_{ij} Percentage contribution of each muscle for various motions e.g. flexion, inversion, adduction, etc.

Equations 1-4: Active muscle model

CAE Wissen by courtesy of:
Elemance, LLC

VIRTUAL TESTING

ONLINE

The carhs Virtual Testing Series

Cost pressures and ever shorter development times in the automotive industry, combined with increasing regulatory and consumer protection testing requirements, are accelerating the use of virtual testing as an alternative or complement to physical testing.

The benefits of virtual testing are numerous and contribute to the attractiveness of using virtual tools and tool chains:

- Reduced time to evaluate the product performance
- Cost reduction by eliminating expensive prototypes or expensive physical testing
- The ability to evaluate millions of scenarios for real-world situations and assess product robustness under varying conditions
- Product lifecycle management and rapid validation of product updates in the software-defined vehicle

While physical testing is a well-known and accepted method of certifying and evaluating new products, virtual test-based assessments have yet to prove themselves as a valid alternative. Validation of virtual tool chains will be an integral part of future regulatory and consumer requirements, and product manufacturers will need to provide sufficient evidence and documentation of such validity.

The carhs Virtual Testing Series will present the status of virtual testing for automotive certification and assessment, address the open questions and provide guidance on the validation of the methods and toolchains. The carhs Virtual Testing Series will initially target different areas of automotive development such as active and passive safety, ADAS/ADS and battery safety.

UPCOMING EVENTS:

VIRTUAL TESTING
#5: ADAS DEVELOPMENT CHALLENGES

Virtual Testing #5
April 29, 2025

ADAS Development Challenges

VIRTUAL TESTING
#6: BATTERY SAFETY ASSESSMENT

Virtual Testing #6
June 06, 2025

Battery Safety Assessment

VIRTUAL TESTING
#7: OCCUPANT PROTECTION ASSESSMENT

Virtual Testing #7
October 07, 2025

Occupant Protection Assessment

Missed a Virtual Testing Event?
Get the replay:

www.carhs.de/VT

ENGINEERING KNOWLEDGE FOR TOMORROW'S AUTOMOTIVE

REGISTER NOW FOR FREE

HBM CONNECT™

Transforming Virtual Testing and Product Development

HBM Connect™ by Humanetics is a family of Human Body Models (HBMs) developed to meet the ever-evolving demands of virtual testing and product development. The current portfolio includes the 50th percentile male (HBM Connect™ 50M) and the 5th percentile female (HBM Connect™ 5F) anthropometries. The model development strategy ensured an optimum balance between anatomical features and biofidelity. This enabled reliable kinematics and injury assessments while offering the best possible robustness and computational efficiency. The approach seamlessly supports product development, upcoming New Car Assessment Program (NCAP) virtual testing protocols and research studies.

HBM Connect™ models are integrated within the RAMSIS™ Safety Studio™ (the most widely used Ergonomics packaging software) to establish a direct link between ergonomics and crash safety domains. This integration enables the development of vehicle designs that are both ergonomically comfortable and safe, right from the early stages of the design cycle.

HBM Connect™ models have been specifically developed to meet the needs of product development engineers in mind. The goal is to empower product development engineers with a sophisticated and user-friendly HBM model that requires no pre-requisite biomechanics knowledge.

Figure 1: HBM Connect™ family of models

Model development and biofidelity:

The anthropometries are obtained from the globally recognized University of Michigan Transport Research Institute [UMTRI] Statistical Model database. This approach eliminates subject-specific variations and supports development of multiple HBMs from the same database.

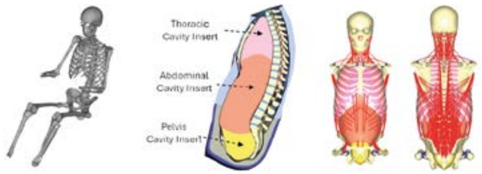

Figure 2: HBM Connect™ 50M modeling details: Skeletal, Inner Organs and Muscles

The model comprises a detailed deformable skeletal system, with both cortical and trabecular parts represented appropriately according to human anatomy. The flesh surrounding the long bones is meshed to ensure seamless nodal connections, improving stability and integration. All articulations in HBM Connect™ models are based on appropriate stiffness and applicable ranges of motion. Internal organs for the thorax, abdomen, and pelvis are lumped into three regions respectively to capture overall mechanical behavior, ensuring a balance of biofidelity, stability, and computational efficiency. All major muscle groups are modeled with 1-D elements, maintaining appropriate insertion and routing to provide muscle tone.

The models have been thoroughly validated with over 100 load cases at tissue, component, sub-assembly, and full system levels using available data from literature. These load cases include those defined by the Euro NCAP working group (HBM4VT) to qualify the HBMs for adoption in the Euro NCAP assessment protocol.

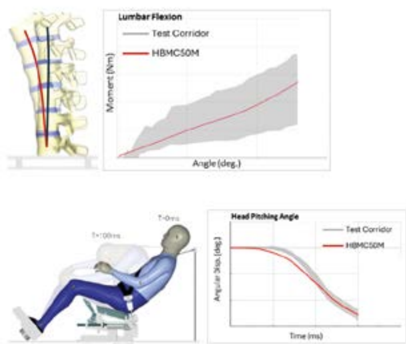

Figure 3: Validation examples for HBM Connect™ 50M: (left) lumbar spine flexion response (Demetropolous et. al. 1998) and (right) full body response for Richardson et. al. (2020)

Model handling and injury assessment:

HBM Connect™ models feature a neutral and universally recognized tree structure, enabling quick adaptation by product development engineers. This structure integrates with all major commercially available pre-processors offered by Ove-Arup, GNS, ESI, BETA-CAE, and Altair. Additionally, HBM Connect™ models are integrated into Humanetics' APT Connect™ software, which offers marker-based positioning, seat squash, and belt routing capabilities. APT Connect™ for HBMs also incorporates spine curvature adjustment based on the UMTRI ergonomic positioning database [Reed (2002)], currently under consideration in the Euro NCAP frontal assessment protocol for HBM positioning in vehicles. Furthermore, APT Connect™ offers seamless integration with RAMSIS™ Safety Studio™, allowing for direct data transfer from comfort position to crash simulation position.

HBM Connect™ models are equipped with a wide range of output responses, including accelerations, loads in various deformable tissue sections, and stresses and strains in skeletal structures, particularly ribs, enabling diverse injury assessment possibilities. All HBM Connect™ models use consistent naming and numbering for output responses, facilitating adoption of customer-specific scripts. To support post-processing of simulation outputs, a dedicated in-house software tool has been provided for comprehensive injury assessment. This tool calculates injury risk for various body regions, including the head, neck, chest, ribs, tibia, and femur, with a key feature being its ability to calculate the probability of rib fracture risk. All outputs from the standalone injury assessment tool are automatically compiled into a comprehensive report. Additionally, post-processing is fully compatible with standard post-processing tools.

The HBM Connect™ models are also equipped with mapping functions to compare responses between ATDs and HBMs upon request. This feature provides additional insights for safety engineers optimizing restraint system performance based on integrated applications of ATD hardware, ATD models and HBMs.

CAE Wissen by courtesy of:
Humanetics Europe GmbH

Advanced Pre and Post Processing of Human Body Models for Safety Simulations with ANSA and META

Autonomous vehicles and virtual certification introduce new challenges for safety simulations. Out-of-position load cases and simulations for other vulnerable road users, like pedestrians and cyclists, are increasingly needed, and HBMs are the only technology that can address these needs. Nevertheless, industrial-level positioning, pre-processing and post-processing of such models have not been straight-forward until now.

Combining Morphing and Kinetics

The main problem currently prohibiting the wide use of HBMs in production for safety simulations is the difficulty in positioning and articulating. Unlike ATDs, HBMs have continuous solid meshes, representing various tissues, such as muscles, skin, ligaments etc. At the same time, the kinematic model of the human body is extremely complex.

Pre-simulation and Morphing has been used to position HBMs, but not without problems. The procedures are cumbersome and lengthy, while they don't guarantee correct kinematics and good final mesh quality.

The novel approach we followed in ANSA was to couple a complex kinematic model handled by our MBD solver with our morphing engine that handles the deformation of the soft tissues. The algorithm follows an optimization approach where, apart from satisfying the kinesiology defined by the kinematic model, morphing is constrained with mesh quality and volume/mass conservation criteria.

For instance, when modeling the knee motion, the gliding trajectory of the patella on the femur needs to be considered, while ensuring the proper rotation of the tibia around the femur's moving axis of rotation. At the same time all the tissues must be morphed. This includes quadriceps, biceps, tendons, ligaments, and skin.

Figure 1: Knee Extension of an HBM. (GHBMC M50-O model courtesy of ELEMANCE)

In contrast, positioning the spine is much more challenging due to its complex kinematic behaviour; multiple position solutions are possible, indicative of the big differences we observe among humans. To model this, we orchestrated a dynamic model which produces, on average, a decent kinematic response of the spine. Adding the possibility to define the ratio between pelvis and spine tilt, offers a way to the engineer to examine different spine kinesiology without getting into modelling details.

Morphing into different anthropometries

HBMs are typically available in a limited range of specific anthropometries, often representing 5^{th} and 50^{th} percentile females and 50^{th} and 95^{th} percentile males. A scaling tool is needed to be able to morph any FE HBM to any target anthropometry.

To generate such variants of a FE Human Body Model, a tool has been developed. The tool utilises as input anthropometric measurements sourced from well-established databases, such as ANSUR or CEESAR, of the requested ("target") part of the population. The produced HBM exhibits this defined input anthropometry.

The method uses advanced morphing techniques to scale and morph the original HBMs, while simultaneously maintaining the structural and functional coherence between the various body parts. The underlying muscles, bones, and internal organs, adjust to the scaling of the skin surface, reflecting the interconnected nature of the body tissue. The resulting HBMs portray a high mesh quality and ensure continuity across different body segments.

Figure 2: Reduced (1.6 m), 50^{th} (1.75 m), and enlarged model (2.0 m) (GHBMC M50-O model courtesy of ELEMANCE)

Post Processing

Post processing HBMs requires specialized functions. META's HBM Post tool creates PPTX and PDF reports including videos and images of the kinematics, strain contour plots, elements erosion identification and injury criteria calculations for GHBM, SAFER and THUMS models.

Injury Criteria

Brain Cumulative Strain Damage Measure (CSDM) is calculated for GHBM and THUMS models. There is the option to calculate the contribution of each part of the brain to the total CSDM result as well as the individual CSDM result of each part.

The Brain Major Principal Strains are reported and the 100th, 99th, 95th and 50th percentile values and elements are identified. For the SAFER HBM, the Concussion Risk (mTBI) is calculated according to *Fahlstedt M, Meng S, Kleiven S. 2022. Influence of Strain Post-Processing on Brain Injury Prediction,* using the 99th percentile value.

For the ribcage, the probability of fracture is calculated for each rib according to *Karl-Johan Larsson, Amanda Blennow, Johan Iraeus, Bengt Pipkorn1 and Nils Lubbe. 2021. Rib Cortical Bone Fracture Risk as a Function of Age and Rib Strain: Updated Injury Prediction Using Finite Element Human Body Models.* Rib fracture probability is calculated by default for 25, 45 and 65 years of age, or for any other selected age. The parameters of the Weibull or the Log-normal distribution can be also adjusted.

The Strain Energy Density (SED) criterion is calculated for the soft tissue abdominal organs (Liver, Spleen, Kidneys).

Heading into the Future

HBMs will be increasingly important for safety assessment during the next decade. Software tools for creation, articulation and personalization of the FE models are already in the pipeline. Our goal is to be able to morph any FE HBM to any position and any anthropometry, (ultimately) equipping engineers globally to design safe vehicles for everyone.

CAE Wissen by courtesy of:
BETA CAE Systems International AG

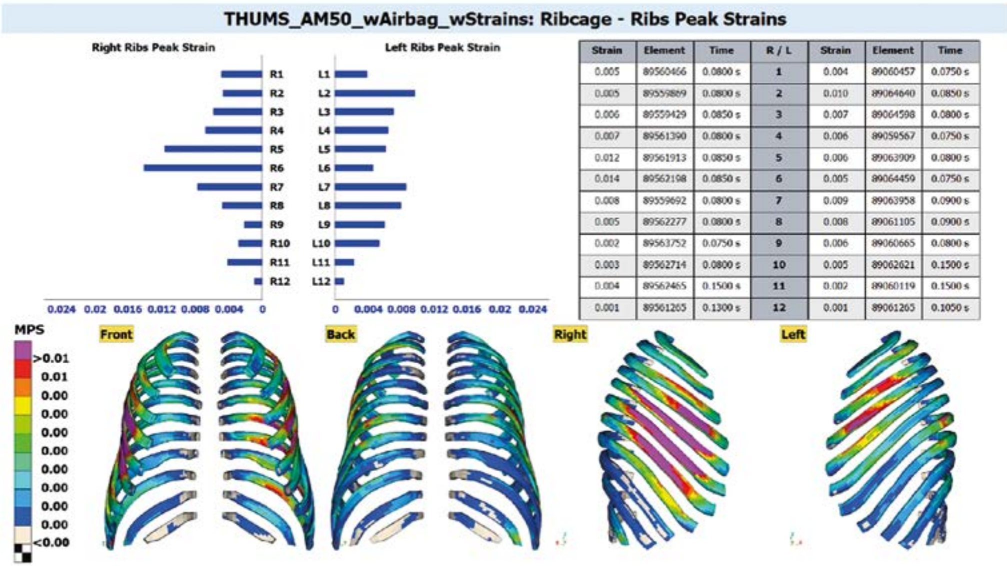

Strain	Element	Time	R / L	Strain	Element	Time
0.005	89560466	0.0800 s	1	0.004	89060457	0.0750 s
0.005	89559869	0.0800 s	2	0.010	89064640	0.0850 s
0.006	89559429	0.0850 s	3	0.007	89064598	0.0800 s
0.007	89561390	0.0800 s	4	0.006	89059567	0.0750 s
0.012	89561913	0.0850 s	5	0.006	89063909	0.0800 s
0.014	89562198	0.0850 s	6	0.005	89064459	0.0750 s
0.008	89559692	0.0800 s	7	0.009	89063958	0.0900 s
0.005	89562277	0.0800 s	8	0.008	89061105	0.0900 s
0.002	89563752	0.0750 s	9	0.006	89060665	0.0800 s
0.003	89562714	0.0800 s	10	0.005	89062621	0.1500 s
0.004	89562465	0.1500 s	11	0.002	89060119	0.1500 s
0.001	89561265	0.1300 s	12	0.001	89061265	0.1050 s

Figure 3: Ribs Peak Strains

Introduction to Impact Biomechanics and Human Body Models

Course Description

To prevent human injury in traffic it is necessary to understand the biomechanics of impact. This can be done through experimental studies with human subjects, volunteers, or post-mortem human subjects (PMHS), after ethical approval. The individual variation is large in experiments with human subjects, due to the wide spread of anthropometry and material properties that depend on factors such as gender, age, and health status. Mechanical anthropometric crash test dummies were developed to provide repetitive tools for development and assessment of safety systems for specific loading scenarios, representing mid-size males, large males, small females and children of different ages. With the development of advanced safety systems, the need for repetitive tools with increased biofidelity and anatomical details, initiated development of numerical human body models. With increasing computer capacity, human body models have become popular tools for traffic safety research, crash simulations, safety evaluations and to study the effects of population diversity on traffic safety. This course covers the basic topics of impact biomechanics, such as human anatomy, population variance, mechanical properties of human tissues, and injury criteria. Finally, it focuses on computational models of the human body and their use to develop and evaluate safety systems.

Course Objectives

The objective of this course is to introduce impact biomechanics, injury biomechanics, and to provide an overview of computational models of the human body. You will learn about the most important topics and get a chance to understand how it relates to your work and traffic safety in general.

Who should attend?

This seminar addresses everyone who wants to obtain an up-to-date overview or who needs a deepened understanding of the field of impact biomechanics, such as university graduates, career changers, management, project assistants, internal service providers, qualified technicians from the crash-test lab or anyone basing product development or decision-making on simulation results with human body models.

Course Contents

- Introduction to impact biomechanics
  - Human anatomy & physiology
  - Medical terminology
  - Injury scaling scores
  - Epidemiology
  - Human substitutes
- Material properties
  - Soft tissues
  - Hard tissues
- Injury mechanisms, tolerances & criteria
  - Head and neck
  - Thorax
  - Upper and lower extremities
- Population variability
  - Biomechanics of children
  - The aging population
  - Gender differences
- Human body models
  - Introduction to numerical methods
  - Methodology for model development
  - Validation of models
  - State of the art models
  - Strengths and limitations

Instructor

Prof. Dr. Karin Brolin (Lightness by Design AB) has worked in the field of impact biomechanics throughout her career. Karin Brolin earned her Ph.D. in 2002 at the Royal Institute of Technology, and since then she has worked in both academia and industry on the topic of human body injury mechanisms and tolerances. The past ten years she led a research group focusing on human body simulations for traffic safety and injury prevention, as Professor in Computational Impact Biomechanics at Chalmers University of Technology. Since 2019 Dr. Brolin has worked as an independent consultant and researcher.

Facts

27.-30.10.2025	193/4488	Online	4 x 4 Hrs.	1.450,- EUR till 29.09.2025, thereafter 1.750,- EUR	

VIVA+ Open Finite Element Models for Injury Assessment

VIVA+ is a lineup of open-source finite element human body models (FE-HBMs). It is available for assessment of skeletal injury primarily, with special focus on robustness and computational efficiency. The lineup consists of average seated female (50F) and seated male (50M) models, and the corresponding standing versions. Positioned models (TB024, cyclists, pedestrians, e-scooter riders) are also available from the VIVA+ community.

The VIVA+ ecosystem adopts an Open Science approach, where the models and its validation catalog are available freely under open-source licenses. These are maintained by the VIVA+ community on open repositories hosted on OpenVT.

VIVA+ model workflow

The workflow used to develop and maintain the VIVA+ HBM lineup is presented in Figure 1. The base model where all development and bug fixing are carried out is the model representing the seated average female. The geometry for this model and all other models is based on anthropometry data developed by University of Michigan Transport Research Institute. This is the same data that is used for the HERMES™ HBM and is presented as regression models with sex, stature, BMI, and age as covariates. Thus, the geometries are not based on single individuals (usually the case for other HBMs), but rather on the "average" of the subpopulation of interest, e.g. the average female or male.

When the base model has been updated it is morphed to the (currently three) derivative models, the seated 50M, the standing 50F and the standing 50M models. One major benefit of this approach is that all model definitions except the node coordinates are shared between the models. The models are organized in include files, with only two files being different between the different models (the main file and the node file), while the rest of the files are shared.

Next, a QA step makes sure all models fulfill the element criteria, and that they are free of initial penetrations and intersections for all contacts. The model robustness is checked by running each model in a selection of robustness load cases. For major updates the model validation is rechecked using the validation pipeline described further down.

VIVA+ injury risk evaluation

The design philosophy for the VIVA+ model lineup is that skeletal bones are modelled in detail to enable detailed (tissue-based using the finite element strains) injury prediction, while the soft tissues surrounding the skeleton are modelled to accurately transfer loads to the skeleton, but not for injury prediction (of the soft tissues). For bones with thin (< 1 mm) cortical bone, for example the ribs (see Figure 2 left) the cortical bone is modelled with shell elements. For bones with thick cortical bone, for example the femur (see Figure 2 right) the cortical bone is modelled using multiple layers of solid elements. For the ribs, the femur, and the tibia tissue-based risk curves are currently available for fracture prediction.

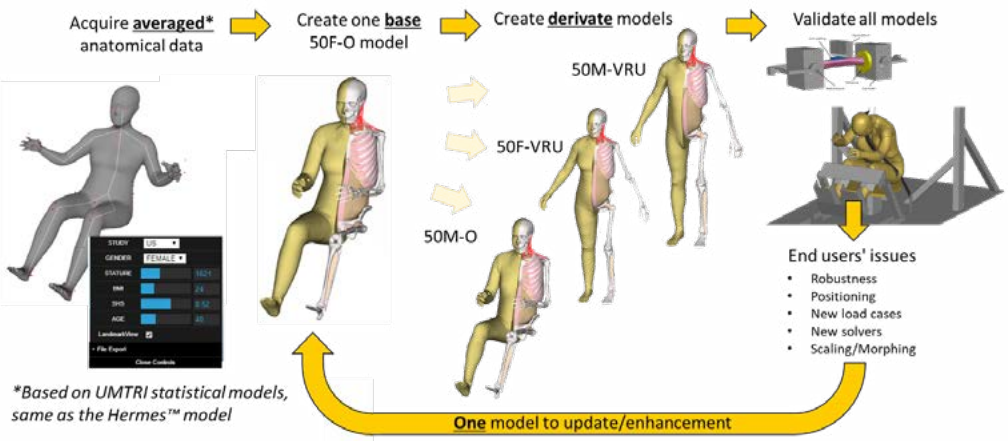

Figure 1: The workflow used to update and maintain the VIVA+ HBM lineup.

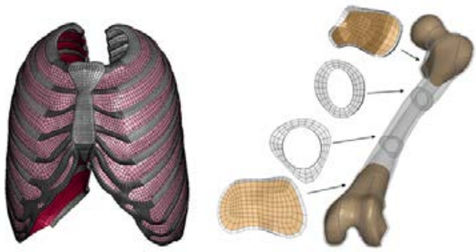

Figure 2: Some body parts are modelled with a higher level of detail to enable tissue-based injury predictions.

VIVA+ validation catalogue

All model validation has been documented in Jupyter notebook format, see Figure 3 for an example, using the Dynasaur python library (https://gitlab.com/VSI-TUGraz/Dynasaur) for post processing the simulation results. The Jupyter notebook format combines formatted descriptive text with code snippets for calculations and visualization. This makes it possible for the users to easily download the validation catalogue, rerun the validation simulations and the postprocessing, to make sure everything looks the same on their hardware. The notebooks and the simulation input files are shared under the Apache open-source license. After a major release all notebooks (for each validation load case) are updated with the latest results, and is compiled to an openly accessible Jupyter book, which is shared on ReadtheDocs (see link at the end of this document).

Figure 3: An example of a validation catalogue Jupyter notebook on OpenVT.

An application example

The VIVA+ model lineup was used to study the effect of autonomous emergency braking (AEB) (Leo, et. al. "Holistic pedestrian safety assessment for average males and females", doi: 10.3389/fpubh.2023.1199949). In particular the advantage of having both an average female and an average male model was used to study if there are any sex related differences in injury risk and if both sexes benefit to the same degree when introducing a generic AEB system.

A summary of the results can be seen in Figure 4. The baseline injury risk (without AEB) varied between the sexes, with the most notable difference in proximal femur fracture risk. This is most likely a geometrical effect, where the proximal femur of the average female impacts the bonnet leading edge, while the average male impacts further up on the bonnet (which is usually a softer area), see Figure 5. By reducing the impact speed, the AEB system reduces the injury risk for most body parts, but in particular for the body parts that initially had the highest injury risk. Both sexes benefit from the AEB system.

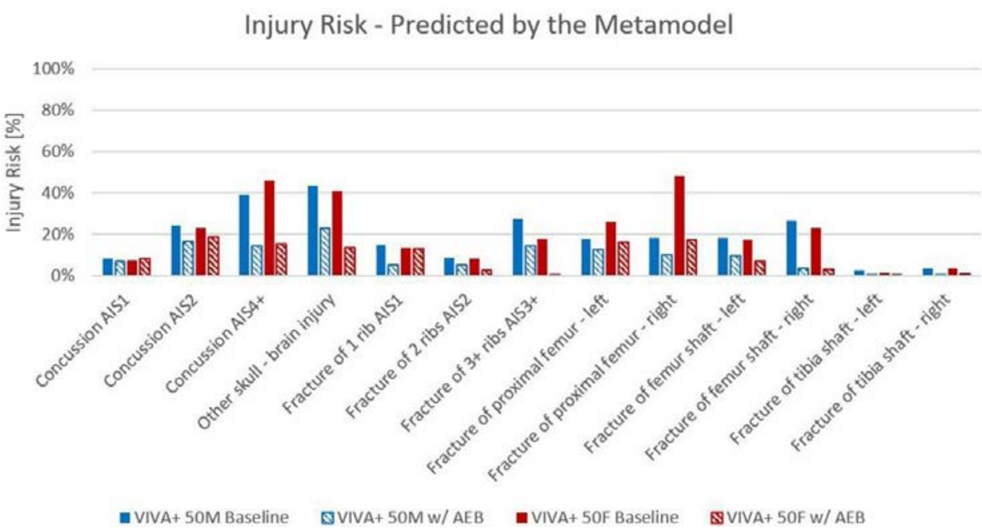

Figure 4: Comparison of the predicted injury risk for the average female and male models, with and without the AEB system.

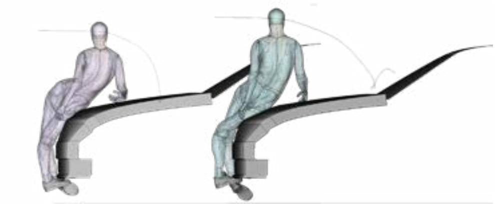

Figure 5: A snapshot of the simulation results at the time of the proximal femur impacting the bonnet leading edge. The impact speed in these simulations was 40 km/h.

Highlights of VIVA+ HBM lineup

- A unique modeling workflow where all the models share the same mesh structure and shared definitions for consistent modeling between different anthropometries and road users.
- Open model repository and validation catalog hosted on OpenVT, creating transparent workflows that enables reproducibility of model performance.
- Open source, with no restrictions on users (industry and research) and an open license fully compatible for use with proprietary models. No contract to sign.
- Low computational cost for a FE model, and high robustness, to enable large parameter studies.

More Information and Download Links

Downloads and Documentation:
https://vivaplus.readthedocs.io/

Validation Catalogue:
https://vivaplus-validation.readthedocs.io/

Contact

The VIVA+ maintainer team can be reached at vivaplus@ovto.org

The VIVA+ HBM lineup was developed in the EU-funded project VIRTUAL. This project has received funding from the European Union’s Horizon 2020 research and innovation programme under grant agreement No 768960.

New Material- and Failure Criteria for Modelling of Glass Models for Crash

Introduction

High quality simulation of safety glass, used for making windshields in automotive industry, is still a challenging topic for commercial crash solvers.

Holistic modelling of the behavior of glass becomes more important due to its influence on structural behavior in several load cases, like for dynamic crashworthiness and pedestrian protection or consumer goods like drop tests.

The main requirement from the industry is to use the same model and the same mesh for all load cases. Local refinement, like adaptive meshing, will lead to localization and at the end to failure in the refined area. Adaptive meshing is a suitable method for stamping simulation where the final deformed shape is known. It is not recommended in crash applications.

To overcome this drawback, ALTAIR has developed further the eXtended Finite Element Method X-FEM [1] (figure 1) and implemented it in the crash solver Altair Radioss [2]. Anyway, there is still ongoing research and development on improving the quality of the results of the prediction of the stiffness and fracture of glass as used in windshield applications.

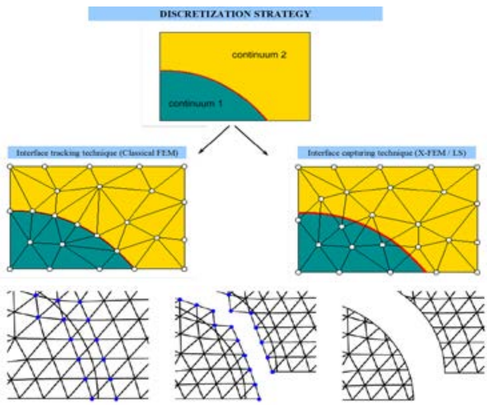

Figure 1: Modelling of crack propagation with X-FEM

The simulation of the fracture behavior of laminated safety glass is still a great challenge (figure 2). The commonly used element erosion technique for the representation of failure leads to a significant underestimation of the stress tensor at the crack tip and thus of the crack pattern in the simulation.

In addition to the X-FEM approach (figure 3) a non-local failure method was developed by Christian Alter et al [3]. The proposed failure model uses a decrease of the rate dependent fracture stress (figure 4) in the direction of a propagating crack instead of an upscaling of the stress tensor.

The Modell was validated in the context of the head impact on windscreens (figure 5) and is already available in ALTAIR RADIOSS (as /FAIL/ALTER).

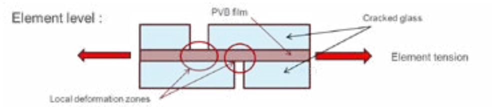

Figure 2: Windshield glass treatment during fracture

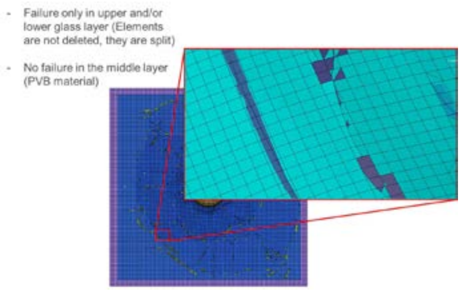

Figure 3: Finite element simulation (RADIOSS) results on a validation structure – safety glass

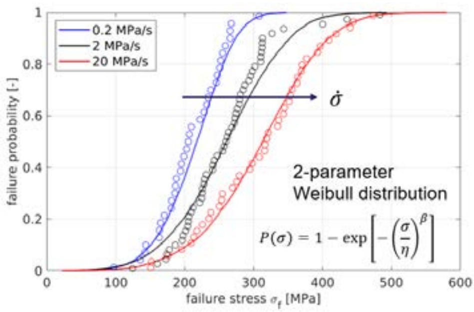

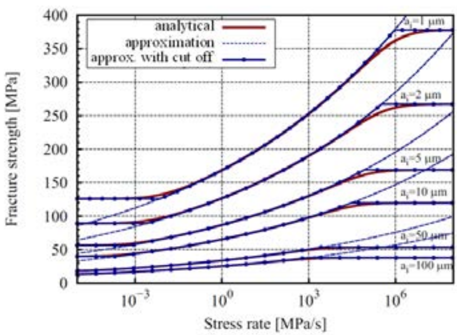

Figure 4: Stress-rate dependency on fracture of glass by C. Alter

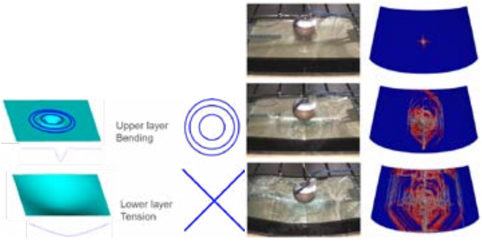

Figure 5: Different crack shapes due to different stress conditions, over the thickness

Due to the existence of initial microcracks in any glass structure (figure 6), this model was enhanced by this feature by the developed of Christopher Brokmann [4] (figure 7). This research and development were done within a public founded research project, using a stochastic approach to model this physical phenomenon. It is also embedded into the recent implementation of this failure criterion. These enhancements allow to consider the stochastic behavior of crack initiation as well as model the thermal or chemical threated outer surface of a single layered glass. These new features extend the ranges of applications from automotive driven applications in windshields to consumer goods, where tempered glass is used.

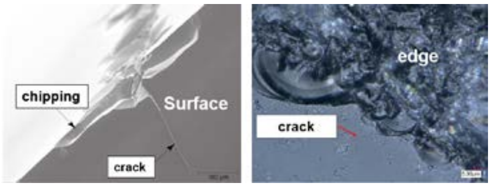

Figure 6: Imperfections observed in glass

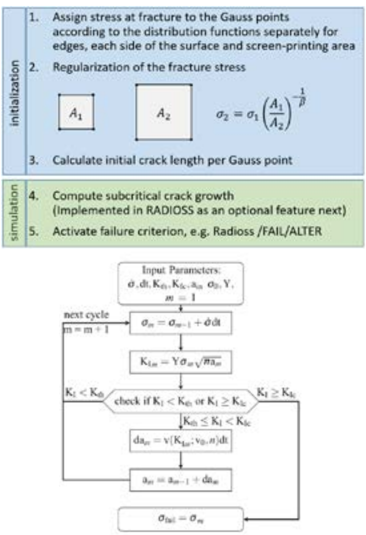

Figure 7: Initialization by C. Brokmann and implementation in Altair Radioss

Theory

X-FEM is a numerical method for geometries containing discontinuities and singularities without the need of building a conforming mesh. This numerical method was developed for modelling large (displacement) as well as slight (strain) discontinuities within a standard finite element framework. It is based on the Partition of Unity Method [5].

X-FEM will be applied for the simulation of crack initiation and propagation without the need of re-meshing [6]. With X-FEM, cracks are represented as surfaces of discontinuous displacements continuously propagating through finite elements. Figures 8 and 9 show different load-cases applied on the same model, without and adjustment to the mesh nor material or failure criteria.

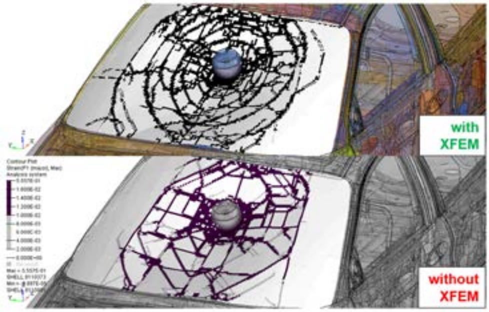

Figure 8: Industrial application: Pedestrian Head impact

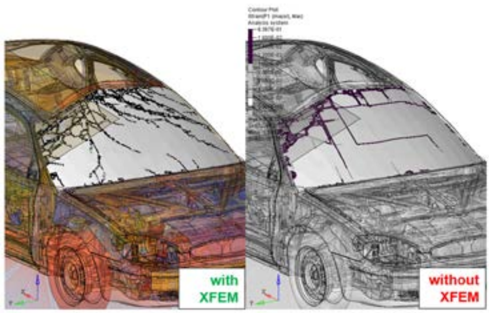

Figure 9: Industrial application: Roof crush

With the new enhancements developed by C. Alter and C. Brokmann the dynamic crack initiation and propagation is an application domain for which X-FEM is particularly suitable because the most prevalent method for treating crack growth, where re-meshing, is not suitable for a solution of this problem.

Application for simulating the windshield behaviour in crash

The X-FEM method is designed as a module and can be added to the existing failure criteria, like Forming Limit Diagram (FLD), Johnson-Cook, tabulated failure-strain-vs-triaxiality and others. For the usage of any application, it is highly recommended to validate the material and failure model first, before activating the X-FEM extension.

The typical safety glass consists of: Glass – Polyvinylbutyral (PVB) foil – Glass

It is obligatory for the FEM method, to be able to represent the correct behaviour of a windshield, to mimic independent cracks within one shell-element, depending on the state of stress and strain, in the individual layer.

Due to different stress states, different crack shapes are expected. The validation model shows exactly the expected behaviour of the layers through their thickness, where the dominant shape on the upper layer is circular and on the lower layer the star-shape becomes dominant. It can be seen that the cracks propagate nearly mesh independent.

After final validation, material-, failure criteria and the X-FEM approach can be applied to industrial cases, especially well-suited for modelling fracture in brittle materials as well as in multi-layered shells with different materials.

Figure 10 shows the very good agreement between real tests and Altair Radioss simulation results using the latest implementation by Christian Alter and Christopher Brokmann with the corresponding acceleration vs. time plots, which are needed for final HIC-value calculation. Deeper information and validation examples can be found in [7].

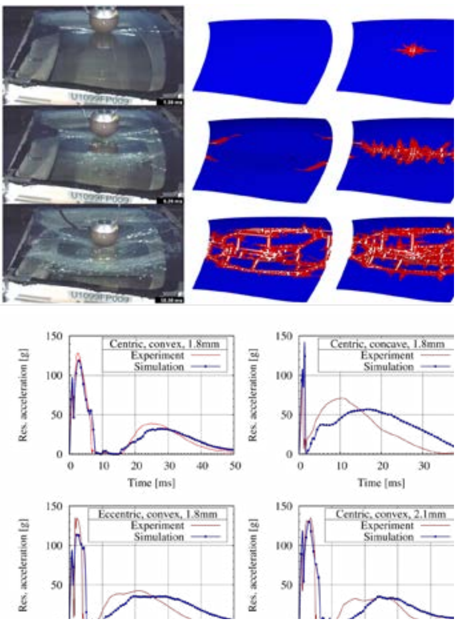

Figure 10: Comparison of measured and computed acceleration. Fracture pattern of a centric head impact test. Left: Experiment, Middle: Exterior glass layer, Right: Interior glass Layer.

Conclusion

X-FEM together with the considered stochastic approach provide more physical results in terms of cracks simulation. Besides, X-FEM aims at avoiding extremely small and CPU expensive meshes. It is successfully implemented in Altair Radioss, where it is able to realistically reproduce crack patterns in laminated glass, like in windshields, and thermal or chemical threated single layered glass. There is also the possibility of crack initiation which is important for design improvement and stochastic analysis.

With the recent enhancements, the field of applications covers windshields as well as single layered glasses with tempered outer surface (temperature or chemically), used in mobile cell phones and others consumer goods.

Advanced failure criteria and X-FEM are easy to use in Altair Radioss: It's just one Flag.

Achnowledgement:

This article is based on the results of two completed research projects at the Giessen Institute of Mechanics and Materials (IMM, working group of Prof. Kolling) in cooperation with the Research Association for Automotive Technology (FAT).

CAE Wissen by courtesy of:
Marian Bulla – ALTAIR Director Program Management
Maciek Wronski - ALTAIR Director Software Development
Mircea Istrate - ALTAIR Senior Software Developer

References

[1] T. Belytschko, T. Black, "Elastic crack growth in finite elements with minimal remeshing", Int. J. Numer. Methods Engrg., 45:601–620, 1999.

[2] HyperWorks RADIOSS Theorie Manual: Nov 2021

[3] C. Alter et al., "An enhanced non-local failure criterion for laminated glass under low velocity impact", Int. J. Imp. Eng. 109:342–353, 2017.

[4] C. Brokmann et al.,"Subcritical crack growth parameters in glass as a function of environmental conditions", Glass Structures & Engineering 6:89–101, 2021.

[5] J.M. Melenk, I. Babuska, "The Partition of Unity Finite Element Method: Basic Theory and Applications", Comput. Meths. Appl. Mech. Engrg., 139:289-314, 1996.

[6] N. Moës, J. Dolbow, T. Belytschko, "A finite element method for crack growth without remeshing", Int. J. Numer. Methods Engrg., 46:131–150,1999.

[7] C. Brokmann, "A Model for the Stochastic Fracture Behavior of Glass and Its Application to the Head Impact on Automotive Windscreens", Springer Vieweg, 63, 2022

Material Models for Metallic Materials

Metals are the dominant material group for the body-in-white. A CAE based development includes the metal forming simulation of the different parts and the simulation of misuse and crashworthiness of subcomponents and the whole body-in-white. The phenomenological models for the elastoviscoplastic behaviour and failure initiation of metals are discussed in general. The implementation of those models can differ between the commercial FEA codes.

A comprehensive material model must cover the following effects:

- Description of elastic material behaviour
- Stress state dependent criterion for the onset of a plastic deformation (stress yield locus) and criterion for derivation of plastic strain components (plastic potential)
- Model for strain hardening and strain rate sensitivity (in case of pronounced viscoplastic behaviour)
- Criteria for onset of material failure (mainly strain-based for metallic materials)

Elastic Behaviour

The elastic behaviour of metals is assumed to be linear. For most technical alloys the elastic properties are assumed to be isotropic on a macroscopic scale (single grains can exhibit a pronounced orthotropy of the elastic properties). Isotropic linear-elastic behaviour can be described by 2 independent values, for example by the

- Young's modulus E with $\sigma = \varepsilon E$ and the
- shear modulus G with $\tau = \gamma G$
- From these values two further dependent elastic constants may be derived:
- bulk modulus K: $K = \dfrac{E}{3(1-2\cdot\nu)}$
- Possion's ratio ν: $\nu = \dfrac{E}{2\cdot G} - 1$

Yield Locus and Plastic Potential

The proportional limit R_p or the technical 0.2% yield strength of a tensile test indicates the onset of plastic deformation in metallic materials. In a finite element analysis a criterion for the onset of plastic deformation is needed for general multiaxial stress states. The yield locus is used for this purpose. Figure 1 shows the yield locus according to *von Mises* in the stress space. Stress states inside the cylinder are still elastic. Stress states on the cylinder shell indicate the onset of plastic flow. The body diagonal in Figure 1 represents the hydrostatic stress p. As volume constancy is assumed for the plastic deformation of metals the onset of plastic deformation is not influenced by the level of hydrostatic stress. In case of a plane stress condition (σ_3=0) for shell elements the yield locus reduces to an ellipse in the σ_1-σ_2-plane.

Typically an associated flow rule is applied for metallic materials. This means that the yield surface or yield locus is also used as a plastic potential. The plastic potential defines the components of the plastic strain rates by the direction of the normal on the surface.

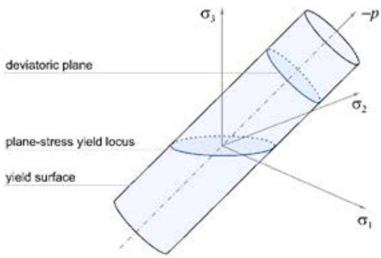

Figure 1: Yield surface according to von Mises

If the *von Mises* plasticity is used the only user input is the yield stress from uniaxial tension. The yield stress and the corresponding hardening curve defines the initial size of the cylinder and its increase during strain hardening.

Sheet metals typically exhibit an orthotropy of the plastic behaviour due to the rolling process. In this case an orthotropic yield locus should be used. *Hill-1948* offers an orthotropic extension of the *von Mises* yield locus. This locus is available in nearly all commercial FEA codes. The orthotropy parameters are typically defined via three Lankford coefficients r_0, r_{45} and r_{90} which are derived from tensile tests in 3 orientations to rolling direction. The Lankford coefficient is defined as follows:

$$r_i = \frac{\ln(b/b_0)}{\ln(t/t_0)}$$

Here b_0 and b are the initial and current width of the tensile specimen. t_0 and t are the initial and current thickness of the tensile specimen. The Lankford coefficient is typically evaluated between 2% and uniform elongation. The *Hill-1948* locus based on Lankford coefficients is appropriate for mild and high strength steel sheets. However advanced high strength steel sheets and aluminium sheets are not represented adequately by this model. More complex yield loci should be used.

Strain Hardening and Strain Rate Sensitivity

The strain hardening can be derived from the classical tensile tests. The input for the FEA codes, however, is true stress versus true plastic strain. The raw data of the tensile tests are force F and elongation ΔL of the extensometer. Based on the initial cross section A_0 and the initial length of extensometer L_0 of the tensile tests the curve can be expressed as engineering stress $\sigma_{eng}=F/A$ and engineering strain $e=\Delta L/L_0$. This curve can be used only up to uniform elongation as the strain is no longer homogeneous in the specimen for a higher elongation. The true stress σ_{true} and true plastic strain ε can be derived as follows:

$$\sigma_{true} = \sigma_{eng} \cdot (1+e);\ \varepsilon_{tot} = \ln(1+e);\ \varepsilon_{pl}=\varepsilon_{tot} - \sigma_{true} / E$$

This hardening curve has to be approximated and extrapolated for the input in FEA. In general cases higher strains than the uniform elongation can be reached in a deformed structure. A well known and robust hardening law is the Swift model:

$$\sigma_{true} = K(\varepsilon_0+\varepsilon)^n$$

K, ε_0 and the strain hardening exponent n are material dependent parameters. Most of the metallic materials show a positive strain rate sensitivity, i.e. the flow stress increases with strain rate. Steels show a pronounced strain rate sensitivity. In general the strain rate sensitivity decreases with increasing yield strength of the steel. Aluminium alloys show a low or even negative strain rate sensitivity at low strain rates, but a positive one for high strain rates. The strain rates of a deep drawing simulation are in the range of 0.001-0.1 1/s. The strain rate in a high speed crash simulation can reach locally strain rates of 500 1/s. The strain rate sensitivity can be expressed either by analytical laws which scale the quasi-static hardening curve as a function of the strain rate or by providing multiple hardening curves for the relevant strain rate regime.

Failure Criteria

As metallic materials are typically ductile, strain-based failure criteria are dominant for this group of materials. Many CAE engineers favour to use the total elongation or engineering fracture strain from the tensile test as a fracture criterion. However this value is not a real material parameter as the specimen elongation does not resolve the local strain in the diffuse neck of a tensile test. In addition the fracture strain is a strong function of the stress state. A sheet under bending will fail first on the surface with tensile load despite the same equivalent strain appears in compression without failure. Completely wrong conclusion can be drawn from this simple criterion.

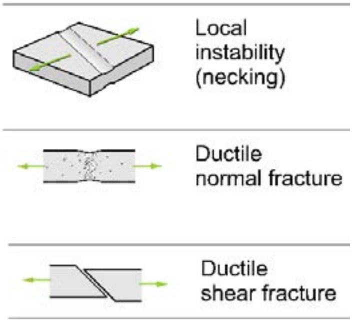

Figure 2: Failure modes for metallic materials

The main failure mechanism of metallic sheets in sheet metal forming and crash is the onset of necking. At a sudden point of deformation the strain hardening and the strain rate sensitivity can no longer avoid a localization of the strain. Due to strain localization a fracture appears inside the neck after a small increase of the global strain. Therefore the necking itself can be used as a failure criterion. As industrial sheet metal forming simulations and crashworthiness simulations are mainly based on shell discretization the localized necking cannot be resolved directly – the width of the neck is in the dimension of the sheet thickness. Forming Limit Curves (FLC) are the standard approach to predict the onset of necking. The FLC is expressed as major principal strain versus minor principal strain at the onset of necking. However the classical FLC is limited to linear strain paths. More advanced models have to be used in case of nonlinear strain paths. For advanced high strength steels and aluminium sheets fracture can happen prior to localized necking. This fracture can be caused either by void growth and void coalescence (ductile normal fracture) or by shear band localization (ductile shear fracture). The fracture limit curves for these fracture modes can be expressed by the equivalent plastic strain at fracture as a function of the relevant stress state parameter.

CAE Wissen by courtesy of MATFEM Partnerschaft, Munich (www.matfem.de)

Latest info about this course

Modeling of Materials & Connections Seminar

Material Models of Metals for Crash Simulation

Course Description

Besides an appropriate spatial discretisation of the structure and a profound knowledge of the required load cases, appropriate material modelling is a key ingredient for predictive crash simulations. The load carrying structure of a car today still mainly consists of metallic materials. The materials to be described are diverse.

The seminar deals with the following materials:

- Mild and high strength steels,
- cold formable AHSS and UHSS steels,
- hot formable and quenchable boron steels,
- wrought Al and Mg alloys,
- cast Al and Mg alloys,
- metalic material produced by additive manufacturing.

The objective of this 1-day course is to give the participants an overview of material models of metals used in crash simulation. Within the first chapter the deformation behavior and the failure mechanisms of each material class are explained based on the material structure. In the second chapter phenomenological models for crash simulation of metals are introduced. This includes elasticity, viscoplasticity and failure due to localized necking, ductile normal fracture and ductile shear fracture. In case of crashworthiness simulation the influence of strain rate on the aforementioned properties is of high interest. In the third chapter the tests needed for the characterization of materials are described and the parameter identification for the material models is discussed. The manufacturing process can have a significant impact on the material properties (pre-straining of sheets, paint bake heat treatment, local heating in joining processes etc.). Within the fourth chapter simulation examples are discussed which show the sensitivity of simulation results regarding the identified material parameters. In the final chapter the influence of the discretization on the predictive quality of a crashworthiness model is discussed. This includes both the element size and the type of element (shell vs. solid).

Who should attend?

The course addresses engineers working in the field of crash simulation and heads of simulation departments interested in the important topic of material modelling.

Course Contents

- Overview of metallic materials used in cars
- Influence of material structure on mechanical behavior
- Phenomenological material models for metals
- Overview of experimental methods for material characterization
- Identification of material parameters from experiments
- Discussion of the sensitivity material parameters

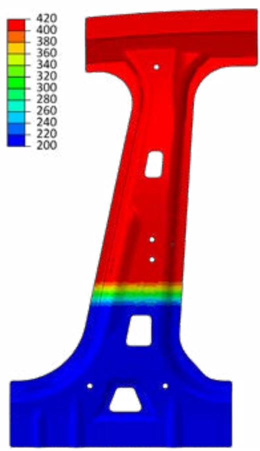

Instructor

Dr.-Ing. Helmut Gese (MATFEM Ingenieurgesellschaft mbH) founded the engineering consultancy MATFEM in 1993 (from 1999 the company has been named MATFEM partnership Dr. Gese & Oberhofer; in 2022 the legal status has changed to MATFEM Ingenieurgesellschaft mbH). MATFEM offers technical and scientific consultancy services at the intersection of material science and finite element methods. Besides performing FEM analysis projects the area of activity covers experimental and theoretical characterization of materials and the development of new material models for simulation.

Facts

16.-17.09.2025	70/4539	Online	2 x 4 Hrs.	890,- EUR till 19.08.2025, thereafter 1.090,- EUR	English
10.03.2026	70/4635	Alzenau	1 Day	890,- EUR till 10.02.2026, thereafter 1.090,- EUR	German

Advanced Constitutive Models for Challenging Forming Simulations

by Frédéric Barlat, Toshihiko Kuwabara and Seong-Yong Yoon

The results of finite element (FE) simulations involving large plastic deformation such as forming depend on many parameters. Beside numerical parameters, physical input such as boundary condition, contact and interface, and material behavior are playing a key role. This article deals only with the latter, more precisely, the influence of the constitutive description on forming simulation results. This article focuses on the forming simulations of laboratory scale specimens, in particular, the hole expansion test. Large scale simulations performed in industry on real scale products are very challenging because of the size of the FE model. Such an example is briefly discussed at the end of this article.

Constitutive modeling

As an example, an accurate prediction of springback in U-draw bending for a simple rectangular blank made of advanced high strength steel is difficult to achieve. Better results are usually obtained if an advanced constitutive model is employed. First, this requires to make the elastic cord modulus as a function of the accumulated plastic strain because of elastic degradation. Second, the plasticity model should consist of a non-quadratic anisotropic yield condition and an anisotropic hardening approach. The latter is necessary because of the forward-reverse loading occurring when the material flows through the proximity of a die corner. It is well known that strain hardening with a large transient effect occurs during non-linear strain paths. Of course, this type of constitutive description requires the measurement of mechanical properties in different directions and for various stress states. Moreover, it should include a few cycles in a forward-reversal mode of deformation, which requires proper equipment and operation for material testing.

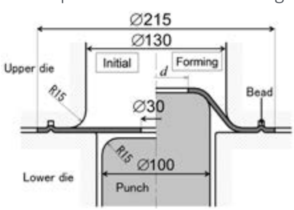

Figure 1: Sketch of hole expansion (HE) test

Finally, although the plastic behavior is assumed to be independent of the hydrostatic stress in most plasticity theories, a small influence is measurable and becomes significant for very high strength steel such as AHSS, commonly used in automobile structures. In fact, since a uniaxial compression test develops a high pressure and uniaxial tension a high hydrostatic tension, the flow curve in compression is higher than in tension. This is called the strength-differential (S-D) effect and the difference may be as large as 7 % for martensitic steel over 1.5 GPa. This effect is significant in itself but it also complicates the analysis of permanent softening occurring during load reversals.

Other simple challenging simulations include cup drawing of a circular blank [1], indentation of a pre-stretched panel [2] and expansion of a circular hole [3]. In the case of cup drawing, the prediction of the earing profile, that is, the strain field in the product, requires a precise description of the material behavior in stress states that are close to those encountered in the flange of a cup. These states fluctuate between plane strain and plane stress states, in which the thickness strain variation is limited. For this purpose, uniaxial tension tests are the easiest to conduct but many loading directions should be considered, typically, at every 15° from the rolling direction (RD). Even with an advanced anisotropic yield condition, some discrepancies with experimental results are expected if hardening is assumed to be isotropic because the material flowing over a die radius experiences forward-reverse deformations cycles. The indentation of a pre-stretched panel requires the use of an advanced constitutive model as well because the pre-strain and indentation correspond usually to two different stress states. In addition, the variation of the elastic modulus must be characterized for a balanced biaxial stress state.

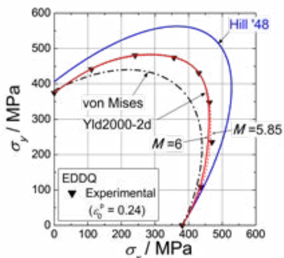

Figure 2: Yield loci for different models: von Mises, Hill's 48 and Yld2000-2d for *M = 5.85* and *M = 6*.

Hole expansion simulations

Experiments were conducted on a high *r*-value, extra deep drawing quality steel (EDDQ), with the set-up represented in Fig. 1. The contact between the punch and the sheet was lubricated with Teflon and Vaseline leading to a friction coefficient μ=0.03. A constant blank holding force of 60 kN was applied to the blank and the experiment ended at a punch stroke of 30 mm. After this test, the specimen radial strains were measured along the RD, transverse (TD) direction, and at 45° from the RD. Simulations were conducted with Abaqus/standard 6.12 using 4-node shell elements SR4 assuming isotropic hardening with the same stress-strain curve for all the cases but different yield conditions. The isotropic von Mises, anisotropic Hill's 48 and anisotropic Yld2000-2d yield conditions were employed with, for the latter, a characteristic exponent *M*. Two cases were considered, namely, M=5.85, which was determined from best approximation of biaxial test data, and *M*=6, which is the standard value for

BCC materials. The constitutive model characterization and calibration, as well as the FE simulations were conducted with utmost care.

Fig. 2 represents the experimental yield locus determined at a constant plastic work corresponding to an effective strain of 0.24. It also provides the predicted loci calculated with von Mises, Hill's 48 identified mostly with uniaxial *r*-values, and Yld2000-2d with *M*=5.85, determined from best approximation of biaxial test data, and *M*=6. This figure indicates that the two Yld2000-2d predicted loci are in good agreement with the experimental points, with a slightly better approximation when *M*=5.85. However, the yield loci predicted with von Mises and Hill's 48 yield conditions are far from the experimental data. This figure illustrates that the choice of a yield condition is important and many studies, such as this one, have shown that von Mises and Hill's 48 are rarely suitable for metallic materials.

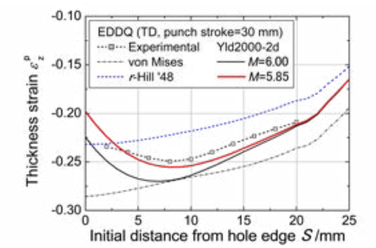

Figure 3: Experimental radial thickness strain profile in TD for HE specimen and predictions with different yield conditions

Figure 4: HE specimen showing neck and crack initiation at 45° from RD (Reproduced from [4] with the permission of AIP Publishing.)

Fig. 3 shows the radial strain distribution from the hole edge towards the specimen outside, experimentally determined in TD and simulated with the four constitutive descriptions as discussed above. It is clear that the results obtained with Hill's 48 and von Mises are not in good agreement with the experiments. Even the trends of the strain profile, which exhibits a minimum at about 8 mm from the hole edge, cannot be captured with von Mises and Hill's 48. In contrast, the curves predicted with Yld2000-2d are much closer to the experimental points. In addition, a minimum is predicted at distances of 8 and 7 mm for *M*=5.85 and 6, respectively, in agreement with the experiment. Finally, there is a significant strain difference depending on the value of the exponent *M* with 5.85 leading to the best agreement with the experiments. Experimentally, Fig. 4 indicates that the crack initiates at about 45° from the RD after strain localization occurs. This is consistent with the minimum thickness strain measured for this orientation (not shown here). This example clearly illustrates that the predicted strain field in the hole expansion test is extremely sensitive to the constitutive equations of plasticity. In these conditions, accurate simulations results can be achieved only at the expense of advanced mechanical characterization techniques [4] and constitutive models.

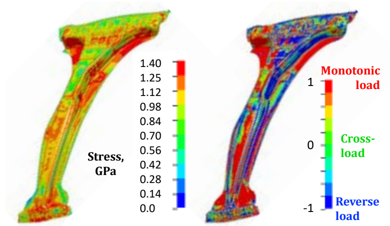

Figure 5. Simulated residual stress field of a B-pillar and strain path change severity map at the end of forming (1 for monotonic loading, i.e. no strain path change; –1 for load reversal, i.e., most severe change)

B-pillar simulations

This example pertains to the simulation of a B-pillar, a complex part for an automotive structure (POSCO EV concept). The forming and springback simulations were conducted by accounting for the influence of strain path change such as Bauchinger effect, permanent softening, transient hardening and cross-loading contraction. In addition, the influence of the hydrostatic stress on the flow curve, leading to the observed S-D effect, was considered [5]. This involved the use of a pressure sensitive, distortional plasticity model with an anisotropic yield function and a reference flow curve for isotropic hardening. Fig. 5 shows residual stress and strain path change severity maps. This example indicates that, with a robust and accurate implementation scheme in FE [6], advanced plasticity models can be used successfully to conduct challenging forming simulations of complex parts.

References:

[1] Yoon, JW, Barlat, F, Dick, RE, Karabin, ME, 2006. Int. J. Plasticity 22, 174-193.

[2] Lee, JY, Lee, M-G, Barlat, F, Chung, KH, Kim, DJ, 2016. Int. J. Solids Structures 87, 254–266.

[3] Nakano, H, Hakoyama, T, Kuwabara, T, 2017. ESAFORM, AIP Conference Proceedings, Vol 1896, 020014.

[4] Kuwabara, T, 2014. In Comprehensive Materials Processing; Van Tyne, CJ, Ed.; Elsevier Ltd., Vol. 1, pp 95-111.

[5] Barlat, F., Yoon, S.Y., Lee, S.Y., Wi, M.S., Kim, J.H., 2020. Int. J. Solids Structures 202, 947–962.

[6] Yoon, S.Y., Barlat, F., Lee, S.Y., Kim, J.H., Wi, M.S., Kim, D.J., 2022. J. Mat. Proc. Technology 302,117494.

CAE Wissen by courtesy of

Frédéric Barlat and Seong-Yong Yoon

Pohang University of Science and Technology, Republic of Korea.

Toshihiko Kuwabara

Tokyo University of Agriculture and Technology, Japan

Material Models for Polymeric Materials

Polymer is a chemical notion comprising many different materials that strongly differ from the physical behaviour of metals. From an engineering point of view it is instructive to subdivide polymers broadly according to their mechanical behaviour into materials with and without permanent deformation. In automotive structures, these are typically:

- Elastomers, recoverable foams, plastics at small deformation
- Crushable foams, plastics at large deformation

All polymers consist of long chain molecules. The differences relate to the number of crosslinks between them (Figure 1).

a) Thermoplastic b) Thermoset c) Elastomer

Figure 1: Molecular structure of polymers

Elastomers

Elastomers are types of polymers that exhibit rubber-like qualities where disorder of the molecule arrangement is a measure of loading (entropy elasticity). Elastomers can be described phenomenologically by hyperelasticity where the stress σ can be obtained by derivation of an appropriate energy function W with respect to the principle stretch ratio λ:

$$\sigma_i = \frac{1}{\lambda_j \lambda_k} \frac{\partial W}{\partial \lambda_i}$$

As an example, Ogden's energy functions is given as

$$W = \sum_{i=1}^{3} \sum_{j=1}^{n} \frac{\mu_j}{\alpha_j} \left(\lambda_i^{*\alpha_j} - 1 \right) + K \left(J - 1 - \ln J \right)$$

where $J = \lambda_1 \lambda_2 \lambda_3$ and $\lambda_i^* = \lambda_i J^{-1/3} = \dfrac{\lambda_i}{J^{1/3}}$

In the case of strain-rate sensitive rubbers, some linear dampers are considered additionally in parallel. As an example, Figure 2 shows the head certification test for pedestrian protection where the skin of the head impactor consists of highly strain rate dependent rubber.

a) Setup b) Head certification test c) Resultant acceleration

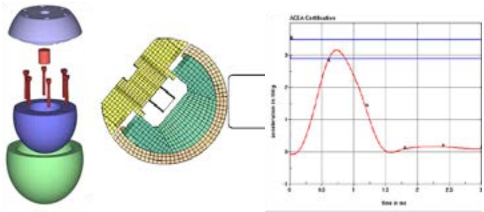

Figure 2: Head impactor for pedestrian protection

Foams

Polymer foams are unique gas-polymer composites that are used in a variety of applications based on their ability to absorb energy. Under compression, foams can be considered as materials with a Poisson coefficient close to zero (Figure 3).

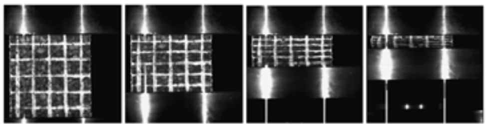

Figure 3: Compression test of an EPP foam

If they are completely recoverable, i.e. there is no permanent deformation during mechanical loading, the mathematical description of the material response can be formulated by the same theory as for elastomers, i.e. hyperelasticity. Contrary for foams that exhibit permanent deformation, a non-isochoric elasto-plastic description can be used.

In both cases, modern explicit finite element packages allow for a tabulated input of the stress-strain relation, even strain rate dependent. It is therefore sufficient to describe the principal stress-strain behavior mathematically, e.g. by

$$\sigma(\varepsilon, \dot{\varepsilon}) = \frac{a_0}{E} \left[1 + K\varepsilon - \exp\left(-\frac{C}{B} \right) \right] \exp\left(\frac{D}{D - E^{c_0}} \right)$$

where the parameters $a_0(\dot{\varepsilon}) = A + H \log\left(\dfrac{F + \dot{\varepsilon}}{F} \right)$ and $c_0(\dot{\varepsilon}) = C + \dfrac{G}{G + \dot{\varepsilon}}$ describe the strain-rate dependency of the material, see Figure 4.

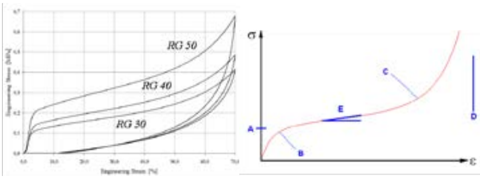

Figure 4: Typical stress-strain relation of a foam under compression for different densities and its mathematical parameterisation.

Plastics

Thermoplastics are polymers with non-crosslinked chain molecules in amorphous or crystalline structure. They turn to liquids when heated and freeze to very glassy states when cooled sufficiently. The same effect occurs if we increase and decrease the strain rate respectively. At small strains, thermoplastics behave viscoelastic, i.e. they have a certain strain rate dependency but (almost) no permanent deformation. At large strains, thermoplastics can be described in a pretty good approximation by viscoplasticity, i.e. strain rate dependency below the yield surface is neglected. Effects like

- increase of volume during plastic flow (crazing),
- different yield stress under tension/compression/shear/biaxial tension and
- decrease of Young's modulus for increasing strain (damage)

also need to be considered to obtain a reasonable material formulation for thermoplastics.

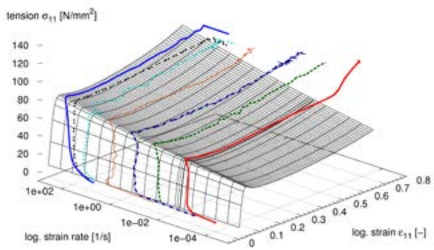

Figure 5: Parameterization of dynamic stress-strain curves.

Also for plastic materials, modern material laws allow for a direct input of the stress-strain relation, but only at constant strain-rates. This, however, is hard to achieve experimentally. It is therefore useful to parameterize the material response e.g. by a simplified G'Sell-Jonas law

$$\sigma(\varepsilon,\dot{\varepsilon}) = \sigma(\varepsilon,\dot{\varepsilon}_0)\left(\frac{\dot{\varepsilon}}{\dot{\varepsilon}_0}\right)^m$$

from which the stress-strain curves at constant strain-rates may be computed. However there are, similar to metals, a lot of open questions due to the influence of the process chain. The influence of fibre orientation and weld lines that lead to a much more brittle behavior (Figure 6,7) can be considered by coupling of the analysis of injection moulding and structural analysis ("integrative simulations") which are topics of ongoing investigations.

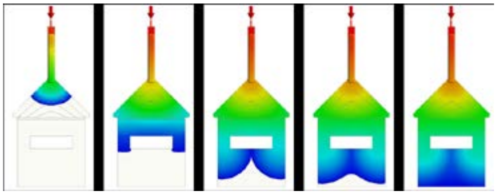

Figure 6: Fill study of a specimen enforcing weld lines

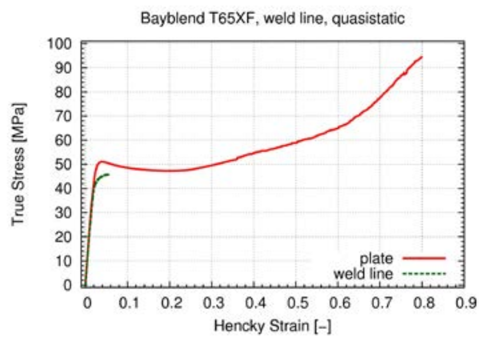

Figure 7: Influence of weld lines during tensile test

Multiscale Material Models for Short-Fiber-Reinforced Plastics

What is Multiscale Modeling?

Multiscale modeling approaches are increasingly used in structural simulation. By means of such approaches, the material behavior of inhomogeneous materials can be described. In particular, such models are used for injection molded short fiber reinforced plastics. The idea here is to resolve the complex material structure in the component by changing the length scale range (localization or downscaling) to such an extent that the relationships in the higher-resolution length scale range (micro or meso level) are more accessible to a mathematical description (Figure 1).

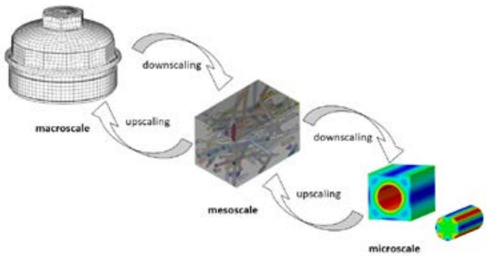

Figure 1: Multiscale Modeling Approach

Thus, it is possible to calculate the behavior of a composite material only on the basis of the material properties of its constituents, i.e. matrix polymer and reinforcing fiber. The constituents with their specific properties and their spatial configuration then determine the material behavior of the composite also at the macroscopic component level (Figure 2).

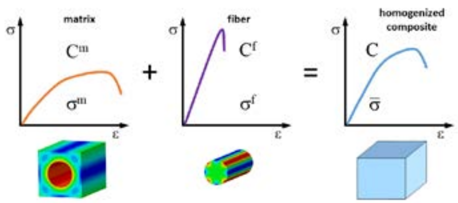

Figure 2: Material Modeling at the Micro Level

For reasons of efficiency, it is now not appropriate to represent a complete component by completely modeling its microstructure. For this reason, a so-called homogenization (upscaling) is carried out. Starting from the properties of the inhomogeneous material at the micro or meso level, equivalent homogenized properties (e.g. stiffnesses) are determined. The material is then regarded as a homogeneous continuum. In the case of short fiber reinforcement, the homogenized material then exhibits analogous anisotropic behavior as the real inhomogeneous composite material. The homogenized material characteristics can then be used to perform numerically efficient FEM analyses of the component. The material modeling at the micro or meso level including the homogenization can be done in different ways. This is the main difference between the various multiscale modeling approaches. In the following, some of the frequently used approaches are presented.

Various Multiscale Approaches

The basis of the approaches is the definition of a so-called representative volume element (RVE). The RVE represents a cutout of the macroscopic component structure. On the one hand, the RVE must comprise the typical microstructure of the material to such an extent that, when the volume section is further enlarged, its external mechanical properties no longer change. It must be representative in a statistical sense, i.e. it must allow a reasonable averaging in the considered section. On the other hand, the RVE must be smaller than the characteristic dimensions of the component. As a rule, several RVEs must be defined for a component, since the local microstructure in the component also differs as a result of the fiber alignment. Basically, the multiscale modeling approaches can be divided into numerical and analytical procedures. Both approaches are presented in the following as examples.

Numerical Multiscale Approaches

Numerical multiscale models represent the real microstructure on the meso level in a defined section of the component, the RVE (Figure 3).

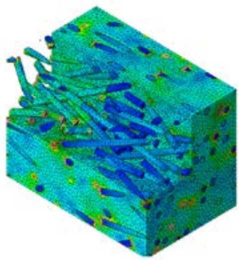

Figure 3: Numerical RVE [IPF, Dresden, 2022]

FE models are typically used for this purpose. The challenge here is to model the microstructure with sufficient accuracy while keeping the model size within acceptable limits. For the model to be representative of the component section under consideration, a sufficient number of fibers must be modeled, e.g. 100 fibers. These are then randomly distributed in the volume according to the assumed spatial fiber orientation distribution (angle classes). Periodic boundary conditions are imposed on the bounding surfaces of the RVE.

The displacement boundary conditions of the respective opposing surfaces of the RVE are coupled. This satisfies the assumption that the cutouts of the microstructure line up in the component.

Macroscopic displacements can now be imposed on the RVE, which are obtained from the corresponding position in the component via an FE analysis. Again, by means of an FE analysis of the RVE, the strain and stress distribution in the RVE is determined. In a further step, homogenization is then performed via volume averaging of the strain and stress distribution in the RVE:

$$\bar{\boldsymbol{\sigma}} = \frac{1}{V}\int_V \boldsymbol{\sigma}\, dV; \qquad \bar{\boldsymbol{\varepsilon}} = \frac{1}{V}\int_V \boldsymbol{\varepsilon}\, dV \quad (1)$$

with: $\boldsymbol{\varepsilon}$ strain tensor, $\boldsymbol{\sigma}$ stress tensor, $\mathbf{V}$ volume, ($\bar{}$) volume averaged values

This then gives the averaged stiffness tensor:

$$\mathbf{C} = \frac{\bar{\boldsymbol{\sigma}}}{\bar{\boldsymbol{\varepsilon}}} \quad (2)$$

with: $\mathbf{C}$ volume averaged composite stiffness

This can then be transferred back to the FE simulation of the component to calculate the next load step.

Due to the nested FE analyses of component and RVE, the term FE² is used for this procedure. This already indicates the high numerical effort. For this reason, different variants of the procedure were developed. In the case of linear-elastic material behavior, the stiffness tensor does not change over the load steps. In this case, it is possible to work with pre-analyzed RVEs whose stiffnesses are then stored in a database and assigned to the respective local microstructure in the component. Instead of an FEM analysis of the RVE, it is also possible to work with a voxel-like structured mesh that is calculated using a so-called FFT solver. This can significantly reduce the computation time for the RVE. There are also approaches that use numerical RVEs to train a neural network (AI). The neural network then provides an analytical model for the mechanical behavior of the RVE, which can be efficiently passed to the simulation of the component.

Numerical RVEs have basically no limitations in terms of material description. In addition to linear-elastic material behavior, plastic and viscoelastic behavior can also be described. Furthermore, a high resolution with regard to the cause and localization of damage can be achieved within the scope of failure evaluation. For example, it is possible to differentiate between fiber fracture, matrix fracture and fiber/matrix debonding. The price for this, however, is the high modeling effort and very long computing times, so that an analysis of complete components with this approach is not suitable for practice, at least at present.

Analytical Multiscale Approaches

Historically, the analytical multiscale approaches known today are based on micromechanical models that have been known for many decades. Here, too, all methods aim to homogenize a physically inhomogeneous material and to provide averaged mechanical properties that exhibit equivalent behavior as the inhomogeneous material. In connection with analytical multiscale approaches, this is also referred to as mean-field homogenization (MFH). This expresses the fact that mechanical field quantities such as strain and stress are averaged in the RVE to calculate the effective stiffness of the homogenized composite.

Mixing Rules

The simplest models are mixing rules that calculate the stiffness or compliance of the composite from the fiber volume fraction and the stiffnesses of fiber and matrix. The approaches of Voigt and Reuss are worth mentioning here:

$$\mathbf{C}^{\text{Voigt}} = \mathbf{C}^{m} + v_f\left(\mathbf{C}^{f} - \mathbf{C}^{m}\right) = v_f\mathbf{C}^{f} + v_m\mathbf{C}^{m} \quad (3)$$

$$\mathbf{S}^{\text{Reuss}} = \mathbf{S}^{m} + v_f\left(\mathbf{S}^{f} - \mathbf{S}^{m}\right) = v_f\mathbf{S}^{f} + v_m\mathbf{S}^{m} \quad (4)$$

with: $\mathbf{C}$ stiffness tensor, $\mathbf{S} = [\mathbf{C}]^{-1}$ compliance tensor, v_f fiber volume fraction, $v_m = (1-v_f)$ matrix volume fraction

Since the fiber weight fraction is usually better known, the fiber volume fraction can be calculated as follows:

$$v_f = \frac{1}{1 + \frac{1-\mu_f}{\mu_f}\frac{\rho_f}{\rho_m}} \quad (5)$$

with: μ fiber weight fraction, ρ density

Voigt's approach assumes that fiber and matrix experience identical strain in the RVE, whereas Reuss assumes identical stress. Voigt therefore calculates the stiffness of the composite, while Reuss calculates the compliance. The Reuss approach is also known as the inverse mixing rule. Since no information about the fiber geometry is included in either model, they are only rough approximations for geometrically oriented (non-spherical) inclusions. The Voigt approach is an upper bound and the Reuss approach a lower bound for the composite stiffness.

Models Based on the Eshelby Theory

A number of more powerful models exist than the mixing rules described above, which can also take into account different fiber geometries and allow significantly better predictions of the composite properties even of anisotropic materials. Among the best known models are those based on the work of Eshelby (1957). The starting point of Eshelby's theory is an RVE consisting of an ellipsoidal inclusion, in the case of short fiber reinforced plastics, a single fiber surrounded by an infinitely extended matrix.

A fundamental concept of the theory is the introduction of so-called strain and stress concentration tensors $\mathbf{A}$ and $\mathbf{B}$. These are the ratios between the averaged strain (stress) in the fiber and the corresponding averaged values in the composite:

$$\bar{\boldsymbol{\varepsilon}}^f = \mathbf{A}\,\bar{\boldsymbol{\varepsilon}} \qquad (6)$$

$$\bar{\boldsymbol{\sigma}}^f = \mathbf{B}\,\bar{\boldsymbol{\sigma}} \qquad (7)$$

with: $\mathbf{A}$ strain concentration tensor, $\mathbf{B}$ stress concentration tensor

The concentration tensors $\mathbf{A}$ and $\mathbf{B}$ have the task of transforming the macroscopic external strains $\bar{\boldsymbol{\varepsilon}}$ and stresses $\bar{\boldsymbol{\sigma}}$ at the boundary of the RVE to the local averaged strains $\bar{\boldsymbol{\varepsilon}}^f$ and stresses $\bar{\boldsymbol{\sigma}}^f$ in the fiber. The averaged composite stiffness can then be calculated using the following relationship:

$$\mathbf{C} = \mathbf{C}^m + v_f\left(\mathbf{C}^f - \mathbf{C}^m\right)\mathbf{A} \qquad (8)$$

The volume-averaged stiffness $\mathbf{C}$ of the composite is calculated in this way from the known stiffnesses for fiber and matrix material $\mathbf{C}^f$ and $\mathbf{C}^m$, the fiber volume fraction and the concentration tensor $\mathbf{A}$. The only question that remains is how to determine the concentration tensor $\mathbf{A}$. The literature provides various procedures for this.

Eshelby gives the strain concentration tensor $\mathbf{A}$ as follows.:

$$\mathbf{A}^{\text{Eshelby}} = \left[\mathbf{I} + \mathbf{E}\mathbf{S}^m\left(\mathbf{C}^f - \mathbf{C}^m\right)\right]^{-1} \qquad (9)$$

with: $\mathbf{I}$ identity tensor, $\mathbf{E}$ Eshelby tensor

The Eshelby tensor $\mathbf{E}$ is calculated from the known values of the stiffness tensor of the matrix $\mathbf{C}^m$ and the length/diameter ratio of the fiber (see related literature). Thus, all quantities for the calculation of the composite stiffness are known. However, the calculation of the composite stiffness by means of the strain concentration tensor $\mathbf{A}^{\text{Eshelby}}$ is only accurate up to fiber volume fractions of approx. 1 %. In this context, one therefore also speaks of the dilute Eshelby model. Consequently, this is not directly applicable to short-fiber-reinforced plastics of practical relevance.

For this reason, **Mori** and **Tanaka** proposed an alternative definition of the strain concentration tensor $\mathbf{A}$ for non-dilute materials, which is frequently used for modeling short-fiber-reinforced plastics. The basic idea of Mori and Tanaka is that a fiber around it sees only properties of the matrix and not those of the homogenized composite (see Eq. (6)):

$$\bar{\boldsymbol{\varepsilon}}^f = \mathbf{A}^{\text{Eshelby}}\,\bar{\boldsymbol{\varepsilon}}^m \qquad (10)$$

Thus, the fibers are so far apart that they have no interaction with each other. Using Eshelby's fundamental solution for the mechanical relations of a single fiber embedded in an (infinitely extended) matrix, the strain concentration tensor $\mathbf{A}^{MT}$ of Mori and Tanaka can be calculated under this assumption to:

$$\mathbf{A}^{MT} = \mathbf{A}^{\text{Eshelby}}\left[\left(1 - v_f\right)\mathbf{I} + v_f\mathbf{A}^{\text{Eshelby}}\right]^{-1} \qquad (11)$$

Using the strain concentration tensor $\mathbf{A}^{MT}$ and Eq. (8), the stiffness of the composite material finally follows. The equation initially applies to any material behavior in fiber and matrix, since no restrictions have been made so far for the stiffness tensors $\mathbf{C}^f$ and $\mathbf{C}^m$. Under the limiting assumption of linear-elastic material behavior, **Tandon** and **Weng** give an analytical solution with which the composite stiffness can be calculated directly in terms of the engineering constants. However, if, for example, the matrix is described elasto-plastically, an anisotropic stiffness tensor always follows in general. In this case, no analytical solution can be given, and the composite stiffness must be determined iteratively numerically.

A restriction of the Mori-Tanaka theory, and all relations based on it, which is significant for practical applications, is based on the assumption that a fiber is not coupled with a neighboring fiber. Thus, strictly speaking, the Mori-Tanaka approach applies only to low fiber volume contents. However, practice shows that the Mori-Tanaka approach can also be successfully applied for fiber volume contents of 30% and more.

Orientation Averaging

Since the Mori-Tanaka approach is based on the Eshelby solution, the relationship initially applies only to microstructures in which the fibers in the representative volume under consideration are all oriented in the same direction, i.e. unidirectionally (transversely isotropic). This is not the case for real microstructures in injection molded parts. Rather, there is a spatial fiber orientation distribution. In addition to the volume averaging of the composite stiffness shown above by means of the various methods, an averaging of the composite stiffnesses over the various fiber orientation angle classes must also be carried out in a second step.

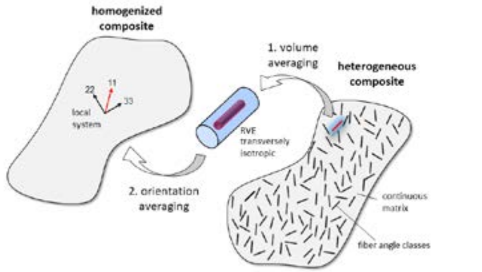

Figure 4: 2-Step Homogenization

This is referred to as a 2-step homogenization. The result of both steps is the homogenized effective total stiffness of the composite for the given fiber orientation distribution (Figure 4).

The total stiffness of the composite is then calculated to:

$$\mathbf{C} = \mathbf{C}^{m} + \sum_{i=1}^{N} w_i \, v_f \left(\mathbf{C}^{f} - \mathbf{C}^{m}\right) \mathbf{A}_i^{\angle\,\text{Eshelby}} \; \bar{\mathbf{A}}^{MT} \qquad (12)$$

with: w_i weight per angle class, $\mathbf{A}_i^{\angle\,\text{Eshelby}}$ strain concentration tensor transformed into local element coordinate system, $\bar{\mathbf{A}}^{MT}$ averaged strain concentration tensor

The weighting factors w_i are obtained from the reconstruction of the orientation distribution function, which is further described below. The type of homogenization given in Eq. (12) is called full-Mori-Tanaka homogenization in contrast to the so-called pseudo-grain homogenization. In pseudo-grain homogenization, not only the fibers are divided into different fiber angle classes, but also the surrounding matrix (grains). The strain concentration tensor is calculated independently of all other fibers. That is, coupling of the strain concentration tensor for each individual fiber to the situation in the surrounding composite is not considered. As a result, the interaction between fibers of different orientations is lost. In the full Mori-Tanaka formulation, on the other hand, the matrix is treated as a continuous phase. This seems to be closer to the real situation in the composite in terms of common sense.

Reconstruction of the Orientation Distribution Function

Both numerical and analytical multiscale models always require knowledge of the local microstructure in the component. This can be determined experimentally, e.g. by means of µCT measurements (Figure 5). Of course, this already assumes the existence of a component. Therefore, the fiber orientation distribution is usually determined numerically by means of an injection molding simulation. However, the injection molding simulation provides the fiber orientation distribution only indirectly via the orientation tensor. The spatial distribution of the fibers must be reconstructed from the orientation tensor using suitable mathematical methods (Figure 5).

The 2-step homogenization based on the full Mori-Tanaka approach is implemented in PART Engineering's multiscale software CONVERSE for the determination of the linear elastic behavior of the composite. For the linear elastic case, such an approach is computationally very effective and provides the elastic properties in good agreement with experiments. However, for the plastic part of the material behavior, it is known that the predictive ability of analytical micromechanical models is generally poor.

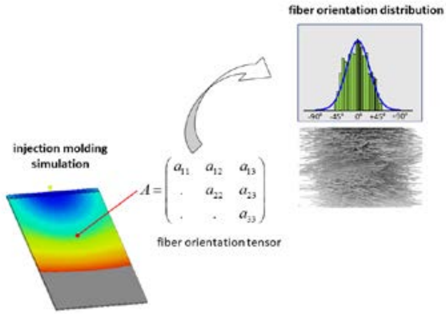

Figure 5: Reconstruction of the Fiber Orientation Distribution from the Orientation Tensor.

Moreover, accounting for plastic effects at the microscale implies an incremental numerical solution approach to the entire set of micromechanical equations, which is numerically very expensive. Therefore, plastic effects are accounted for in CONVERSE by introducing an orientation-dependent yield criterion already defined for the homogenized composite, which is computationally very effective and easy to handle with respect to the calibration of the model. Thus, with the help of the analytical modeling approaches presented in this paper, so-called pre-homogenized material cards are computed which are then transferred to the respective FE solver (Figure 6).

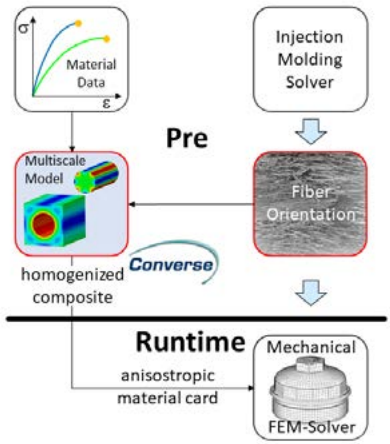

Figure 6: Pre-Homogenized Material Cards

CAE Wissen by courtesy of Dr. Wolfgang Korte

Managing Director, korte@partengineering.com, phone 02204 -306 77 20

PART Engineering GmbH, Friedrich-Ebert-Str. 75, 51429 Bergisch Gladbach, Germany

Material Models of Composites for Crash Simulation

Many different types of composites exist today, but generally there is a common aim to combine two or more constituents to give a better material than each of the individual constituents. The most popular composites today combine strong stiff fibres (e.g. Carbon, Glass or Aramid) with a low strength polymer matrix (e.g. Epoxy or Polyester). Great flexibility is possible in combining these materials to obtain required cost and performance.
The fibres are first brought together as yarns having, typically, 6k (k=1000) and possibly up to 48k fibres. These yarns may be directly used to manufacture a 'preform', which is the basic textile structure of the composite; or they may be further processed into fabrics. The fabrics would then be formed (draped), combined and trimmed for the preform. Generally, Aerospace applications use 6k or 12k tows for best performance, whereas 'thicker' 24k or even 48k tows are preferred for Automotive applications where low cost fast preforming is the priority. Many different types of fabrics are produced having widely different drape, infusion or final part mechanical properties for stiffness, strength or impact. Generally, fabrics fall into two groups and either have intertwined yarns (e.g. Plain weaves and Twills) or have straight yarns (Non Crimp Fabrics) for better stiffness. In this case yarns are overlaid and held together with light stitching.

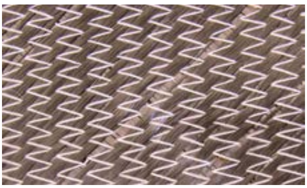

Bi-axial NCF (tricot stitch)

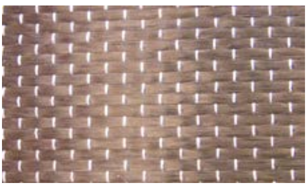

Uni-directional NCF

The function of the resin is to protect fibers and transfer stresses between them; particularly for load redistribution at the ends of any fibres that may break. Again, an enormous variety or resin types are commercially available ranging from low performance, low cost, polyester systems to high performance epoxy resins and super high performance/cost PEEK thermoplastic resins. Finally, manufacturing methods for composites broadly fall into two camps. First, there are the high performance pre-preg composites in which a laminate is made from stacking plies which have resin pre-impregnated into the fibres; and second, there are Liquid Resin Infusion technologies where resin is only added after the dry fabrics are placed and shaped.
Regardless of the fibre, fabric or resin types there are usually common analysis methods available to predict composites mechanical performance; these range from simple analytical methods for stiffness to advanced Finite Element methods for stiffness, failure and impact or crash loading. Some simple formulae based on mechanics of materials can be helpful to obtain basic mechanical data; these so-called micro-mechanics laws combine fibre and matrix properties to give homogenized composite properties.

$$E_1 = E_f \cdot V_f + E_m \cdot V_m$$

Voigt model: This law of mixtures gives accurate axial composite modulus E_1 from fibre modulus (E_f), resin modulus (E_m), fibre volume ratio (V_f = vol. fibres/ total vol.) and the matrix volume ratio V_m (=1-V_f/ total vol.).

$$\frac{1}{E_2} = \frac{V_f}{E_{2f}} + \frac{V_m}{E_m}$$

Reuss model: This reciprocal law of mixtures for E_2 gives a poor estimate for transverse modulus since transverse stresses are non-uniform and poorly represented by the assumed simple spring model. Improved relations are given by the Halpin-Tsai or Hopkins-Chamis models.

Despite considerable research it has been difficult to extend micro-mechanics models to woven textile composites for accurate failure prediction. If homogenized properties are available, from test or micro-mechanics, then Classical Laminate Theory (CLT) can be used to compute laminate stiffness of a stack of plies. Software tools are available to help automate these calculations. Typically, for a given applied loading, these codes compute overall laminate strains and individual ply stresses and strains in the fibre directions. Classical failure criteria can then be used to compute maximum load limits.

During the past 30 years many ply failure criteria have been proposed with the main ones being Maximum Stress (or Strain) and the Tsai-Hill and Tsai-Wu 'quadratic' criteria. Each of these describes a failure envelope in stress, or strain space, and gives the limits of safe loading. These criteria have points determined from coupon tests and assumptions are used to complete the envelope. The Maximum Stress-Strain criteria assumes no interaction of stress components on failure, whereas the quadratic criteria more correctly assumes stress interactions but can be unrealistic for some load combinations. In recent years the physically based Puck criteria for UD composites has gained popularity and does overcome many of these limitations.

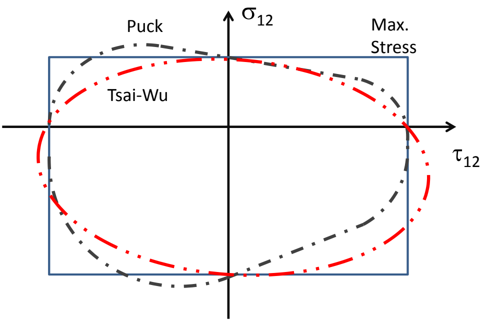

For impact and crash classical criteria are not appropriate and progressive ply damage laws should be used since these allow the different ply failure modes to be represented and damaged independently. For a UD composite failure modes may be fibre tension or compression failure, transverse matrix tension or compression failure, or matrix shear failure. In addition delamination of the weak resin layer between plies may occur. The popular approach to model ply damage is via damage variables that modify initial linear stiffness; delamination is usually approximated with damaging spring elements that tie plies together and absorb resin fracture energy during progressive failure.

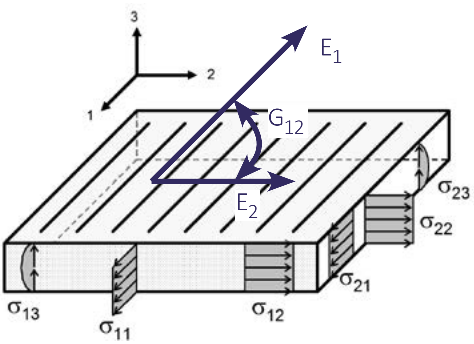

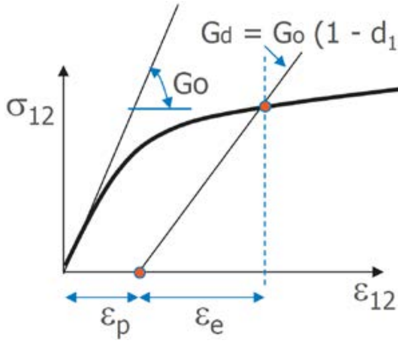

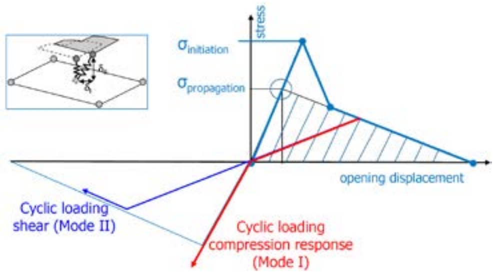

A further important crash mode is axial crushing. Here ply and delamination models are not applicable and specialized techniques to model composites fragmentation are needed. Fragmentation is initiated via a trigger device (usually a chamfer) that creates local micro-cracking; this then steadily propagates through the part as it is crushed. An important feature is that material at the crash front is fundamentally different to the intact undamaged materials and both must be properly represented in the numerical model.

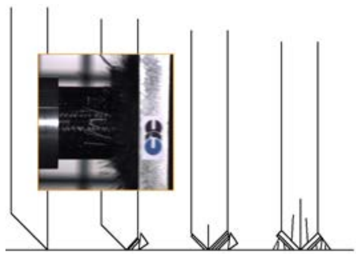

CAE Wissen by courtesy of Dr. Anthony Pickett, IFB University of Stuttgart.

Latest info about this course

Material Models of Composites for Crash Simulation

Course Description

Increasing demands for weight reduction paralleled by requirements for improved crash performance and stiffness of structures have strongly pushed the development of advanced composites. The use of composite materials today is not limited to niche applications or secondary parts; they are increasingly used for important load carrying structural components in series production.

In this one day seminar Prof. Thomas Karall presents the foundations of structural impact and crash analysis of composites with the Finite Element Method. At the beginning of the seminar an overview of current and upcoming industrial applications of composite materials is given. Thereafter concepts for the correct physical modeling of the complex load degradation and failure mechanisms in numerical simulation are presented. The course concentrates on the numerical simulation of the crash behavior of composites and is accompanied with demonstrations using the PAM-CRASH code.

Who should attend?

The course addresses simulation and project engineers, project managers as well as researchers involved in the analysis and design of composite parts and structures.

Course Contents

- Current and upcoming areas of application of composite materials
- Analysis of composite materials
- Available material models and their application
- Modeling methods for plies and laminates
- FEM modeling of composites
- Failure mechanisms and their representation
- PAM-CRASH ply and delamination models
- Necessary material tests
- Examples

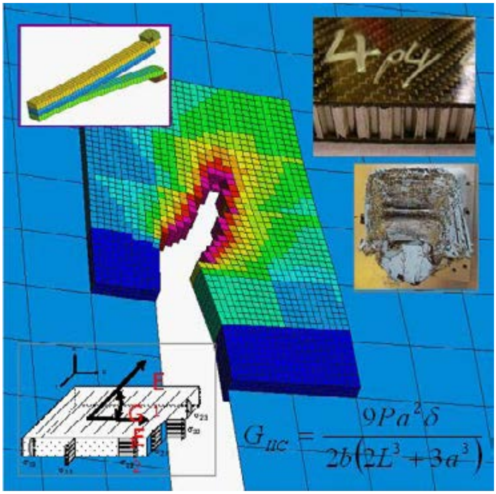

Instructor

Prof. Dr. Thomas Karall (Hof University of Applied Sciences) studied mechanical engineering at the Technical University of Vienna and received his PhD as Assistant Professor at the University of Leoben in the field of fibre-reinforced plastics and the calculation by finite elements. From 2006 to 2010 he was head of department at the Austrian Research Institute for Chemistry and Technology in Vienna in the field of mechanical and thermal testing / fibre composites, and Secretary General of the Austrian Working Group for reinforced plastics. From 2010 to 2015 he worked as Lead Researcher for lightweight design at Virtual Vehicle Research Center in Graz. He was also a lecturer at the Technical University of Graz and lecturer at the FH Joanneum Graz. Since 2015 he has been Professor at the Engineering Department of the Hof University. His areas of work include lightweight design, fibre-reinforced composites and the finite element method.

Facts

09.-10.10.2025	68/4536	Online	2 x 4 Hrs.	890,- EUR till 11.09.2025, thereafter 1.090,- EUR	

Static and Dynamic Analysis of Long-Fibre-Reinforced Plastics

Course Description

Due to increasingly strong social and political demands for a reduction of the energy demand of automobiles, systematic lightweight construction is becoming more and more important in this industry sector. Special opportunities are offered by the use of fibre-reinforced composites as prime materials for lightweight constructions. A major challenge of these materials is the anisotropic material behavior and its calculation. Given the fact that composites are constructed entirely different and behave completely different compared to the classic metallic materials, the engineer must learn to deal with this class of materials to use the advantages of composites for the design of vehicle structures. In the seminar the attendees are first introduced to examples from practice and gain a basic understanding of the tasks. After that, the theoretical and practical aspects of computing methods are explained in order to be able to calculate statically and dynamically loaded structures of long fibre-reinforced plastics.

Course Objectives

After participating in the seminar "Static and dynamic analysis of long-fibre-reinforced plastics", participants are able to compute composite structures and to identify the effective mechanisms of the associated physics. They understand the different requirements of a fibre composite structure and the associated calculation concepts. A particular focus of the seminar is aimed at the challenges, the problems and limitations in the analysis of long-fibre-reinforced composites. Accordingly, it provides knowledge for the design and the detailed FE analysis. Furthermore, the various damage mechanisms and failure criteria are explained.

Who should attend?

The seminar is especially designed for engineers and technicians in the development and simulation departments of automobile manufacturers, suppliers and engineering service providers dealing with the simulation and development of fibre composite components, and fibre composite structures.

Course Contents

- Introduction
- Mechanics of Composite Materials and Structures
- Characteristics and parameter determination of composite materials
- Calculation of long-fibre-reinforced plastics
- FEM modeling
- Material models for structural-mechanical description
- Calculation of static loads
- Calculation of dynamic loads
- Failure criteria of composites
- Damage and failure mechanisms of composite materials

Instructor

Prof. Dr. Thomas Karall (Hof University of Applied Sciences) studied mechanical engineering at the Technical University of Vienna and received his PhD as Assistant Professor at the University of Leoben in the field of fibre-reinforced plastics and the calculation by finite elements. From 2006 to 2010 he was head of department at the Austrian Research Institute for Chemistry and Technology in Vienna in the field of mechanical and thermal testing / fibre composites, and Secretary General of the Austrian Working Group for reinforced plastics. From 2010 to 2015 he worked as Lead Researcher for lightweight design at Virtual Vehicle Research Center in Graz. He was also a lecturer at the Technical University of Graz and lecturer at the FH Joanneum Graz. Since 2015 he has been Professor at the Engineering Department of the Hof University. His areas of work include lightweight design, fibre-reinforced composites and the finite element method.

Facts

14.11.2025	145/4535	Alzenau	1 Day	890,- EUR till 17.10.2025, thereafter 1.090,- EUR	
20.03.2026	145/4629	Alzenau	1 Day	890,- EUR till 20.02.2026, thereafter 1.090,- EUR	

Spot Weld Modeling for Crash Simulation

Joints are often the weak points of a vehicle when overload occurs e.g. in crash situations. They join the single components to the load-bearing body in white. The crash simulation needs reliable and applicable tools for the prediction of the load bearing capacity and energy absorption of all kinds of joints to ensure the crash safety of vehicles.

Joints are modeled with simplified models in crash simulations of whole cars due to efficiency. The simplified models should be able to reproduce the deformation and failure behavior as well as the energy absorption of the joints with less computational cost but with adequate accuracy. Simplified modeling techniques for point-shaped, line-shaped and plane joints are available in different crash codes and still new models are developed because of an increasing variety of new joining techniques. The procedure of determination of damage and fracture parameters of the models is a more or less standard procedure of inverse simulation. The procedure of calibration of model parameters of spot welds is shown in this article.

Definition of spot weld model

Here, as example a solid element is used for the geometric representation of a spot weld as one possibility for the simplified modeling of spot welds. Figure 1 shows the dimensions and the position of a solid element representing one spot weld. The solid element is bound to the shell elements in the mid position of the sheet metal using tied contact definitions

The weld nugget diameter d = 5.4 mm and the metal sheet thickness $t_1 = t_2 = 1.5$ mm give the height

$$h = (t_1 + t_2)/2$$

and the element edge length

$$L_e = \sqrt{\pi d^2/4}$$

of the hexahedron.

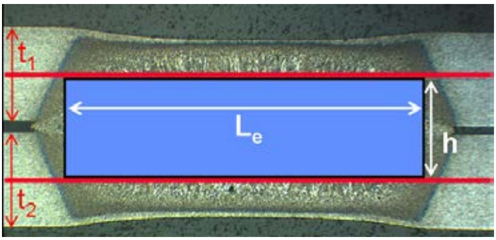

Figure 1: Position and size of spot weld model hexahedron

The failure model is given according to

$$\left(\frac{f_n}{F_n}\right)^2 + \left(\frac{f_s}{F_s}\right)^2 + \left(\frac{m_b}{M_b}\right)^2 + \left(\frac{m_t}{M_t}\right)^2 = 1$$

where f_n, f_s, m_b and m_t are the actual normal and shear force, bending and torsion moment calculated in the hexahedron, respectively. F_n is the critical normal force, F_s the critical shear force, M_b the critical bending moment and M_t the critical torsion moment at fracture. Because of minor importance the critical torsion moment is neglected. The exponents are all equal and set to 2 what results in a quadratic, equal distributed superposition of normal, shear, bending and torsional loading in a mixed loading case.

Procedure of failure parameter determination

The three remaining failure parameters are determined by simulation of specimen tests of spot welded tension, lap-shear and peel specimens. The finite element models of the specimens are shown in Figure 2. The stepwise procedure of calibration of the failure parameters, the critical normal force F_N, the critical shear force F_s and the critical bending moment M_b is described in Table 1. First the tension specimen test is simulated using the spot weld model. Under tension loading the easiest case occurs, because f_s and m_b are zero. If the global maximum force measured in the test is reached by the calculated global force, the local value of f_n is evaluated and gives the value of the critical normal force F_n. In the second step the peel specimen test is simulated. If the calculated global force reaches the measured value of maximum force the local values f_n and m_b of the hexahedron are evaluated, f_s still remains zero. These values are put in the failure model using the already determined value of F_N and the critical bending moment M_B can be calculated by easy transformation of the equation. In the third step the lap-shear specimen is simulated. The values of f_n and f_s are evaluated if the calculated global force reaches the value of the measured maximum force in the lap-shear test. F_S can be calculated by putting these values for f_n, f_s and the already determined value for F_N in the failure equation, because m_b remains zero. With this procedure the triple of parameters of the failure model is determined which is specific for the tested material, spot weld diameter and loading velocity.

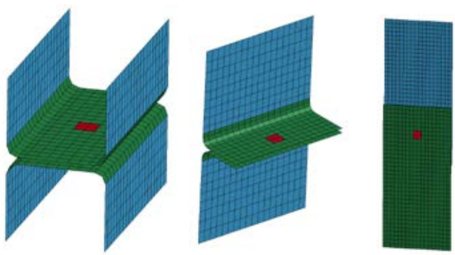

Figure 2: Finite element models of spot welded specimens: tension, peel and lap-shear specimen (from left to right)

step	procedure	result
1	determination of critical normal force by simulation of tension test	F_N
2	determination of critical bending moment by simulation of peel test with fixed value of FN	M_B
3	determination of critical shear force by simulation of lap-shear test with fixed value of FN and MB	F_S

Table 1: Stepwise determination of failure parameters

Results of parameter determination

The result of the determination of parameters is shown in Figure 3. The dashed lines are the measured load vs. displacement curves of the three specimen tests used for parameter calibration. The calculated load vs. displacement curves are shown in straight lines and reproduce the measured load bearing capacities quite well. The determined parameters are shown in Table 2 and are specific for the investigated DP600 spot weld with nugget diameter of 5.4 mm and quasi-static loading.

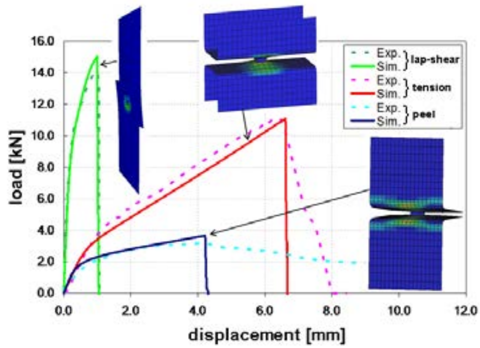

Figure 3: Comparison of the measured and calculated load vs. displacement curves of lap-shear, tension and peel tests using solid elements and MAT_100 in LS-Dyna

F_N	M_B	F_S
11.1 kN	15.7 Nm	15.4 kN

Table 2: Failure parameters for spot welded joints in DP600 with a nugget diameter of 5.4 mm and quasi-static loading

CAE Wissen by courtesy of Dr. Silke Sommer, Fraunhofer IWM, Freiburg

Modeling of Joints in Crash Simulation

Course Description

For the efficient assembly of components and complete structures many different joining techniques are available. Joints have to ensure that the assembly will fulfill crashworthiness, durability and other requirements. Therefore the best joining technique has to be selected for each application. Modern lightweight design often uses a material mix. Using different materials, like various steel grades, lightweight alloys, plastics or composites for applications for which the individual material is best suited allows for weight savings. The efficient and reliable joining of different materials is even more challenging. Failure of joints can be a reason for collapse of vehicle structures during crash testing. Therefore failure of joints must be precisely predicted in numerical crash simulation applied in the virtual design process of vehicle development.

Course Objectives

The objective of this one day course is to give the participants an overview of failure modelling of different joints (punctiform, linear, planar joints) for crash simulation and also of the characterization tests and methods that are necessary for calibrating the model parameters. Also recommendation for validation tests and simulations of calibrated joint models are given. Examples of typical and used models are shown in all common crash codes.

Who should attend?

The course addresses engineers working in the field of crash simulation and heads of simulation departments interested in the important topic of modelling of joints including failure.

Course Contents

- Overview of modeling techniques for different joining techniques
- Tests and methods for characterization of joints
- Local loading conditions at joints during testing under shear, tension and bending load
- Characteristics of failure behavior
- Failure modeling of
  - Spot welded joints including spot welds in press hardened steels
  - Self-piercing riveted joints
  - Laser welded joints
  - Adhesive joints
- Calibration methods for determination of model parameters
- Validation of calibrated models through testing and simulation

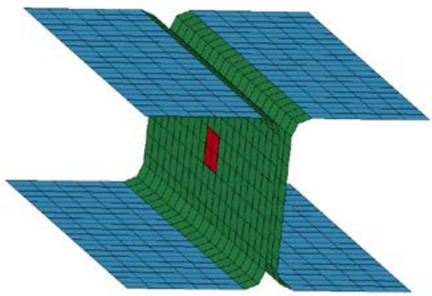

Instructor

Dr.-Ing. Silke Sommer (Fraunhofer-Institut für Werkstoffmechanik) studied Physics at the RWTH Aachen University and obtained her PhD degree at the Karlsruhe Institute of Technology about modeling of the deformation and failure behaviour of spot welds. She has been working at the Fraunhofer Institute for Mechanics of Materials IWM in Freiburg since 2000 in the field of damage and failure modeling of materials and joints for crash simulation. Since 2013 she has been a group leader for joining and joints.

Facts

Date	#	Location	Duration	Price	Language
05.-06.11.2025	155/4525	Online	2 x 4 Hrs.	890,- EUR till 08.10.2025, thereafter 1.090,- EUR	English
19.03.2026	155/4633	Alzenau	1 Day	890,- EUR till 19.02.2026, thereafter 1.090,- EUR	German

Material Parameter Identification - Reverse Engineering

The utilization of new materials such as plastics, composites, foams, textiles or high-strength steels requires the application of highly complex material models. These material models generally bring along numerous material parameters, which are difficult to define. Design optimization can be a useful method to identify those parameters.
Design optimization can be defined as an automated procedure for achieving the best outcome of a given operation while satisfying certain restrictions. This objective has always been central to the design process, but is now assuming greater significance than ever because of the maturity of mathematical and computational tools available for design optimization. These tools are used in different scenarios. Mathematically the problem is always reduced to minimizing a system outcome criterion while satisfying other system responses. A typical example would be the weight reduction of a car body by changing sheet thicknesses under achieving different NVH and crash criteria.

Reverse engineering

Nowadays these optimization tools are often used for "reverse engineering". This method is applied due to the fact that complex interacting problems in measurement and simulation often can't be transformed into a simple problem description, e.g. in the process of material calibration:

- $\sigma(\varepsilon,\dot{\varepsilon})$ couldn't be measured directly or the effort to measure it is too high (e.g. bending test)
- sample preparation doesn't allow or the effort is too high to gain specimens for each loading condition (e.g. compression, shear, tension, ...) or material (e.g. sandwich, glue,...) needed
- the material model parameters are interacting with simulation parameters (e.g. hour glassing) or model idealization (e.g. mesh size, contact formulation of multi material mix)

Parameter identification is commonly used to solve those issues.
Parameter identification problems are non-linear inverse problems which can be solved using mathematical optimization. In most cases the objective is to minimize the mismatch between two curves, typically a two-dimensional experimental target curve, e.g. a stress-strain curve or a force-displacement curve, and the corresponding computed curve extracted from a simulation. The computed curve depends on system parameters that can be varied, e.g. material constants. The main essential components of such an algorithm designed for system identification are

- the optimization algorithm (e.g. metamodel-based or direct optimization)
- the curve matching metric (e.g. Mean Squared Error)
- the formulation of the material "parameter" law (e.g. Johnson Cook)

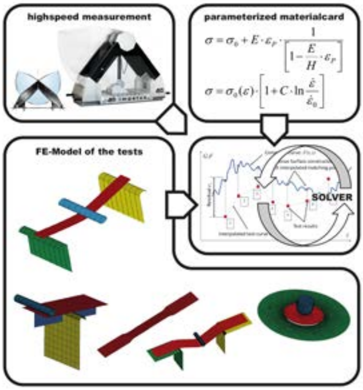

Figure 1: Reverse Engineering - Parameter Identification

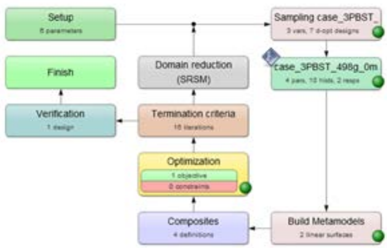

Figure 2: Optimization process diagram

Optimization algorithm

The idea of direct optimization is to use only simulation results to find the optimal value. A typical algorithm is the Genetic Algorithm, e.g. MOGA-NSGA II. The GA is a population based stochastic optimizer inspired by Darwin's "Survival of the fittest" principle. But since direct optimization requires many simulation runs, this method is usually too expensive and hence rarely used.

The idea of metamodel-based optimization is to approximate the relation between parameters and simulation output by simple functions (e.g. a linear polynomial) and perform the optimization on that surrogate model. Only a few simulation runs are required to fit the metamodel. The method is very effective, especially for highly non-linear optimization problems.

The nature and capacity of the simulation environment as well as the purpose of the optimization effort typically dictate the strategies for metamodel-based optimization. The strategies depend mostly on whether the user wants to build a metamodel that can be used for global exploration or he is only interested in finding an optimal set of parameters.

An important criterion for choosing a strategy is also whether the user wants to build the metamodel and solve the problem iteratively or he has a "simulation budget", i.e. a certain number of simulations he wants to use as effectively as possible to build a metamodel and obtain as much information about the design as possible.

In case of iterative solving polynomial response surfaces are typically used, together with the strategy "Sequential Response Surface Method with domain reduction" (SRSM). In case of a "simulation budget" or of complex problem descriptions Feedforward Neural Networks or Radial Basis Function Networks are used more often nowadays. To solve parameter identification problems, SRSM is usually used.

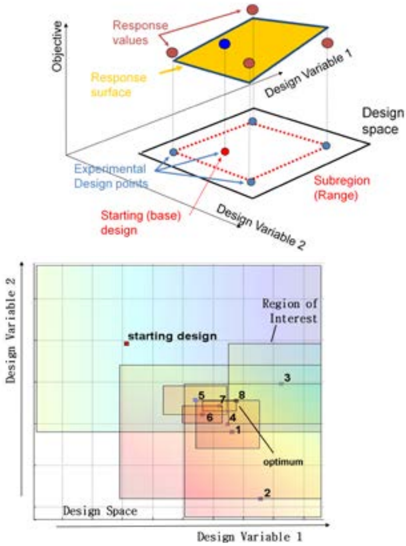

Figure 3: Sequential Response Surface Method

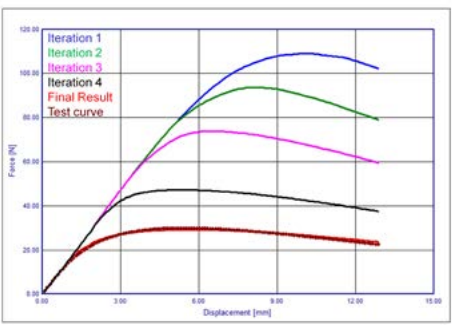

Figure 4: Material characterization of the yield behavior based on a three point bending test (4a impetus process).

Curve matching metric

The objective of a parameter identification problem is to minimize the mismatch between the target curve and the simulation curve. To judge on the mismatch between two curves, a curve matching metric is required.

The commonly applied Mean Squared Error uses the vertical coordinate distance between two specified curves to compute the matching error. The mismatch is quantified by the sum of the squares of the distances in the y-coordinate between the target points and the interpolated points on the computed curve. Thus, the mismatch of the abscissa is not explicitly included.

$$\varepsilon = \frac{1}{P}\sum_{p=1}^{P} W_P\left(\frac{f_p(x) - G_p}{s_p}\right)^2 = \frac{1}{P}\sum_{p=1}^{P} W_P\left(\frac{e_p(x)}{s_p}\right)^2$$

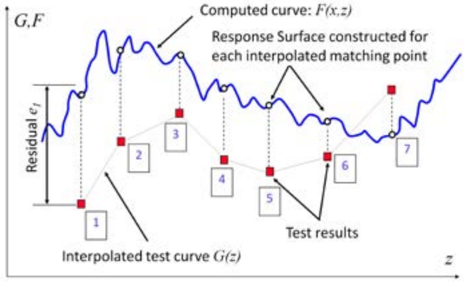

Figure 5: Mean Squared Error

A major difficulty with ordinate-based curve matching is that steep parts of the curve are difficult to incorporate in the matching. Failure material models have the characteristic of a steep decline of the stress-strain curve towards the end of the curve while steep curves also feature in models in which part of the behavior (the leading part of the curve) is linear.

In case of curve hysteresis the ordinate values of the curve are not unique. To solve this problem one can use time dependent measurement descriptions, which are unique or a different curve matching algorithm has to be used, e.g. Partial Curve Mapping.

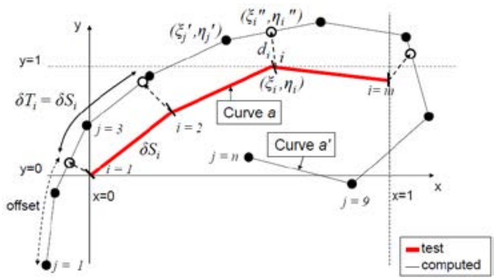

Figure 6: Partial Curve Mapping

Partial Curve Mapping normalizes the curves to the test (experimental) curve to avoid problems with different magnitudes for abscissa and ordinate. It maps the short curve onto the long curve so that the lengths are equal. The error is defined by the area between the short curve and the mapped curve. The sum of the volumes representing the individual segment errors is the criterion which is minimized in the optimization process.

Formulation of the material "parameter" law

Typical material cards in commercial solvers for elastic viscoplastic material behavior are defined by true stress- true strain curves for different strain rates. Internally the commercial solvers are using a table lookup algorithm to get the current material state during an explicit simulation.

To use reverse engineering for material characterization, the curves $\sigma(\varepsilon,\dot{\varepsilon})$ have to be described by a parameterized material law. Before simulating each loadcase the material card has to be created by a script using the design parameter values submitted by the optimizer.

Well known material laws for describing the yield behavior can be found in Table 1, those describing the strainrate behavior in Table 2.

Bi-Linear	$\sigma = \sigma_0 + E_T \cdot \varepsilon_p$
Ludwik	$\sigma = A + B\varepsilon_p^n$
Bergström	$\sigma = A + k\sqrt{1 - \exp(-0.5\ \varepsilon_p\ )}$
G'sell Jonas	$\sigma = \sigma_0 + K \cdot (1 - e^{-w \cdot \varepsilon_p}) \cdot e^{h \cdot \varepsilon_p^n}$
Johnson Cook	$\sigma = [A + B \cdot (\varepsilon_P)^n] \cdot [1 - (T^*)^m]$
Swift	$\sigma = A \cdot (B + \varepsilon_P)^C$
Voce	$\sigma = A + (B - A) \cdot e^{-C^*\varepsilon}$
4a three parameter	$\sigma = \sigma_0 + E \cdot \varepsilon_p \cdot \dfrac{1}{\left[1 - \frac{E}{H} \cdot \varepsilon_p\right]}$

Table 1: Material laws for yield curves

PowerLaw	$\sigma = \sigma_0(\varepsilon)\dot{\varepsilon}^n$
Cowper Symonds	$\sigma = \sigma_0(\varepsilon)\left[1 + (\frac{\dot{\varepsilon}}{D})^{\frac{1}{P}}\right]$
Johnson Cook	$\sigma = \sigma_0(\varepsilon)\left[1 + C\ In\frac{\dot{\varepsilon}}{\dot{\varepsilon}_0}\right]$
Kang	$\sigma = \sigma_0(\varepsilon)\left[1 + C_1 In\frac{\dot{\varepsilon}}{\dot{\varepsilon}_0} + C_2(In\frac{\dot{\varepsilon}}{\dot{\varepsilon}_0})^2\right]$

Table 2: Strain rate dependence

Evaluation of optimization results

Since parameter identification problems have target values or curves, the easiest way to judge on the quality of the optimization result is to compare the optimal simulation results and the target. If the fit is not good enough, the following issues could be a reason among others:

First the convergence of the optimization algorithm should be checked. If a sensitive parameter still varies, the results can be improved by continuing the optimization. If the optimum is found at a bound for one or more parameters, those variable ranges should be enlarged. In case that not any of the curves found in the optimization process fits the test curves quite well, the material model might not be appropriate and should be changed.

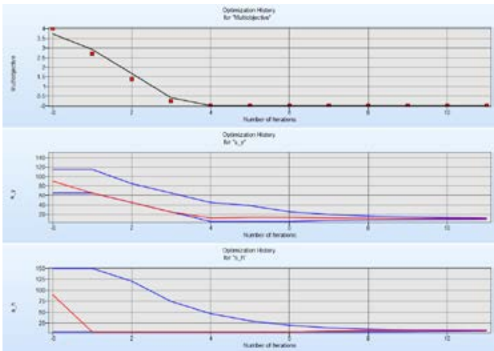

Figure 7: Optimization History

Further information:

http://impetus.4a.co.at

http://www.lsoptsupport.com

CAE Wissen by courtesy of
4a engineering GmbH, Austria (www.4a-engineering.at)
and
Dynamore GmbH, Stuttgart (www.dynamore.de)

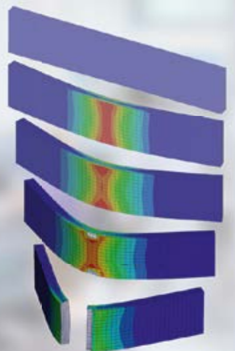

Model Order Reduction Techniques for Real-time Parametric Crash and Safety Simulations

Introduction

Model order reduction (ROM) techniques are interpolation methods exploiting exiting data sets (input and output) derived from an existing model or experimental setup. The starting point is a DOE-type design which covers as best as possible the design space (space filling property). Contrary to response surface (polynomial based) designs where the selection of design points at particular positions is important due to a-priori properties of the fitted surface, for ROM techniques, the most important issue is the space-filling capacity and sufficient "modal" representation of the response.

In some cases ROM can be considered as algebraic solutions, exploiting decomposition of time-dependent phenomena into spatial and temporal components, for reducing the volume of a data set while preserving the most important parts of the information contained within the data which is necessary for retrieving all or the most essential part of the data when needed. Else we can also consider ROM as clustering or other "lossy" efficient data compression techniques, allowing for the reduction of the amount of data required for the reconstruction of the complete data set. Both such techniques allow for creating on-board and real-time applications based on voluminous experimental or simulation results (ex. Finite element).

In this paper we shall present the major idea behind the reduction (or fusion) methods as well as providing three potential applications for crash and safety simulations. The results are obtained by ODYSSEE (Lunar) software [2] and compared to LS-DYNA FEM results.

Reduced Order Modeling

In 2015 Kayvantash [1] reported on an innovative solution and presented results based on model reduction techniques in order to exploit fully the results of time dependent DOE's such as in the case of Crash or ALE. An explanation of the algorithm (based on POD standing for Proper Orthogonal Decomposition) was given and a demonstration of the method was provided for a typical safety simulation model as well as an ALE application (ballistic impact including detonation and fluid/structure interaction). In 2017 Yasuki [5] presented a full sled test demonstration using solutions developed by Kayvantash [2] and provided detailed comparative studies of the FEM and ROM solutions. Further, in 2018 Yasuki [6] presented a population based comparison of 100 sled tests using an FE dummy + sled simulation and compared it to ROM reconstructions of the same scenario. Additionally, after validation of the comparative studies, a Pareto Front profile of Nij for 10000 hypothetic individuals was established. In 2018 Ovazza and Kayvantash [4] developed new methods of decomposition based on clustering techniques and machine learning which improved yet further the computation speed and reduced the data storage required for implementing ROM on on-board devices. These works have launched an interest in applications of ROM for crash and safety simulations, parametric studies and optimizations. In this work we shall explain the principles and discover further the potential of such reduction methods.

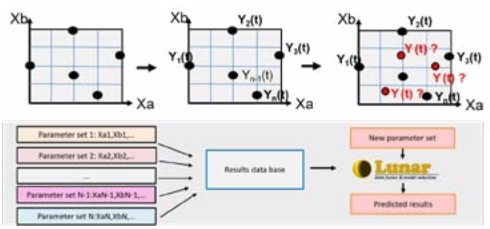

Figure 1: Procedure for ROM modeling (using ODYSSEE (Lunar) Software).

Some reduction techniques are based on reducing the order of the operators representing the set of algebraic operations resulting from discretization of differential equations. These are commonly referred to as PGD (Proper Generalized Decomposition) and are directly applicable to PDE solvers. These solutions are considered as "intrusive" since they require extensive modifications or even rewriting of solver code. However, recent research has shown that using machine learning techniques other physical phenomena - for which a PDE (partial differential equation) is not known, or does not exist, or not fully or efficiently handled from a computation effort point of view - may also be explored and predicted using ROM methods. In particular, "non-intrusive" or a posteriori techniques of results post-processing are of interest. These methods (such as POD) require simply the establishment of a new vector base (orthogonal or reference vector as opposition to the original Cartesian-temporal reference axes) and a projection of the known model or experimental results on that new base. This technique is similar to a PCA (Principal Component Analysis) projections.

Independent of the method selected, a ROM technique implies three steps: Decomposition, Reduction and Reconstruction. In the next paragraphs we shall describe shortly these steps and then proceed with a few crash and safety related applications.

In what follows we shall use the following conventions:

X = Table of design parameters (or variables) defining experiments (we may also call this a DOE)

Y = Results of the experiments associated with X

XN = A new table of parameters for which we seek results without actually performing experimenting or computing

YN = Results of the new experiments associated with XN (to be computed by ROM)

G, H, S = Decomposition matrices of which Gr, Hr, Sr are sub-matrices.

y = Spatial or latent metrics of system (sometime called coefficients)

t = time

m, n, p, r = indices (dimensions of matrix)

Note – The **N** in (**XN** and **YN**) stands for **NEW** since we do not include **XN**, which is known, in the decomposition process and we don't know the **YN** (since we want to predict it).

Decomposition

Assuming we have a set of data representing a time dependent phenomena such as **Y**(**y**, t), where **y** represent a "spatial" but latent variables associated to the response.

We define the decomposition:

$\mathbf{Y}(\mathbf{y}, t) = \mathbf{G}(\mathbf{y}) \cdot \mathbf{s} \cdot \mathbf{H}(t)$ where **G** is a "spatial" operator (a matrix) , **s** is a transfer matrix (diagonal or semi-diagonal) and **H** is a "modal" operator (a matrix). Indeed a popular method often used at this phase is called Singular Value Decomposition in which case the **s** matrix includes the singular values of **Y**.

We may obtain similar decomposition via an appropriate clustering method such that:

$\mathbf{Y}(\mathbf{y}, t) = \sum \boldsymbol{\alpha} \cdot \boldsymbol{\Psi}\ (\mathbf{y})$

Where **Ψ** are "weights or cluster functions and **α** are coefficients both obtained via an appropriate learning or clustering algorithm (Support Vector Machines, PCA, MLP, etc.).

In both cases we can claim to have decomposed the original data set from the physical or Cartesian reference frame on to a new set of basis with special and very useful properties such as orthogonality (in case of SVD decomposition) or compactness (in case of clustering).

As common in most supervised techniques, let's assume also that we know of another set of data **X** (representing a sampling table of some properties or criteria which have resulted in the variations of the responses. In short, **X** represents a Design of Experiments and **Y** the corresponding outcome at the **X** sampling points. We are interested in establishing a function (the ROM operator) which relates **Y** to **X** as in the case of a "supervised" learning algorithm.

In particular by applying the decomposition and the projection we have separated the variables **y** and t (similar to modal decomposition techniques in transient dynamic problems). We can claim to have obtained a decoupled version of the original set of data, in another vector basis other than the original Cartesian (or physical) basis. Secondly, we can now perform separate operations on any of the two major components (matrices **G** or **H** or **α** or **Ψ**) in order to further exploit the data, in association with many available interpolation techniques.

Reduction

The primary objective of all ROM techniques is to compress or reduce the volume of data to be handled and in consequence, the number of floating point operations required for the response prediction. The purpose of this compression and reduction is to allow for real-time computation providing reliable parametric studies based on existing DOE's.

In general matrix **s** contains a set of singular values (if SVD based decomposition is performed) of descending order, corresponding to the effect of the corresponding singular value on the complete reconstruction of original base. This is very similar to the approach used in modal analysis where only lower (or higher) modes are retained. If all non-zero components of **s** are used for the reconstruction (see next phase), we can claim a "non-lossy" reconstruction whereas an abandon of smaller singular values can lead to a "lossy" form of the reconstruction compression.

Similar argumentation holds for a clustering based decomposition, where coefficients **α** and weights matrices **Ψ** may be maintained or removed from the reconstruction phase due to the importance (often called " inertia") representing contribution to the overall information content of the data base.

This results in using only subsets of **G** and **H** (or **α** and **Ψ**) based on some tolerance criteria is simply a compression (fusion) of the original data base.

In this case only the "reduced" matrices need be considered with important consequences for CPU and storage issues which are essential for on-board computing solutions. In matrix form, if the original data **X** and **Y** are of dimensions $\mathbf{X}_{m,n}$ and $\mathbf{Y}_{m,p}$ (assuming p>>m which is reasonable for time responses,) then the decomposed matrices may have the dimensions $\mathbf{G}_{m,r}$, $\mathbf{S}_{r,r}$ and $\mathbf{H}_{rxp}$ (where r represents the number of retained modes or clusters). We can observe that if a new set of parameters is experimented such as $\mathbf{XN}_{q,n}$, the reduced matrices still provide a result matrix $\mathbf{YN}_{m,p}$ (same order as $\mathbf{Y}_{m,p}$).

At any instance we can either reconstruct the original set of data either completely (using decomposed operators) without loss or partially (using reduced operators) with some loss of information. A partial reconstruction would mean that we only retain selected parts of **G** and **H**, a technique which can be assimilated to filtering or lossy compression. This allows a reduction of the volume of the "on-board" data as well as a filtering of noise or other high frequency sources of uncertainty in the results

Reconstruction

In what follows we shall only refer to the SVD based approach (POD) since the computational steps are identical for clustering based solution.

In case of predictions which require the results **YN** for a new parameter set **XN**, we observe that we can replace **G** or **H**, by their modified updates **G'** or **H'**, taking into account of the change in the parameters, and obtain a new set of response corresponding to slightly modified new positions **XN** compared to the original **X**. In simple terms we can make predictions of effect of **X** moving to **XN** on **Y** (moving to **YN**) via considering its effect on **G**, moving to **G'** or **H** moving to **H'** only. If we need to compute **YN**, we need to compute the effect of **XN** on **G** or **H**. It turns out that the updates **G'** or **H'** may be simply obtained by an adequate interpolation technique such as radial basis functions, kriging, etc. A final back multiplication provides the results **YN**.

Lastly, it is important to point out that it is possible to mix the experimental and numerical results and construct a unified data base ($\mathbf{Y}_{experiments+simulation}$) in which case we could call the data base a fusion of real and virtual information. This alone open ups new horizons in modeling which until now was always suffering from "correlation" and "validation" issues. We can claim that we have a new tool which benefits from the best of both experimental and numerical technologies.

Applications

Three applications will be presented hereafter showing different potential of the proposed method and solution software. The starting point is, as in many other parametric design projects, the construction of the DOE samples and the time dependent response of the system for each case present in the DOE table (Figure 1). Note that the response may be measured experimentally or computed via discretization techniques such as Finite Elements, etc.

For all three applications a Desktop version of the software ODYSSEE (Lunar) has been used running on a Laptop (DELL M4800, INTEL i7 4910 MQ, 2.9GHz, 2.9GHz, 16 GB RAM) was used.

Simply supported plate without or with rupture

A simply supported plate with variable thickness and moving support position is considered in order to compute the deflection at the loaded side of the plate (Figure 2). A DOE of 15 cases was first assumed and analysed via FEM. The results were obtained for four new points by ROM methodology (Figure 3) A finite element based solution (1000 elements) is compared with a real-time (instantaneous, ~1sec) solution. CADLM's ODYSSEE (Lunar) software [2] was used for the ROM modeling.

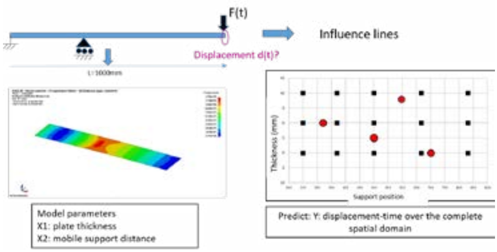

Figure 2: Computing influence lines for moving support point – Black square points represent the DOE samples and the red circles represent the prediction points.

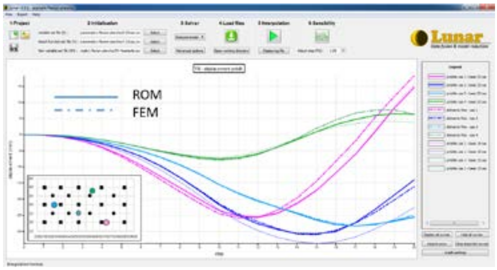

Figure 3: Computing influence lines for moving support point at four combinations of model parameters (colored circle points) – Results (Finite Elements versus ROM)

Simplified Bonnet head impact

A simply supported plate with a spherical impactor is considered as a simple model of a head impact on a bonnet as in the case of pedestrian impact. The plate is made of composite material allowing for failure corresponding to rupture of fibers (Figure 4). It is intended to evaluate the capabilities of the ROM solution in case where rupture (or bifurcation occurs). This clearly shows that the method is not limited to simple, linear or smoothly non-linear cases. A finite element based solution (1000 elements is compared with a real-time (instantaneous, ~1sec) solution. CADLM's ODYSSEE (Lunar) [2] [3] was used for the ROM modeling as well as conducting the DOE runs.

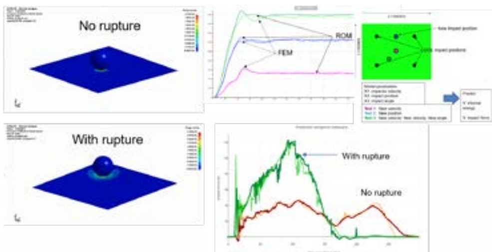

Figure 4: Plate-sphere impact (representing bonnet-head in pedestrian case) including possible rupture of composite material – Results (Finite Elements versus ROM)

Sled with airbag and uncertain impact velocity

A typical sled test is considered. An FEM model is constructed using LS-DYNA dummy and the results of the FEM model are obtained for a DOE of 9 Optimal Latin Hyper Cube augmented by 6 additional "space filling" type samples. A DOE of 15 cases was first constructed and the results were computed via LS-DYNA. CADLM's ODYSSEE (Lunar) software was used [2]. The results of the pelvis acceleration and chest displacement are compared (Figure 5 & Figure 6) Additional parametric studies were also conducted and animation screen shots are also obtained and compared.

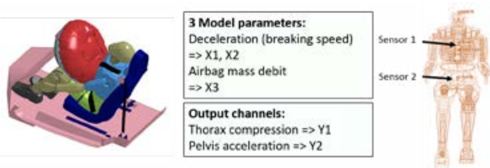

Figure 5: Sled test + airbag with variations on airbag mass injection and impact velocity - DOE with 3 parameters, 9 (OLH) + 6 "space filling" samples

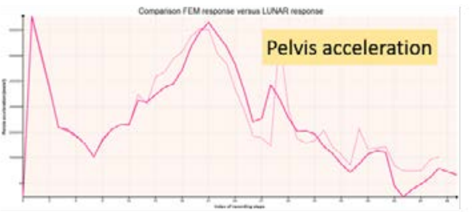

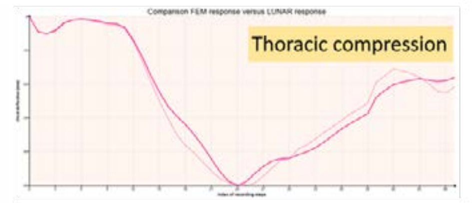

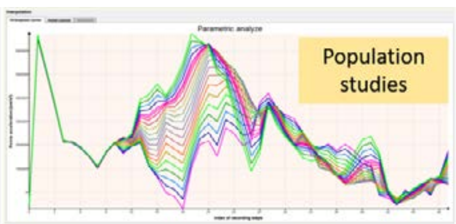

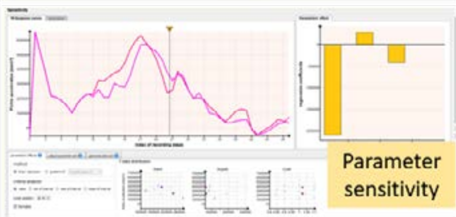

Figure 6: Results of sled test comparing FEM (LS-DYNA) and ROM (ODYSSEE/ Lunar). ROM method may be used with simplicity for inverse optimization (model fitting) as well as sensitivity and population studies.(1)

Summary and conclusions

All three comparative studies undertaken during this work were used to compare results accuracy and computing time. All the results were satisfactory in terms of differences with the FEM counterparts (difference in the range of 1 - 10 %). All the ROM CPU times were at most in the order of a few seconds.

Results obtained by ROM lie within 1 - 10 % of the finite element counterparts. The computing time for ROM models is often in the order of seconds whereas the FE models range from minutes of computing (applications 1 & 2) to hours for sled test model. In practice any new set of parameters could be studied in a matter of seconds or "quasi real-time" with a gain of many orders of magnitude in terms of computation time.

Finally, comparative performance and portability studies were also investigated on an on-board version (Raspberry PI 3) of ODYSSEE/Quasar (The results will be published in a separate work). It has been shown that nearly all the presented applications may be conducted on a very small CPU while the current limitations concern the storage available on such on-board devices.

Literature

[1] Kayvantash, K.: "European LS-DYNA Conference", Wurzburg, Germany, Proceeding, 2015

[2] Kayvantash, K.: "ODYSSEE (Quasar/Lunar) software package for Machine learning, Model Fusion, Forecasting and ", CADLM, www.cadlm.com , Wissous, France, Release 9/2017

[3] Le Duc, T., Kayvantash, K.: "Quasar Online software implementation for web-based Model Reduction and Machine learning", CADLM, www.cadlm.quasaronline , Wissous, France, Release 10/2018

[4] Ovazza, H., Kayvantash, K.: "An onboard implementation of Quasar software for Raspberry PI 3 for Lidar/ Radar/ MobileEye data - Fusion and forecasting of Autonomous Vehicle Data recordings", Internal Report, CADLM, www.cadlm.com , Wissous, France, 8/2018

[5] Yasuki, T.: "Application of reduced model to estimating Nij of HYBRID3 AF05 dummy in sled FE simulation, DYNA conference, Salzburg, Austria, 2017

[6] Yasuki, T.: "Application of Reduced Model to Simulations of Occupant Protection and Crashworthiness at Toyota", Advanced CAE Division, Toyota Motor Corporation,15th International LS-DYNA® Conference & Users Meeting, Detroit, USA, 2018

CAE Wissen by courtesy of
Dr. Kambiz Kayvantash, Hexagon

Introduction of Reduced Order Modelling and its Application for Model based real-time Optimization

Course Description

The cost of computing and simulation has become an important component of the total design cycle. In particular, anything related to iterative computing such as optimization, reliability or robustness studies requires frequent relaunch of models. This is costly even for one design or simulation, due to the fact that any sensitivity related analysis requires detailed models, sufficiently sensitive to changes of model variables (endogenous) or parameters (exogenous).

The associated results are simulation outputs, experimental measurements or both while the primary purpose of simulation models is to replace real-life experiments by lower cost and easier to control counterparts. Unfortunately, the desired simplicity of models (often formulated in terms of oversimplified surrogate models) has its limits due to often complex physics or lack of representative models.

The introduction of Reduced Order Modelling (ROM), is aimed at solving two problems at a time, namely the requirement for precision accompanied by the constraints on computational effort. The ROM technique is an innovative and promising solution to advance engineering to yet another limit in terms of what we can call real-time modelling.

In recent years the concept of ROM, initiated originally from system modelling, has been introduced and has picked up acceptability and efficiency both in applications and algorithmic maturity. The fundamental idea is to exploit compression techniques borrowed from classical matrix algebra and signal processing, combined with new concepts related to machine learning and image processing, to reduce the computational effort necessary to calculate and exploit existing models and/or experimental results. Given an existing dataset (know-how) on the behavior of a system subject to variations of its internal components or external loadings it is intended to exploit this know-how in form of a black-box in order to predict its behavior without extensive computing, thus enabling re-design, etc.

Who should attend?

Anyone interested in accelerating sensitivity analysis, optimization, reliability, robustness and globally anyone who needs to understand and initiate the application of ML techniques in CAE is a candidate for participating to this seminar. You don't need any deep understanding of machine learning nor complex mathematics or matrix algebra. Your engineering education is enough, even though experience in simulation techniques (various solvers) and optimization processes (not algorithms) is very useful. The participants can be academics, above MSC level students, designers, architects, engineers or project managers and team leaders at various design or decision-making stages of CAD/CAE based manufacturing. Topics from automotive, aeronautics, medical and civil engineering will be exploited for demonstrations.

Course Contents

- Model Reduction
- Introduction
- Theoretical background
  - Regression
  - Eigenvalue problem
  - Singular value decomposition
- Methods of Reduction
  - Proper Orthogonal Decomposition
  - Clustering
  - Central Voronoi Tessellation
  - Fast Fourier Transforms
  - Neural Networks
  - Support Vector Machines
  - Dynamic Mode decomposition
- Application of ROM as a surrogate model
  - Optimization
  - Reliability & Robustness
  - Entropy and Complexity
- Examples
  - Box-beam
  - Sled Test

Instructor

Dr. Kambiz Kayvantash (Hexagon) has a PhD from University GHS of Essen, Germany, and an executive MBA from HEC, Paris, France. In the past he has occupied various technical and managerial positions both in academia and industry (University of Essen, MECALOG, ALTAIR, Cranfield University/Cranfield Impact Centre, CIVITEC, CADLM/ École spéciale des travaux publics. He is currently the CTO of Hexagon/CADLM and develops Artificial Intelligence based solutions for predictive, real-time industrial applications such as Autonomous Vehicle, Crash and Safety, Health Monitoring, etc.

Facts

21.-24.10.2025	194/4446	Online	4 Days	1.450,- EUR till 23.09.2025, thereafter 1.750,- EUR	

Introduction and Examples of Multiphysics Simulation

Over the last decade, the multiphysics simulation approach replaced the artificial segregation of different physics with a single, unified simulation environment that replicates the real behavior of natural systems. This allowed engineers to simulate the way physics influence one another in the real world in a matter of minutes, drastically reducing the risk of product failure and delays to market.

Multiphysics is based on the design to simulate coupled physics effects by solving its underlying mathematical representation based on partial differential equations (PDEs). The user interface should allow the user to include just about any physics effects of interest that are relevant to a specific application, allowing the user to set up a simulation in minutes. For all common multiphysics problems the coupling between the physics involved is fully automated. Joule heating, thermal stress, electrochemical reactions, fluid-structure interaction (FSI) are but a few examples of the many predefined couplings that are available in software packages such as COMSOL Multiphysics. The software then automatically compiles the system of PDEs, representing predefined physics as well as user-defined physics, and computes a numerical solution to that system.

There are a lot of examples where multiphysical simulation comes into play in automotive applications, starting from sound-vibration couplings via couplings of chemical reactions, heat transport and free or porous flow as e.g. in catalytic converters or batteries and fuel cells, to thermal management simulations when designing the electronic system in the car. Sometimes the coupling is just one-directional, where one physics influences the other, sometimes it is bidirectional, where both physical processes influence each other.

True multiphysical: The Thermoacoustic Effect

The thermoacoustic effect is a truly multiphysical phenomenon as it describes the interaction between acoustic pressure, density and temperature variations. When sound propagates in structures and geometries with small dimensions, the sound waves become attenuated because of thermal and viscous losses. More specifically, the losses occur in the acoustic thermal and viscous boundary layers near the walls. This is a known phenomenon that needs to be included when studying and simulating systems affected by these losses in order to model these systems correctly and to match measurements.

The example which is shown here takes this effect into account while modeling an acoustic muffler with perforates. It also shows that this multiphysical approach can be used just for those parts of the model where it plays a significant role while in other parts, modeling the acoustic pressure variations is sufficient to adequately represent real conditions. This point leads to a second way of Multiphysics coupling: The multiscale-coupling by combining a full-scale model of the system with a detailed sub-model of a cutout of the system.

Theoretical background of Thermoacoustics

For many applications simulating acoustics, a series of assumptions are then made to simplify these equations: the system is assumed lossless and isentropic (adiabatic and reversible). Yet, if you retain both the viscous and heat conduction effects, you will end up with the equations for thermoacoustics that solve for the acoustic perturbations in pressure, velocity, and temperature.

The governing equations used in this model are the continuity equation:

$$i\omega\rho = -\rho_0(\nabla \cdot \mathbf{u})$$

where ρ_0 is the background density;
the momentum equation:

$$i\omega\rho_0\mathbf{u} = \nabla \cdot \left(-p\mathbf{I} + \mu\left(\nabla\mathbf{u} + (\nabla\mathbf{u})^T\right) + \left(\mu_B - \frac{2}{3}\mu\right)(\nabla \cdot \mathbf{u})\mathbf{I} \right)$$

where μ is the dynamic viscosity and μ_B is the bulk viscosity, and the term on the right hand side represents the divergence of the stress tensor; the energy conservation equation:

$$i\omega(\rho_0 C_p T - T_0\alpha_0 p) = -\nabla \cdot (-k\nabla T) + Q$$

where C_p is the heat capacity at constant pressure, k is the thermal conductivity, α_0 is the coefficient of thermal expansion (isobaric), and Q is a possible heat source; and finally, the linearized equation of state relating variations in pressure, temperature, and density:

$$\rho = \rho_0(\beta_T p - \alpha_0 T)$$

where β_T is the isothermal compressibility.

In thermoacoustics, the background fluid is assumed to be quiescent so that $\mathbf{u}_0$=0. The background pressure p_0 and background temperature T_0 need to be specified and can be functions of space.

The left-hand sides of the governing equations represent the conserved quantities: mass, momentum, and energy (actually entropy). In the frequency domain, multiplication with $i\omega$ corresponds to differentiation with respect to time. The terms on the right-hand sides represent the processes that locally change or modify the respective conserved quantity. In two of the equations, diffusive loss terms are present, due to viscous shear and thermal conduction. Viscous losses are present when there are gradients in the velocity field, while thermal losses are present when there are gradients in the temperature. Both is usually the case close to solid boundaries, where so-called viscous and thermal boundary layers are created at the solid surfaces.

The model

The aim of the present model is to determine the impedance Z(ω) using a detailed thermoacoustic model of a single hole as it is computationally impossible to model the whole perforated plate. The model of one hole will give a precise value of Z including thermal losses and viscous losses as well as all hole-hole interactions (see Figure 1). Moreover, there are no free parameters here. The so-called end correction is included explicitly when solving this detailed thermoacoustic model.

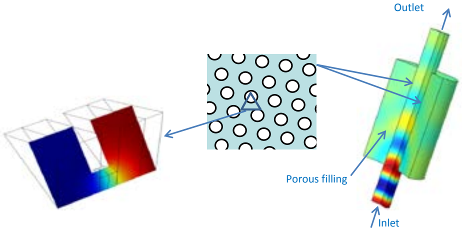

Figure 1: The thermoacoustic sub-model of one of the perforated plate holes (left) is used to determine lumped parameters which are then applied as internal impedance boundary condition in the full-scale model of the muffler (right).

The effect of having a porous backing on one side of the perforated plates is however not included in the initial model. The semi-analytical Kirby-Cummings impedance model, taking a porous backing into account, is implemented for comparison.

Now the simulation is performed in four steps:

Step 1: The thermoacoustic sub-model of the single hole is solved;

Step 2: The pressure acoustics model using the default perforated plate boundary condition is solved;

Step 3: The pressure acoustics model using the impedance determined from the sub model is solved;

Step 4: The pressure acoustics model using the Kirby and Cummings impedance model is solved.

The results are shown in Figure 2: The transition loss has been plotted as a function of frequency for the different model versions and for experimental results by Selamet et al, 2003. The model that matches the experimental values best is the one including the thermoacoustic effect.

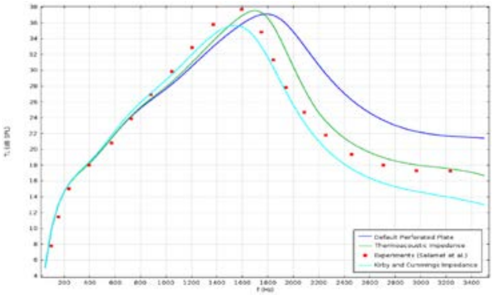

Figure 2: Transition loss as a function of frequency: Blue: without including the thermoacoustic effect, green: Thermoacoustic effect included, turquois: thermoacoustic and effect of porous backing included. The red dots show experimental results.

References:

Selamet et al., JSV, 262, p. 509 (2003)

COMSOL, Acoustics Module User's Guide, chapter 6, pp. 327-339 (2014)

CAE Wissen by courtesy of Comsol Multiphysics GmbH

Imprint

Published by

carhs.training gmbh, Siemensstrasse 12,
D-63755 Alzenau, Germany
Tel. +49 (0) 6023-9640-60, Fax +49 (0) 6023-9640-70
Managing Director: Constantin Hoffmann
Commercial Register: Aschaffenburg HRB 9961

Principles and Applications of FDM, FVM and FEM

Introduction

The behaviour of mechanical systems in general is described by a set of partial differential equations (PDE, in case of a distributed parameter system) or by a set of ordinary differential equations (ODE, in case of a discrete parameter system). They have to be fulfilled within the domain of the considered (structural) problem subjected to detailed geometrical and other boundary conditions. A closed solution in general is not possible. Hence approximated numerical solutions are applied during the analyzing phase within the engineering design process. Suitable tools of computer aided engineering (CAE) are the Finite Difference Method (FDM), the Finite Volume Method (FVM), and the Finite Element Method (FEM). They should be discussed briefly in the following sections with respect to their principles and major focus of application.
A final section provides a top level comparison of the three considered methods.

The Finite Difference Method (FDM)

The Finite Difference Method (FDM) is probably the oldest of the three considered methods. It is based on an approximation of the derivative expressions of the PDE or ODE by appropriate finite differences. As an example a set of two points in space (or time) may be considered, where some function values are provided. In this case the slope of the underlaying function may be approximated by the difference of the function values at these two points divided by the spatial (or time) distance between the locations. Higher order derivatives are equivalently obtained. In case of a PDE (or ODE) problem description the function values at those locations are the unknown to be evaluated. Then an appropriate set of "measurement points" is defined within the considered domain and the PDE (or ODE) is formulated based on the just described finite differences with respect to the provided boundary conditions. As a result a system of algebraic equations for the unknown function values is obtained and finally solved. The more "measurement points" are defined within the considered domain, the better in general the obtained function values approximate the solution of the PDE (or ODE). A typical application of this approach within engineering analysis is the investigation of a system behaviour at the time domain. Classical time integration methods are formulated on the base of FDM, i.e. Runge Kutta and the central difference time integrator.

$$\left.\frac{\mathrm{d}f}{\mathrm{d}x}\right|_{x^-} = \frac{f(x) - f(x-\Delta x)}{\Delta x}$$

$$\left.\frac{\mathrm{d}f}{\mathrm{d}x}\right|_{x^c} = \frac{f(x+\Delta x) - f(x-\Delta x)}{2\,\Delta x}$$

$$\left.\frac{\mathrm{d}f}{\mathrm{d}x}\right|_{x^+} = \frac{f(x+\Delta x) - f(x)}{\Delta x}$$

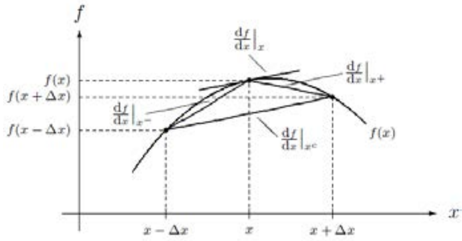

Figure 1: Derivatives Approximated by Finite Differences

The Finite Volume Method (FVM)

The Finite Volume Method (FVM) is newer than the FDM. As indicated by its name, a subdivision of the entire domain of the considered problem is applied into a set of finite volumes of simple geometry like triangles, quadrilaterals, tetrahedrons, hexahedrons, etc. Within each of these volumes the considered problem-specific PDE (or ODE) may be easily integrated by assuming average values for the unknown functions (i.e. at the center of those finite primitives). Possible derivative expressions of the PDE or ODE may be approximated by appropriate finite differences obtained from the mean functional values between the centers of neighbouring finite volumes. This approach is equivalent to the one of the FDM described at the previous section. In a similar way the possible flux of physical quantities through the finite volume boundaries is treated. The mean function values at the finite volumes are the unknowns to be evaluated at the FVM. In this way for every finite volume a set of algebraic equations is obtained. All of them together with the problem defining boundary conditions (as mentioned at the introductional section) describe a system of algebraic equations to be subsequently solved for the unknown mean function values. The more finite volumes are defined within the considered domain (! mesh refinement), the better in general the obtained function values approximate the solution of the PDE (or ODE). A typical application of this approach within engineering analysis is the investigation of flow fields in fluid dynamics. Hence the FVM is today the major tool for computational fluid dynamics (CFD).

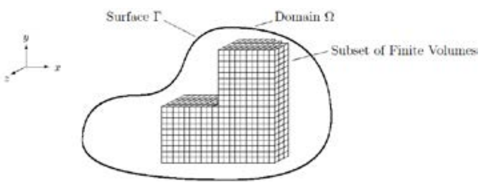

Figure 2: Subdivision of the Spatial Domain into Finite Volumes

The Finite Element Method (FEM)

The Finite Element Method (FEM) to some extend is similar to the FVM discussed in the previous section. Hence it subdivides the entire domain of the considered problem into a set of primitive domains like triangles, quadrilaterals, tetrahedrons, hexahedrons, etc. These are called Finite Elements. Within each of these elements the unknown field is interpolated by a combination of (initially unknown) function values and spatial shape functions. These shape functions are specific to each finite element. Based on this approach and by applying the Virtual Displacement Method (or equivalently the Weighted Residual Method or the Galerkin Method), the considered PDE or ODE may be integrated over the elemental domain with the still unknown function values as parameter variables For each element a set of algebraic equations is obtained. All of them together with the problem defining boundary conditions (as mentioned at the introductional section) describe a system of algebraic equations to be subsequently solved for the unknown parameter values. The more finite elements are defined within the considered domain (→ mesh refinement), the better in general the obtained function values approximate the solution of the PDE (or ODE). A typical application of this approach within engineering analysis is the investigation of mechanical structures with respect to their static or dynamic behaviour like deformation and mechanical stress distribution. But the wide field of application of the FEM includes as well safety aspects (i.e. computer crash analysis at the automotive industry) and the simulation of production processes like sheet metal forming.

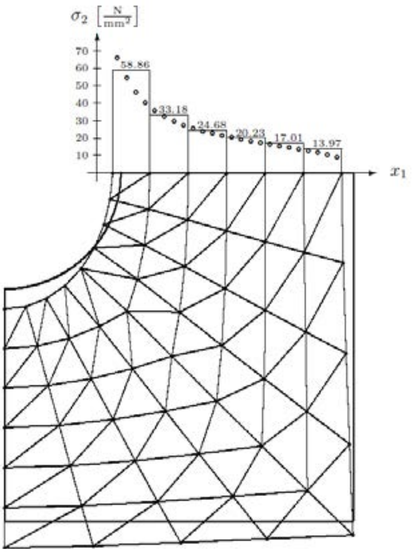

Figure 3: Deformed Finite Element model and border stresses

Properties of the Methods

The three methods FDM, FVM and FEM as described in the previous sections contain some similarities. I.e. the obtained solution of the considered problem is always an approximation depending on the applied number of objects, either function evaluation points, finite volumes or finite elements. Hence the quality of the result always depends on the applied effort. But in details each of the method behave in a different way depending on its individual methodical approach. The FDM is purely based on the differential description of the PDE or ODE defining the considered problem. The FVM and FEM are based on a (numerical) integration of the underlaying PDE or ODE. Practical tests reveal a high precision for the FDM compared to (physical) measurements. The real strength of the FEM lies on the flexibility with respect to its application. The FVM is found to be somewhere located between FDM and FEM, both with respect to flexibility and precision. Over the past decades these properties have surely defined the major field of engineering application for the three methods FDM, FVM and FEM.

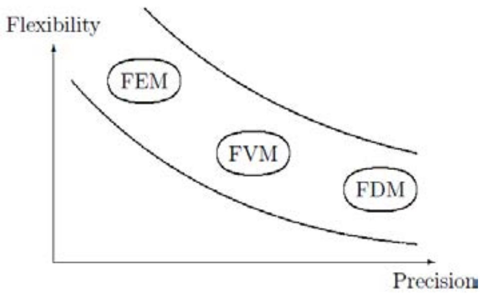

Figure 4: Flexibility and rrecision of the discussed methods (see [4])

References

[1] Bathe, K.J., Finite Element Procedures, Prentice-Hall, Englewood Cliffs, NJ, 1996

[2] Ferziger, J.H., Peric, M., Computational Methods for Fluid Dynamics, Springer Verlag, Berlin, 1996

[3] Hughes, T.J.R. The Finite Element Method, Prent. Hal. Int. Ed., Englewood Cliffs, New Jersey, 1987

[4] Lecheler, S. Numerische Stömungssimulation, Vieweg-Teubner Verlag, Wiesbaden, 2009

[5] Wissmann, J., Sarnes, K.-D., Finite Elemente in der Strukturmechanik, Springer Verlag, Berlin, 2005

Arbitrary Lagrangian-Eulerian Method (ALE)

Introduction

Before performing a numerical simulation of a multidimensional problem the choice for a suitable kinematical description of the continuum has to be made. When it comes to solid mechanics this choice normally leads to a Lagrangian formulation. Here the mesh nodes follow each motion of the material (material configuration) which makes it easy to track free surfaces or edges to treat with contact algorithms. However, when it comes to large deformations appearing for instance in forming simulations, the mesh distortion can lead to a strongly decreasing accuracy of the results. The numerical simulation of fluid dynamics usually uses an Eulerian formulation where the continuum moves through a fixed mesh (spatial configuration). However, this means that a boundary does not necessarily have to remain with the initial defining nodes which makes the imposition of boundary conditions more complicated. ALE, as the name insinuates, is a simulation approach for the coupled numerical simulation of interacting Lagrangian and Eulerian continua combining their strengths and ruling out their disadvantages as far as possible. In the following passages we first recall the principles of Lagrangian as well as Eulerian continua. After this the necessary adaptations for an ALE approach are presented. In the end some examples for the practical use of the ALE method shall be given.

Lagrange vs. Euler

To describe the motion of particles in continuum mechanics usually two domains are used. One is the material domain R_X consisting of material particles **X** and the other one is the spatial domain R_x consisting of spatial points **x**. In the Lagrangian description the reference configuration R_X is identified via the material coordinates **X**. The relation between the material coordinates **X** and the spatial coordinates **x** is realized through the motion of the material points. By means of a mapping $\varphi(X,t) = (x,t)$ it is possible to link **X** and **x** in time by the law of motion (see Fig. 1). The material velocity **v** for this formulation is $v(X,t) = \frac{\partial x}{\partial t} |_X$. By the inversion $(X,t) = \varphi^{-1}(x,t)$ it is possible to identify the reference position of any given material particle occupying a coordinate **x** at a given time **t**.

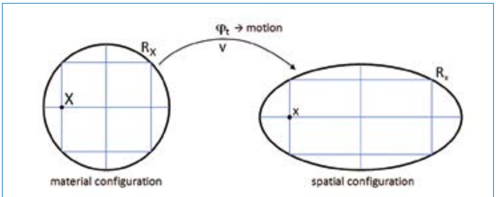

Figure 1: Lagrangian approach

The disadvantage of the Lagrangian approach and in particular of the coincidence of grid points and material points arises when it comes to problems with excessive mesh distortions, for instance explosions, fluid dynamics, etc. For such cases often the Eulerian description is used which is formulated based on the spatial coordinates **x** and time **t** using a continuum which moves through a fixed mesh. Due to this the Eulerian description only involves variables with significance for the current point of time. The current configuration serves as reference configuration which means that a deduction of a former point in time as it is possible with the Lagrangian approach is inhibited.

In the Eulerian approach the material velocity of a node corresponds to the velocity of the material point which is coincident with the node in question at the considered time. It is expressed as $v = v(x,t)$ with a reference to the fixed mesh but without a reference to the initial configuration of the continuum and thus without a reference to the initial material coordinates. The relative motion of the material opposite the fixed grid leads to advective effects.

Arbitrary Lagrangian-Eulerian (ALE) Approach

In the ALE approach an external reference system is introduced since neither the Lagrangian configuration nor the Eulerian configuration can be used as a reference. Fig. 2 shows the relations between the three configurations. The motion that was introduced as φ before can now be expressed as $\varphi = \Phi \circ \Psi^{-1}$. The Φ mapping from the reference configuration to the spatial domain which is equivalent to the motion of the mesh points in the spatial configuration yields the mesh velocity $\hat{v}(\chi,t) = \frac{\partial x}{\partial t} |_\chi$ For practical purposes we can directly regard the mapping of Ψ^{-1} which yields the velocity of $w = \frac{\partial \chi}{\partial t} |_X$. The latter representing the particle velocity in the reference configuration.

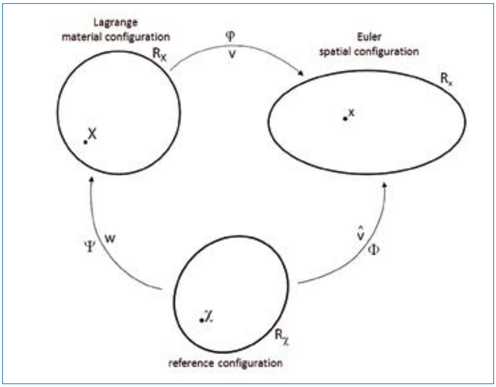

Figure 2: Arbitrary Lagrangian-Eulerian (ALE) approach

The relation between the three velocities v, $\hat{v}$ and **w** can be derived from the relation of $\varphi = \Phi \circ \Psi^{-1}$ and leads to the advective velocity $c := v - \hat{v} = \frac{\partial x}{\partial \chi} w$. It constitutes the particle velocity relative to the mesh from the viewpoint of the spatial configuration since both v and $\hat{v}$ are variations of the coordinate **x**.

Numerical implementation

To deal with the necessary advection for the Eulerian part it has proven useful to split a simulation into a Lagrangian step and an Eulerian step. In the first step all advection is inhibited so there is generally no difference between this step and an ordinary simulation process in structural mechanics. As long as the distortions of the mesh are reasonable the Lagrangian formulation is applied. However as soon as the distortions exceed a certain threshold a so called “rezoning” process is executed as shown in Fig. 3.

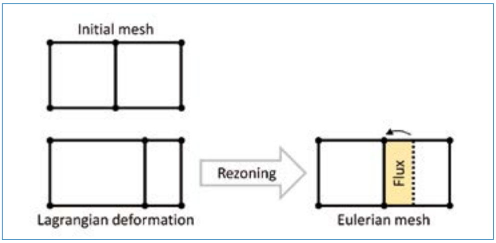

Figure 3: Rezoning Process for highly distorted elements

During this process the nodes of the mesh are moved back to their initial positions. At the same time all material volume and state variables (in Fig. 3 called „Flux“) are transported between the elements in an advection-step. The advection rules however can differ from solver to solver.

Examples of application

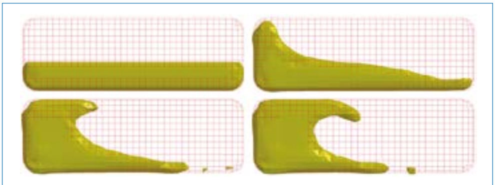

Figure 4: Water sloshing in a tank

One classical application is the analysis of the effects of sloshing water in a tank. Fig. 4 shows the relative movement of water during a deceleration of the tank from a certain initial velocity. Not only the connection-forces to the carrying structure can be analyzed but also different measures to lessen the sloshing effects can be simulated and evaluated.

In the same manner Fig. 5 shows the effects of water movement caused by the drop test of a customary PET-bottle.

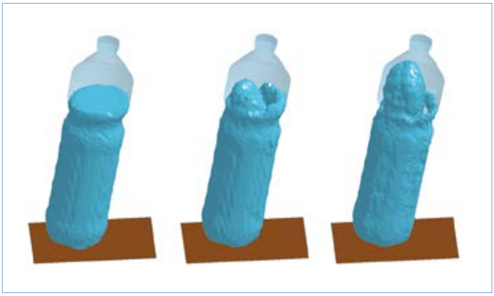

Figure 5: Movement of Water in a drop-test of a PET-bottle

Another large area for ALE simulation is the capability to simulate shockwave propagations induced by explosions. Fig. 6 shows the propagation of a dust deflagration inside a filter housing. By means of ALE simulations the influence of different measures such as flame traps or gates on the shockwave propagation and thereby on the deformation of the housing can be evaluated.

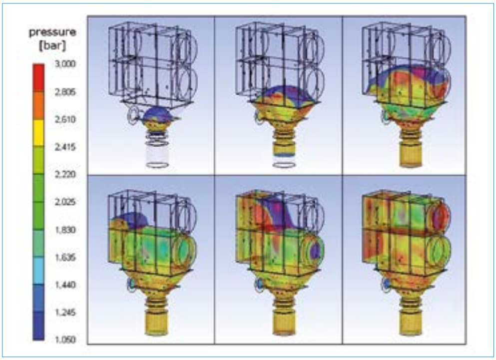

Figure 6: Shockwave propagation in a filter housing resulting from a dust explosion

CAE Wissen by courtesy of Heiko Honermeier, Ingenieurbüro Huß & Feickert GbR, www.ihf-ffm.de.

Advances in Direct Time Integration Schemes for Dynamic Analysis

by Robert Kroyer, Kenth Nilsson, Klaus-Jürgen Bathe

The accurate solution of dynamic response in finite element analyses has been the subject of extensive research for the last few decades. In general, implicit schemes are used when the transient response can be obtained with a relatively small number of large time steps, typically of order 10^{-3} s, and explicit schemes are used when many time steps of small size need be used, typically of order 10^{-6} s. The most widely-used schemes in implicit solutions are the Newmark trapezoidal rule and alpha generalized method, and in explicit solutions the central difference method [1]. However, these schemes have some undesirable characteristics, and recently more effective methods have been proposed, which we want to expose briefly in this short article.

Implicit Time Integration: Bathe Method

The trapezoidal rule is unconditionally stable in linear analyses, and has the characteristics of no amplitude decay and a reasonable amount of period elongation. Hence, on first sight, the solution errors seem to have excellent qualities. However, in fact, the quality of no amplitude decay can cause major solution problems, because frequencies may be sampled that should be suppressed (for example, because they are an artifact of finite element modeling). In linear analysis this phenomenon can be easily and directly seen (an example is given below), and in nonlinear analysis, the phenomenon can also render the iterative solution difficult to converge. We illustrate the solution behaviors below.

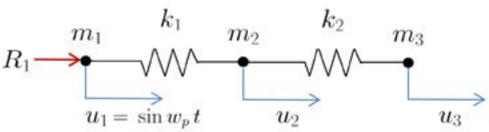

Figure 1: Model problem of three degrees of freedom spring system $k_1 = 10^7$, $k_2 = 1$, $m_1 = 0$, $m_2 = 1$, $m_3 = 1$, $\omega_p = 1.2$

Figure 1 gives a simple two spring model solved [2,3]. While very simple, the model contains the essence of many practical finite element models. The stiff spring represents stiff components in a structural model, which may be largely due to modeling constraints with stiff elements, while the soft spring represents the rest of the model. The aim is to only solve for the response in the soft part of the structure, like in a mode superposition solution. The trapezoidal rule gives very large errors in this linear analysis, see Figures 2 and 3. The response prediction can be improved by introducing damping, numerical or physical, but then the question will always be how much damping to introduce when not knowing the desired response. The same holds when using the generalized alpha method.

A new scheme is the Bathe method, which combines the use of the trapezoidal rule and Euler backward method [1-3]. In the Bathe method, no parameter is (usually) set and the accuracy of solution is simply dependent on the size of the time step used. As the time step becomes smaller the accuracy increases. Figures 2 and 3 show that the method gives the desired response, just like obtained in a mode superposition solution including only the lowest mode response with the static correction. Further results are given in ref. [3] where it is also shown that the error in the reaction using the Newmark method is very large.

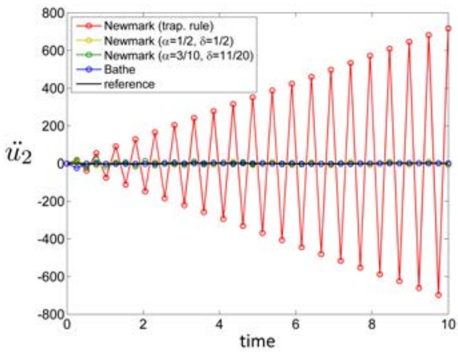

Figure 2: Acceleration of node 2 for various methods

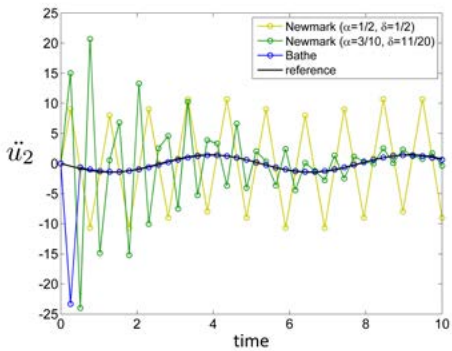

Figure 3: Acceleration of node 2 for various methods (the overshoot in the first time step of the Bathe method could be eliminated by using in the Newmark method $\delta = 3/4$, $\alpha = 1.0$ for the first step only).

There is also a parameter in the Bathe method on the size of the sub-step (but this parameter, changing the accuracy, is by far mostly used in its default value, see refs. 1-3). Hence the advantage of the Bathe method is that no parameter values need to be chosen.

While the Bathe method is about twice as expensive per time step (since two sub-steps are used), the higher accuracy in general allows to use less steps in linear response solutions. In nonlinear analysis the Bathe method is overall frequently more effective because it converges much better in the nonlinear iterations of the time steps, larger time steps can be employed, and the method remains stable when the Newmark and alpha generalized methods become unstable (unless sufficient damping is introduced).

The above observations are demonstrated in the solutions given in Figures 4 to 10.

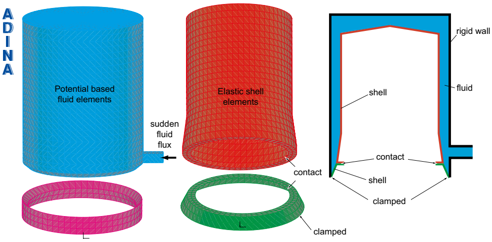

Figure 4: Schematic of the shell-fluid problem considered; results shown in Figures 5 - 8

Figure 4 shows the model considered, which consists of an elastic shell fully clamped at its base and a fluid surrounding it contained by an exterior rigid wall. Shell elements and subsonic potential based fluid elements are used to represent the media. The shell structure consists of two parts with frictional contact conditions between them. The model is subjected to a sudden fluid flux representing a pipe break. The resulting shock waves cause the internal parts of the model that are in contact to rapidly change status. For the implicit dynamic analysis of such problems usually the Newmark time integration is used. However, when contact conditions are included between internal parts, the contact surfaces repeatedly stick and slip, which results in rapid pressure pulses in the fluid. As a consequence, high frequency vibrations are observed. These high frequency oscillations are spurious in the Newmark method solution and grow with time. After a while, the solution becomes obviously very erroneous and may even diverge. The results using the Newmark method without damping are shown in Figure 5. Note the highly oscillatory response of the flange, the non-smooth contact status between the internal parts and the parasitic pressure distribution.

To overcome this problem, different techniques can be used, such as adding physical damping to the model (e.g. Rayleigh damping). In this case the damping will only be applied to the structure and the question is how much damping to introduce when physically it is negligible. Alternatively, the Newmark method can be used to introduce numerical damping. This reduces the numerical oscillations, but also reduces the physical response which should be solved for, and the question is how much numerical damping to introduce in order to obtain acceptable results.

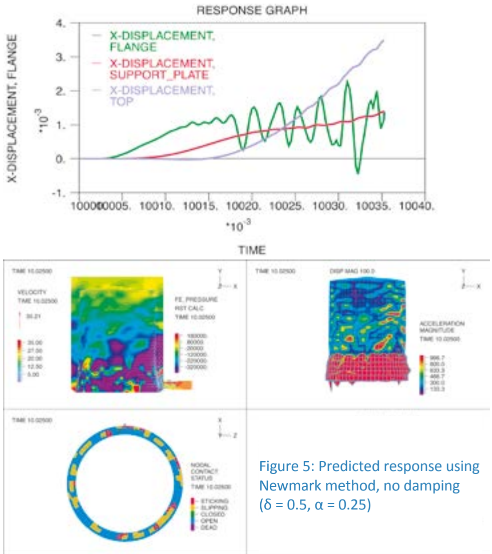

Figure 5: Predicted response using Newmark method, no damping ($\delta = 0.5$, $\alpha = 0.25$)

Figures 6 and 7 show that while the presence of physical damping or numerical damping improves the results using the Newmark method, to suppress all oscillations, the damping must be increased to high levels, which is not desirable. However, when using the Bathe method, no numerical parameter had to be adjusted and no artificial physical damping was introduced in the model, see Figure 8. The results achieved in this analysis led to the subsequent use of the Bathe method in the analyses of large finite element models.

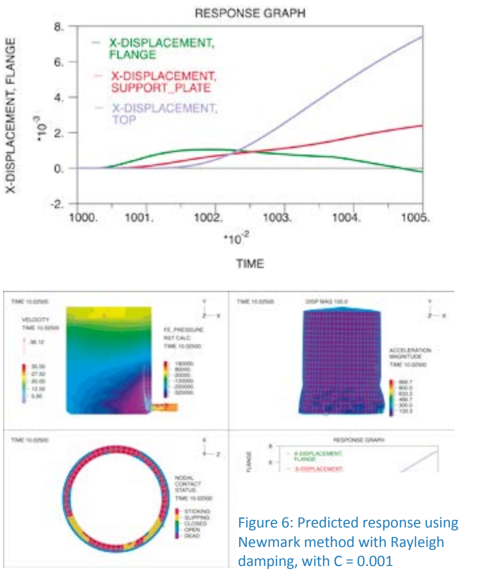

Figure 6: Predicted response using Newmark method with Rayleigh damping, with C = 0.001

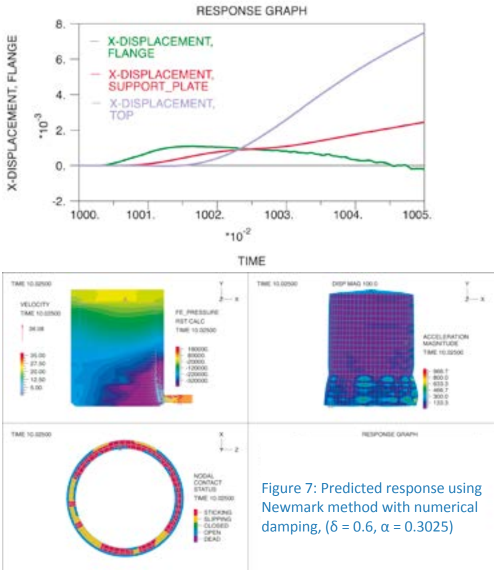

Figure 7: Predicted response using Newmark method with numerical damping, (δ = 0.6, α = 0.3025)

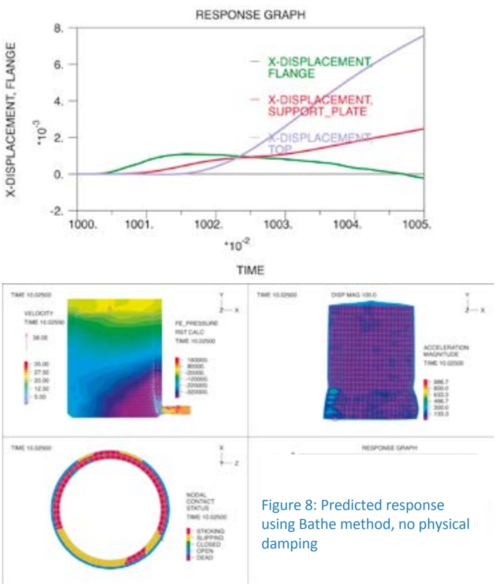

Figure 8: Predicted response using Bathe method, no physical damping

Another example solution pertains to the rotation of a heavy antenna structure, with focus on high accuracy of the antenna positioning and orientation. In this application, we see very large displacements over long time ranges in the transient analysis, and numerical stability can be difficult to achieve. Figure 9 shows the model of the antenna, which is rotated with various angular velocities using the classical trapezoidal rule and the Bathe method for time integration.

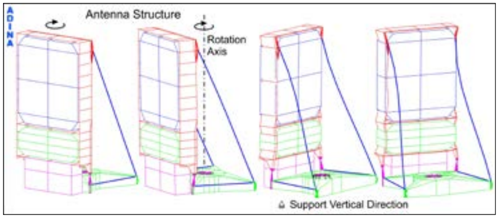

Figure 9: Antenna model in various rotational positions using Bathe Method

When using the Bathe method, the solution is obtained very accurately for many revolutions, whereas the Newmark time integration procedure fails before finishing the second revolution, see Figure 10 for the antenna rotation instability occurring in the solution. The numerical instability is also well seen when studying the axial forces in the antenna stabilizers, see Figure 10, and occurs quite suddenly. No physical damping, e.g. Rayleigh damping, is used in the model. This antenna rotation problem may be seen as an extension of the problem of a rotating stiff pendulum[2].

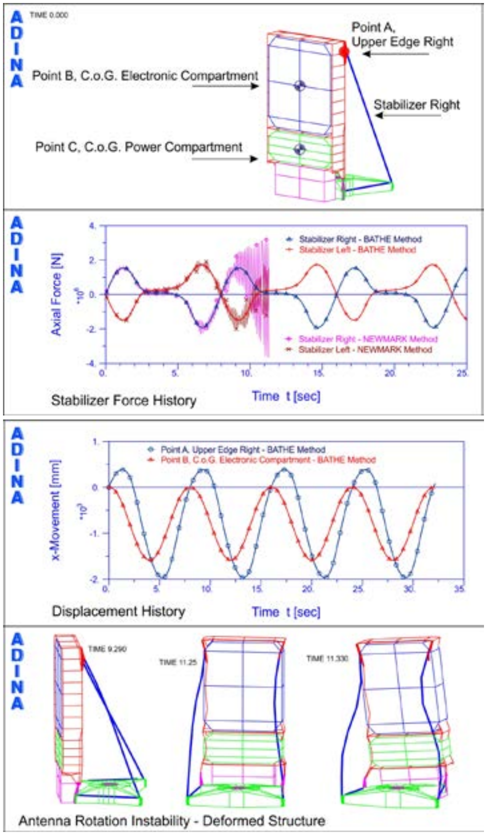

Figure 10: Predicted transient response of antenna using Newmark and Bathe Method

Although the above analyses focus on relatively simple problems, the mentioned solution phenomena are rather general and occur in many large-scale practical analyses of structures and fluid-structure interactions. In particular, considering contact problems, a spurious response of oscillatory nature can cause the nonlinear iterations not to converge.

While the above discussion refers to implicit integration, of course, explicit time integration is also widely used in practice. Using explicit integration, mostly wave propagation problems are considered, but structural vibration and even static problems are also solved.

Similar to the above observations regarding the trapezoidal rule, the predicted response obtained using the central difference method can show spurious oscillations in the high frequency modes [4]. These are frequencies and modes that cannot be represented by the chosen mesh. Ideally, any response in these modes would be automatically suppressed — but without loss of accuracy in the frequencies and modes that can be represented by the mesh.

Explicit Time Integration: Noh-Bathe Method

A new explicit time integration scheme, referred to as the Noh-Bathe method was developed with the same aim as for the implicit Bathe scheme [4]. The method automatically suppresses spurious high frequency response, without using any non-physical parameters, while accurately integrating those modes that can be spatially resolved. The computational cost of using the procedure is only slightly larger than the cost with the central difference method, when using the same mesh, but frequently coarser meshes can be used with the Noh-Bathe scheme.

Figures 11 and 12 show the analysis of the crushing of a tube. Figure 11 shows the deformations at three different times, and Figure 12 shows the acceleration-time solution curves of the impactor. We see that spurious oscillations are present in the central difference method solution, while the Noh-Bathe method solution does not show such oscillations.

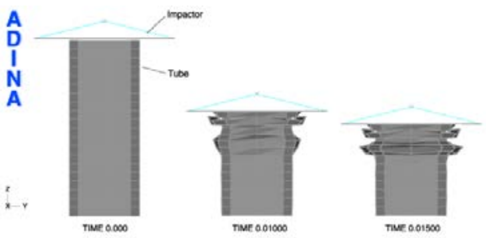

Figure 11: Tube-crush problem: Noh-Bathe method predicted deformations at t = 0.000, 0.010, and 0.015 s

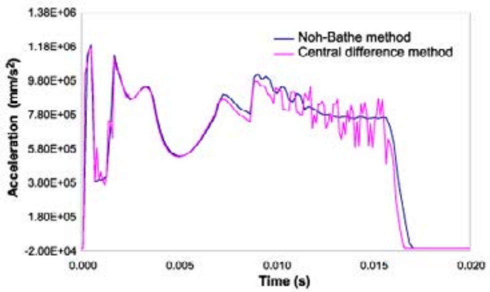

Figure 12: Impactor acceleration-time response for the tube

Further solutions of problems, algorithmic details and observations are given in the additional references [5-8].

References

[1] K. J. Bathe, “Finite Element Procedures”, Prentice Hall, 1996, Second Edition, K. J. Bathe, Watertown, Massachusetts, 2014.

[2] K. J. Bathe, “Conserving energy and momentum in nonlinear dynamics: A simple implicit time integration scheme”, Computers & Structures, 85:437-445, 2007.

[3] K. J. Bathe and G. Noh, “Insight into an Implicit Time Integration Scheme for Structural Dynamics”, Computers & Structures, 98-99:1-6, 2012.

[4] G. Noh and K. J. Bathe, “An Explicit Time Integration Scheme for the Analysis of Wave Propagations”, Computers & Structures, 129:178-193, 2013.

[5] G. Noh, S. Ham and K. J. Bathe, “Performance of an Implicit Time Integration Scheme in the Analysis of Wave Propagations”, Computers & Structures, 123:93-105, 2013.

[6] Z. Kazanci and K. J. Bathe, “Crushing and Crashing of Tubes with Implicit Time Integration”, Int. J. Impact Engineering, 42:80-88, 2012.

[7] K. J. Bathe, “Frontiers in Finite Element Procedures & Applications”, Chapter 1 in Computational Methods for Engineering Technology, (B.H.V. Topping and P. Iványi, eds.) Saxe-Coburg Publications, Stirlingshire, Scotland, 2014.

[8] http://www.adina.com/newsgrp.shtml

CAE Wissen by courtesy of

Dr. Robert Kroyer

MBDA Deutschland GmbH

Senior Expert Structural Mechanics/-dynamics

Hagenauer Forst 27, 86529 Schrobenhausen, GERMANY

Kenth Nilsson MSc

Analysis & CAE

AB Volvo Penta,CB74680, Z5.1

SE-405 08, Gothenburg, SWEDEN

Prof. Dr. Klaus-Jürgen Bathe

Massachusetts Institute of Technology,

Cambridge, MA 02139, USA

Meshfree Numerical Modeling of Flows and Continuum Mechanics

The complexity and difficulties of a flow simulation is highly dimensional. In many cases, we have only little or diffuse knowledge about boundary conditions or material properties. Moreover, the geometry might be extensive and very detailed, it may deform/move/change during the flow process. The flow might contain free surfaces or phase boundaries. It might contain fluid structure interaction (such as airbags, aquaplaning). In many cases, prior to the modeling, we do not know which part of the geometry will be impacted by the flow (rain water management in cars). These and other reasons can make flow simulations very inefficient.

To judge efficiency of a flow simulation, we have to measure not only the CPU-hours taken by a particular task, but also the time and effort it needs for preprocessing, postprocessing, and how well the simulation can be coupled to other tools (fluid-fluid and fluid-structure interaction).

Fraunhofer ITWM is developing, together with Fraunhofer SCAI the simulation tool MESHFREE. As the name suggests, it is a completely gridless numerical idea for fluid and continuum mechanics, that might considerably improve efficiency and accuracy of flow simulations. Our understanding of “flow” goes beyond classical CFD, we also consider non-Newtonian materials such as granular media, polymer melts etc. The simulation idea can overcome some of the difficulties mentioned above and is therefore a very efficient tool in many aspects.

The method evolved from the coupling of the classical Finite Pointset Method (FPM), developed in ITWM, with the Algebraic Multigrid Method (SAMG) of the Fraunhofer SCAI. The fluid is represented by a set of numerical points (Figure 1). Each point carries problem-relevant physical information, e.g. density, momentum, and total energy as the basic flow information in general. In contrast to methods like SPH or DEM, points do not carry a mass as they are purely numerical. Mass conservation is given by solving the appropriate differential equation, see (1).

The point cloud is automatically established and maintained due to user given constraints of point density, no need to mesh the flow domain. It is sufficient to provide a geometry model of the boundaries (walls, inflows, outflows) by stl- or similar formats.

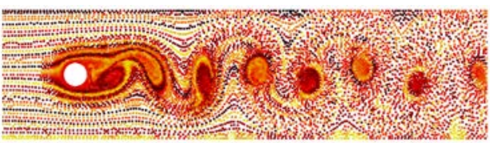

Figure 1: MESHFREE simulation of Karman vortex street with adaptive point refinement due to the gradient of velocity.

The method is Lagrangian, the numerical points move with flow velocity. In this way, we achieve an almost perfect self-adaptivity of the simulation towards moving geometry or free/phase boundaries. As the points are purely numerical, we can easily add or remove points, which gives rise to a truly adaptive numerical scheme, see again figure 1.

The conservation laws are modeled in their differential form:

$$\begin{aligned} &d\rho/dt+\rho\left(\nabla^T\mathbf{v}\right)=0 && \text{mass}\\ &d\left(\rho\mathbf{v}\right)/dt+\rho\mathbf{v}\left(\nabla^T\mathbf{v}\right)=-\nabla p+\left(\nabla^T\mathbf{S}\right)^T+\mathbf{g} && \text{momentum}\\ &d\left(\rho E\right)/dt+\rho E\left(\nabla^T\mathbf{v}\right)=-\nabla^T\left(p\mathbf{v}\right)+\nabla^T\left(\mathbf{S}\mathbf{v}\right)+\rho\left(\mathbf{g}^T\mathbf{v}\right)+\nabla^T\left(k\nabla T\right) && \text{energy}\end{aligned} \qquad (1)$$

This set of partial differential equations (PDE) is solved locally on each numerical point. The substantial derivative d/dt describes the change-rate of physical quantities of a point moving with fluid velocity. The material properties are settled in the stress tensor $\mathbf{S}$ and in the heat conduction k, and we need to provide thermodynamic closure relations $p=p(\rho,\rho\mathbf{v},\rho E)$, $T=T(\rho,\rho\mathbf{v},\rho E)$.

The solution of the PDE requires the computation of local derivatives, such as $\nabla^T\mathbf{v}$ and ∇p, which is achieved by the so-called moving least squares approach. Here, around each point, we establish local best-fit polynomials of user-given order to meet the discrete function values of the neighbor stencil. Around some space position $\mathbf{y}$ and with respect to some given function u, we search for the local best-fit polynomial $a_{\mathbf{y}}^u$ by minimizing the functional

$$\sum_{j=1}^{N(\mathbf{y})} W^2\left(\mathbf{y},\mathbf{x}_j\right)\cdot\left(a_{\mathbf{y}}^u\left(\mathbf{x}_j\right)-u_j\right)^2 \overset{!}{=} \min \qquad W\left(\mathbf{y},\mathbf{x}_j\right)=\exp\left(-\frac{c}{h^2}\left(\mathbf{y}-\mathbf{x}_j\right)^2\right) \qquad (2)$$

with $N(\mathbf{y})$ the number of neighbor points considered around $\mathbf{y}$, u_j the discrete function values at the point locations $\mathbf{x}_j$, and $W(\mathbf{y}, \mathbf{x}_j)$ the generic weight function with coefficient c and local interaction radius h to be chosen by the user. The gradient of any function can be approximated by the gradient of the best fit polynomial, for example the pressure gradient would simply be $\nabla p\left(\mathbf{y}\right)\approx\nabla a_{\mathbf{y}}^p\left(\mathbf{y}\right)$, second order derivatives like the heat diffusion can be approximated as $\nabla^T\left(k\nabla T\right)\left(\mathbf{y}\right)=k\Delta T+\nabla^T k\cdot\nabla T\approx k\Delta a_{\mathbf{y}}^T(\mathbf{y})+\nabla^T a_{\mathbf{y}}^k(\mathbf{y})\cdot\nabla a_{\mathbf{y}}^T(\mathbf{y})$. Thus, with (2), we are able to represent any derivative needed by the PDE in (1), and so we can integrate mass, momentum, and energy on each point of the cloud concluding the numerical scheme.

The method convinces by very short preprocessing times. Due to the absence of the computational mesh, the user can concentrate on the definition of boundary conditions and physical/numerical parameters. In this way, convergence and parameter studies, a “must” for any numerical study, becomes a straight-forward task.

For better visualization and comparison, free surfaces and boundaries are triangulated, as for example shown in figure 2.

Figure 2: Simulation and experiment of deep water crossing, cooperation with Volkswagen

The original implementation of the method is an explicit upwind formulation, which is used for airbag inflation simulation. For this purpose, ESI and ITWM have developed a generic interface between VPS and FPM/MESHFREE (fluid-structure-interaction). It has become an inherent feature of VPS and has proven reliability as an industrial tool already since 2004.

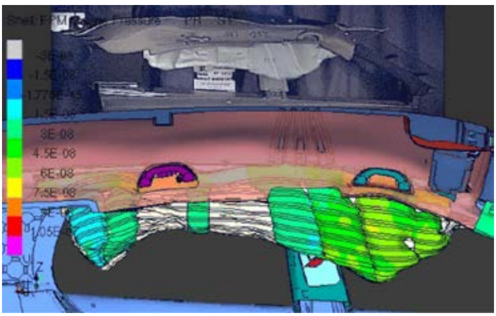

Figure 3: Simulation and experiment of curtain-airbag-inflation

The current focus of development is on the implicit formulation, especially questions of computational performance and incorporation of material models. For the solution of the arising big linear systems, we employ the above mentioned SAMG-solver. For car development, this meshfree method covers watercrossing applications (Figure2), tank filling, sloshing, just to mention the most traditional ones. As a recent development, we put special focus on water/rain management. For example, two separate simulations of airflow around a car and a droplet phase are coupled in order to capture soiling effects (fluid-fluid-interaction).

Figure 4: MESHFREE coupling of wind and water for soiling analysis. Droplet injection line in front of the wind shield. Cooperation with ESI

Another recent development is the modeling of granular flows by the Drucker-Prager model, such as given due to the roll-over interaction of cars with sand or gravel. For this purpose, we employ once more the coupling interface with VPS, already used for airbags. The sand is modelled by MESHFREE, and the car dynamics is modelled by VPS. The aim is to employ higher quality material models like Barodesy, which is our current focus.

Figure 5: Car interaction with sand, comparison of simulation and experiment, cooperation with Volkswagen

CAE Wissen by courtesy of Dr. Jörg Kuhnert, Fraunhofer Institute for Industrial Mathematics ITWM

Meshless Methods: Smoothed Particle Hydrodynamics Method

Introduction

Advanced engineering applications have traditionally relied upon numerical methods like the Finite Element Method (FEM) in order to achieve the accuracy that closed-form mathematical solutions could not possibly offer. However, when the applications moved from the linear elastic domain to the non-linear large displacement / large strain domain, the classical FEM suffered strong limitations due to the loss of accuracy within highly distorted meshes. The practical restrictions imposed upon the usage of FEM in scenarios involving strong topological changes (like fracture) or involving Fluid-Structure Interaction (FSI) meant that a new class of methods had to be adopted, which would not suffer from the topological non-uniqueness problems that highly distorted FEM meshes suffer. This was achieved by adopting "particle-type" methods that do not maintain a strict connectivity in the domain, hence they do not follow a "mesh" (meshless methods). The most fundamental of these methods is the Smoothed Particle Hydrodynamics method, or SPH, which is a cornerstone in the Virtual Performance Solution (VPS) suite of codes of ESI Group.

Overview of SPH Method in VPS

SPH is a gridless Lagrangian method whose corner stones are two approximations, namely :

- The Kernel approximation, and
- The Particle approximation

The Kernel approximation is derived from the following identity :

$$\langle A(r) \rangle = \int_{\Omega} A(\bar{r}')\delta(\bar{r}-\bar{r}')d\bar{r}', \qquad (1)$$

$$\int_{\Omega} \delta(\bar{r}-\bar{r}')d\bar{r}' = 1 \qquad \text{(delta function)} \qquad (2)$$

which says nothing else than that the "value at a point" of a continuous function over a continuous domain could be extracted from its integral by using a delta function as a "filter".

Assuming now that the delta function is replaced by another function which spans a certain "range" but still obeys the basic delta function property

$$\lim_{h \to 0} W(\bar{r}-\bar{r}',h) = \delta(\bar{r}-\bar{r}') \qquad \text{(delta function)}$$

then equation 1 will yield the following form

$$\langle A(\bar{r}) \rangle = \int_{\Omega} A(\bar{r}')\, W(\bar{r}-\bar{r}',h)\, d\bar{r}', \qquad (3)$$

which is similar in appearance as before except for the function W which will be called the KERNEL function and the range of influence it spans is controlled by the "smoothing length". What that equation says is that the value of a function at a point contains information about not just that point but of the range around that point that the Kernel in question is spanning.

Therefore, a "smoothing" of the domain has taken place, hence the term "smoothed" particle hydrodynamics.

Although the SPH concept may differ completely from that of Finite Elements, there are similarities such the continuity of some basic variables within a limited region in space and that the SPH method may also be derived from a Galerkin formulation

The Particle approximation is the next step after the Kernel approximation and it says that the domain around the point in question where we seek to define the value of a function, is NOT continuous. Instead it consists of a number of "topologically unconnected finite elements" which we will call from now on PARTICLES in order to distinguish them from the classical finite elements which have a pre-defined and rigid topological connection (the "connectivity" defined at the input level). The consequence of this approximation is in replacing the integral by a sum and modify the algebra to account for the "number density" of the domain (ie. how many particles can be found within a given domain volume defined by the Kernel we use). This is expressed as below :

$$\langle A(\bar{r}) \rangle = \sum_{j=1}^{J} (m_j / \rho_j) A_j W\left(\left|\bar{r}-\bar{r}_j\right|,h\right). \qquad (4)$$

The above equation reads like : the contribution of each particle within the Kernel range (taking into account its number density) is summed over all the particles in order to produce the smoothed value of a function at a point.

Hence the above approximation has also its roots close to those of the classical FE method.

In order for the Kernel and Particle approximations to be pragmatic, the choice of Kernel should be such that the following is satisfied :

- Compact form ie. acting over a finite range, zero outside that range
- Positive within this range
- Respecting the "delta function properties"
- Monotonically decreasing
- Degenerating in the limit to a delta function

The reader should be reminded that indeed the first two requirements listed above are the same for the classical interpolation functions of the FE method. Therefore the Kernel should be seen as a form of an interpolation function.

Figure 1 illustrates graphically the similarity between the FE and the SPH approximations. A patch of 9 elements is shown in both the FE and the equivalent SPH approximation. The interpolation functions have been overlaid upon the central element of the FE mesh while the Kernel of the central particle has been "sketched" as spanning its neighbors in the SPH mesh.

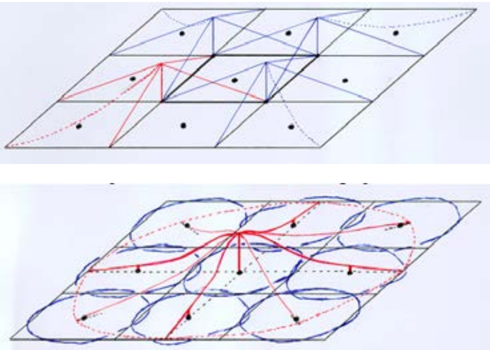

Figure 1: Comparison between FE and SPH modeling of the same patch of 9 elements

The above mentioned approximations can be applied to solve the continuity equations by parts whereby the partial derivatives of the unknowns are replaced by derivatives of the (known) kernels, yielding :

$$\dot{\rho}_i = \sum_{j=1}^{J} m_j (\bar{u}_i - \bar{u}_j).\bar{\nabla}_i W_{ij}, \qquad (5)$$

$$\frac{du_i}{dt} = -\sum_j m_j \left\{ \frac{p_i}{\rho_i^2} + \frac{p_j}{\rho_j^2} \right\} \nabla_i W_{ij} \qquad (6)$$

$$\dot{e}_i = -\frac{1}{2} \sum_{j=1}^{J} m_j (\bar{u}_i - \bar{u}_j) \left\{ P_i / \rho_i^2 + P_j / \rho_j^2 \right\} \bar{\nabla}_i W_{ij} \qquad (7)$$

Observe that these equations are different from those we habitually solve in the FE method. Moreover, starting from the same equation but following a different set of algebraic operations and approximations we could arrive at the following alternative momentum equations :

$$\frac{du_i}{dt} = -\sum_j m_j \left(\frac{p_i + p_j}{\rho_i \rho_j} \right) \nabla_i W_{ij} \qquad (8)$$

$$\frac{du_i}{dt} = -\sum_j m_j \, 2 \frac{\sqrt{p_i p_j}}{\rho_i \rho_j} \nabla_i W_{ij} \qquad (9)$$

Artificial viscosity to handle shock discontinuities is required, just as for existing numerical integration methods. Note that the above set of resulting equations is not unique, but it has been found that the differences are usually small.

Examples of Applications

The pictures below give a brief but not exhaustive overview of the basic ranges of application of the SPH method:

Hypervelocity impact: This is a typical application where matter behaves like a fluid under the extreme pressures generated during hypervelocity impact. A full 3D simulation is an ideal application fo SPH due to the large material phase and state changes (solid-liquid-gaz, fragment clouds etc.)

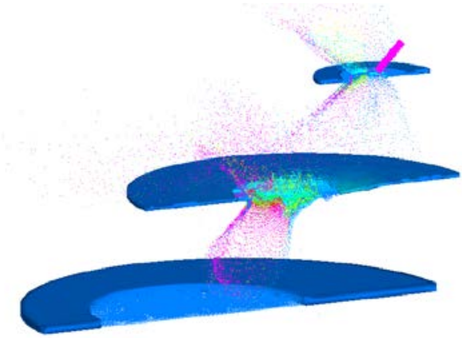

Figure 2: Double bumper penetration at 11 km/s by a cylindrical projectile (Courtesy of ESA)

Vulnerability analysis: In aeronautics this involves primarily birdstrike, hail strike etc. Birstrike is in particular well adapted for SPH applications due to the large deformations and fragmentation of the bird upon impact with the wings or rotor blades of an aircraft or helicopter.

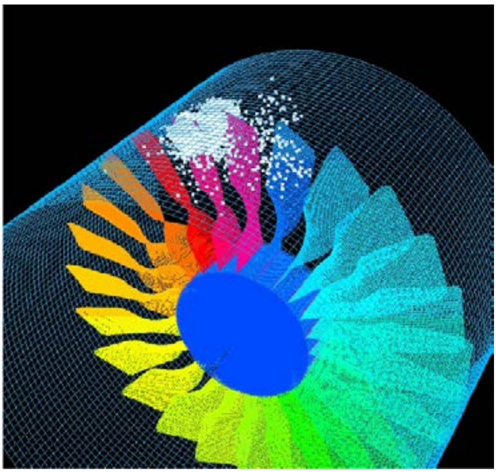

Figure 3: Birdstrike upon jet engine fan-blade

Another typical such application is forced water landing (splashdown).

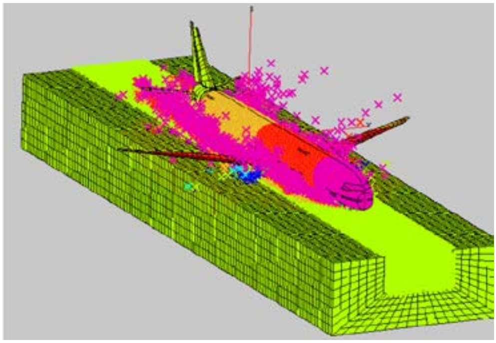

Figure 4: Airbus A321 Splashdown (courtesy of EC project CRAHVI)

Natural Hazzards: Excessive marine phenomena like tsunamis imply very strong FSI simulation requirements in terms of capability, functionality and computatuional efficiency due to the complexity and size of the problems in question. The SPH option in VPS is fully parallelized in DMP and can be used within the Multi Scale Option of VPS (Multi-Model Coupling). The images below show typical tsunami simulations regarding the effect upon a Liquid Natural Gas tank and the flooding of a building. Critical information can be gathered in terms of the strength of the associated structures or the survival time window the infrastructure has in a given scenario.

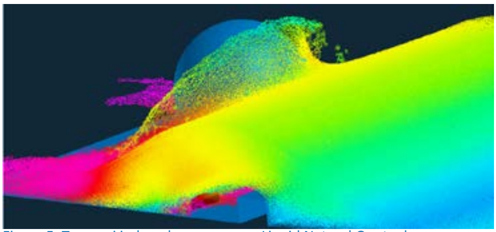

Figure 5: Tsunami induced surge upon a Liquid Natural Gas tank

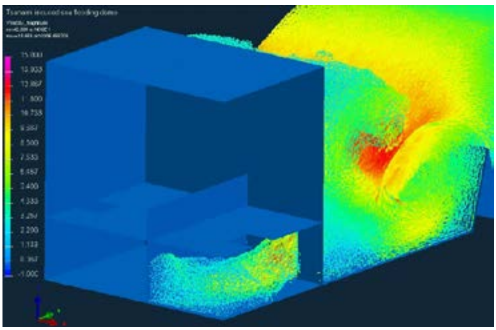

Figure 6: Tsunami induced flooding of building infrastructure

CAE Wissen by courtesy of Dr. Argiris Kamoulakos, Scientific Director, ESI Group

Simulation of Fluid Structure Interaction

Since the invention of the computer, several CAE methods for structure and fluid dynamics analysis were successfully developed by universities, research institutions and engineering software vendors and have been established as standard tools in the daily design practice in the automotive, aerospace, energy, manufacturing and other industries. On the other hand and for several reasons, development of CAE methods for flow and structure analysis was done for both, flows and structures, independently from each other in most cases, without really realizing it, a kind of thought had been established during this time which left interactions between both engineering disciplines for several years practically aside. As a consequence, despite the fact that both numerical algorithms for fluid-structure interactions (today referred by most authors as „iterative" and „direct" or „monolithic") were developed by the author already in the mid eighties having highly nonlinear membrane problems like parachutes, sails and hang-gliders in mind, it took at least two additional decades to stimulate the interest of the industry on fluid-structure interaction simulations. Starting from established integral simulation programs like the famous ADINA, which offers to the user not only the full (i.e. both „direct" and „iterative") fluid-structure interaction (FSI) capability but also full thermal fluid-structure interaction analysis (TFSI) in a really seamless development environment, down to highly specialized FSI simulation tools like PARA2G for gliding parachutes, it is very gratifying to see that in recent years more and more researchers and software vendors started to deal with solutions for a continuously increasing number of FSI applications.

Fluid Structure Interaction Basics

In fluid structure interaction analysis, fluid forces are applied on the solid and the solid deformation changes the fluid domain. The computational domain is divided into the fluid domain and the solid domain, where the fluid and the solid model are defined respectively, through their material data, boundary conditions, etc. The interaction occurs along the interface of the two domains. This is called the fluid-structure interface. Having the two models coupled, simulations and predictions of many physical phenomena can be performed.

In general we distinguish between two general algorithms for fluid-structure interaction:

- Iterative or two-way coupling:

  This algorithm is sometimes also called the partitioned method. In this iterative solution method, the fluid and solid solution variables are fully coupled. The fluid and the solid equations are solved individually in succession, always using the latest information provided from the other part of the coupled system. This iteration process is continued until convergence is reached in the solution of the coupled equations.

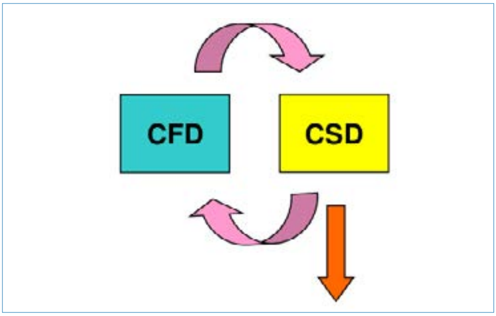

Figure 1: Iterative two-way coupling

- Direct or monolithic coupling:

  This algorithm is sometimes also called the simultaneous solution method. In this direct solution method, similar to the procedure in the above iterative solution method, the fluid and the solid solution variables are also fully coupled but here the fluid and the solid equations are combined and treated in one single system.

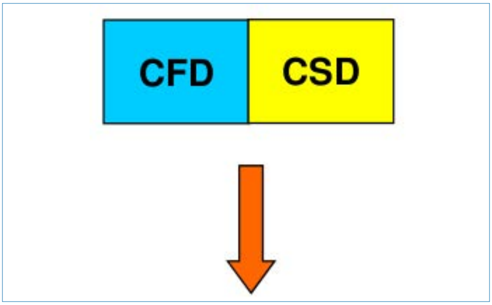

Figure 2: Direct (or monolithic) coupling

The direct coupling algorithm requires a code developed for a particular combination of the physical problems while the iterative coupling algorithm preserves software modularity because existing flow and structural solvers can be coupled in order to implement it. In addition the iterative approach facilitates solution of the flow equations and the structural equations with different, possibly more efficient numerical techniques which have been developed specifically for either the flow or the structural part of the problem. Explicit airbag simulation is an example for this kind of procedure. On the other hand, development of a stable and accurate coupling procedure, something practically impossible for a wide range of FSI problems, is required in the iterative coupling method.

Problem Dependency of Algorithm of Choice

Depending on the physics of the FSI problem someone should consider carefully the FSI algorithm of choice:

- Direct or monolithic coupling

  In the direct FSI coupling solution method the fluid and solid equations are combined and treated in one system (one stiffness matrix for both problems) and solved using an iterative solver such as the Newton-Raphson method. The direct FSI coupling algorithm offers great robustness when solving very difficult FSI problems, for example, large deformations with soft structures or highly compressible flows around very stiff structures. Due to occurring instabilities like the so-called "artificial added-mass effect" and similar these types of problems are difficult to solve using the iterative FSI solution method.

- Iterative or two-way coupling

  In general the Iterative FSI coupling solution method requires less memory than the direct FSI Coupling method and therefore may be more applicable to solve very large problems despite occurring instabilities which can be handled, sometimes more sometimes less efficiently, by numerical intervention like e.g. relaxation factors.

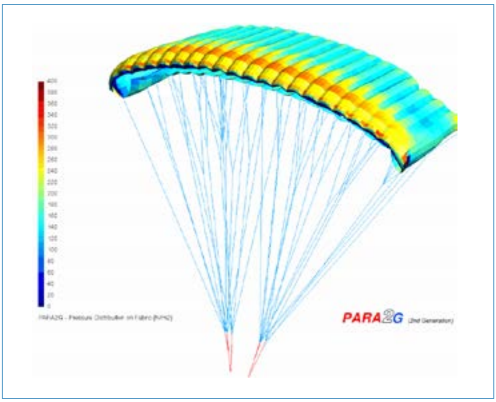

Figure 3: Iterative two-way FSI coupling example: Ram-Air Parachute

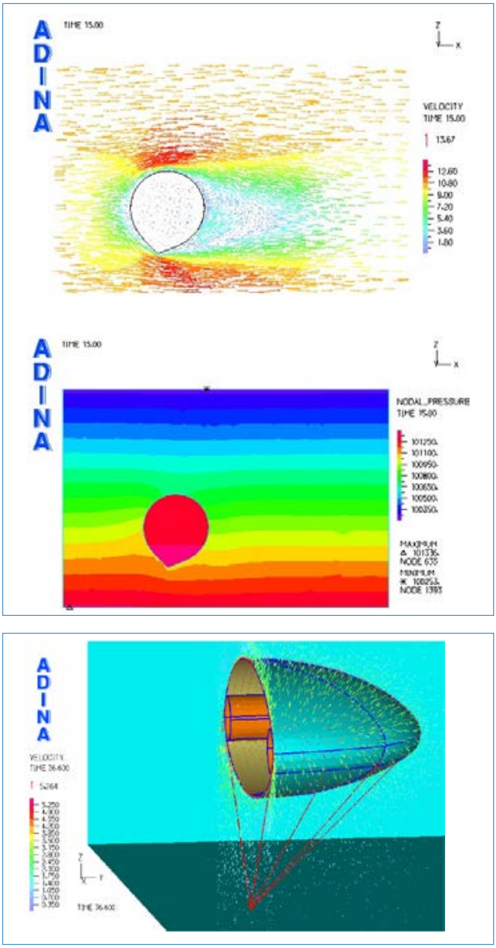

Figure 4 a+b: Direct FSI coupling examples:
a) Tethered Helium Balloon
b) Dirigible Free Flying Helium Lighter than Air Aircraft

CAE Wissen by courtesy of
Dr.-Ing. Thomas Chatzikonstantinou (Aachen)

Introduction to Passive Safety of Vehicles

Course Description

Ever increasing requirements regarding vehicle safety have led to rapid developments, with major innovations in the field of Active and Passive Safety. Especially legal requirements in the USA (FMVSS 208, 214), the consumer information tests U.S. NCAP, Euro NCAP, C-NCAP and IIHS, as well as pedestrian protection regulations are drivers behind this trend.

The seminar provides an introduction to Passive Safety of Vehicles. Passive Safety is about initiatives and legal provisions for the limitation of injuries following an accident. All important topics are covered in the seminar, from accident statistics and injury-biomechanics, which are decisive parts of accident research, to the crash-rules and regulations that are derived from the latter, and also to consumer information-tests with protection criteria and test procedures, and eventually to crash tests, where the compliance with the compulsory limits is tested and proven in test procedures. Specific attention is given to dummies, with which the potential loads on a person in an accident can be measured. Finally the basic principles of occupant protection are explained, and the components of occupant protection systems, respectively restraint-systems in motor vehicles such as airbags, belt-system, steering wheel, seat, interior, stiff passenger compartment and others, as well as their increasingly complex interaction, also in terms of new systems, will be discussed.

Course Objectives

It is the primary objective of this seminar to communicate an understanding for the entire field of Passive Safety with all its facets and correlations, but also for its limits and trends. In the seminar you are going to learn about and understand the most important topics and can then judge their importance for your work. With the extensive, up-to-date documentation you obtain a valuable and unique reference book for your daily work.

Who should attend?

The seminar addresses everybody who wants to obtain an up-to-date overview of this wide area. It is suited for novices in the field of Passive Safety of Vehicles such as university graduates, career changers, project assistants, internal service providers, but also for highly qualified technicians from the crash-test lab.

Course Contents

- Introduction to vehicle safety
  - Overview active and passive safety
  - Crash physics
- Accident research
  - General accident research
  - Classifications
  - Statistics
- Biomechanics
  - Human anatomy
  - Injury mechanisms, Injury criteria
- Dummy technology
- Crash testing
- Crash regulations and NCAP tests
  - Institutions
  - Passive safety regulations
  - NCAP tests
  - Insurance tests (IIHS, RCAR, C-IASI, ...)
- Protection principles, occupant protection systems
  - Protection principles of passive safety
  - Occupant protection systems with sensors, airbag, belt
  - Passenger compartment, interior with steering wheel and steering column, seat
  - OOP, pre crash, post crash, sensor system, vehicle body
  - Optimization of restraint systems, adaptive systems
  - Integrated safety

Instructor

Ralf Reuter (carhs.training gmbh) studied mechanical engineering and business administration at the technical universities of Darmstadt and Eindhoven. Since 1997 he has worked for carhs in various management positions. He deals with vehicle safety issues intensively, in particular with the latest developments in rules and regulations as well as consumer testing. As he is in charge of the SafetyWissen which has been published by carhs for many years, he keeps his knowledge up-to-date and profits from the inputs of carhs' trainer and expert network.

Facts

14.-17.07.2025	17/4516	Online	4 x 4 Hrs.	1.450,- EUR till 16.06.2025, thereafter 1.750,- EUR	
16.-17.09.2025	17/4517	Alzenau	2 Days	1.450,- EUR till 19.08.2025, thereafter 1.750,- EUR	
10.-13.11.2025	17/4518	Online	4 x 4 Hrs.	1.450,- EUR till 13.10.2025, thereafter 1.750,- EUR	

Introduction to ADAS and Active Safety

Course Description

Increasing demands on the protection of vehicle occupants have led to a continuous reduction in the number of injured and killed persons. While more than 20,000 persons have been killed on German roads in the early 1970s, this number is now just over 3,000. Passive safety, i.e. measures which are designed to minimize the consequences of an accident, has made a significant contribution to this achievement.

While the potential of passive safety is considered to be largely exhausted and huge efforts are required to achieve further progress in occupant protection, active safety has become increasingly important in recent years. Active Safety means measures which prevent an accident or at least reduce the collision speed and thus the energy input.

While technologies such as ABS or ESC have been established years ago and have proven their effectiveness, new techniques such as the emergency brake or the lane keeping assist and numerous other driver assistance systems are just entering the market. It can be assumed that these systems will be widely used in the next few years and will lead to a further decrease in the number of traffic victims.

Automated driving can be seen as the next step of active safety. Although there is still a lot of development needed in this area, it can be assumed that vehicles which will driven at least partially automatically in certain traffic scenarios will enter the market over the next ten years.

In the seminar first a brief introduction to active safety, in contrast to passive safety is given. This is followed by a presentation of current active safety systems and an overview of the requirements of legislation and consumer protection organizations. In addition, current and upcoming developments in the area of driver assistance systems and automated driving are presented.

Who should attend?

The seminar is aimed at new and experienced engineers working in the field of active vehicle safety in research and development departments of automotive OEMs or suppliers, as well as for all other interested parties, which want to receive an overview of current and future developments in the areas of active vehicle safety, driver assistance and automated driving.

Course Contents

- Fundamentals of active safety
  - Basic principles of action
  - Legal requirements
  - Euro NCAP requirements
- Current active safety systems
  - ABS
  - ESC
  - Brake assist
  - Pre-crash systems
- Driver assistance systems
  - Basic requirements and design strategies
  - Current and future driver assistance systems
- Automated driving
  - State of the art
  - Opportunities and risks
  - Human machine interface
  - Market introduction strategies

Instructor

Dr. Gerd Müller (Technical University Berlin) has been working at the department automotive technology of the Technical University of Berlin since 2007. From 2007 to 2015 he was a research assistant. Since 2015 he has been a senior engineer of the same department. His research focuses on vehicle safety and friction coefficient estimation. Dr. Müller gives the lecture "Fundamentals of Automotive Engineering" and conducts parts of the integrated course "Driver Assistance Systems and Active Safety".

Facts

29.-30.04.2025	51/4476	Online	2 x 4 Hrs.	890,- EUR till 01.04.2025, thereafter 1.090,- EUR	

SAFETYWEEK

The Future of Automotive Safety

Supporting automotive development engineers to further improve automotive safety, that is the essence of SafetyWeek.

In a unique combination of knowledge congress, events and exhibition, SafetyWeek offers participants and visitors the opportunity, to bring their expertise up-to-date and to learn about the latest developments and technologies in product development and product verification.

In 2025 SafetyWeek will feature numerous highlights:

- The knowledge congress **SafetyUpDate** with the latest updates on requirements and solutions in active and passive safety.
- The **SafetyTesting*Challenge*** with the innovations from the leaders in testing and simulation of components and systems in active and passive safety
- **Auto[nom]Mobil**, the expert forum on L3 and beyond
- The accompanying exhibition **SafetyExpo**, the meeting point for suppliers and decision makers in automotive safety.

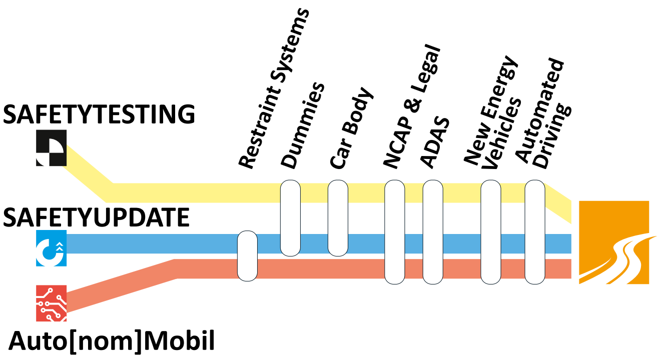

Who should attend?

SafetyWeek is the meeting point for everyone involved in vehicle safety. This includes developers as well as test and simulation engineers from OEMs and suppliers, manufacturers of test systems, representatives of governments and consumer protection organizations and researchers from universities and research institutes.

ON SITE & ONLINE

Facts

May 13 – 15, 2025

Hanau, GERMANY & ONLINE

www.carhs.de/safetyweek

English

AUTOMOTIVE Safety Summit Shanghai 2025

Safety Requirements & Technologies for the intelligent, autonomous and electrified Automobile of the Future.

Since 2014, the »Automotive Safety Summit Shanghai« is attracting every year more than 500 automotive safety experts from China and beyond to discuss the latest requirements and innovations in active and passive safety. Accompanied by a comprehensive trade show with the worldwide vendors in development technologies and services, the summit is the leading event for everyone involved in automotive safety. The 2025 event will focus on automotive safety in the context of the dominating megatrends: ADAS, ADS and NEV.

Join »Automotive Safety Summit Shanghai« at the Kerry Hotel in Pudong, Shanghai, China.

Keynotes from international experts, presentations on requirements and innovations, the latest developments in testing and simulation for active and passive systems will make this event a true highlight for every decision maker and engineer in the fields of active and passive safety.

The event will have dedicated sessions on the following topics:

- Safety in Autonomous Driving Systems
- Legal Requirements for Level 3 and beyond
- Advances in World-wide NCAP Programs
- Safety of New Energy Vehicles
- Vulnerable Road Users
- New Testing Technology for ADAS and ADS
- Safety Assurance for ADS
- Human Modeling and Simulation for Safety

Who should attend?

»Automotive Safety Summit Shanghai« is addressing decision makers and experts at all stages of the development phase, managers during the conceptual phase who need to understand upcoming global requirements, design engineers, testing and simulation specialists.

ON SITE & ONLINE

Facts

July 16 – 17, 2025

Shanghai, CHINA & ONLINE

www.carhs.de/safetysummit

English / Chinese with simultaneous translation

theADAS experience 中国

The requirements by New Car Assessment Programs regarding safety-supporting driver assistance systems for passenger cars are constantly increasing: Oncoming traffic scenarios, tests in darkness and higher expected speed reductions are some of the prerequisites for a 5-star rating in the Euro NCAP or an IIHS Top Safety Pick.

The introduction of emergency brake assistants for passenger cars is being driven forward by legislation: Since 2022 UN Regulation 152 has been applicable for passenger cars in the EU. The lane departure warning functions have also been incorporated into UN R 79.03.

At **The ADAS Experience**, the framework relevant for the development will be presented: Requirements, technical principles, development and release methods on the Theory Day in the conference hotel, followed by hands-on experience on the test track on the Demo Day. Various test scenarios will be performed and examples of how the test technology is best used, will be shown live in the different test setups.

This is what awaits you:

- The presentation of current and future requirements on emergency braking, evasion and highly automated driving functions, as well as development strategies that lead to a robust system.
- Face to face talk with the people who set the framework for the development of safety assist functions: Legislative representatives, consumer protection organizations, OEM representatives and suppliers of simulation and testing technologies.
- Practical experience with various test setups, targets, driving robots and control software on the Demo Day.

Who should attend?
The ADAS Experience addresses everyone, who works in the field of safety-related driver assistance systems. The Conference is the right place to broaden and deepen your network: You will meet key players in development, system integration, regulation and verification of Safety Assist Systems.

Facts

September 23 – 24, 2025

tba, China

www.carhs.de/adasCN

Automated Driving - Safeguarding and Market Introduction

Course Description

The seminar presents the necessary and sufficient conditions for bringing automated vehicles onto the market. In addition, requirements for product monitoring and market surveillance will be derived, which can be used to ensure that the technology proves itself throughout the entire product life cycle. The question is addressed as to what forms automated driving can be expected to take in private transport, local passenger and freight transport, long-distance transport and in very special areas of application, and what opportunities connectivity and digitization of the technology open up.

Course Objectives

The course teaches the steps necessary to bring an automated vehicle to the market. In particular, it deals with how the safety of such vehicles can be proven and documented.

Who should attend?

The seminar is aimed at engineers who are faced with the task of making automated vehicles ready for the market and providing legally compliant proof of the safety of these vehicles.

Course Contents

- National and international laws and regulations
- Safety standards (functional safety, safety of the intended function, cyber security)
- Positive risk balance
- Technically unavoidable residual risks
- Proof of operational reliability
- Epidemiological and systemic approaches in safety and risk analyses
- Development of automation in
  - Customer vehicles
  - People & goods movers
  - Heavy commercial vehicles
  - Special applications
- Connectivity and digital mobility ecosystems

Instructor

Udo Steininger (TESACO GmbH) earned his diploma in Nuclear Physics in 1986 and began working in nuclear safety research with a nuclear power plant operator. Since 1991, he has been with TÜV SÜD, working in various fields including reactor safety supervision, railroad control and safety technology, and general road vehicle safety. In 2005, he shifted his focus to the safety of automated driving. In 2024, he co-founded TESACO GmbH, where he serves as Managing Director. TESACO's mission is to provide technical and regulatory support for the development and operation of vehicles and systems for connected cooperative automated mobility.

Facts

03.06.2025	198/4493	Alzenau	1 Day	890,- EUR till 06.05.2025, thereafter 1.090,- EUR	

International Safety and Crash-Test Regulations
Current Status and Future Developments

Course Description

Since the 1960's, the regulation of vehicle safety performance has had a major impact on vehicle and system design. As automotive manufacturing has evolved into an integrated global system, understanding and anticipating legal requirements has become an immense challenge. Regulators collaborate and diverge in how they address road-safety policy goals. Regulatory changes in a single market can translate into global customer requirements. And these requirements are continuously evolving. In a compact program, this two-day seminar provides a worldwide update on the passive safety landscape, covering local, national, regional, and international policy and rulemaking developments.

The first segment of the seminar focuses on regulatory institutions and processes. By understanding the regulatory environment, including the trend towards an integrated global regulatory system, businesses can better prepare for changes that impact competitiveness and customer satisfaction.

The second segment applies this knowledge to current and future regulatory requirements. The seminar covers crashworthiness (frontal, side, rear impact, etc.) as well as pedestrian protection and new technologies.

Course Objectives

This course informs participants of recent developments and discussions within the global regulatory community concerning passive safety. The seminar explores differences in regulatory systems and philosophies, in compliance and enforcement, and in the forces behind the regulation of vehicle safety. The course provides participants with a broad understanding of current regulatory directions and guidance on how to follow, and even influence, future requirements.

Who should attend?

This seminar should be of interest to anyone involved with meeting and anticipating legal requirements for vehicle safety performance across international markets. The course provides a compact review of changes in passive safety requirements and current priorities across the international regulatory community. Moreover, the course provides knowledge critical to understanding differences in the way regulators establish and enforce these legal requirements.

Course Contents

- History of safety regulation and development of legal regimes (e.g., self-certification, type approval, product liability, in-use surveillance)
- Regulatory agencies and rulemaking processes (e.g., UN, EU, U.S. NHTSA, etc.)
- Regulatory drivers and priorities (e.g., accident data, injury dynamics, injury criteria, test tools, harmonization, whole vehicle approval, competitiveness, etc.)
- Types and purposes of regulations (UN Regulations, GTR, FMVSS, EU Regulations and Directives, etc.)
- Developments in crashworthiness and occupant protection requirements (frontal impact, side impact, pole-side impact, full width barrier, ODB, MDB, etc.)
- Vulnerable road user (VRU) protection (e.g., pedestrian safety, cyclist safety)
- Safety of new propulsion technologies (electric vehicles, hydrogen fuel-cells, minimum vehicle noise levels)
- Passive safety implications of new safety technologies (e.g., e-call, collision avoidance, VRU detection, AD)

Instructors

John Creamer (GlobalAutoRegs.com) is the founder of GlobalAutoRegs.com and a partner in The Potomac Alliance, a Washington-based international regulatory affairs consultancy. In his client advisory role, Mr. Creamer is regularly involved with meetings of the UN World Forum for the Harmonization of Vehicle Regulations (WP.29). Previously, he has held positions with the US International Trade Commission and the Motor & Equipment Manufacturers Association (representing the US automotive supplier industry), as the representative of the US auto parts industry in Japan, and with TRW Inc. (a leading global automotive safety systems supplier).

Dr. Thomas Kinsky (Humanetics Europe GmbH) completed his studies of automotive engineering at TU Dresden in 1991 and received a doctorate at TU Graz in 2015. From 1991 to 1995 he worked as an officially certified expert for TÜV Rheinland. Afterwards he managed from 1995 to 1998 the vehicle construction department in a small medium-sized company. From 1999 to 2018 Dr. Kinsky worked for the car manufacturer Opel in the area of vehicle regulations. Lastly as a senior expert, he was responsible for the development of legislation on passive vehicle safety and represented Opel in the discussion with authorities and associations. Since 2018 he is Director of Business Development at Humanetics. In this role he is the contact for all topics regarding dummy development as well as for requirements on passive and active safety at Humanetics.

Facts

14.-15.04.2025	16/4478	Alzenau	2 Days	1.450,- EUR till 17.03.2025, thereafter 1.750,- EUR	
05.-08.05.2025	16/4494	Online	4 x 3 Hrs.	1.450,- EUR till 07.04.2025, thereafter 1.750,- EUR	
12.-13.11.2025	16/4479	Alzenau	2 Days	1.450,- EUR till 15.10.2025, thereafter 1.750,- EUR	

Vehicle Safety under Self-Certification
Principles, Obligations, Enforcement and Remedies

Course Description

When looking at regulatory requirements across different markets, it's common to think in terms of technical specifications, checking for differences in test procedures and performance criteria. However, failure to consider how the regulations are used can be a fatal mistake because safety authorities differ in how they apply and enforce their requirements.

This seminar looks at the self-certification compliance and enforcement system which focuses heavily on monitoring the performance of vehicles in use. Compliance with the legal standards is only one part of a much larger, more complex system requiring the assurance of safety throughout the lifetime of every vehicle on the road. Manufacturers must have systems in place to detect possible safety concerns regardless of whether they relate to compliance with specific standards and must communicate continuously with safety authorities or run the risk of damaging recalls that can place the company in peril.

Course Objectives

This seminar provides a review of self-certification compliance and enforcement mechanisms toward helping manufacturers avoid expensive recalls, costly penalties, and lost reputation.

Who should attend?

The seminar is aimed at employees from the development departments of automobile manufacturers and suppliers who develop vehicles for the U.S. market as well as all employees in the areas of product strategy, sales and warranty and defect management for the U.S. market.

Course Contents

- Background and origins of self-certification
- Players and processes in U.S. rulemaking
- Principles of U.S. safety compliance and enforcement
- Role of product liability laws
- Role of Federal Motor Vehicle Safety Standards (FMVSS)
- NHTSA and FMVSS compliance
- NHTSA and safety monitoring
- Non-regulatory methods to ensure safety
- Safety defects and motor vehicle recalls
- Manufacturer roles and responsibilities
- Outlook for U.S. safety policies

Images: NHTSA

Instructor

John Creamer (GlobalAutoRegs.com) is the founder of GlobalAutoRegs.com and a partner in The Potomac Alliance, a Washington-based international regulatory affairs consultancy. In his client advisory role, Mr. Creamer is regularly involved with meetings of the UN World Forum for the Harmonization of Vehicle Regulations (WP.29). Previously, he has held positions with the US International Trade Commission and the Motor & Equipment Manufacturers Association (representing the US automotive supplier industry), as the representative of the US auto parts industry in Japan, and with TRW Inc. (a leading global automotive safety systems supplier).

Facts

14.-15.10.2025	183/4496	Alzenau	2 Days	1.450,- EUR till 16.09.2025, thereafter 1.750,- EUR	

NCAP - New Car Assessment Programs Tests, Assessment Methods, Ratings

Course Description

In 1979 the first New Car Assessment Program (NCAP) was established by NHTSA in the United States. The goal was to motivate competing car manufacturers to enhance the safety level of their cars beyond the minimum safety standards defined by regulations. The same approach has been followed globally by other organizations (e. g. by Euro NCAP, IIHS, ANCAP, JNCAP, KNCAP, C-NCAP, ...). Euro NCAP which has been established in 1997 has taken a leading role and has significantly influenced other countries and regions. The NCAP programs in many cases are highly dynamic, especially in comparison with rulemaking activities. In order to reach the goal to continuously improve the safety level of cars, the requirements need to be permanently adapted to the state of technology. Developers in the automotive industry need to know about upcoming changes at an early stage in order to be able to design or equip their vehicles accordingly.

In this seminar attendees get an overview of the organizations in charge of the NCAP programs and become familiar with the various test and assessment methods.

The seminar is conducted several times a year with changing focuses:

- **Focus passive safety:** Here the focus is on test and assessment methods for passive safety. Frontal and side impact, whiplash, child protection and pedestrian protection are discussed in detail. Tests for active safety are only mentioned in as far as they are relevant for the overall rating.
- **Focus active safety:** Here the focus is on active safety systems such as AEB or lane assistance. The tests and assessments for these systems are explained in detail. Tests for passive safety are only mentioned in as far as they are relevant for the overall rating.

In both focusses the current overall rating methods are described and explained. In addition to that an outlook is given on the roadmaps and future developments of the NCAP programs.

Who should attend?

The seminar addresses design, simulation, testing and project engineers as well as managers who want to get a current overview on the global range of NCAP programs with an outlook on upcoming topics and trends from an insider. Depending on the focus of their work attendees should chose the appropriate focus of the seminar.

Course Contents

- Basics of New Car Assessment Programs
- Euro NCAP
  - Background, Principles and Organisation
  - Products, Rating and Rules
  - Adult Occupant Protection (AOP)
  - Child Occupant Protection (COP)
  - Vulnerable Road User Protection (PP / VRU)
  - Safety Assist (SA)
  - Automated Driving
  - Commercial Van Safety
  - Roadmap 2030
- IIHS
- China NCAP

Instructor

Director and Professor Andre Seeck (German Federal Highway and Transport Research Institute) has been Vice President of the Federal Highway Research Institute (BASt) since April 2022, where he heads the Vehicle Technology division. In this position he is responsible for the preparation of European Safety Regulations. Furthermore he represents the German Federal Ministry for Digital and Transport in the Board of Directors of Euro NCAP and he is the chairman of the strategy group on automated driving and of the rating system. These positions enable him to gain deep insight into current and future developments in vehicle safety. In 2017 NHTSA awarded him the U. S. Government Special Award of Appreciation.

Facts

01.-02.07.2025	164/4473	Alzenau	2 Days	1.450,- EUR till 03.06.2025, thereafter 1.750,- EUR	
25.-28.08.2025	164/4472	Online	4 x 4 Hrs.	1.450,- EUR till 28.07.2025, thereafter 1.750,- EUR	
23.-24.09.2025	164/4474	Alzenau	2 Days	1.450,- EUR till 26.08.2025, thereafter 1.750,- EUR	
18.-21.11.2025	164/4475	Online	4 x 4 Hrs.	1.450,- EUR till 21.10.2025, thereafter 1.750,- EUR	

Crash Safety of Hybrid and Electric Vehicles

Course Description

During recent years, electric vehicles have achieved an ever-increasing importance for the automotive market. In addition, established OEM suffer increasing pressure by new competitors with innovative vehicle concepts. A compliance of restrictions for CO2 emissions in EU since 2020 is not possible without electrified powertrains. All major OEM offer an increasing variety of hybrid vehicles (HEV), plug-in hybrid vehicles (PHEV) and pure electric vehicles (BEV). Also a first offer of fuel cell electric vehicles (FCEV) is in the market. Market acceptance and consumer demands exceed delivery capacity for some models. In 2020 more than 3 million electrified vehicles (BEV and PHEV) were sold worldwide. The breakthrough of the automotive electrification is evident. For the development of future vehicle generations, the integration of electrified powertrains has not to be considered, it's the baseline.

Nevertheless, several challenges for vehicle safety arise with these technologies. Electric shock risks on high-voltage systems, fire hazards in case of lithium-ion batteries and risks of rupture in case of gas tanks are the most important issues here. For every mode of drive, specific drive components and their particular safety requirements are described. In addition to common rules and standards, specific needs based on real-life accidents are being discussed.

For all relevant vehicle components the respective safety requirements, safety concepts and exemplary safety initiatives will be discussed. The state of the art concerning test standards, verification methods and possibilities for virtual safety will be shown. Future trends will be presented with the help of current research projects and results. Practical experience of rescuing, recovering and towing of electric vehicles complete the spectrum of accident safety.

Course Objectives

Participants will get an overview about automotive safety of electric vehicles and will learn the special challenges and solutions which come along. Participants will be able to apply test methods and safeguarding concepts and to pursue development strategies in a target-oriented way.

Who should attend?

The seminar addresses development and research engineers as well technicians in the fields of testing and engineering with electric vehicles. Due to its current relevance the course suits young professionals as well as experienced engineers who want to deepen their knowledge in this field.

Course Contents

- Overview alternative drive systems: hybrid, electric vehicles, fuel cell, gas vehicles
- Challenges for vehicle safety
- Legal requirements and standards, safety requirements for real-world accidents
- Safety of high voltage systems
- Battery safety
- Gas tank safety
- Fuel cell safety
- Structural safety
- Safety concepts
- Rescuing, recovering and towing of electric vehicles

Instructor

Rainer Justen (Mercedes-Benz AG) has more than 30 years of experience in the field of vehicle safety. After his studies in mechanical engineering with a focus on automotive engineering he started his career in the automotive development at Daimler AG in 1987. Several career milestones in the fields of vehicle safety, project management, safety concepts and active safety / driver assistance systems made him an expert on all relevant topics of automotive safety. Since 2008 he is working in the field of safety for alternative drive systems. Rainer Justen is author of numerous publications and papers on this topic. In 2015 Rainer Justen received the SAE Automotive Safety Award for his work on the Safety of Li-ion Batteries in Electric Vehicles from the American Society of Automotive Engineers (SAE).

Facts

	#				
29.-30.04.2025	173/4532	Alzenau	2 Days	1.450,- EUR till 01.04.2025, thereafter 1.750,- EUR	
28.-31.07.2025	173/4533	Online	4 x 3 Hrs.	1.450,- EUR till 30.06.2025, thereafter 1.750,- EUR	
18.-19.11.2025	173/4534	Alzenau	2 Days	1.450,- EUR till 21.10.2025, thereafter 1.750,- EUR	

Development of Frontal Restraint Systems meeting Legal and Consumer Protection Requirements

Course Description

Belts, belt-load limiters, airbags, steering column, knee bolster, seat ... - only if all the components of a frontal restraint system are in perfect harmony it is possible to meet the different legal limit values as well as the requirements of consumer tests. However, these requirements, e.g. FMVSS 208, U.S. NCAP, Euro NCAP et al. are manifold and extensive, partly contradict each other, or the requirements superpose each other. Therefore it is a challenge for every development engineer to develop a restraint system by a clear, strategic procedure; time-saving and target-oriented with an optimal result.

In this 2-day seminar this strategic way of development will be shown. You will learn a procedure how to ideally solve the complex development task of a typical frontal restraint-system design within the scope of the available tools test and simulation. Especially the importance and the influence of individual system components (e.g. belt-load limiters) for the accomplishment of development-sub tasks (e.g. minimum chest deflection) will be covered. In addition the influence of the airbag module design on the hazards of Out-of-Position (OoP) situations is going to be discussed, and a possible development-path for the compliance with the OoP requirements according to the FMVSS 208 legislation will be shown. The possibilities and limits of the development tools test and simulation will be discussed and communicated. Last but not least tips and tricks for a successful overall system design will be part of this seminar.

In this seminar you will become familiar with a procedure for the successful development of a frontal restraint system. Furthermore you will learn which development tool, simulation or test, is best suited for the respective sub task. Moreover you will be made aware of the influence of the individual components of a restraint system (belts, belt-load limiters, airbags, steering column, knee bolster, seat, ...) on the efficiency of the entire system.

Finally future topics such as the compatibility of vehicles as well as pre-crash preparation and prevention of accidents are integrated into the seminar.

Who should attend?

The seminar addresses simulation and test engineers, project engineers and project managers as well as the heads of development departments in the field of passive safety who work on the design of restraint-systems for vehicles.

Course Contents

- Identification of the relevant development load cases
- Procedures for the development of a restraint system
- Influence and importance of individual system components on the overall performance
- Development strategy for UN regulations and NAR restraint systems
- Development path for the conformance to the OoP requirements according to FMVSS 208

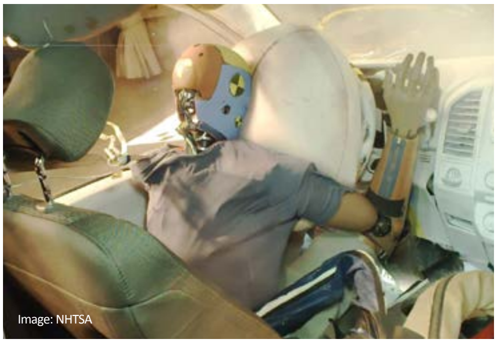
Image: NHTSA

Instructor

Kai Golowko (Bertrandt Ingenieurbüro GmbH) has been working in the area of vehicle safety since 1999. He started his career as a test engineer for passive safety at ACTS. Since 2003 he has been working as senior engineer for occupant safety and pedestrian protection. Since 2005 he has managed the department vehicle safety at Bertrandt in Gaimersheim. He has also been responsible for active and passive vehicle safety for the Bertrandt Group since 2017.

Facts

17.-18.06.2025	20/4568	Gaimersheim	2 Days	1.450,- EUR till 20.05.2025, thereafter 1.750,- EUR	
19.-20.11.2025	20/4569	Alzenau	2 Days	1.450,- EUR till 22.10.2025, thereafter 1.750,- EUR	

Model Based Head Injury Criteria for Head Protection Optimization - SUFEHM

Introduction

The head and more specifically the brain is among the most vital organs of the human body.

Over the past decades, a slant has been put by the biomechanical research on the understanding of the head injury mechanisms. Nevertheless, an injury is always a consequence of an exceeded tissue tolerance to a specific loading. Even if local tissue tolerance has very early been investigated, the global acceleration of the impacted head and the impact duration are usually being used as impact severity descriptors. The Wayne State University Tolerance Curve has therefore been proposed since the early Sixties thanks to several works by Lissner et al. (1960) [1] and Gurdjian et al. (1958) [2]. Hence, after the work of Gadd (1966) [3], the National Highway Traffic Safety Administration (NHTSA) proposed the Head Injury Criterion (HIC) in 1972. This is the tool used nowadays in safety standards for the head protection systems using headforms. Since it is based solely on the global linear resultant acceleration of a single mass head model, some limitations of this empiric criterion are well-known, such as the fact that it is not specific to direction of impact and that it neglects the angular accelerations.

A proposed alternative method for assessing head injury risk is to use a human head Finite Element Model (FEM), which can enable the investigation of the intra-cranial response under impact conditions. This method is well known since 1975 when one of the first three dimensional models was developed by Ward et al [4]. This method thereby leads to added useful mechanical observables which should be closer to the description of known injury mechanisms. Hence, new injury criteria can be proposed. In the last decades, more than ten different three dimensional finite element head models have been reported in the literature. Fully documented head impact cases can be simulated in order to compute the mechanical loadings sustained by the head tissues and to compare it to the real injuries described in the medical reports. It has for example been shown in Zhou et al. (1996) [5], Kang et al. (1997) [6] and more recently in King et al. (2003) [7], Kleiven et al. (2007) [8] and Deck et al. (2008) [9] that the brain shear stress and strain rates predicted by their Finite Element Head Models agree with the location and the severity of the axonal injuries described in the medical report. Since these FE head models exist, new injury prediction tools based on the computed intracranial loadings become available for protective systems design.

Human Head Model Development and Validation

The proposed head geometry is based on a digitized human skull. Membranes (falx and tentorium) are based on anatomic atlas and a brain-skull interface has been considered in order to represent the CSF. Brain, CSF and scalp are modeled with brick elements. As a function of application, three approaches exist for the skull model, i.e. a rigid skull, a frangible and deformable skull modeled by a three layered composite structure with constant thickness and finally a detailed skull description with non-constant thickness. Figure 1 illustrates the skull, the CSF, the membranes and the brain structure of Strasbourg University FE Head Model (SUFEHM). The constitutive laws implemented under LS-DYNA for the different parts of the human head are reported in Deck et al 2008 [9] for the material supposed to be elastic (scalp, CSF, membranes, face), and visco-elastic brain material for the composite frangible elasto-plastic behavior of the skull. In order to ensure that this mechanical head model presents a realistic response under impact it was validated against data reported in the literature as reported in [9]. Validation focused on intra-cerebral pressure, brain deformation and skull deformation. Anatomical and structural analysis of the children head-neck system as a function of age showed that the scaling down method was applicable to children over 6 years old. For younger children, specific geometrical and structural specifications such as sutures, fontanels, skull homo-

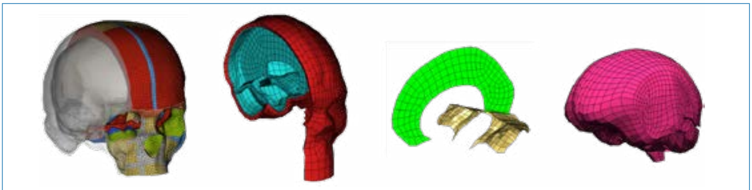

Figure 1: SUFEHM (Strasbourg University FE Head Model): skull, CSF, membranes, brain

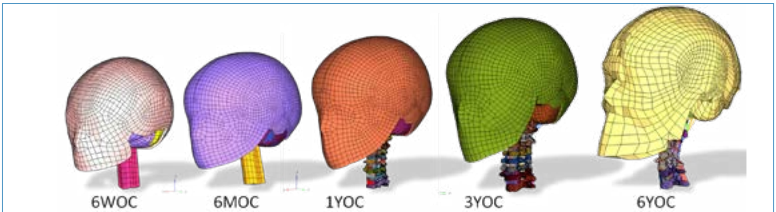

Figure 2: Illustration of the children head and neck FE models with specific structural and geometrical characteristics of the 6 weeks, 6 months, 1,3,6 years old.

geneity should be considered. Figure 2 reports the head-neck models developed for the 6 weeks, 6 months, 1 , 3 and 6 years old child models.

Model Based Head Injury Criteria and Applications

In order to establish human head tolerance limits, no less than 125 real world head trauma involving adults and children have been simulated with the above head models. Several cranial and intra-cranial mechanical parameters have been computed and correlated with the occurrence of skull fracture, subdural hematoma and neurological injuries respectively. It has been shown that a under 50 % risk of subdural hematoma appears for maximal pressure of the CSF of about -135kPa, the 50 % risk of neurological injury exists for an intra-cerebral von Mises shearing stress of around 37 kPa, both, for the adult and the child. Coming to skull fracture prediction it was shown that the relevant mechanical parameter is skull strain energy and that the critical value (50 % risk) is strongly age dependent as it varies from 0.5 J for the adult to 6 J for the youngest child.

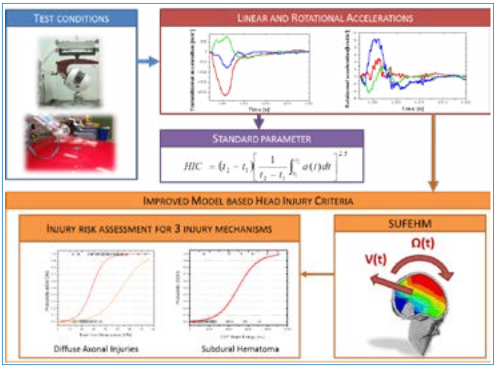

Figure 3: Implementation of the head injury prediction tool into a standard test method according to the coupled experimental versus numerical test method.

The proposed head models and injury criteria transform the model to numerical head injury prediction tools with a number of possible applications in the field of evaluation and optimization of head protection systems or advanced virtual testing. The coupled experimental versus numerical test procedure is illustrated in figure 3 and is implemented in a so-called SUFEHM-Box. For helmet applications, a FE-model free solution based on deep learning method has been developed by Bourdet et al. 2021[10].

Figure 4: Implementation of the head injury prediction tool into a full FE approach considering the coupled head-protective system model in the framework of car bonnet or helmet optimization.

Further, a full FE approach is possible when the protective system has been previously modelled. In this case a virtual evaluation and optimization of the protective system is possible as reported by Tinard et al 2012 [11] and illustrated in figure 4 for a car bonnet and a motorcyclist helmet optimization.

Conclusion

Background of head injury criteria based on single head acceleration and on advanced head FE models are presented. Further, the Strasbourg University Finite Element Head Model (SUFEHM) has been presented and validated. In an attempt to develop model based head injury criteria a total of 125 real world head trauma that occurred in motorcyclist, American football and pedestrian accidents were reconstructed with SUFEHM.

Tolerance limits to specific injury have been computed for a 50% injury risk of skull fracture, SDH and neurological injuries Finally it is shown how the proposed model based head injury criteria can be applied to experimental and numerical head protection systems evaluation and optimization.

References

[1] Lissner H.R., Lebow M., Evans F.G., Experimental studies on the relation between acceleration and intracranial pressure changes in man, Surgery, Gynecology and Obstetrics, vol. 111, 1960.

[2] Gurdjian E.S., Webster A., Head Injury, Little Brown Company, Boston, 1958.

[3] Gadd C.W., Use of a weighted – impulse criterion for estimating injury hazard, Proc. of the 10th STAPP Car Crash Conf., pp. 164-174, 1966.

[4] Ward C.C., Chan M., Nahum A.M., Intracranial pressure: a brain injury criterion, SAE, 1980.

[5] Zhou C., Kahlil T.B., Dragovic L.J., Head injury assessment of a real world crash by finite element modelling, Proc. of the AGARD Conf., 1996.

[6] Kang HS,, Willinger R., Diaw BM, Chinn B : Validation of a 3D human head model and replication of head impact in motorcycle accident by finite element modelling. Proceed. of the 41th Stapp Car Crash Conf. Lake Buena Vista USA, pp 329-338, 1997.

[7] King A., Yang K., Zhang L., and Hardy W. Is head injury caused by linear or angular acceleration? IRCOBI Conference, pp 1–12, 2003

[8] Kleiven S (2007) Predictors for traumatic brain injuries evaluated through accident reconstructions. Proceedings 51th Stapp Car Crash Conference, SAE paper 2007-22-0003:81-114.

[9] Deck C., Willinger R., (2008) Improved head injury criteria based on head FE model, International Journal of Crashworthiness, Vol 13, No 6, pp. 667-678.

[10] Bourdet N., Deck C., Trog A., Meyer F., Noblet V., Willinger R.: Deep Learning methods applied to the assessment of Brain Injury Risk, IRCOBI Conference Paper IRC-21-81,Sept. 2021

[11] Tinard V, Deck C, Willinger R.: New methodology for improvement of helmet performances during impacts with regards to biomechanical criteria. J of Materials and Design 37 (2012) 79-88.

CAE Wissen by courtesy of Dr. Caroline Deck & Prof. Dr. Remy Willinger, University Strasbourg & CNRS, France

Model Based Head Injury Criteria for Innovative Protection Design

Course Description

To prevent injuries resulting from head impacts inside and outside the car, the next generation of head protection design will have to be based on improved model-based head injury criteria including virtual or coupled experimental and virtual methods. These novel approaches will consider linear and rotational head acceleration vs time and take into account a range of head injury mechanisms. By implementing recent research tools into new design methods, it will be possible in a near future, to propose protective structures and panels to be optimized against biomechanical injury criteria including the challenging aspect of mild brain injury. An analysis of how SUFEHM is monitored within Euro NCAP and how an Artificial Intelligence version of SUFEHM has been implemented into helmet testing will be exposed as well.

Course Objectives

The objective of this course is to provide an overview of head trauma biomechanics and existing head injury criteria. Focus will then be on the state of the art in the domain of human head FE modeling, both its limitations and its recent achievements. Special attention will be paid to real world head trauma reconstruction and the derivation of model based head injury criteria. Finally the novel head injury prediction tool SUFEHM (Strasbourg University Finite Element Head Model) will be presented, with special focus to its implementation into an industrial environment It will be shown how the assessment of head injury risk is conducted in the context of an experimental crash scenario and how new protection design is evaluated in a virtual testing environment.

Who should attend?

This seminar is especially suited for engineers and technicians who work on experimental or numerical development of vehicle interior parts or pedestrian protection, who want to prepare the next generation of head protection design based on virtual methods.

Course Contents

- Introduction
- Human head surrogates and existing head injury criteria
- Overview of head protection standards
- The state of the art in human head FE modeling
  - Overview of existing head models
  - Model validation issues
- Real world head trauma simulation
  - Head trauma database
  - Victim kinematics and head impact conditions
  - FE modeling of the head trauma
- Model-based head injury criteria
  - Methodology
  - Injury criteria for different injury mechanisms
  - Age dependent issues (elderly and children)
- Application to head protection
  - Optimization against biomechanical injury criteria
  - Focus on the implementation of the tool SUFEHM within an industrial environment (experimental and virtual testing)
- Conclusion and next steps

Instructor

Dr. Caroline Deck (University of Strasbourg) obtained her Ph.D Thesis in biomechanics in 2004 and a research manager habilitation in 2014. Since 2004 she has a permanent research position in Biomechanics at Strasbourg University. She is specialized in finite element modeling of the human head, head trauma numerical accident reconstruction and head injury criteria development as well as head protective system evaluation and optimization.

Facts

12.-13.11.2025	141/4524	Online	2 x 4 Hrs.	890,- EUR till 15.10.2025, thereafter 1.090,- EUR	

Whiplash Testing and Evaluation in Rear Impacts

Course Description

In real-world accidents, distortions of the cervical spine or so-called whiplash injuries following a rear impact are among the most expensive injuries for the insurance industry. About 75 % of all injury costs of the insurers are caused by whiplash injuries in highly-motorized countries. About 80 % of all injuries in a rear impact are whiplash-injuries. This is why this type of injury - even though it is neither very serious nor lethal - has reached a high priority in the endeavors to develop test procedures and assessment criteria which help in designing constructive measures in the car in order to avoid this type of injury.

As an introduction, this seminar refers to the different accident data for whiplash injuries, which offer many realizations but no consistent pattern with regard to the biomechanical injury mechanisms. However, some organizations - mainly from the field of consumer information and insurance institutes - are working on the development of test procedures and assessment criteria. The most active ones are Thatcham (UK) and IIHS (USA) which are united in the group IIWPG (International Insurance Whiplash Prevention Group), SNRA and Folksam (Sweden) and the German ADAC.

In 2008 Euro NCAP introduced a whiplash test procedure as part of its rating system. In 2014 an additional static assessment for the rear seats was added. In 2020 Euro NCAP introduced a new Whiplash assessment on front seats. Where concepts and methods from the future legal requirement the Global Technical Regulation No. 7 Phase II (Head Restraints) can be recognised. The Euro NCAP assessment will be explained in detail in the seminar. Furthermore, the EEVC working group 20 is active as a consulting authority concerning whiplash injuries for the legislation in Europe. The Global Technical Regulation No. 7 Phase I (Head Restraints, short GTR 7) was unsatisfactory from the European point of view. Therefore the United Nations published a second phase of this regulation. The content of the GTR 7 Phase II gives the legal base for the future HR development requirements. The focus of this work is on improving the BioRID dummy and on the definition of so called Seat Performance Criteria.

All discussions about the assessment of whiplash injuries within the framework of consumer information have in common, that the protection effect in a rear-end impact needs to be examined in an isolated vehicle seat by means of a sled test using a generic acceleration pulse. It turns out to be problematic, however, that presently there is no traumato-mechanical explanation of the phenomenon “whiplash injury” and that all the currently discussed dummy criteria with the respective limit values follow a so-called “black-box approach”. Experts try to correlate the measured dummy criteria with the findings from accident data and to thus derive limit values. In this context the available dummy-technology with the different measuring devices and criteria, as well as the proposed limit values are going to be presented.

In the last part of the seminar different seat design concepts (energy-absorbing, respectively geometry-improving), sub-divided into active and passive systems will be introduced, and their advantages and disadvantages will be discussed.

Who should attend?

The seminar addresses development engineers who are new in the field of rear impacts or who have already got some experience in the field of safety, as well as developers of sub-assemblies which have to fulfill a crash-relevant function. It is furthermore especially interesting for project managers and managers who deal with the topic of rear-end impacts and who would like to obtain a better knowledge of this subject in order to use it for an improvement of procedures.

Course Contents

- Introduction into the characteristics of a rear-end impact
- Overview of the most important whiplash requirements
- Injury criteria
- Dummy-technology for rear impacts
- Presentation of the Euro NCAP and FMVSS 202-dynamic test procedures
- Outlook on possible harmonization-tendencies
- Explanation of the possible design measures in car seats

Instructor

Thomas Frank (LEAR Corporation GmbH) joined the passive safety department of LEAR Corporation in 2002 after graduating from the Technical University of Berlin in physical engineering sciences. At LEAR Thomas Frank initially worked as a test engineer in crash testing, later he developed head rests. Today he is expert for head restraints and low speed rear impact safety. In his position he guides the seat development with respect to meet whiplash protection requirements in regulations and consumer tests.

Facts

18.09.2025	50/4538	Alzenau	1 Day	890,- EUR till 21.08.2025, thereafter 1.090,- EUR	English

Latest info about this course

Safety Seminar

Side Impact - Requirements and Development Strategies

Course Description

In addition to the frontal impact, the protection in a side impact has a fixed place in the development of vehicles. Continuous aggravation of consumer tests and legal regulations, due to new pole tests (UN ECE R135 and U.S. NCAP), enhanced deformable barriers and the introduction of World-SID Dummies (5 / 50%ile) with test specific measuring methods are causing a need to further improve side impact protection. In order to achieve this enhancement, it is necessary to get a much more profound understanding of the highly complex phenomena and modes of action in a side impact which goes far beyond the simple application of additional airbags. The seminar provides a comprehensive overview of today's standard test procedures including country-specific variations, the legal regulations and the requirements of consumer protection as well as an outlook on changes in the near future. In addition, tools, measuring methods and criteria, and virtual methods such as crash and occupant simulation, as well as the analysis of the performance of the restraint systems will be discussed. Furthermore it will be explained how a target-oriented use of CAE-simulation and hardware tests can lead to optimal passenger values, while at the same time obeying to boundary conditions such as costs, weight and time-to-market. A workshop with crash-data analysis finally deepens the understanding.

Who should attend?

The seminar addresses development engineers who are new in the field of side crash, or who have already gained some experience in the field of safety, as well as developers of assemblies that have to fulfil a sidecrash-relevant function. Furthermore it is also interesting for project managers and managers, who deal with side impact and who would like to gain a deeper understanding of this topic in order to use it for an improvement of procedures.

Course Contents

- Challenges of side impacts
- Explanation of the different measuring means, in particular the different dummies
- Overview of current test procedures and side impact relevant protection criteria
  - Legal tests (FMVSS 214, UN ECE R95, UN ECE R135, ...)
  - Other tests (Euro NCAP, U.S. NCAP, further NCAPs, IIHS, manufacturer specific tests)
- Development methods and tools:
  - Crash and occupant simulation, range of application and limitations.
  - Analysis of the performance of protection and restraint systems in side impact. Discussion of the boundary conditions, limits, conflicts and problems
  - Development strategy for an optimal restraint system for side impact
  - Target oriented use of CAE-simulation and hardware tests to develop optimal occupant load values
- Workshop with analysis of crash-data and discussion of the results

Instructors

Stephanie Wolter (BMW AG) studied engineering physics at the University of Applied Sciences Munich. Since 1995 she has been working at BMW AG in different functions in the field of side protection, such as pre-development, development of side airbags and as a project engineer in various car lines. Moreover, she represents BMW Group in various national and international bodies that deal with side impact and other aspects of side protection, e. g. ISO Working Groups, etc.

Joachim Peest (BMW AG) studied Mechatronical Engineering at the Leibniz University Hannover, focussing on automation and control systems engineering. He has been working in passive safety since 2011 in different functions, starting as a test- and project-engineer, and later as a requirement- and process-developer. Since 2017, he has been working at BMW AG as a specialist in the side-crash-development of various vehicle projects.

Facts

02.-05.06.2025	28/4522	Online	4 x 4 Hrs.	1.450,- EUR till 05.05.2025, thereafter 1.750,- EUR	
11.-12.11.2025	28/4523	Gaimersheim	2 Days	1.450,- EUR till 14.10.2025, thereafter 1.750,- EUR	

Head Impact on Vehicle Interiors: FMVSS 201 and UN R21

Course Description

To prevent injuries resulting from impacts of the occupants' heads on vehicle interior parts, these parts need to be designed in a way which allows sufficient deformation space to reduce the loads on the head. Internationally there are two important regulations regarding the design of interiors, such as cockpits, roof and door liners: The U.S. FMVSS 201 and the Regulation UN R21. Both regulations stipulate requirements concerning the maximum head acceleration or the HIC in impacts on interior parts.

The objective of this course is to provide an overview of the legal requirements and to show how these can be fulfilled. The focus of the seminar is on the development process and the development tools and methods. In particular the interaction of testing and simulation will be described and different design solutions will be discussed. Typical conflicts of objectives in the design - e.g. to fulfil NVH requirements, static stiffness, or misuse, while fulfilling the safety standards at the same time - are addressed in this seminar. Examples of practical solutions will be shown and discussed.

In addition, the development according to the head impact requirements in the overall-context of vehicle development is described in this seminar.

In a workshop exemplary head impact locations in a vehicle interior and impact areas on a dashboard are determined.

Who should attend?

This seminar is especially suited for engineers and technicians who work on the development of vehicle interior parts and who want to become familiar with the safety requirements that are relevant for these parts.

Course Contents

- Introduction
- Rules and regulations concerning head impact
  - FMVSS 201
  - UN R21
- Development tools
  - Numerical simulation
  - Test
- Workshop: Determination of impact locations in a vehicle
- Development process and methods
  - Solving of conflicts of objectives
  - Typical deformation paths, padding materials

Instructor

Torsten Gärtner (Opel Automobile GmbH) has been working as a simulation expert since 1997. From numerous projects he has extensive experience in the field of occupant simulation and interior safety. He is Technical Lead Engineer Safety Analytics at Opel Automobile GmbH. Before that he worked as department manager for safety with TECOSIM GmbH and spent 10 years in various management positions with carhs gmbh.

Facts

02.06.2025	46/4553	Alzenau	1 Day	890,- EUR till 05.05.2025, thereafter 1.090,- EUR	

General Terms for the Participation in Seminars and Events

Subject and Scope of Application
These General Terms and Conditions (AGB) apply exclusively to participation in seminars and events organized and held by carhs.training GmbH (hereinafter referred to as carhs.training), Siemensstraße 12, 63755 Alzenau, Germany. General terms and conditions or other general contractual conditions of the customer or third parties are not valid, even if carhs.training does not expressly object to them in individual cases.

Registration
You can register for the seminar, for the event directly via our webpage www.carhs.de. By sending the e-mail/internet registration, the participant accepts the conditions of participation. Your registration data will be stored for internal purposes.

Registration Confirmation / Invoice
You will receive a written registration confirmation and an invoice immediately after receipt of your registration. Invoices are due for payment 30 days after the invoice is issued, but no later than 7 days before the start of the seminar or before the start of the event without deductions. We reserve the right to exclude participants from the seminar or event if payment is not made in time.

Participation Fee
The participation fee for a seminar, an event is per person plus VAT and includes training material, certificate of participation, food and drinks during breaks and lunch. Since the place of performance for seminars and events held in Germany is Germany (§ 3a Abs. 3 Nr. 3 lit. a German UStG), participants from abroad must also pay VAT (but it may be possible to apply to the German Federal Central Tax Office for a refund of VAT). Participation in our seminars and events only temporarily does not entitle to a reduction of the participation fee. If you would like to book a larger number of seminar days and/or event days within a year, it is advisable to conclude a framework agreement. Please contact us in this regard!

Discount for Participants from Universities and Public Research Institutions
We grant participants from universities and public research institutions a discount of 40 % on the respective seminar prices, event prices.

Number of Participants
The number of participants is limited in order to guarantee an efficient execution of the seminars, the events. Registrations will be considered in the order in which they are received. Early registration is therefore recommended. For registrations beyond this date, we will try to offer an alternative date.

Cancellation
1. Cancellation of the registration up to 4 weeks before the seminar is free of charge. For cancellations up to 2 weeks before the start of the seminar we have to charge a flat rate of 100 Euro. If a cancellation is made after this date or if the participant does not appear at the seminar, the fee is to be paid in full. In this case, the participant has the right to participate in the next seminar without further costs.
2. For the conferences and events listed under the heading "Events", the following deviating cancellation conditions apply: Cancellation of registration up to 4 weeks before the start of the event is free of charge. Cancellation up to 2 weeks prior to the start of the event will be charged half the participation fee. If the cancellation is made after this date or if the participant does not appear at the event, the fee is payable in full.

Replacement Participants
A substitute participant can be named at any time instead of the registered participant at no additional cost. The same conditions of participation apply to this substitute as to the registered participant. If two persons share the participation (1 participant per day), both will receive the complete documents. A surcharge of EUR 100 plus VAT will be charged.

Program Changes
carhs.training reserves the right to change the program of the seminar or event.

Cancellation or Postponement of Seminars and Events
We reserve the right to cancel or postpone seminars and events for organizational reasons (e.g. if the minimum number of participants, which depends on the type of seminar or event, is not reached or if the speaker is unavailable at short notice). In case of cancellation by us, we will try to rebook you on another date and/or venue, if you wish so. Otherwise you will be refunded the fees already paid, further claims are excluded.

Liability
Naturally, the speakers will present their own opinions, publish or make available information and data. We cannot accept any liability for the content of the statements, for information and data or for the success of the training. We are not liable for loss of or damage to items brought to seminars or events unless the loss or damage to these items is due to intentional or grossly negligent conduct by our employees or other vicarious agents. We would therefore ask you not to leave any valuables or important materials in the conference room during breaks. We do not guarantee that the products, processes and names mentioned in seminars, events and documents are free of property rights.

Copyrights
The materials handed out within the context of our seminars and events are protected by copyright and may not be reproduced or commercially used, even in part, without the consent of carhs.training GmbH and the respective instructors.

Image Recordings
carhs.training is entitled, within the framework of the seminar, the event, to create, reproduce, broadcast or have created, reproduce or have broadcast, make available to the public or have made available to the public, as well as to use or have used in any other way in audio-visual media, image recordings of the participants that go beyond the reproduction of an event of current events (right to one's own image) without remuneration.

Partner Seminars and Events
At the seminars, events of our partner companies Automotive Solution Center for Simulation e.V., BGS - Böhme und Gehring GmbH and Verkehrsunfallforschung an der TU Dresden GmbH we only act as a broker and forward your registration to the respective provider. Your contractual partner becomes the respective seminar or event provider. Their conditions of participation apply exclusively.

Validity of the Conditions of Participation
For all seminar bookings, event bookings (with the exception of partner seminars, partner events) these terms and conditions of participation apply exclusively. Deviating terms and conditions of our clients shall not apply even if the client refers to his own terms and conditions in the course of correspondence required due to the contractual relationship.

Written Form, Validity of German Law and Place of Jurisdiction
1. All agreements made at the time of the conclusion of the contract or thereafter, which deviate from the provisions of these AGB, must be in writing to be legally effective. This also applies to a cancellation or waiver of the written form requirement. For the compliance with the written form it is also sufficient to send it by fax or e-mail.
2. The present AGB and all individual contracts concluded between carhs.training and the customer are subject exclusively to the laws of the Federal Republic of Germany, excluding the UN Convention on Contracts for the International Sale of Goods (CISG).
3. If the customer is a merchant, legal entity under public law, or special fund under public law, or has no general place of jurisdiction in Germany, the exclusive place of jurisdiction is the headquarters of carhs.training.

Registration at www.carhs.de

Index

Advertisers Directory

Seminar Calendar 2025

carhs Empowering Engineers

April

08.-09.04.2025 | Frankfurt/Hanau | p. 12
automotive CAE Grand Challenge

14.-15.04.2025 | Alzenau | p. 159
International Safety and Crash-Test Regulations

29.04.2025 | Online | p. 95
Virtual Testing #5 ADAS Development Challenges

29.04.2025 | Chongqing China | www
Euro NCAP HGV Workshop

29.-30.04.2025 | Alzenau | p. 162
Crash Safety of Hybrid and Electric Vehicles

29.-30.04.2025 | Online | p. 154
Introduction to ADAS and Active Safety

May

05.-08.05.2025 | Online | p. 159
International Safety and Crash-Test Regulations

06.-07.05.2025 | Alzenau | p. 16
Crashworthy and Lightweight Car Body Design

13.-14.05.2025 | Frankfurt/Hanau | p. 155
SafetyWeek

20.-21.05.2025 | Alzenau | p. 80
Introduction to the Python Programming Language

20.-21.05.2025 | Online | p. 14
Early Increase of Design Maturity of Restraint Systems

June

02.06.2025 | Alzenau | p. 169
Head Impact on Vehicle Interiors

02.-05.06.2025 | Online | p. 84
Python based Machine Learning w. Automotive Applications

02.-05.06.2025 | Online | p. 168
Side Impact - Requirements and Development Strategies

03.06.2025 | Alzenau | p. 158
Automated Driving - Safeguarding and Market Introduction

03.-04.06.2025 | Landsberg am Lech | www
Euro NCAP Passive Safety Workshop

04.-05.06.2025 | Alzenau | p. 13
Virtual Testing for Vehicle Safety Assessment

06.06.2025 | Online | p. 95
Virtual Testing #6 Battery Safety Assessment

17.-18.06.2025 | Gaimersheim | p. 163
Development of Frontal Restraint Systems

25.-26.06.2025 | Bergisch Gladbach | p. 41
PraxisConference Pedestrian Protection

July

01.-02.07.2025 | Alzenau | p. 161
NCAP - New Car Assessment Programs

14.-17.07.2025 | Online | p. 153
Introduction to Passive Safety of Vehicles

16.-17.07.2025 | Shanghai | p. 156
Automotive Safety Summit Shanghai

22.-23.07.2025 | Tokyo | www
SafetyUpDate Japan

28.-31.07.2025 | Online | p. 162
Crash Safety of Hybrid and Electric Vehicles

August

05.-07.08.2025 | Online | p. 38
Pedestrian Protection - Development Strategies

25.-28.08.2025 | Online | p. 161
NCAP - New Car Assessment Programs

September

01.09.2025 | Alzenau | p. 18
Crash-Course Additive Manufacturing

01.09.2025 | Alzenau | p. 18
Implementation of Additive Manufacturing Processes

04.-05.09.2025 | Alzenau | p. 19
Design for Additive Manufacturing

16.-17.09.2025 | Alzenau | p. 153
Introduction to Passive Safety of Vehicles

16.-17.09.2025 | Online | p. 110
Material Models of Metals for Crash Simulation

18.09.2025 | Alzenau | p. 167
Whiplash Testing and Evaluation in Rear Impacts

23.-24.09.2025| China | p. 157
The ADAS Experience 2025 China

23.-24.09.2025 | Alzenau | p. 161
NCAP - New Car Assessment Programs

25.-26.09.2025 | Alzenau | p. 86
Simulation for Automated Vehicles

29.09.-02.10.2025 | Online | p. 63
NVH - Background, Practice and Simulation Methodology

October

07.10.2025 | Online | p. 95
Virtual Testing #7 Occupant Protection Assessment

09.-10.10.2025 | Online | p. 121
Material Models of Composites for Crash Simulation

10.10.2025 | Alzenau | p. 68
Design and Simulation of Vehicle Vibration

14.-15.10.2025 | Alzenau | p. 160
Vehicle Safety under Self-Certification

Seminar Calendar 2025/26

carhs Empowering Engineers

15.10.2025 | Gaimersheim | p. 163
Development of Frontal Restraint Systems - Advanced

08.-09.10.2025 | Klettwitz | www
The SafeBattery Experience

21.-22.10.2025 | Alzenau | p. 85
AI and Machine Learning for ADAS and ADS

21.-22.10.2025 | Landsberg am Lech | www
Euro NCAP Passive Safety Workshop

21.-24.10.2025 | Online | p. 134
Introduction of Reduced Order Modelling and its Application for Model based real-time Optimization

27.-28.10.2025 | Alzenau | p. 84
Python based Machine Learning

27.-30.10.2025 | Online | p. 72
Structural Optimization in Automotive Design

27.-30.10.2025 | Online | p. 100
Introduction to Impact Biomechanics and HBMs

29.10.2025 | Alzenau | p. 100
Introduction to Impact Biomechanics and HBMs

30.-31.10.2025 | Shanghai | p. 91
Human Modelling and Simulation in Automotive Engineering

November

03.-04.11.2025 | p. 38
Pedestrian Protection - Development Strategies

05.11.2025 | Alzenau | p. 14
Early Increase of Design Maturity of Restraint System ...

05.-06.11.2025 | Online | p. 125
Modeling of Joints in Crash Simulation

10.11.2025 | Alzenau | p. 154
Introduction to ADAS and Active Safety

10.-13.11.2025 | Online | p. 153
Introduction to Passive Safety of Vehicles

10.-13.11.2025 | Online | p. 16
Crashworthy and Lightweight Car Body Design

11.-12.11.2025 | Gaimersheim | p. 168
Side Impact - Requirements and Development Strategies

12.-13.11.2025 | Online | p. 166
Model Based Head Injury Criteria for Innovative Protection Design

12.-13.11.2025 | Alzenau | p. 159
International Safety and Crash-Test Regulations

14.11.2025 | Alzenau | p. 122
Static and Dynamic Analysis of Long-Fibre-Reinforced Plastics

17.-18.11.2025 | Alzenau | p. 17
Design of Composite Structures

18.-19.11.2025 | Alzenau | p. 162
Crash Safety of Hybrid and Electric Vehicles

18.-21.11.2025 | Online | p. 161
NCAP - New Car Assessment Programs

19.-20.11.2025 | Alzenau | p. 163
Development of Frontal Restraint Systems ...

25.-26.11.2025 | Alzenau | p. 13
Virtual Testing for Vehicle Safety Assessment ...

26.-27.11.2025 | Landsberg am Lech | www
The Safe Seats Experience

December

02.-05.12.2025 | Online | p. 80
Introduction to the Python Programming Language

10.-11.12.2025 | Frankfurt/Hanau | www
Euro NCAP UpDate 2025

February 26

23.-24.02.2026 | Alzenau | p. 63
NVH - Background, Practice and Simulation Methodology

March 26

03.-04.03.2026 | Alzenau | p. 72
Structural Optimization in Automotive Design

05.-10.03.2026 | Online | p. 13
Virtual Testing for Vehicle Safety Assessment

10.03.2026 | Alzenau | p. 110
Material Models of Metals for Crash Simulation

19.03.2026 | Alzenau | p. 125
Modeling of Joints in Crash Simulation

20.03.2026 | Alzenau | p. 122
Static and Dynamic Analysis of Long-Fibre-Reinforced Plastics

April 26

14.-16.04.2026 | Frankfurt/Hanau | p. 155
SafetyWeek

May 26

19.-20.05.2026 | Frankfurt/Hanau | p. 12
automotive CAE Grand Challenge

Find the latest information on our seminar program at
www.carhs.de


Unmatched In-Design Multiphysics Analysis solutions
Our advanced software, processes, and service solutions for Engineering Simulation-Driven Design empower you to navigate the virtual product development process with precision. Gain deeper insight into your products from the initial design phase, while mitigating innovation risks through faster, smarter decision-making as you transition from concept to reality.
www.beta-cae.com
BETA CAE Systems is now part of Cadence
BETA
SIMULATION SOLUTIONS
cadence

TECOSIM, a Hinduja Tech company, is a leading partner in innovative product development. Leveraging advanced CAD, CAE, and digital engineering, we support clients in the mobility sector and beyond. Our global team of 650 experts deliver tailored solutions – from the initial concept to series production – bringing your ideas to live. Building on our core engineering services, we also offer virtual benchmarking, software solutions, and talent management.

Engineering better living

Since Dec 2024, TECOSIM has been integral to Hinduja Tech Ltd., a mobility-focused global engineering and R&D technology company. As the company's center of excellence for simulation-led design engineering, TECOSIM is a strategic partner for leading automotive manufacturers and mobility providers. With Hinduja Tech, our 2,650 engineers offer comprehensive solutions encompassing powertrains, body engineering, vehicle integration, virtual validation, embedded electronics, and digital technologies to global OEMs and leading Tier-1 suppliers worldwide.

TECOSIM Group
Gutenbergplatz 1 | 65187 Wiesbaden, Germany
info@tecosim.com | www.tecosim.com

Follow us on

Bangalore | Basildon | Bucharest | Cluj-Napoca | Cologne | Coventry | Detroit | Hamburg | Irvine | Munich | Norwich | Osaka | Pune | Stuttgart | Wiesbaden